Combined Measurement of Noise Exposure and Induced Auditory Fatigue Using a Digital Hearing Protector

by

Vincent NADON

MANUSCRIPT-BASED THESIS PRESENTED TO ÉCOLE DE TECHNOLOGIE SUPÉRIEURE
IN PARTIAL FULFILLMENT FOR THE DEGREE OF
DOCTOR OF PHILOSOPHY
Ph.D.

MONTREAL, APRIL 14, 2020

ÉCOLE DE TECHNOLOGIE SUPÉRIEURE
UNIVERSITÉ DU QUÉBEC

BOARD OF EXAMINERS

THIS THESIS HAS BEEN EVALUATED

BY THE FOLLOWING BOARD OF EXAMINERS

Prof. Jérémie Voix, thesis supervisor
Department of mechanical engineering, École de technologie supérieure

Prof. Chakib Tadj, president of the board of examiners
Department of electrical engineering, École de technologie supérieure

Prof. Olivier Doutres, member of the jury
Department of mechanical engineering, École de technologie supérieure

Dr. Hugues Nélisse, member of the jury
Researcher, Institut de recherche Robert-Sauvé en santé et en sécurité du travail (IRSST)

Prof. Tony Leroux, external examiner
School of speech-language pathology and audiology, Faculty of Medicine,
Université de Montréal

Dr. Philippe Fournier, external independent examiner
Post-doctoral researcher, Université d'Aix-Marseille

THIS THESIS WAS PRESENTED AND DEFENDED

IN THE PRESENCE OF A BOARD OF EXAMINERS AND THE PUBLIC

ON JANUARY 31, 2020

AT ÉCOLE DE TECHNOLOGIE SUPÉRIEURE

ACKNOWLEDGEMENTS

This doctoral project was very challenging in many ways. The technical difficulties for the design of the DPOAE systems have slowed down the pace of the project. These difficulties include an earpiece makeover in addition to software coding and recoding due to hardware limitations. Moreover, software recording issues discovered at a late stage of the project required several months of problem solving to finally submit a scientific article. I am therefore grateful to finalize this project after all these years in this long adventure, and I would like to thank:

The IRSST for their flexible and comprehensive financial support during my doctoral studies from 2014 to 2017.

Jérémie Voix, my thesis supervisor, for all these great years working together from my masters to my doctorate. His ambitions inspired me to push my limits and become a better researcher.

My doctoral jury for accepting to evaluate my work. I truly believe I am surrounded by the best researchers to challenge me.

Nick Laperle who opened his "EERS" when I had a difficult time.

All my colleagues in the CRITIAS lab, but especially Valentin Pintat not only for his PCB assembling and debugging skills, but also for following me in my cycling adventures like when he did my support for the Ultra Défi 2017.

Hami Monsarrat-Chanon who spent several hours helping and developing code for the new ARP3 and the SoundBoard.

Fabien Bonnet for his humoristic touch, and helping me out with my doctorate when he could give a hand.

Rachel Bou Serhal for her patience with the article and moral support during difficult times.

Gabrielle Crétot-Richert for being more than a desk neighbour, a precious confidant. Thanks for being there to let the steam out and telling me about all your crazy stories.

Annelies Bockstael who invited me at Ghent University in Belgium. In addition to my international friends Mirjana Adnadjevic, Gemma Echavaria, Maria Lappano, Ivar Stam and Caroline Forlim for the good times together and their help in Belgium.

Clément Drapeau for his precious help finding students exposed to noise and allowing the experiment to be conducted in his workshop. I'd also like to thank the École Nationale du Meuble et de l'ébénisterie (ENME) in Montreal for their contribution in this important doctorate study.

Karolina Charaziak, postdoctoral Fellow at University of Southern California, for all her help with the forward pressure level calibration method.

Éric Lacourse at Université de Montréal and Jill Vandermeerschen at the Université du Québec à Montréal (UQAM) for their precious help in statistics for the multilevel models.

Robocyclo cycling club in Ghent, for my therapy on the bike and helping me discover a new passion in 2015. In addition to Club Cycliste de l'Université de Montréal and Team IBIKE to help me continue this therapy on the bike in Montreal and integrate me in their teams.

My love, Amélie Marcil-Roy for her support to manage the crisis the last year of this crazy adventure.

My family Réjean Nadon, Josée Guimond and Benoit Nadon for trying to help me out the best they could by showing their support in my studies, helping me to find factories to conduct my experiments and giving me motivation to finish this ambitious project. My father Réjean helped me out to find an expert in mixed model analysis, which was a crucial part to finalize this thesis.

Mesure combinée de l'exposition au bruit et la fatigue auditive induite en utilisant un protecteur auditif numérique

Vincent NADON

RÉSUMÉ

Malgré les efforts pour intégrer les programmes de conservation de l'ouïe en milieux de travail et l'utilisation de protection auditive. La perte auditive induite par le bruit demeure la maladie du travail la plus commune et dispendieuse. Les travailleurs portent donc une protection auditive pour réduire le risque de développer cette maladie professionnelle. Cependant, il est difficile d'estimer le niveau d'exposition au bruit résiduel derrière la protection auditive et son impact sur l'audition. D'une part, plusieurs facteurs doivent être considérés pour estimer le niveau de bruit résiduel, comme le niveau de protection du protecteur auditif, la qualité du positionnement du protecteur, etc. D'autre part, les mesures pour détecter la perte auditive sont conduites sur de trop grands intervalles. Généralement après que le dommage soit fait. Elles ne préviennent donc pas la perte auditive induite par le bruit en milieu de travail. Par ailleurs, il n'y a pas de moyen de s'assurer que la limite d'exposition au bruit de 90 dBA au Québec, basée sur une journée de travail de 8 heures, est adéquate pour un individu en particulier étant donné sa propre susceptibilité au bruit. Des études récentes montrent que le niveau d'exposition équivalent sur une journée n'est pas suffisant pour expliquer les changements dans la santé auditive. Afin d'améliorer l'estimation du risque, les variations temporelles en plus du spectre de fréquence devraient donc être considérées.

Dans le but d'établir la relation entre l'exposition au bruit et ses effets sur la santé auditive, une approche est suggérée pour faire le suivi continu des émissions otoacoustiques (OAE) pendant le quart de travail tout en mesurant l'exposition au bruit. Les objectifs de cette thèse par articles sont premièrement de tester la santé auditive des individus dans un environnement bruyant simulé pour valider le premier prototype du système de mesure des OAE développé. Ensuite, développer une méthode pour mesurer le niveau de bruit résiduel derrière le bouchon ainsi que le niveau d'atténuation du bruit *in situ* du protecteur auditif en utilisant le système portable conçu. Ce qui permet finalement d'estimer la relation dose-réponse entre l'exposition au bruit et la santé auditive. Les résultats obtenus dans cette thèse montrent qu'il est possible de détecter des changements dans la santé auditive pendant l'exposition à des niveaux de bruit modérés. Des méthodes de prévention sont donc suggérées pour conserver l'ouïe.

Mots-clés: suivi de santé auditive, émission otoacoustique, dosimétrie, perte auditive induite par le bruit, surdité professionnelle

Combined Measurement of Noise Exposure and Induced Auditory Fatigue Using a Digital Hearing Protector

Vincent NADON

ABSTRACT

Despite the efforts to integrate hearing conservation programs in the workplace, noise-induced hearing loss (NIHL) remains the most common and expensive occupational disease. Although industrial workers do wear hearing protection devices (HPD), it is difficult to estimate the effective noise exposure using a personal dosimeter placed on their shoulder, since the residual ambient sound pressure level (SPL) behind the hearing protector is usually unknown. Many factors need to be considered when estimating the effective residual noise exposure, such as the attenuation rating of the hearing protector, the quality of the HPD fit, the duration the protector was removed during noise exposure, as well as how the human auditory mechanisms interact with changes in noise exposure levels. Moreover, hearing assessment with audiometric measurement is often conducted on too long intervals, after the hearing damage might have appeared, and thus do not prevent the occupational hearing loss. There is also no way to ensure that the recommended maximum noise exposure of 90 dBA, based on an 8-hour work shift, in Quebec is suitable for a given individual due to his own susceptibility to NIHL. Besides, recent studies show that global noise exposure levels are not sufficient to explain changes in hearing health and temporal fluctuations in noise in addition to noise spectral balance measurements should be considered in NIHL risk assessment.

In order to establish a dose-response relationship between noise exposure and its effects on hearing health, an approach is suggested to continuously monitor the workers' otoacoustic emissions (OAE) levels during their work while recording the noise exposure. The objectives of the thesis project are first to assess the individual's hearing health with OAEs in a simulated noisy environment to validate the first prototype of the developed OAE measurement system. Then, develop a method to monitor the residual ambient sound pressure level behind the earplug and the hearing protection level *in situ* using the designed portable system. This finally allows to estimate the dose-response relationship based on the effective noise exposure and OAE levels. The results obtained in this thesis show that it is possible to detect changes in hearing health during moderate noise exposure levels. Hearing conservation methods are therefore proposed to reduce the risk of NIHL.

Keywords: hearing health monitoring, otoacoustic emissions, dosimetry, occupational hearing loss, noise-induced hearing loss

TABLE OF CONTENTS

Page

LIST OF TABLES

LIST OF FIGURES

Page

LIST OF ABREVIATIONS

AIC	Akaike Information Criterion
ARP	Auditory research platform
BIC	Bayesian Information Criterion
CAS	Contralateral Acoustic Stimulation
CAD	Canadian Dollar
CRITIAS	NSERC-EERS Industrial Research Chair in In-Ear Technologies (CRITIAS)
CNESST	“Commission des Normes, de l’Équité, de la Santé et de la Sécurité du Travail”
CIRMMT	Centre for Interdisciplinary Research in Music Media and Technology
DSP	Digital Signal Processor
DP	Distortion Product
DPOAE	Distortion-Product Otoacoustic Emission
EOAE	Evoked Otoacoustic Emission
ÉTS	“École de technologie supérieure”
HCP	Hearing Conservation Programs
HPD	Hearing Protection Device
HTL	Hearing Threshold Level
ICC	Intraclass Correlation Coefficient
IEM	In-Ear Microphone
IEND	In-Ear Noise Dosimeter

IRSST	“Institut de recherche Robert-Sauvé en santé et en sécurité du travail”
MOC	Medial Olivocochlear
MEM	Middle-ear muscle
NIHL	Noise-Induced Hearing Loss
NIOSH	National Institute for Occupational Safety and Health
NIPTS	Noise-Induced Permanent Threshold Shift
NSERC	Natural Sciences and Engineering Research Council
OAE	Otoacoustic Emission
OC	Olivocochlear
OEM	Outer-ear microphone
OHC	Outer Hair Cells
OSHA	Occupational Safety and Health Administration
PAR	Personal attenuation rating
PEL	Permissible exposure limit
PTS	Permanent Threshold Shift
PTA	Pure-Tone Audiometry
REL	Recommended exposure limit
SD	Standard Deviation
SEM	Standard Error of the Mean
SOC	Superior Olivary Complex

SPL	Sound Pressure Level
TEOAE	Transient-Evoked Otoacoustic Emission
TTS	Temporary Threshold Shift
USB	Universal Serial Bus
WID	Wearer-Induced Disturbance
WHO	World Health Organization

LIST OF SYMBOLS AND UNITS OF MEASUREMENTS

β	kurtosis
dB	decibel
dBA	A-weighted decibel
dB(HL)	decibels Hearing Level
dB(SPL)	decibels Sound Pressure Level
Δ	coherence variation
Hz	Hertz
kHz	kilohertz
Fs	sampling frequency
L_{eq}	equivalent continuous sound level
$L_{eq,\,T}$	equivalent continuous sound level over duration T
$L_{Aeq,\,T}$	A-weighted equivalent continuous sound level over duration T
$L_{ex,\,8h}$	noise exposure level that is energy-averaged over an 8-hour work shift
ms	milisecond
Pa	Pascal
mPa	milipascal
μPa	micropascal
ϕ	phase

INTRODUCTION

0.1 Context

According to the National Institute for Occupational Safety and Health (NIOSH) (NIOSH, 2016), more than 22 million North American workers are exposed every day to noise exposure doses that may induce hearing loss according. Many workers use hearing protection such as earmuffs or earplugs inserted in the earcanal in order to limit their noise exposure. Unfortunately, these hearing protectors are generally not correctly fitted (Smith, P. S., Monaco, B. A. & Lusk, S. L., 2014) nor worn for a sufficient duration (Groenewold, M. R., Masterson, E. A., Themann, C. L. & Davis, R. R., 2014; HSE, 2019a), therefore exposing workers to an excessive noise dose that may lead to permanent hearing damage.

As a result, in the province of Quebec these hearing disorders represent more than 58% of the files received and accepted in 2011 for occupational diseases (CNESST, 2011) and this number increased to 72.5% in 2017 (CNESST, 2017) . The amount of hearing disorders cases has tripled over the last 15 years, when the number of other reported occupational diseases decreased (CNESST, 2015). The evolution of hearing injury requires a continuous follow-up of workers and frequent hearing aids adjustment. Eventually hearing disorders can cause other problems between family members due to the lack of communication, isolation, depression, etc., thus increasing the societal costs of the disease (Gates, G. A. & Mills, J. H., 2005; Ruberg, K., 2019). Hence, hearing disorders are the most expensive occupational disease (CNESST, 2015) with an average cost by case of 153 618$ (CAD) between 2005 and 2007 (Lebeau, M., 2014). The prevention of permanent damage with adequate hearing protection is obviously less expensive to the society. However, despite the efforts in the implementation of hearing conservation programs, Noise-Induced Hearing Loss (NIHL) remains one of the biggest causes of invalidity and indemnity in North America (CNESST, 2015,1; NIOSH, 2016).

0.2 Research problem

NIHL is a hearing impairment resulting from exposure to loud sounds and often leads to a loss of perception for a narrow range of frequencies (Alberti, P. W., 1992) or a change in sensitivity to sound or ringing in the ears, also known as tinnitus. The loss of sound perception can lead to communication problems, which in turn leads to isolation and can cause depression (Alberti, 1992).

Current practices to prevent NIHL in occupational health and safety programs (CCOHS, 2019a) involve monitoring noise exposure coming from machinery with sound level meters and noise dosimeters. When the workers are exposed to 8-hour equivalent sound levels ($L_{\text{eq, 8h}}$) exceeding 85 dBA (CCOHS, 2019a) a hearing conservation program (HCP) must be developed and implemented in the workplace. Such HCP can require noise control at the source to reduce the instantaneous noise level close to workers' ears below 85 dBA (CCOHS, 2019a) and the use of individual hearing protection devices (HPD) such as earplugs and earmuffs. To limit the workers' noise exposure further, administrations may restrict the amount of time spent in noisy areas. To detect the onset of NIHL, occupational health and safety administrators and other practitioners in the workplace, such as industrial hygienists, have the legal obligation to monitor noise exposure levels at work and require workers to perform an annual audiometric test (CCOHS, 2019a) to monitor the workers' hearing threshold levels. However, many traumatic noise events , such as loud sporting events or noise coming from loud machinery at work for example, can occur during a year and it is difficult to track back the exact causes of hearing loss. The annual hearing tests also measure the damage once it is already permanent, and thus do not actually prevent the occupational hearing loss. A year is a long time interval, hence hearing assessment should be performed on a daily basis and, depending on the worker's susceptibility to NIHL, measurements may need to be conducted on 20-minute intervals for example. Where susceptibility to NIHL represents a human's level of vulnerability to the effects of noise on his

hearing health due to environmental and physiological factors. However, this would be difficult with current bulky audiometer devices and would disturb the workers routine. Hence, these methods are somehow obsolete since they mostly document NIHL instead of using noise control methods for proper occupational hearing loss prevention (Lee D. Hager, 2019).

Besides, the recommended maximum noise exposure of 90 dBA based on an 8-hour work shift and exchange rate of 5 dB in Quebec is less strict compared to the limit of 85 dBA , 3 dB exchange rate, in the rest of Canada (CCOHS, 2019b). At the moment, there is no way to ensure that the permissible exposure limit (PEL), or recommended exposure limit (REL), is suitable for a given individual since everyone can have a different susceptibility to NIHL. As a result, even with the current noise regulations in Quebec, workers still have a risk of 18% to suffer from NIHL according to the ISO1999 standard (ISO, 2013). This standard suggests a reference method to estimate the risk of NIHL by taking into account the effects of aging. It is based on the relationship between noise exposures and noise-induced permanent threshold shifts (NIPTS) estimated using statistics from populations of various ages from three industrialized societies. However, this risk of hearing trauma assessed in the ISO1999 standard does not consider the frequency spectrum balance of the noise exposure. This could be an important factor for NIHL considering the low frequency weaknesses of passive HPD (Nélisse, H., Gaudreau, M.-A., Boutin, J., Voix, J. & Laville, F., 2011) and greater ear sensitivity in higher frequencies (Maison *et al.*, 2013). This risk of NIHL assessed in the ISO1999 standard is also based on an equal sound energy hypothesis (Alberti, 1992), whereas recent studies show that noise temporal variation characteristics should also be included in the risk assessment (Davis, R. I., Qiu, W., Heyer, N. J., Zhao, Y., Yang, M. Q., Li, N., Tao, L., Zhu, L., Zeng, L., Yao, D. et al., 2012).

Excessive noise exposure levels can damage the hair cells in the cochlea. This organ is responsible for the generation of electrical nerve signal resulting from acoustical stimulation. These nerve signals are then transmitted to the auditory cortex by the auditory nerve. Once the hair cells

are damaged due to high noise exposure levels, the nerve signal transmitted loses amplitude and frequency resolution, which leads to an increase in hearing threshold levels (HTL). Current advances in hearing research showed that moderate noise exposure levels can also cause some hearing damage (Bharadwaj *et al.*, 2015). Although such moderate noise levels may not induce changes in auditory thresholds in quiet conditions in the short term. They may induce damages to the cochlea's Inner Hair Cell (IHC) synapses (synaptopathy) and to the auditory nerve fibres (neuropathy). These hearing damages are therefore "hidden" since they are not detected with pure-tone audiometry, but usually impede speech intelligibility in noisy conditions (Kujawa, S. G. & Liberman, M. C., 2015; Liberman, M., 2016). Current techniques to assess hidden hearing loss on humans, with Auditory Brainstem Responses (ABR) for example, only measure the symptoms once the damage is irreversible and therefore do not prevent the onset of these damages.

In order to assess the health of the cochlea's Outer Hair Cells (OHC), otoacoustic emission (OAE) measurements can be used. These low amplitude acoustic signals are the responses of the OHC to a sound stimulated by a miniature loudspeaker in the earcanal. They are captured with an in-ear microphone positioned in the earcanal between the earpiece tip and the eardrum. These measurements are objective, fast and do not require the active participation of the worker. Hence, they are ideal to measure the reversible OHC damages *in situ* before the damage becomes permanent. In spite of the technological advances in the clinical devices available at the moment, OAE measurement devices and their test duration does not allow to continuously monitor the accumulated hearing fatigue in an industrial workplace. Very few experiments (Zare, S., Nassiri, P., Monazzam, M. R., Pourbakht, A., Azam, K. & Golmohammadi, T., 2015) were previously conducted with systems currently available in an industrial working environment, close to traumatic noise events, where it is difficult to obtain a reliable measurement due to noise disturbance in the recorded signal. Hence, there is no device on the market that measures all

the necessary noise metrics and tests hearing health on a short-time interval during the noise exposure for proper NIHL risk assessment.

0.3 Research objectives

To address the issues highlighted above, the main objective of this research project is to develop and validate a method to observe the effects of noise exposure on hearing health of industrial workers in their noisy work environment.

To achieve this main objective, the project includes the following 3 sub-objectives:

1. Design a robust and portable system able to evaluate the cumulative hearing fatigue of industrial workers in their own environment.

2. Establish the dose-response relationship between the noise exposure and its induced effects on hearing health.

3. Find which predictors are the most relevant for NIHL risk assessment. These predictors can be based on the individual's characteristics, the cumulative noise exposure level and other noise metrics.

0.3.1 Doctoral Thesis Objectives

The design of the OAE system, the first sub-objective of this research, was partially achieved during the candidate's master thesis (Nadon, V., 2014) and validated in laboratory conditions afterwards (Nadon, V., Bockstael, A., Botteldooren, D., Lina, J.-M. & Voix, J., 2015a,1). However, the system was not tested in realistic industrial noise environments. To complete the envisioned research, the doctoral thesis objectives are to:

1. Assess the individual's hearing health with OAEs in a simulated noisy environment to validate that the developed OAE system can monitor the effects of noise on the outer hair cells.

2. Develop a method to monitor the residual ambient sound pressure level behind the earplug and the hearing protection level *in situ* using the designed system. These methods will be used to find the relationship between the noise exposure and changes in hearing health.

3. Integrate the latest findings in hearing health research (e.g. hidden hearing loss) in the experimental protocol by implementing new OAE measurement settings and functions in the designed system. This would allow to finally estimate the dose-response relationship between the noise exposure and OAE levels to recommend better hearing conservation practices based on the most significant predictors of NIHL.

0.4 Thesis outline

This doctoral thesis details all the scientific developments achieved in order to complete the research project. The thesis starts with an exhaustive literature review (Chapter 1) to cover the available knowledge that is necessary for this doctoral project and set the objectives to bridge the knowledge gaps. Chapter 2 is added to detail the design process for the materials and methods used for this research. Afterwards, the thesis is mainly divided into three scientific peer-reviewed articles, contained in Chapters 3-5. It is followed by Chapter 6 that shows the experimental results of the longer-term effects of noise on hearing health. Finally Chapter 7 summarizes the findings and outcomes in this doctoral thesis. The content of each chapter is presented hereafter.

Chapter 1 - Literature Review

This first chapter covers important knowledge on the epidemiology of NIHL, noise exposure assessment and hearing health monitoring techniques. A few longitudinal studies on the effects

of noise exposure on the auditory system are also presented and reviewed. Finally, an overview of statistical methods to analyze noise-induced hearing status changes is presented.

Chapter 2 - Developed materials and methods

This second chapter presents the development process of the portable systems and calibration methods used for the laboratory and in-field experiments. The chapter details the technological advances and limitations of the developed systems regarding otoacoustic emission and noise exposure measurement. It is followed by a presentation of the *in situ* fit-test and calibration methods developed and used to ensure proper earpiece fit and improve the reliability of the DPOAE results.

Chapter 3 - Field Monitoring of Otoacoustic Emissions During Noise Exposure: Pilot Study in Controlled Environment (peer-reviewed article 1)

This chapter is a peer-reviewed article published by the *American Journal of Audiology* in October 2017. This article presents a preliminary study that fulfills the first objective of the doctoral project. The introduction of this article restates the necessity to measure the noise exposure levels and its effects on hearing health in order to prevent occupational NIHL. An approach is then proposed in the Method section to monitor hearing health using otoacoustic emissions while measuring the noise exposure continuously with a sound level meter. The variations in OAE levels over a few hours were analyzed and a model, built from the experimental results, showed the effects of the duration and levels of noise exposure on the OAE levels. In conclusion, this study shows that monitoring OAE levels on an individual during noise exposure is useful to observe temporary hearing status changes induced by ambient noise and is an interesting tool for effective hearing conversation programs in the workplace.

Chapter 4 - Method for protected noise exposure level assessment under an in-ear hearing protection device: a pilot study (peer-reviewed article 2)

This chapter is an article submitted for review to the *International Journal of Audiology* in September 2019. This article presents a method to estimate the residual noise behind the earplug by rejecting some noise artifacts, referred to as Wearer-Induced Disturbances (WID), to fulfill the second objective of this doctoral project. The introduction of this article details the needs and limitations of commercial in-ear noise dosimeters (IEND). One limitation being that current IEND do not reject WID events from the cumulative noise exposure levels over a day and these WIDs can potentially over-estimate the effective residual ambient noise level which has a real effect on hearing health. Therefore, a method using digital adaptive filtering is proposed to use the outer-ear microphone signal to estimate the effective residual ambient noise levels behind the earplug and discard the energetic contribution of the WIDs. This proposed method can also be used to estimate the Personal Attenuation Rating (PAR) of the HPD in real-time during noise exposure. The results of the proposed adaptive filter approach show that rejecting the WIDs can have an important effect on the daily accumulated noise exposure levels and that the PAR estimates of the proposed estimation method can be used to observe the hearing protection level *in situ*. In conclusion, the proposed method is of low-complexity and removes WID events from the residual noise level calculated over a day, which in turn gives more accurate information on the real effects of ambient noise exposure on hearing health.

Chapter 5 - In Situ Otoacoustic Emission Monitoring to Assess the Effects of Noise Exposure on Hearing Health (peer-reviewed article 3)

This chapter consists in an article submitted for review to the *Annals of Work Exposures and Health* journal in November 2019. To fulfill the third objective of this doctoral research, this article presents the proposed continuous hearing health and noise exposure monitoring approach to see which noise metrics and individuals' information are important predictors for the onset

of NIHL. An overview of the limitations of current hearing conservation programs to reduce NIHL is presented in the introduction. Then, the approach to monitor hearing health changes through short-interval otoacoustic emission measurements is detailed. Such approach was tested in-field on workers with moderate-exposure levels in their industrial working environment. The OAE results are analyzed using multilevel models with various predictors such as noise exposure levels, kurtosis, crest factor and frequency spectrum balance to find the most significant predictors of NIHL. This study shows that moderate levels of impulsive noise exposure can have detrimental effects on individuals' cochlear mechanisms and most damages are found at high frequencies. In conclusion, it is recommended that hearing conservation programs start to consider integrating the measurements of noise impulsiveness and spectral balance metrics in the workplace to mitigate the risks of NIHL.

Chapter 6 - Experimental results: permanent hearing health changes

In this chapter, the results of the longer-term effects of noise on hearing health evaluated with contralateral acoustic stimulation OAE measurements are presented. The reduction in otoacoustic emission suppression effect and the permanent DPOAE shifts suggest that males exposed to noise are more at risk of permanent hearing health changes.

Chapter 7 - Summary and Outcomes

This last chapter first summarizes the main findings of the doctoral project with their limitations and recommendations for future research. The potential scientific, technological and occupational health and safety outcomes of this project are then presented.

CHAPTER 1

LITERATURE REVIEW

Despite the efforts in hearing conservation programs, NIHL remains a major occupational problem in North America due to excessive noise exposure in the workplace. It is therefore important to conduct a stricter follow-up of the worker's hearing health by using, for example, OAE measurements to detect small changes in outer hair cells (OHC) activity which are a good indicator of the sensorineural hearing health.

To explain how noise affects the auditory system, this literature review covers the epidemiology of NIHL in Section 1.1, followed by noise exposure assessment in Section 1.2 and ways to monitor the effects of this noise on hearing health in Section 1.3. Several longitudinal studies have already found a relationship between noise exposure and changes in hearing health and are shown in Section 1.4. However, additional work is needed to understand the underlying hearing mechanisms that explain the onset of permanent damage. Finally, in order to find the most significant predictors of NIHL, an overview of statistical methods used for the analysis of hearing status changes is presented in Section 1.5.

1.1 Epidemiology

While there can be several causes to hearing loss such as ototoxic drugs, severe ear infections and genetics, studies show that aging (Gates, G. A., Mills, D., Nam, B.-h., D'Agostino, R. & Rubel, E. W., 2002; Huang, Q. & Tang, J., 2010) and noise (Eleftheriou, P. C., 2002; Thiery, L. & Meyer-Bisch, C., 1988) are important risk factors in the onset of permanent hearing loss. These risk factors are especially important in industrial environments, where there is an 11.5% risk of developing hearing loss for a highly screened male population of 50 years of age due to average daily noise exposure levels of $L_{\mathrm{ex,\,8h}}$ = 90 dB for 30 years. This risk is increased to 18% when combined with the effects of aging (ISO, 2013). This age-related hearing loss, also known as presbycusis, is a multifactorial process that varies in severity from mild to substantial. The symptoms of the disorder are reduced hearing sensitivity and speech understanding in noisy

environments, slowed central processing of acoustic information, and impaired localization of sound sources. These symptoms occur due to peripheral (i.e. the cochlea) and central auditory pathways that are affected over time. The communication issues related to presbycusis contribute to isolation, depression, and possibly dementia (Gates & Mills, 2005). To alleviate the symptoms, hearing aids are a widely available solution for mild presbycusis, and cochlear implants can be used for severe hearing loss. However, the elderly have difficulty to accept these solutions because of the stigma around hearing aids and their cost (Gates & Mills, 2005).

Despite the effects of aging, recent studies show that noise exposure is the main risk factor and it is actually the effects of noise exposure at a young age that are aggravated over time. Hence, age on its own is not the first cause of hearing loss (Fernandez, K. A., Jeffers, P. W., Lall, K., Liberman, M. C. & Kujawa, S. G., 2015; Kujawa, S. G. & Liberman, M. C., 2006; Liberman, M. C. & Kujawa, S. G., 2017; Xiong, M., Yang, C., Lai, H. & Wang, J., 2014). Nowadays, the risk of developing NIHL is still present although hearing conservation programs are integrated in the workplace and noise dosimeters are available. This risk can be explained by the recommended exposure limit (REL) considered hazardous for hearing damages which is set at 85 dBA with a 3 dB exchange rate for an 8-hour work day in most North American noise regulations as suggested by the National Institute for Occupational Safety and Health (NIOSH) (NIOSH, 2019), whereas the Occupational Safety and Health Administration (OSHA) sets the permissible exposure limit (PEL) at 90 dBA with a 5 dB exchange rate (OSHA, 2019a). The action level, that is the noise level at which employers must take steps to monitor and limit noise exposure, is usually set at half the PEL (OSHA, 2019b). These limits are based on a population average in which there is a great diversity in each individual's response to a noise dose and are calculated with statistical tools such as linear models (NIOSH, 1998; Rabinowitz, P. M., Galusha, D., Dixon-Ernst, C., Clougherty, J. E. & Neitzel, R. L., 2013). These statistics are sometimes based on a protected population using hearing protection devices for example (Rabinowitz *et al.*, 2013). In which case the efficiency of the protection (Berger, E. H., Franks, J. R., Behar, A., Casali, J. G., Dixon-Ernst, C., Kieper, R. W., Merry, C. J., Mozo, B. T., Nixon, C. W., Ohlin, D. et al., 1998; Groenewold *et al.*, 2014; HSE, 2019a; Smith *et al.*, 2014) comes into play and could

alter the effective noise dose, thus increasing the risk of NIHL. This PEL is usually the same for all individuals and does not consider the differences in individuals' susceptibility. This level could therefore be accurate for some individuals and inaccurate for others. Although there is still a risk of hearing damage with noise exposure levels below the PEL (Bharadwaj *et al.*, 2015; Maison *et al.*, 2013), some long-term studies were not able to find a direct relationship between noise levels below 85 dBA and pure-tone audiometry hearing threshold shift (Prince, M. M., Stayner, L. T., Smith, R. J. & Gilbert, S. J., 1997; Rabinowitz *et al.*, 2013). Hence, there are possibly other noise characteristics that explain this remaining risk to suffer from NIHL (ISO, 2013) with current hearing conservation programs. Other possible reasons for this remaining risk could be that hearing assessment is conducted on too long intervals or that the hearing tests are not sensitive enough.

Amongst the possible noise characteristics that could possibly explain the remaining risk of NIHL, the temporal fluctuations in noise levels could be an important factor. The short peaks in noise level define the impulsiveness of the noise. For example, a Gaussian noise has minimal impulsiveness whereas industrial noise has many fluctuations in noise levels due to impacts and sudden start of machinery, therefore more impulsiveness. An impulsive noise may have different effects (Davis *et al.*, 2012; Lutman, M. E., Davis, A. C. & Ferguson, M. A., 2008; Qiu, W., Hamernik, R. P. & Davis, R. I., 2013) on the various hearing mechanisms involved (Lutman *et al.*, 2008). It also has more risk of inducing hearing loss than Gaussian noise as confirmed by Thiery & Meyer-Bisch (1988)'s and Davis *et al.* (2012)'s studies.

To further reduce the risk of developing NIHL, an individualized PEL could be based on the temporary effects of immediate noise exposure on the cochlea's hair cell response for each worker's ears, such as the method suggested by Czyżewski, A., Kotus, J. & Kostek, B. (2007). This would allow to limit the exposure duration to minimize the worker's risk of NIHL. The temporary effects of noise exposure on hearing can be monitored by simultaneously recording noise levels and otoacoustic emission measurements to observe the instant feedback from outer hair cells' health.

1.2 Noise exposure

1.2.1 Measurement

Noise is measured as an acoustic pressure with a microphone, also known as sound pressure level (SPL) and expressed on a logarithmic scale in decibels (dB). The recorded sound waveforms are first A-weighted with a filter, to mimic the perception of loudness of pure tones by human hearing (Berger, E. H., 2003), and then summed and converted in dB. The SPL can be measured each second, or on a smaller interval. However, instantaneous SPLs are not useful to describe an individual's noise exposure (Berger, 2003). Average levels over a longer duration ($L_{\text{eq, T}}$) on the other hand give more information on an individual's cumulative noise exposure level. The A-weighted equivalent sound level $L_{\text{Aeq, T}}$ can be calculated on the cumulative noise duration T as follows:

$$L_{\text{Aeq, T}} = \frac{b}{\log(2)} \log \left[\frac{1}{T} \sum_{i=1}^{m} T_i 10^{\frac{\log(2)}{b} L_{Ai}} \right], \tag{1.1}$$

where L_{Ai} is the A-weighted noise level measured over each i^{th} duration T_i and b is the exchange rate. An exchange rate of b=3 dB for example means that when the noise level is increased by 3 dBA, the amount of time an individual can be exposed to a certain noise level to receive the same dose is cut in half.

The $L_{\text{Aeq, T}}$, can also be normalized over 8 hours $L_{\text{Aeq, 8h}}$ with a pre-defined exchange rate of either 3 or 5 dB (Berger, 2003), according to local noise regulations. This cumulative level makes it easier to compare individuals with different noise exposure duration and levels, as this equivalent level is calculated on the same time base. The $L_{\text{Aeq, 8h}}$ is also used to calculate the noise dose (%) received by an individual compared to the maximum permissible by the local noise regulations. The L_{ex} can be calculated on the effective duration of the noise exposure and is usually reported on a 8-hour work day. For example, a 4-hour noise exposure $L_{\text{eq, 4h}}$ = 76 dBA would be equivalent to an $L_{\text{ex, 8h}}$ = 76 dBA + (-3) = 73 dBA, considering a 3 dB exchange rate.

To find the relationship between noise exposure levels and auditory fatigue it is preferable to use $L_{\text{Aeq, T}}$ since it is calculated on the effective noise duration. Hence, it is easier to correlate with changes in hearing health as presented in Chapter 5.

1.2.2 Instrumentation

Many devices available on the market can measure noise exposure levels such as: sound level meters, integrating sound level meters and noise dosimeters. Sound level meters record the instantaneous sound levels with a slow response setting at the position of the worker's head, without the worker's head presence. Therefore this type of device does not take into account the impact of the body on the acoustical field. It is accurate for steady noise exposure levels, without impulsive noise content. On the other hand, the integrating sound level meters directly calculate the equivalent sound level L_{eq} over a set period with faster response and can also calculate the C-Weighted peak sound pressure. Therefore they are more accurate in impulsive noise environments. Noise dosimeters are designed to be worn close to the worker's ear, generally with the noise dosimeter's microphone being positioned on the shoulder. Conventional dosimeters therefore measure the free-field noise exposure. When the microphone is positioned at other locations like on the chest for example, it can lead to important errors in the $L_{\text{Aeq, T}}$ (Byrne, D. & Reeves, E., 2008).

To improve NIHL risk assessment, the noise levels should be measured in the earcanal with in-ear noise dosimeters (IEND) (Bonnet, F., 2019; Rabinowitz *et al.*, 2013). Assuming that the risk of NIHL is related to the sound pressure levels at the eardrum, an IEND is a promising approach to continuously monitor an individual's actual noise exposure inside the ear and accurately estimate the SPL that reaches the inner ear. However, IENDs currently available do not allow the direct measurement of SPLs at the eardrum position. Consequently, a microphone to eardrum correction should be included to estimate the $L_{\text{Aeq, T}}$ at the eardrum position.

Besides, the Wearer-Induced Disturbances (WIDs) which are sounds generated by the user such as speech and heartbeats, are also captured by the noise dosimeter's microphone and

contribute to the worker's noise dose. These contributions to the $L_{\text{Aeq, T}}$ may not contribute to the hearing fatigue due to middle-ear mechanisms which protect the inner-ear (Borgh, M., Lindström, F., Waye, K. P. & Claesson, I., 2008; Mukerji, S., Windsor, A. M. & Lee, D. J., 2010), such as the stapedial reflex involved during speech for example. An option to remove these WID contributions from the $L_{\text{Aeq, T}}$ should be included in the next generation of IENDs to find a stronger relationship between noise levels and its induced auditory fatigue. A WID rejection approach using an adaptive filter is suggested and compared to a reference method from the literature (Bonnet, F., Nélisse, H. & Nogarolli, M. A. C., 2019b) in Chapter 4.

1.2.3 Additional noise metrics

Previous studies have demonstrated that various noise characteristics, such as impulsiveness and frequency spectrum (Davis *et al.*, 2012; Qiu *et al.*, 2013; Starck, J., Toppila, E., Pyykko, I. et al., 2003; Vinck, B. M., Van Cauwenberge, P. B., Leroy, L. & Corthals, P., 1999), can have different effects on the auditory system's health. For example, an impulsive noise may induce more hearing damage than a Gaussian noise for the same energy level (Davis *et al.*, 2012; Qiu *et al.*, 2013; Starck *et al.*, 2003). When the noise impulsiveness is taken into account in NIHL risk assessment, it improves the accuracy of the risk estimate (Goley, G. S., Song, W. J. & Kim, J. H., 2011). The noise's frequency spectrum, temporal fluctuations and 8-hour equivalent levels should therefore be analyzed as separate risk factors.

The frequency spectrum of the ambient noise can be analyzed using the difference expressed in dB between the C- and A-weighted overall sound pressure levels, this metric is referred to as the spectral balance (ANSI, 2007; Nélisse *et al.*, 2011). This metric is important considering that threshold shifts and other changes in hearing health are maximal about 1/2-octave above the frequency range with most energy of the noise (Cody, A. & Johnstone, B., 1981; Kujawa, S. G. & Liberman, M. C., 2009; Maison *et al.*, 2013; Rabinowitz *et al.*, 2013).

Temporal fluctuations of the noise can be estimated on a time interval (Δt) as three different metrics: 1) the dynamic range, 2) crest factor and 3) kurtosis. The dynamic range is simply

the difference between the lowest and highest noise levels. The crest factor is an estimate of noise signal impulsiveness, it is calculated as the ratio of the peak magnitude on the root-mean square (RMS) average (Starck *et al.*, 2003). The kurtosis ($\beta(t)$) is defined as the ratio of the fourth-order central moment on the squared second-order moment of the amplitude distribution (Davis *et al.*, 2012; Qiu *et al.*, 2013). It is a metric used to quantify the normality (e.g. Gaussian noises) or non-normality (speech, impulse/impact noise, and complex noises) of noise signals. For normal noise signal distributions $\beta(t) = 3$, whereas distributions that have more outliers have a $\beta(t) \geq 3$ (Davis *et al.*, 2012). Non-normal signals such as complex noises consist of combinations of impact and continuous Gaussian noise , therefore they are non-Gaussian. All variables that characterize a non-Gaussian noise e.g. transient peaks, inter-transient intervals, transient duration and crest factor have different effects on the kurtosis value (Davis *et al.*, 2012). The kurtosis and crest factor metrics assessed on *in situ* measurements are presented in Chapter 4 & 5.

Although all these noise metrics are available through audio recording, they are not sufficient to estimate accurately an individual's actual risk of developing NIHL due to his own susceptibility, the effects of aging (Kujawa & Liberman, 2006) and other factors. Therefore the noise metrics presented should be measured simultaneously with objective hearing tests , such as otoacoustic emission measurements, to ensure proper NIHL risk assessment. Such approach should prevent permanent hearing damage by detecting early signs of temporary changes in hearing health and taking appropriate actions to minimize exposure.

1.3 Hearing health

1.3.1 Physiology of hearing

The cochlea consists in a basilar membrane where miniature cells, called hair cells, move with mechanical (acoustical) stimulation. When the inner hair cells (IHC) are in motion, the signal of this movement is transmitted to the brain as an electrical nerve signal by the auditory nerve. The signal captured by the inner hair cells is analyzed by the auditory cortex and the brain

continuously adapts the input level by sending a signal back through a feedback loop known as the efferent system, as shown in red in Fig. 1.8. This signal travels towards the outer hair cells to control the rigidity of the basilar membrane and decrease or increase the level of the electrical nerve signal transmitted to the brain (Purves, D., 2004). This feedback mechanism helps to reduce the intensity level of the electrical nerve signal for high sound pressure levels. On the other hand, it increases the electrical nerve signal intensity for low sound pressure levels (Purves, 2004). Using such a feedback mechanism, the cochlea acts as an amplifier and compressor depending on the sound pressure level transmitted in the ear and otoacoustic emissions are low intensity sounds generated by this cochlear amplifier in a normal process of a healthy auditory system. The cochlea's inner and outer hair cells are organized to respond to different frequencies from the base (high frequencies) to the apex (low frequencies) of the scala vestibuli. This organization is the cochlea's tonotopy.

Damage to OHCs modifies the amplification of the signal captured at the IHCs and hence change hearing thresholds. These thresholds are a basic evaluation of an individual's hearing status and correspond to the lowest acoustic sound pressure levels to which the individuals respond for a certain number of repetitions (Katz, J., Medwetsky, L., Burkard, R. & Hood, L., 2009). In turn, these cochlear changes reduce the intensity of the nerve signal transmitted to the auditory cortex for low sound pressure levels and can increase the intensity of high sound pressure levels. This phenomenon is referred to as recruitment. The damage to OHCs also reduces the otoacoustic emission levels.

Excessive noise exposures can cause a temporary threshold shift (TTS), also referred to as temporary hearing loss. TTS results from fatigued OHC and usually disappears in the time following the noise exposure (Müller, J. & Janssen, T., 2008). Repetitive noise exposure can gradually induce irreversible damage to the cochlear sensory cells in the long term and result in permanent threshold shift (PTS) (Müller & Janssen, 2008). PTS can also be accompanied by larger auditory filters critical frequency bands. Enlarging the bandwidth of the auditory filters can hinder speech intelligibility due to the difficulty to discriminate the frequencies (Lutman *et al.*, 2008). Hearing loss can also lead to difficulties hearing low sound pressure levels and

can eventually lead to severe consequences like deafness, communication problems, increase in stress levels, psychological problems, etc (Gates & Mills, 2005).

Hidden Hearing Loss

Scientists have assumed for decades that outer hair cell damage was the primary indicator of noise-induced hearing loss (Bramhall, N. F., Konrad-Martin, D., McMillan, G. P. & Griest, S. E., 2017; Kujawa & Liberman, 2009; Le Prell, C. G., 2019; Lin, H. W., Furman, A. C., Kujawa, S. G. & Liberman, M. C., 2011). They also thought that moderate-level noise exposures were benign since they did not cause permanent changes in otoacoustic emission levels nor hearing thresholds (Bharadwaj *et al.*, 2015; Bramhall, N., Beach, E. F., Epp, B., Le Prell, C. G., Lopez-Poveda, E. A., Plack, C. J., Schaette, R., Verhulst, S. & Canlon, B., 2019; Themann, C. L. & Masterson, E. A., 2019). However, recent studies with animal models (Kujawa & Liberman, 2009) have shown that such exposures can cause irreversible damage to IHC-synapses and the auditory nerve. These damages were undetectable prior to advances in immunostaining and microscopy technologies. This undetectable change in hearing health was therefore called "hidden" hearing loss (HHL) by Schaette & McAlpine (2011). However, this change in hearing health is 1) no longer hidden, and 2) it does not result in a permanent hearing loss on the audiogram, details of these statements are explained below:

1) The time gap between permanent changes in outer hair cells, i.e. within hours, and Spiral Ganglion Cells (SGC), i.e. several weeks, is so large that researchers assumed they were not related (Liberman & Kujawa, 2017; Liberman, 2016). As a result, it was assumed that the temporary changes in outer hair cells had no impact on the auditory system in the long-term since it would not show up ("hidden") in audiometric thresholds measured in quiet conditions. Thus, there was a delayed change in hearing health at the SGC, but researchers thought it was not related. However with the latest advances in auditory research, these changes are visible earlier. Therefore, moderate noise levels which were assumed inoffensive in the past could potentially lead to irreversible damages to hearing health (Maison *et al.*, 2013).

2) Hearing loss is a term used to describe the elevation of hearing thresholds measured with classic audiometry in controlled/quiet conditions. A permanent elevation of HTLs indicates damages in OHC and IHC (Furman, A. C., Kujawa, S. G. & Liberman, M. C., 2013; Liberman, 2016). In the case of hidden hearing loss, these HTLs return to normal in the short term and the damages to auditory nerve fibres and IHC-synapses are only observed with speech intelligibility tests in noise (Kujawa & Liberman, 2015; Liberman, 2016).

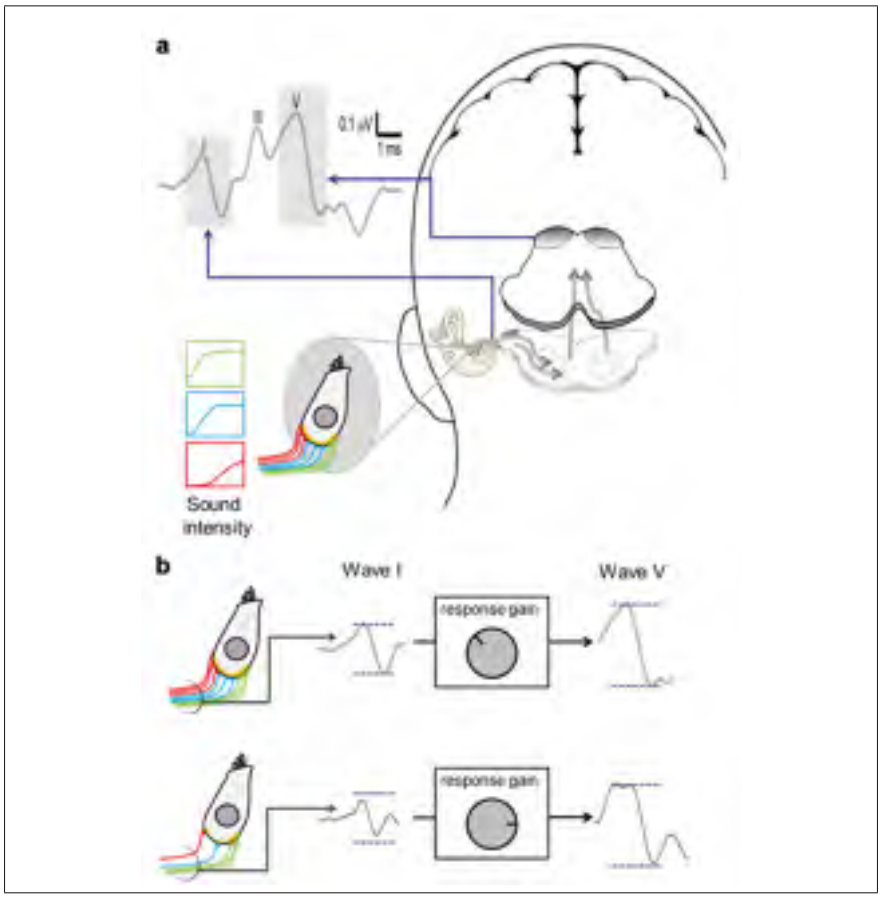

Figure 1.1 Illustration of a) auditory brainstem responses in relation to hidden hearing loss and b) the homeostatic gain control from the auditory system. The different auditory nerve fibres are illustrated in green for low, blue for medium and red for high-threshold. The IHC-synapses are visible in yellow. The action of the homeostatic gain control to normalize the Wave V signal when auditory nerve fibres and synapses are damaged is detailed in b). Reproduced from Schaette & McAlpine (2011)

According to recent studies (Kujawa & Liberman, 2009; Lin *et al.*, 2011), short duration - high level or long duration - moderate level noise exposure can permanently damage the auditory nerve fibres and IHC-synapses. These damages are usually followed by a slower degeneration of the SGC in the following months to years (Kujawa & Liberman, 2009). Hence, age-related hearing loss might be explained by noise-induced damages in IHC-synapses at a young age, that degenerated with aging (Fernandez *et al.*, 2015; Kujawa & Liberman, 2006; Sergeyenko, Y., Lall, K., Liberman, M. C. & Kujawa, S. G., 2013).

Auditory nerve fibres are classified by their spontaneous firing rate and threshold, mainly : low spontaneous rate (LSR) - high threshold fibres and high spontaneous rate (HSR) - low threshold fibres (Bramhall *et al.*, 2017). As shown in Furman *et al.* (2013)'s study, LSR fibres are more susceptible to noise exposure than HSR fibres. Damage to LSR - high threshold fibres result in a difficulty to hear in high ambient noise levels. However, HTLs are not affected in quiet conditions since HSR-low threshold fibres remain healthy. This explains why the audiogram leads to the conclusion of a normal hearing although there is a hidden injury.

Similarly to the slow degeneration of SGC, there is a delayed damage to OHC (Fernandez *et al.*, 2015) and IHC (Bohne, B. A., Kimlinger, M. & Harding, G. W., 2017) caused by previous synaptopathic noise. In mice, although temporary changes in OHC are observable within 24 hours with DPOAE growth functions (see Section 1.3.2.2.2 for description), the permanent changes in OAEs are not synchronized with the changes in synapse counts since OHC damage usually appears later (Fernandez *et al.*, 2015). This supports the hypothesis that noise exposure induces a progressive injury to OHC. These cells seem to have a limited injury/recovery life cycle. After a number of recovery cycles either after a long duration noise exposure, or several short duration noise exposures, the OHC would die due to mechanisms such as oxidation, apoptosis or necrosis. This cycle is also seen for synaptopathy, where non-synaptopathic noise exposure (2h to 91 dB(SPL)) becomes synaptopathic with longer duration (8h to 91 dB(SPL)) (Fernandez *et al.*, 2015; Maison *et al.*, 2013). An effect similar to duration can be observed with intensity of noise levels, when comparing moderate noise levels exposures to high noise levels exposures (Fernandez *et al.*, 2015; Maison *et al.*, 2013; Sergeyenko *et al.*, 2013). However, the lifespan

under noise exposure of the IHC-synapses, for which the damages are visible within 24 hours (Furman *et al.*, 2013), and LSR-high threshold auditory nerve fibres seem to be much shorter than for OHC and SGC which can be up to several months to years past the traumatic noise exposure (Kujawa & Liberman, 2009; Lin *et al.*, 2011). Sergeyenko *et al.* (2013) showed that, in mice, the process of age-related hearing loss starts with the death of IHC-synapse ribbons followed by SGC and then with a drastic change in OHC. The progress of the loss in mice is similar as in humans when the age is normalized to a percentage of the total lifespan (Sergeyenko *et al.*, 2013).

When the auditory nerve fibres and IHC-synapses are damaged, the signal transmitted to the central auditory system is reduced. To stabilize mean neuronal activity, homeostatic plasticity generates increased excitatory gain and reduced inhibitory gain in neurons downstream of the auditory nerve. This restores average neuronal activity to normal levels, as shown in Fig. 1.1. When neurons become more active from the feedback of the homeostatic gain, their spontaneous activity is amplified which leads to hyperactivity. This could potentially explain the generation of tinnitus (Schaette & McAlpine, 2011).

1.3.2 Hearing health assessment

1.3.2.1 Audiometry

To monitor hearing loss, current hearing conservation programs use classic tonal audiometry tests. These tests determine the individual's hearing threshold level (HTL), indicated in dB(HL), by sending pure tones at different acoustic sound pressure levels for 1 to 2 seconds per level (for non-automatic tonal audiometry) (Katz *et al.*, 2009). The HTL corresponds to a specific sound pressure level (SPL) in function of the tested frequency that is based on isophonic curves (ISO226). For example, 0 dB(HL) corresponds to 40 dB(SPL) at 1000 Hz. The isophonic curves were established based on several large-scale studies on a normally hearing population of young adults (Katz *et al.*, 2009).

In general, the test starts either by a stimulus with a level below the normal auditory threshold or by a stimulus with a level over the threshold, so that the person can get familiar with the stimulus (Katz *et al.*, 2009). Hence, the test generally starts with a stimulus of 30 dB(HL) at 1000 Hz. The vast majority of individuals without any major hearing loss should be able to respond to this tone. Hearing thresholds are normally tested using an Up-Down method, such as the Hughson-Westlake method, or a variant of this method (AudSim, 2019; Katz *et al.*, 2009). The audiologist starts with the 30 dB(HL) stimulus, and when the subject responds to the stimulus, the next stimulus will be sent with a -10 dB(HL) step until the subject does not respond anymore. After a few missing responses, the audiologist increases the stimulus level by a step of +5 dB(HL) until the subject responds back again. This method is repeated until a pattern is observed, then the threshold is calculated (Katz *et al.*, 2009). This procedure is repeated for every tested frequency, usually sweeping the octave or 1/2-octave bands from 125 to 8000 Hz to evaluate the functionality of the complete auditory path in one test(Katz *et al.*, 2009). Audiometric frequencies with most changes over time can give information on the type of hearing loss and on the affected region in the auditory system. It also gives information on the severity of the hearing loss (Katz *et al.*, 2009).

However, these audiometric tests have many disadvantages such as the duration of the measurement. It is also a subjective test, therefore individuals can respond differently depending on when they are focused. The noise-induced changes in subjective sensation measured by auditory thresholds may also occur later and therefore might not be immediately detectable after a short noise exposure (Müller & Janssen, 2008) , contrary to OAE levels which can change within a few minutes post-exposure. On the other hand, according to Vinck *et al.* (1999)'s study pure-tone audiometry thresholds recovered to their pre-exposure values faster than OAEs. This suggests that OAEs are more sensitive to measure subtle changes in hearing status (Lutman *et al.*, 2008; Sliwinska-Kowalska, M., Kotylo, P. et al., 2001) since, depending on the moment of the measurement, the changes in HTLs might have already recovered and therefore remain undetected. Hence, it is difficult to identify the exact cause of hearing loss, which may be temporary, due to the variable lag between noise exposure and its effects on HTLs. In addition,

audiometric tests are usually conducted on too long time intervals which makes it even harder to track back the origin of the damage. The long intervals also make it difficult to take actions (hearing protection, reducing noise exposure or using noise control at the source for example) to efficiently prevent permanent hearing loss. Classic audiometry equipment can also be bulky and cannot be worn continuously by workers. Hence, it is not a practical solution to closely monitor an individual's hearing health. Other hearing tests, such as otoacoustic emissions, must therefore be considered for *in situ* hearing assessment.

1.3.2.2 Otoacoustic emission measurements

OAEs can be measured with a sensitive microphone positioned in the outer earcanal, as shown for the first time by David Kemp in 1978 (Whitehead, M., Stagner, B., Lonsbury-Martin, B. L. & Martin, G. K., 1994). For clinical applications OAEs can be evoked with a click (Transient-evoked OAE, TEOAE), the OAE response frequency can be calculated based on the spectrum of the stimulus signal (Whitehead *et al.*, 1994), or with two pure-tone acoustic stimulation signals at frequencies f_1 and f_2 (distortion product OAE, DPOAE). Otoacoustic emissions can also be generated spontaneously by the cochlea (Moulin, A., 2000b) without any acoustical stimuli. However, the latter is not present in all individuals and is sporadic, therefore hard to measure. The pure-tone stimulation signals are transmitted in the earcanal with miniature loudspeakers as illustrated in Figure 1.2. After the acoustic stimuli signals went through the external ear, the tympanic membrane transmits the vibrations to the cochlea by the ossicles. The cochlea then amplifies the sounds to send them to the brain by the auditory nerve. The f_1 and f_2 stimuli are amplified/compressed by the non-linear cochlear amplification process and result in distortion products, i.e. the otoacoustic emissions, which are captured by the in-ear microphone (IEM). The distortion product frequencies are at $f_{dp} = [2f_1 - f_2, 2f_2 - f_1, 3f_1 - 2f_2, 3f_2 - 2f_1, 4f_1 - 3f_2,...]$, however, like other kinds of distortion products most of the energy is concentrated mainly in the first distortion product, that is $f_{dp} = 2f_1 - f_2$ (Probst, R., Lonsbury-Martin, B. L. & Martin, G. K., 1991; Tracy, S., 2001; Whitehead *et al.*, 1994). The amplification process also controls the DPOAE level output in function of the input stimuli levels

L_1 and L_2 (Sutton *et al.*, 1994). Excessive noise exposure can result in damages in cochlear mechanics and alter this DPOAE input/output function, also known as DPOAE growth function. This type of DPOAE measurement is further described in Section 1.3.2.2.2.

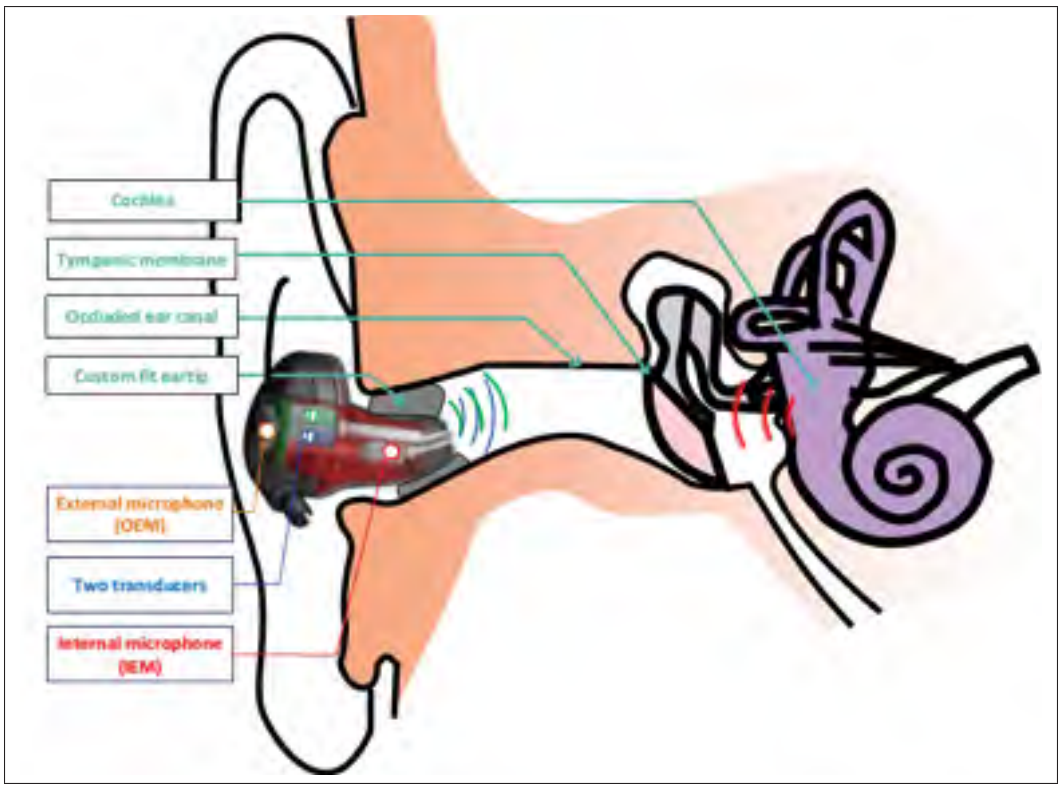

Figure 1.2 Illustration of a distortion product otoacoustic emission stimulation with the two transducers and recording with the internal microphone

Current literature shows that a $f_2/f_1 = 1.22$ ratio between the two stimuli frequency gives an optimal DPOAE level for the majority of the frequency spectrum, but a variable ratio depending on the tested f_2 frequency can give better results according to Moulin, A. (2000a). By their nature, DPOAEs are specific to the stimuli frequencies and therefore they characterize a specific region in the cochlea's tonotopic organization. It is therefore easier to establish a relationship between hearing loss in a specific cochlear region with DPOAE levels than with TEOAE levels. DPOAEs are therefore generally preferred to detect changes in hearing status.

Otoacoustic emissions generally have low sound pressure levels, hence it is difficult to capture them when the noise level in the IEM signal is too high. It is therefore important to set the stimuli parameters to obtain the highest DPOAE level possible, without saturating the cochlear gain, and measure them above the noise floor. The recommended stimuli parameters are therefore L_1 at 65 dB(SPL) for first stimulus (f_1) and L_2 at 55 dB(SPL) for the second stimulus (f_2). These sound pressure levels normally give higher OAE levels compared to other combinations of stimuli sound pressure levels. They were established empirically based on different combinations of levels tested in the literature (Hauser, R. & Probst, R., 1991). According to Sutton *et al.* (1994), specific stimuli levels can maximize the differences in pre- and post-exposure DPOAE levels.

Equilevel and unequal-level stimuli primary tones can produce DPOAEs with similar amplitudes, but unequal-level stimuli DPOAE amplitudes are more affected by noise exposure. This phenomenon can be explained by the excitation patterns evoked by the primary tones which generate a maximal DPOAE response when the two traveling-wave displacement envelopes are equal in magnitude at the overlap location on the basilar membrane (Sutton *et al.*, 1994). This requires an L_2 primary tone level smaller than the L_1 primary tone level, since the f_2 tone is restricted to the tail region of the f_1 tone which is located more towards the apex (low frequencies). The primary tone level $L_1 \neq L_2$ pattern is particularly valid for the sharp excitation envelopes produced by the low level primary tones because the f_2 tone has its maximum amplitude at the overlap location (Sutton *et al.*, 1994). On the other hand, when $L_1 = L_2$, the f_1 tone has a much lower amplitude at the point of maximal overlap compared to f_2 and the equal-amplitude displacement criterion is no longer satisfied.

For higher level primary tones, the $L_1 = L_2$ condition produces DPOAEs of essentially same amplitude as the $L_2 \neq L_1$ condition, because the resulting increased amplitude of the f_2 tone relative to the f_1 tone is beyond the criterion needed to produce maximal DPOAE levels (Sutton *et al.*, 1994). The phenomenon can be further explained by the saturating non-linearity of the cochlear amplifier which generates the DPOAEs since it acts as a compressor when stimuli levels make it saturate, as explained previously in Section 1.3.1. Therefore, for high $L_1 = L_2$

primary tones, the f_2 tone has a substantially larger amplitude at the maximal overlap location and would be closer to the saturation range of the cochlear amplifier than when $L_2 < L_1$ (Sutton *et al.*, 1994). When the f_2 tone is low and therefore the cochlea is operating in the non-saturating range, it is expected that a slight noise-induced cochlear damage would substantially reduce the excitation pattern of f_2 (Sutton *et al.*, 1994) and as a consequence reduce the DPOAE amplitude.

The maximal sensitivity of noise-induced DPOAE shifts are obtained with 55/30 dB primary tone levels (optimal ratio of 1.83) (Sutton *et al.*, 1994). However, such low stimuli levels may generate very low DPOAE levels which may be difficult to measure in higher noise levels for in-field DPOAE monitoring.

Based on Sutton *et al.* (1994)'s study, using equal magnitude stimuli (stimuli ratio = 1) to generate DPOAEs leads to the smallest difference in DPOAE changes. Therefore, primary tone levels of 65/55 dB(SPL) (ratio of 1.18), is a good compromise for the purpose of the current project since it should produce relatively high DPOAE levels to measure them above the noise floor. Plus, the DPOAE shifts should be significant enough between pre- and post-exposure as well as during exposure. It is not recommended to adapt the stimuli ratio between the pre-exposure measurement and following measurements since it would induce an additional bias in the measurements, obviously making the DPOAE levels follow this change in stimuli levels. The selected stimuli levels must be calibrated in the earcanal for accurate DPOAE level measurements, such calibration method is presented in detail in Section 1.3.2.2.1.

1.3.2.2.1 DPOAE probe fit and stimuli calibration procedures

Probe fit Manufacturers of otoacoustic emission measurement systems usually do not provide much detail about their specific probe fit and calibration procedures. However, an early review of otoacoustic emission measurements provided by Kemp, D. T., Ryan, S. & Bray, P. (1990) reveals that a click stimulus is used in his OAE system (Otodynamics Ltd, 2019) to stimulate the ear and measure the earcanal's impulse and frequency responses. If too much ringing artifacts,

that is artifacts that appear as spurious signals near sharp transitions in a signal, is present in the impulse response the probe needs to be re-fit. A re-fit is also required when the frequency spectrum shows a sharp peak followed by a trough or if there is no low-frequency energy.

The EMAV manual(Neely, S. & Liu, Z., 1994) also describes a similar probe fit assessment procedure where it uses either a chirp or white noise to stimulate the ear. The measured response is then displayed as a waveform and spectrum, where a good fit is indicated by a flat frequency spectrum. A new approach for fit-testing using an adaptive filter to identify the earcanal frequency response is proposed in Section 2.2.1.

In-ear stimulus calibration All DPOAE systems include an in-ear calibration procedure to adjust the DPOAE stimuli signals to ensure their levels are the same at each discrete stimuli frequency based on the stimulus level parameter selected and minimize the variability in DPOAE levels between repeated measurements when the probe is re-fitted. According to the EMAV manual (Neely & Liu, 1994), the program presents two chirp signals in sequence, one for each stimuli (f_1 and f_2) loudspeaker. The program then calculates the voltage needed, as a correction factor, to produce the desired SPL at the IEM based on the chirp response calculated with a discrete Fourier transform, therefore accommodating for varying earcanal volumes (Interacoustics, 2019).

However, these in-ear stimulus calibration methods are susceptible to standing waves, which can change the SPL by up to 20 dB around 3 to 4 kHz (Charaziak, K. K. & Shera, C. A., 2017; Scheperle, R. A., Neely, S. T., Kopun, J. G. & Gorga, M. P., 2008; Siegel, J. H., 1994). To improve the accuracy of DPOAE measurements at higher frequencies, a more accurate calibration of the stimuli levels at the eardrum is needed. This can be achieved using the forward pressure level (FPL) calibration presented below.

Forward pressure level calibration The total sound pressure level measured at the IEM is composed of the forward pressure, which is the wave component that propagates away from the sound source, and the backwards traveling wave component reflected from the eardrum as shown in Fig. 1.3. Estimating the forward pressure component gives a personalized calibration of stimuli levels equivalent to measuring the sound pressure level at the eardrum position. This calibration reduces measurement errors due to the phase interference of the standing waves between the forward and reverse wave propagation in the earcanal (Scheperle, R. A., Goodman, S. S. & Neely, S. T., 2011). The FPL is determined from the microphone at the reference plane in the earcanal instead of at the eardrum position (see $\text{SPL}_{\text{terminal}}$ in Table 1.1 and Fig. 1.3), making the FPL calibration method less invasive than measuring with a probe microphone at the eardrum (Scheperle *et al.*, 2011).

Table 1.1 Definition of calibration method terms

$\text{SPL}_{\text{entrance}}$	is the sound pressure level measured at the reference plane in the earcanal or the entrance of the cavity measured with the earpiece in-ear microphone
$\text{SPL}_{\text{terminal}}$	is the sound pressure level measured with a microphone positioned directly at the closed end of a tube or at the eardrum position
FPL	Forward pressure level is an estimate of the emitted pressure level component of a sound source, discarding the reflected pressure level component

The first step to estimate the FPL component, is to calculate the Thevenin equivalent of the probe loudspeaker Z_s, shown in Fig. 1.4. This is achieved by using five metal tubes of known lengths for specific resonance frequencies with a hard termination at one end, these tubes are used as calibration cavities. An example of such a cavity set schematic is presented in Fig. 2.12 in Chapter 2. The sound pressure level is measured in each cavity, as shown in Fig. 1.5. For example in Cavity_1 pressure P_1 is measured.

The choice of the cavity lengths depends on the number of cavities and the probe's loudspeaker response. Ideally the cavity wavelengths are selected with minimal peak resonances and nulls

overlap between cavities to cover a maximum range of the loudspeaker frequency response (Scheperle *et al.*, 2011), as shown in Fig. 1.5.

The second step is to calculate the ideal expression for the cavity impedance Z_{c1} using Eq. 1.2 shown below (taken from Eq. 1 (Scheperle *et al.*, 2008)):

$$Z_c = -iZ_0\cot(kL), \tag{1.2}$$

where Z_0 is the characteristic impedance of a plane wave propagating in the tube, L is the cavity length and k is the wave number.

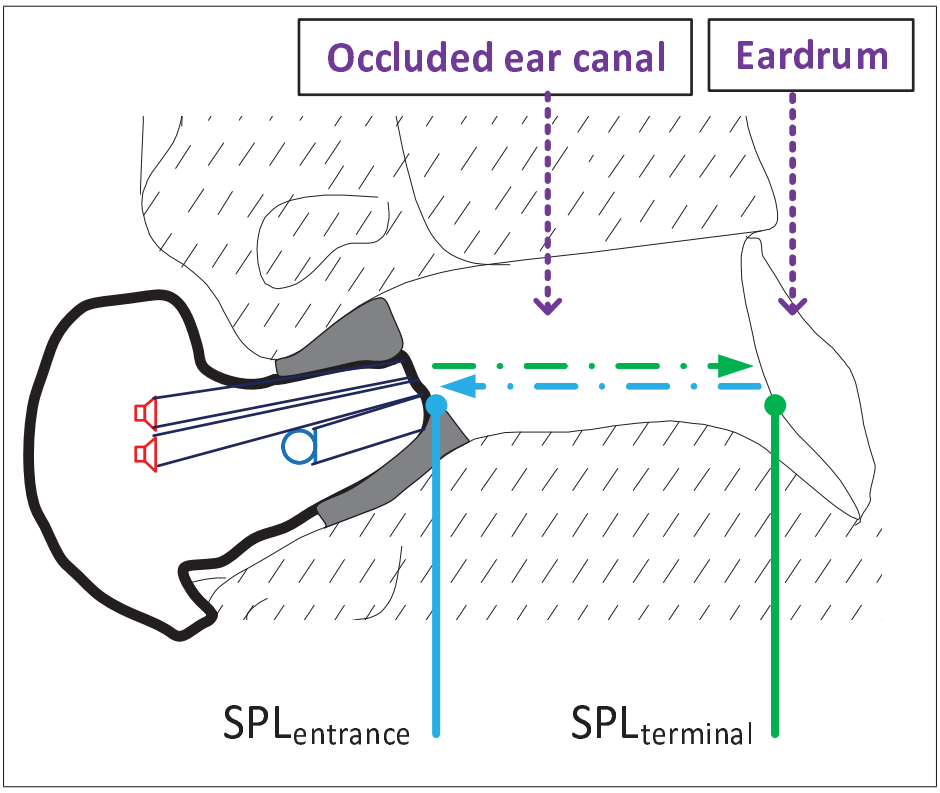

Figure 1.3 Schematic showing the locations for sound pressure levels $SPL_{entrance}$ at the tip of the DPOAE probe and $SPL_{terminal}$ at the eardrum position, the term definitions a presented in Table 1.1. The green arrow shows the forward pressure component and the blue arrow shows the reflected wave

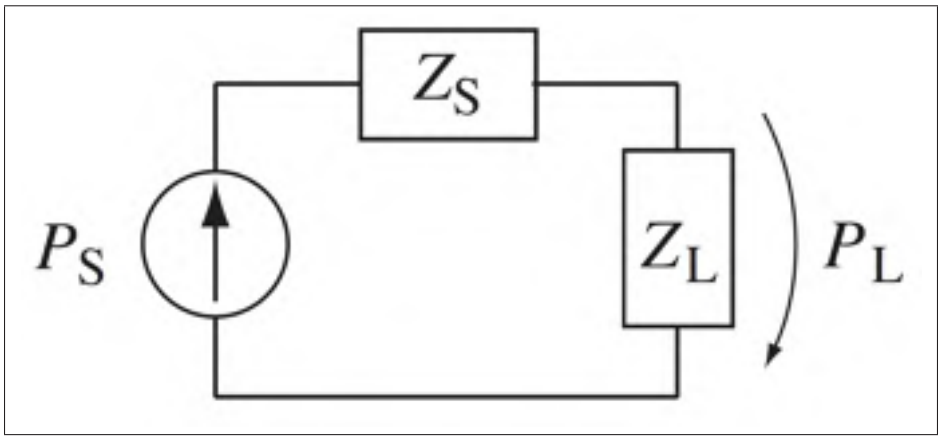

Figure 1.4 Acoustic Thevenin equivalent circuit for the probe loudspeaker (source) impedance Z_s in the earcanal (Z_l), where P_s is the voltage to sound pressure term for the source and P_l the load pressure response. Reproduced from Hiipakka & Tikander (2009)

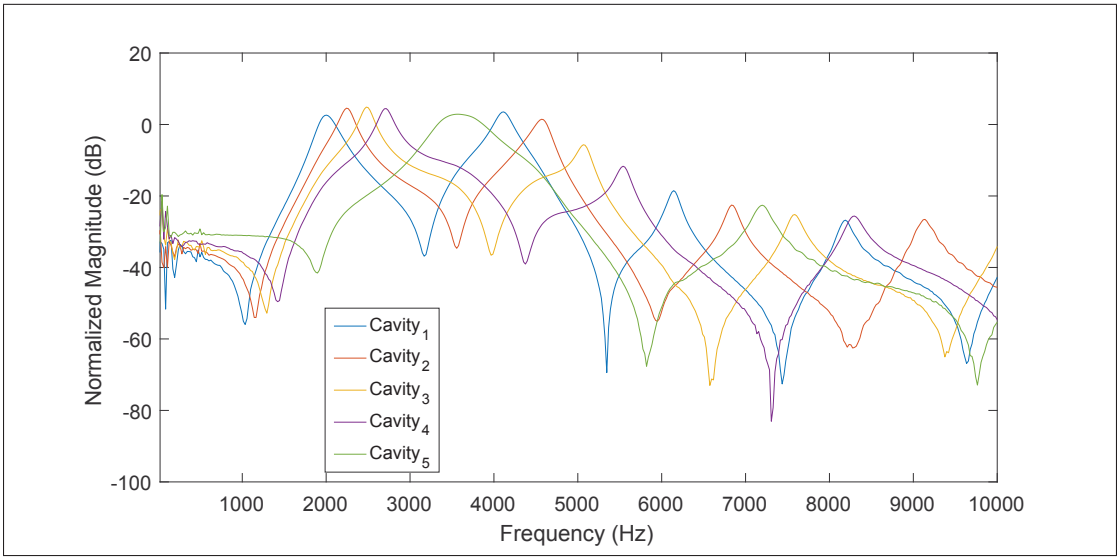

Figure 1.5 Frequency responses (P_1 to P_5) captured with the designed metal tubing DPOAE probe, described in Section 2.2.2.1, showing the cavities' #1 to 5 resonance peaks and nulls (results obtained by the author using the FPL calibration procedure)

The acoustic impedance is calculated as follows (taken from Eq. 1 (Scheperle *et al.*, 2011)):

$$Z_0 = \frac{\rho c}{A}, \tag{1.3}$$

where ρ is density of air, c is the speed of sound, and A is cross-sectional area of the tube.

The acoustic impedance's ρ and c depend on environmental conditions and can be approximated using a table with the temperature in the cavity measured using an infrared temperature sensor. All the pressure and temperature measurements must be done the day of the in-ear calibration for optimal precision in the Thevenin equivalent and the resulting FPL estimate.

Once the two previous steps are finished, the Thevenin equivalent is estimated by solving P_s and Z_s from the following equation for each frequency (taken from Eq.12 (Keefe, D. H., Ling, R. & Bulen, J. C., 1992)):

$$\begin{bmatrix} Z_{c1} & -P_1 \\ Z_{c2} & -P_2 \\ \vdots & \vdots \\ Z_{cm} & -P_m \end{bmatrix} \begin{bmatrix} P_s \\ Z_s \end{bmatrix} = \begin{bmatrix} Z_{c1}P_1 \\ Z_{c2}P_2 \\ \vdots \\ Z_{cm}P_m \end{bmatrix}, \tag{1.4}$$

where Z_{cm} is the mth cavity's impedance (see Eq. 1.2 presented above) and P_m is the pressure measured in this cavity. P_s and Z_s are the Thevenin equivalents for the source pressure and impedance respectively.

An example of the Thevenin impedance Z_s and pressure P_s are shown in the second and third subplots in Fig. 1.6 respectively. Keefe *et al.* (1992)'s overdetermined equation system can be solved using four cavities as shown in (Allen, J. B., 1986). However, for more precision in the Thevenin estimate five cavities are recommended (Charaziak & Shera, 2017).

Finally, once the Thevenin equivalent impedance (Z_s) is estimated with minimal error, it can be used to calculate the load impedance Z_l, i.e. the impedance at the reference plane in the earcanal. This is achieved by measuring the sound pressure (P_l) in the earcanal and calculating Z_l using the following equation (taken from Eq. 3 in (Scheperle *et al.*, 2008)):

$$Z_l = \frac{Z_s P_l}{P_s - P_l}. \tag{1.5}$$

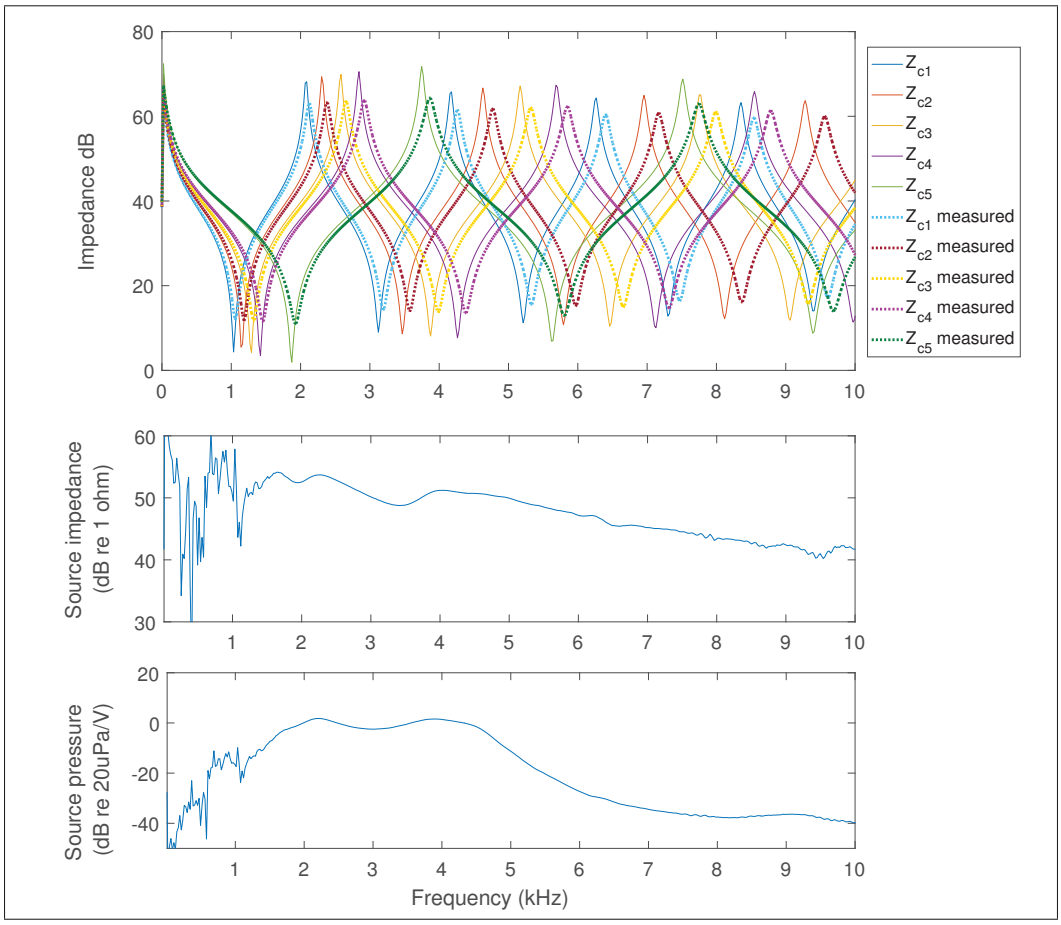

Figure 1.6 Calibration cavities' impedances at the top showing the ideal cavity impedance response which is compared to the measured cavity response. The second plot shows the source Thevenin equivalent impedance and third plot below shows the source pressure from the Thevenin equivalent (results obtained by the author using the FPL calibration procedure as detailed in Section 2.2.2)

The forward pressure (P_{forward}) is then estimated from the pressure P_l measured in the earcanal using the following equation (taken from Eq. 2 in (Scheperle *et al.*, 2011)):

$$P_{\text{forward}} = \frac{1}{2} P_l \left(1 + \frac{Z_0}{Z_l}\right), \tag{1.6}$$

where P_l is the load's pressure (i.e. the total sound pressure), and Z_l is the load impedance determined by both resistive and reactive elements, both P_l and Z_l are frequency-specific.

The FPL calibration method requires many steps, e.g. measuring the pressure in all five cavities, and specific hardware (e.g. special probe design and high quality sound card) to minimize the distortion in the Thevenin estimate. The integration of this method in a portable DPOAE device for *in situ* measurements with workers in industrial environments is therefore quite challenging. On the other hand, this method might reduce the variability in the DPOAE results, especially in the higher frequency range, hence an attempt to integrate the method in the designed DPOAE system has been investigated and is detailed in Section 2.2.2.

1.3.2.2.2 Otoacoustic emission growth functions

DPOAE growth functions are measured by stimulating the cochlea with the DPOAE primary tones at L_2 levels increasing generally from 50 to 75 dBA with a 5 dB step (Engdahl, B. & Kemp, D. T., 1996), L_1 is normally equal to or 10 dB above L_2. Some studies have briefly analyzed the cochlear gain curve and found an equation for the input/output function (Preyer, S., Baisch, A., Bless, D. & Gummer, A. W., 2001; Withnell, R. H. & Yates, G. K., 1998). While other studies have analyzed the growth functions as linear parameters with the DPOAE threshold and the slope of the growth function (Engdahl & Kemp, 1996; Gates *et al.*, 2002). The DPOAE threshold is the lowest stimulus level used to generate a specific DPOAE level. The measurement of these growth functions can help to differentiate between : 1) cochlear dysfunctions visible through changes in the DPOAE growth function slope and 2) other sources of changes in DPOAE levels like stimuli calibration, stapedial reflex or middle-ear dysfunctions which are visible through changes in DPOAE levels at all stimulation levels (Bharadwaj *et al.*, 2015; Gehr, D. D., Janssen, T., Michaelis, C. E., Deingruber, K. & Lamm, K., 2004; Keefe, D. H., 2002; Preyer *et al.*, 2001).

However, testing the entire growth function on the whole DPOAE spectrum on workers *in situ* might be time consuming and inefficient. Considering that the cochlear compression occurs mostly around L_2 = 55-70 dB(SPL) , as shown in Fig. 1.7 (Bharadwaj *et al.*, 2015; Sergeyenko *et al.*, 2013), these stimuli levels would be sufficient to observe changes in cochlear mechanics. These stimuli levels also allow to measure DPOAE levels of approximately 0 dB(SPL) in humans (Dreisbach, L. E. & Siegel, J. H., 2005), which is generally above the noise floor of the designed

DPOAE system during ambient noise exposure. The recommended DPOAE growth function procedure has therefore been integrated in the continuous DPOAE monitoring described in Section 5.3.3.1.

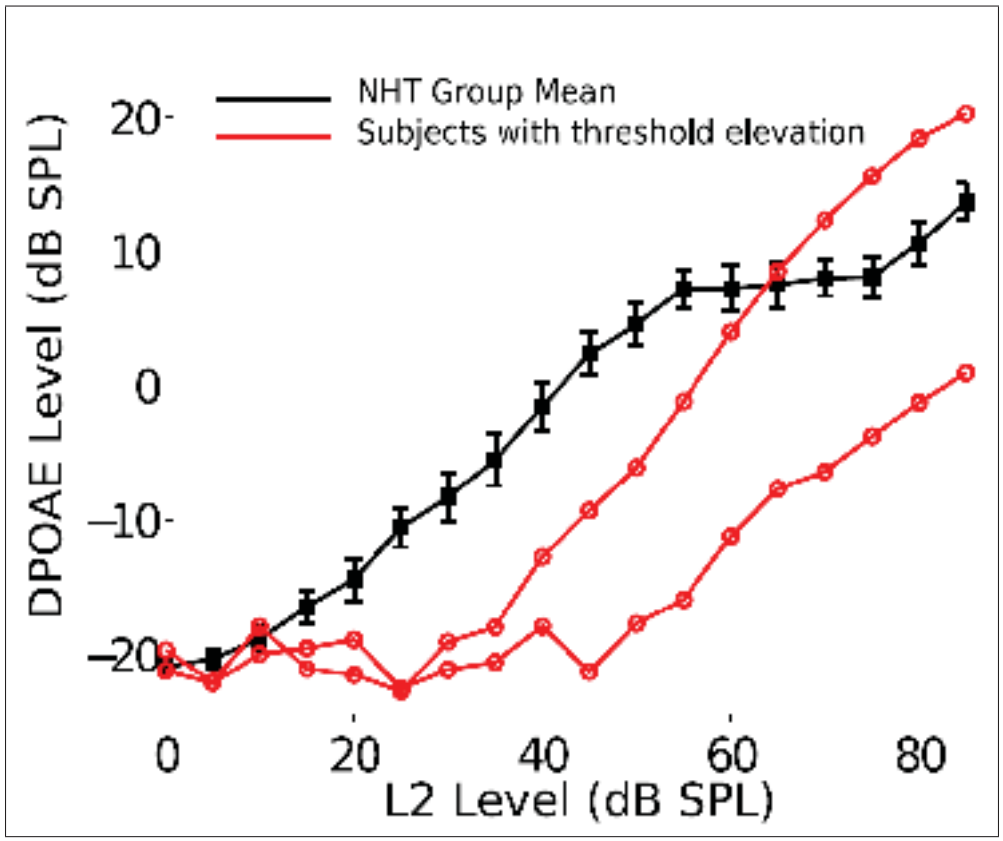

Figure 1.7 DPOAE growth functions (f_2 = 4 kHz) for a normal hearing cohort and two subjects with elevated thresholds. DPOAE thresholds are elevated for subjects with hearing loss, affirming that the measure is sensitive to cochlear mechanical deficits. Reproduced from Bharadwaj *et al.* (2015)

DPOAE growth functions are often used on mice to observe the onset of hidden hearing loss (Fernandez *et al.*, 2015; Furman *et al.*, 2013; Sergeyenko *et al.*, 2013). These studies show that high noise exposure levels (synaptopathic noise) can induce a reversible OHC dysfunction, measured with DPOAE growth functions, and permanent damage to IHC-synapses particularly at high frequencies as observed with immunostaining methods. This reversible OHC dysfunction can eventually become permanent in the long term (Fernandez *et al.*, 2015). This suggests that DPOAE growth functions can be used to observe the progressive onset of IHC-synapse

and OHC injury. These permanent damages degenerate over time and can reduce the medial olivocochlear reflex as detailed in Section 1.3.2.2.3.

1.3.2.2.3 Contralateral Acoustic Stimulation DPOAE

The Medial OlivoCochlear (MOC) efferents are a group of efferents that innervate outer hair cells and control the gain of the mechanical amplification within the cochlea. The Contralateral Acoustic Stimulation (CAS) DPOAE measurement is a practical, non-invasive, method generally used to observe the MOC reflex suppression effect on outer hair cells. This suppression is estimated by calculating the difference between DPOAE levels measured without contralateral stimulation and DPOAE levels measured while stimulating the contralateral ear with a wide-band noise. The measured DPOAE suppression is the consequence of a feedback or control mechanism of the auditory system on the OHCs. This feedback is mediated by the auditory efferent neurons in the OlivoCochlear (OC) bundle in the presence of a sound stimulus in the contralateral ear (Sun, X.-M., 2008). These OC neurons originate from the Superior Olivary Complex (SOC) of the brainstem and their nerve fibres are connected to the cochlea as shown in Fig. 1.8. "The nerve fibres in the medial part of the OC system directly innervate the outer hair cells of the cochlea [...] hence, the suppression is attributed to the MOC reflex" (Sun, 2008).

Cochlear-nerve compound action potential (CAP) is a more direct measurement of MOC activity elicited by contralateral noise. The measured suppression is therefore greater with CAP than with CAS DPOAEs. On the other hand, this measurement requires an electrode placed on the tympanic membrane and a long averaging time (Lichtenhan, J., Wilson, U., Hancock, K. & Guinan, J., 2016). A trans-tympanic electrode to measure the MOC reflex would require less averaging. However, the CAP method is an invasive procedure which requires a local anesthesia and restricts the individual's mobility (Lichtenhan *et al.*, 2016). These CAP measurement methods are therefore not a viable option to monitor individual's MOC reflex daily in an industrial workplace.

The use of CAS DPOAEs as a tool to evaluate the auditory efferent system and to some extent for hearing health monitoring was investigated by a few recent studies (Müller & Janssen, 2008; Sun, 2008; Venet, T., Campo, P., Rumeau, C., Thomas, A. & Parietti-Winkler, C., 2014). Clinical application of CAS DPOAEs is limited by the small suppression of approximately 2 dB by the MOC reflex (Yakunina, N., Kim, J. & Nam, E.-C., 2018). Researchers normally take precautions by selecting a low contralateral stimulation level to avoid activating other feedback mechanisms such as the Middle-Ear Muscle (MEM) reflex (Sun, 2008), which also contribute to the DPOAE suppression. This MEM reflex can reduce the DPOAE levels by an additional 4 dB Sun (2008). According to most studies (Müller & Janssen, 2008; Sun, 2008; Yakunina *et al.*, 2018), the contralateral broadband noise used to stimulate the MOC reflex should be calibrated at either 60 (Müller & Janssen, 2008) or 65 dB(SPL) (Yakunina *et al.*, 2018). These stimulation levels are below the lower range of the Acoustic Reflex Thresholds (ART) normally found between 70 and 100 dB(SPL). The ART is the lowest noise level that produces a measurable change in acoustic admittance/impedance (MEM reflex) (Sun, 2008). The experimental protocol of this doctoral research has therefore been adjusted to prevent triggering the MEM reflex during DPOAE measurements. A special attention was also given so that the effective residual noise level behind the earplug remained below the average ART (< 70 dB(SPL)) before measuring DPOAE levels, see Section 2.1.2 for the details of the integration of this protection in the developed software.

The MEM reflex can be activated by presenting intense sound stimulation in the contralateral or ipsilateral ear. It contracts the stapedius muscle to increase the stiffness of the middle ear which causes an increase in the acoustic impedance of the external ear. When the MEM reflex is activated, the stiffened middle-ear reduces the transmission of acoustic energy to the inner-ear and reduces the OAE level (Sun, 2008). This reflex is assumed to protect the inner-ear from noise-induced hearing damage. However, the impedance change caused by this MEM reflex decreases as the reflex develops fatigue with cumulative noise exposure over time (Borg, E., Nilsson, R. & Lidén, G., 1979) . Monitoring the ART could therefore be helpful to observe short-term effects of noise exposure on the auditory system. Yet, recent developments in acoustic reflex threshold measurement techniques showed that current clinical devices using the

pure-tone activators are less sensitive than the wideband probe stimulation technique (Feeney, M., Schairer, K., Keefe, D. H., Fitzpatrick, D., Putterman, D., Garinis, A., Kurth, M., Kolberg, E., McGregor, K. & Light, A., 2018). Therefore, the wideband probe stimulation technique for ART measurements should be included in future experiment protocols to detect such short-term effects of noise exposure.

The role of the medial olivocochlear reflex in hidden hearing loss Previous studies suggest that the MOC reflex may have many functions, such as 1) a protective role against moderate and high noise exposure levels (Maison, S. F. & Liberman, M. C., 2000; Maison *et al.*, 2013; Müller & Janssen, 2008). This protective role not only affects outer hair cells and inner hair cells (Kujawa & Liberman, 2015), but also minimizes neuropathy possibly due to the feedback reduction of cochlear amplification (Maison *et al.*, 2013). In mice, an 84 dB(SPL) noise exposure caused modest neuropathy in the normal ear, this neuropathy was aggravated in the absence of the MOC feedback (Maison *et al.*, 2013). 2) The MOC reflex is also involved in the ability to listen to someone's voice in high background noise levels (Kim, S., Frisina, R. D. & Frisina, D. R., 2006), also known as the cocktail party effect. In general, noise partially masks the tone-burst response, but with MOC stimulation the response to the background noise is inhibited. This partially restores the auditory nerve fibre dynamic range for responses to short tone bursts. Hence, in a continuously noisy background the MOC reflex can increase the response to transient sounds, such as speech, by reducing the response to the noisy background. This increases the audibility of transient sounds in background noise (Guinan Jr, J. J., 2006). In addition, small changes in the MOC reflex suggest that the central gain feedback may be altered due to noise-induced damages in either peripheral, e.g. IHC-synapses or auditory nerve fibres, or central auditory systems (Bharadwaj *et al.*, 2015). This change in central gain has already been reported in previous studies as a possible explanation for the onset of tinnitus (Schaette & McAlpine, 2011). Further research is needed to understand the complex relationships of long-term plasticity, MOC and middle-ear reflexes with neuropathy (Bharadwaj *et al.*, 2015).

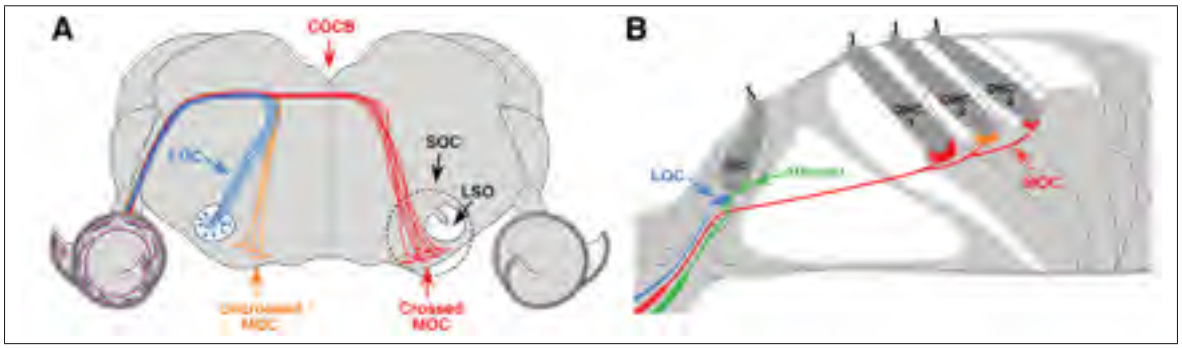

Figure 1.8 Illustration of the brainstem origins and a) peripheral targets of lateral olivocochlear (LOC) and medial olivocochlear (MOC) efferent pathways to the cochlea. a) Where the cross-section through the mouse brainstem also shows the lateral superior olive (LSO), superior olivary complex (SOC), crossed olivocochlear bundle (COCB). In b) the synaptic contacts of the LOC terminals in the IHC and the MOC terminals on OHCs are shown in the organ of corti. Reproduced from Maison *et al.* (2013)

Growth function and CAS DPOAEs are complimentary methods to test cochlear functionality and should be included in hearing conservation programs to better understand the onset of hidden hearing loss. These tests must be accompanied by other hearing tests, such as auditory brainstem responses detailed below, to diagnose synaptopathy.

1.3.2.3 Auditory Brainstem Response

Auditory Brainstem Responses (ABR) are auditory evoked potentials extracted from ongoing electrical activity in the brain. They are recorded via electrodes placed on the scalp. In order to distinguish the damages to the auditory nerve fibres from OHC injury, DPOAE levels measure the cochlear amplification process of the OHC while ABR Wave I measure the neural response of the cochlea. This Wave I assess the auditory nerve function and, furthermore, corresponds to the proportion of intact IHC-synapses (Plack, C. J., Leger, A., Prendergast, G., Kluk, K., Guest, H. & Munro, K. J., 2016). The combination of the DPOAE and ABR measurements is common in studies to identify synaptopathy and neuropathy (Fernandez *et al.*, 2015; Liberman, M. C., Epstein, M. J., Cleveland, S. S., Wang, H. & Maison, S. F., 2016; Maison *et al.*, 2013). These studies usually consider that when DPOAE and ABR Wave I levels change in the long term following a noise exposure, it indicates damages to OHC, upstream of the auditory pathway.

While permanent changes in ABR Wave I levels without a DPOAE shift would indicate damages to underlying mechanisms such as IHC-synapses and auditory nerve fibres (Kujawa & Liberman, 2015).

Despite the reduction in Wave I in both noise-induced and age-related IHC synaptopathy, there is no reduction in the amplitude of Wave V. This Wave V is thought to arise mainly from responses in the inferior colliculus (midbrain) (Kujawa & Liberman, 2015). This could be explained by the homeostatic gain control in the auditory brainstem which would normalize (amplify) the Wave V amplitude after hidden hearing loss (Schaette & McAlpine, 2011). Recent human studies have shown that the ratio of Wave I to Wave V is reduced in tinnitus sufferers with normal audiometric thresholds, compared to non-tinnitus sufferers (Schaette & McAlpine, 2011). This pattern is consistent with the primary degeneration of the auditory nerve fibres resulting in the amplification of central gain. This amplification would elicit tinnitus in the absence of threshold elevations (Kujawa & Liberman, 2015).

In the short term, the similarity of post-exposure thresholds in DPOAEs and ABRs suggests that temporary threshold shifts are due predominantly to reversible damage to the cochlear amplifier (Furman *et al.*, 2013). Considering that the synaptopathic noise exposure has temporary effects on DPOAE levels as shown in (Fernandez *et al.*, 2015), it could be possible to prevent the onset of synaptopathy by monitoring OHC activity with high temporal resolution DPOAE growth functions. A similar approach was also suggested by Liberman & Kujawa (2017). Logically, since DPOAEs result from the cochlear amplification, if there is an onset of synaptopathy the signal transmitted in the auditory nerve fibres should decrease. Hence, the gain control feedback to the OHC should fluctuate. Otoacoustic emissions may not be the optimal tool to detect IHC-synapses and auditory nerve fibres damage which occurred a long time ago. However, in the short term, otoacoustic emissions could be a suitable prevention tool to monitor early signs of synaptopathy as well as other cochlear damage to take actions at the right moment before sensorineural changes become irreversible.

ABRs are a promising approach to measure hidden hearing loss, but they have low amplitudes in humans since electrodes are placed on the surface of the scalp, instead of subdermal needle electrodes with the mouse. They also show a high variability both between and within individuals (Plack *et al.*, 2016). This variability in Wave I may be the result of various factors besides cochlear synaptopathy (Plack *et al.*, 2016). Thus, Wave I can be useful to compare group differences in response to synaptopathic noise exposures, but not to diagnose hidden hearing loss in an individual (Plack *et al.*, 2016). Although the combination of ABR with DPOAE measurements eliminates the possibility that the difference in Wave I magnitude comes from the OHC.

The Frequency-Following Response (FFR) is therefore a better alternative to the Wave I of ABRs as suggested by Plack *et al.* (2016). It is a sustained auditory-evoked potential reflecting neural activity in the brainstem in phase with the stimulus waveform. The FFR can be recorded using a similar electrode setup as the ABR and is a more robust measure than ABR Wave I in low frequencies. This results in a clear response above the noise floor for most humans (Plack *et al.*, 2016). Preliminary evidence of reduced FFR in presence of normal absolute thresholds suggests that the FFR may be sensitive to synaptopathy (Plack, C. J., Barker, D. & Prendergast, G., 2014). However, the FFR technique may also be influenced by central factors unrelated to synaptopathy and variability within-subjects and between-subjects (Plack *et al.*, 2016). One way to circumvent these disadvantages is to use a differential measurement, i.e. two measurements that are compared for each individual, one that is affected by synaptopathy and one that is not. Both measurements would be equally affected by other sources of variability and therefore the variability would be cancelled out (Plack *et al.*, 2016). One solution could be to compare across stimulation levels, since only LSR-high threshold fibres should be affected by a moderate synaptopathic noise exposure compared to the HSR-low threshold fibres. A second solution could be to compare across stimulation frequencies, the high frequency range is more susceptible to damage compared to low frequencies. Hence, if FFRs are measured to observe signs of synaptopathy or neuropathy, two frequencies should be measured to eliminate the within- and between-subjects variability. For example, one frequency around 4 kHz, known to be more

subject to change due to the frequency spectrum of the noise exposure and a second frequency 235 Hz which is less prone to change, as used by Plack *et al.* (2016).

In order to monitor human's IHC-synapses and auditory nerve fibres health in their workplace, ABR and FFR measurements require wearing electrodes on the scalp during a long period. This involves preparation like cleaning the skin for a good electrical contact with the electrodes. The subjects must also remain still otherwise the electrodes could move and induce noise in the measurements. Hence, these tests are not a practical solution for day-to-day hearing health monitoring, especially for industrial workers. Moreover, performing these measurements requires some expertise and time to find the optimal device parameters for proper hearing assessment. DPOAE measurements therefore appear as a more viable solution for elaborate hearing assessment in the workplace. Anyhow, moderate noise exposure does not immediately induce changes in ABRs, at least not within the first hour (Maison *et al.*, 2013). On the other hand, effects of moderate noise exposures appear immediately (within 1h) post-exposure in DPOAEs (Maison *et al.*, 2013). In addition, DPOAEs are easy to measure in humans since the OAE signal is usually strong enough to be recorded in noisy environments with microphones currently used in DPOAE probes. Plus, DPOAE probes are comfortable and can be worn over a long period. Although, most HHL studies generally observe DPOAE levels, they usually use these results to compare them to ABR results. These studies do not analyze the short-term pattern of the DPOAE variations during and after the noise exposure, which could potentially reveal information on underlying mechanisms of the onset of synaptopathy. Rodents are usually used in studies on hidden hearing loss in the first place because the synapses can be counted after the experiment once the animal is sacrificed. Hence, the onset of hidden hearing loss could be monitored in rodents first, before testing on humans, with high temporal resolution DPOAE measurements every 15 to 20 minutes during and after the noise exposure. Then, the noise-induced effects on IHC-synapses could be confirmed by the synapse count using common immunostaining methods.

In a more elaborate experiment to specifically observe hidden hearing loss in humans, ABR and FFR could be used to evaluate the effect of the noise exposure on the auditory nerve

fibres response and, of course, any problem upstream the nerve fibres such as damage to the IHC-synapses for example. In order to ensure that the changes in Wave I amplitude relate to changes in auditory nerve fibres or IHC-synapses, Wave V must also be extracted from the measurement. The ratio of Wave I/Wave V should be compared between the first reference measurement and all the following ABR measurements. The Wave I, Wave V and FFR responses in relation to noise exposure could validate the DPOAE assessment approach as a tool to prevent further damage to IHC-synapses and auditory nerve fibres. For example, FFR tests should be conducted once at the beginning of the experiment, ideally just after the initial screening. Afterwards, following FFR measurements should be conducted within 24 hours of the noise exposure. Finally, one last FFR should be measured approximately one month after the last monitored noise exposure to observe any progress of synaptopathy or neuropathy.

In summary, short-term effects of traumatic noise would result in difficulty to hear in noise as a consequence of synaptopathy or neuropathy. While, long-term effects of traumatic noise would result in difficulty to hear in noise as well as without noise as a consequence of synaptopathy/neuropathy in addition to the loss of OHC. Although most studies are based on animal models, similar conclusions are reported from human studies (Bramhall *et al.*, 2017; Sergeyenko *et al.*, 2013). Considering that the onset of synaptopathy can be measured with DPOAEs (Fernandez *et al.*, 2015), close monitoring of DPOAEs in the workplace is a promising approach for future hearing conservation programs.

1.4 Continuous noise exposure and hearing health monitoring

Although many longitudinal studies report monitoring noise exposure and hearing threshold measurements (Lapsley Miller, J. A., Marshall, L. & Heller, L. M., 2004; Lutman *et al.*, 2008; Müller & Janssen, 2008; Rabinowitz *et al.*, 2013), it is difficult to find the direct relationship between noise and hearing loss (Rabinowitz *et al.*, 2013). A first possible cause of this difficulty is the use of ambient noise exposure levels instead of in-ear noise levels, introduced in Rabinowitz *et al.* (2013)'s study, to find the relationship with noise-induced hearing damage. A second possible cause is the lack of noise impulsiveness measurements to include these measurements

as a NIHL risk predictor (Davis *et al.*, 2012; Qiu *et al.*, 2013; Rabinowitz *et al.*, 2013). A third possible cause is the delay between permanent IHC-synapses damage , resulting in hearing threshold shifts, and the progressive onset of OHC damage following noise exposure (Fernandez *et al.*, 2015). Hence, it is important to monitor the onset of OHC damage continuously with DPOAE measurements to properly identify the relationship between noise exposure and the onset of hearing loss.

In order to establish a dose-response relationship between noise exposure levels and its induced otoacoustic emission changes, it is important to know in the first place how DPOAE levels fluctuate over time pre- and post-exposure. A few studies report on the DPOAE levels recovery time after noise exposure (de Toro, M. A. A., Ordoñez, R., Reuter, K., Hammershøi, D. & others, 2010; Engdahl, 1996; Sutton *et al.*, 1994; Vinck *et al.*, 1999), but these studies do not measure DPOAEs during the noise exposure. Testing DPOAEs in noise conditions requires a robust DPOAE measurement system, which has finally been designed by the candidate for the purpose of the current doctoral project and is presented in Section 2.1.

According to Sliwinska-Kowalska *et al.* (2001) and Engdahl (1996), recovery time patterns for DPOAEs and TEOAEs are very similar to the recovery of behaviourally measured temporary threshold shifts. Similar findings can be observed by comparing the TTS recovery curves in logarithmic scale measured with audiometric thresholds found in Laroche, C., Hetu, R. & Poirier, S. (1989)'s study and the DPOAE recovery curves found in Sutton *et al.* (1994)'s study. The recovery curve can also be observed in the superposed graphs shown in Figure 1.9 (Engdahl, 1996). These results show that the recovery time is quite similar between the audiometric thresholds and the DPOAE levels, with approximately 10 dB (Engdahl, 1996; Laroche *et al.*, 1989) and approximately 3 to 5 dB recovery (Engdahl, 1996; Sutton *et al.*, 1994) respectively within the first 15 to 20 minutes post-exposure for typical subjects, as shown in Fig. 1.9 & 1.10 D. According to Engdahl (1996), there is a more rapid recovery when the DPOAE shift is large. It is therefore advisable to measure DPOAEs as closely as possible to the traumatic noise event to detect the greatest DPOAE shifts between pre-exposure and during exposure. Failing to measure

OAEs at the right moment with the correct parameters may lead to DPOAE shifts that are not statistically significant, as found in (Lutman *et al.*, 2008).

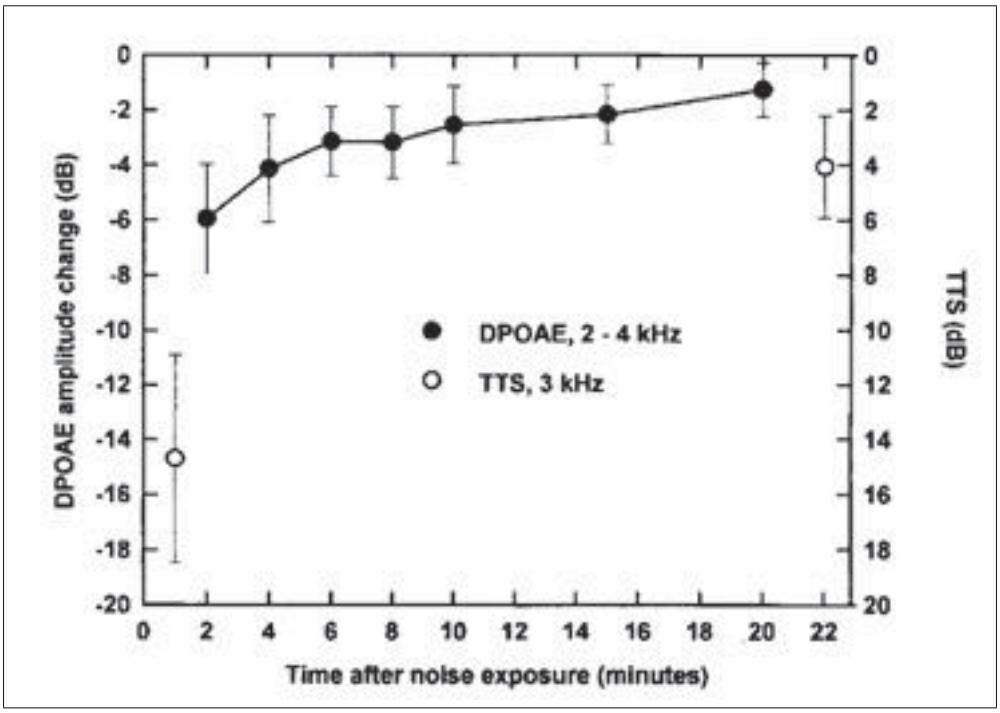

Figure 1.9 DPOAE amplitude change averaged in the 2-4 kHz range, mean ±1 SD and TTS measured as the change between post- and pre-exposure Békésy thresholds at 3 kHz. Reproduced from Engdahl (1996)

Although recovery is normally a logarithmic function and starts within the first minute post-exposure, it takes several minutes (over 70 minutes) for certain subjects' DPOAE levels to recover completely from noise exposure. Usually most of the recovery happens within the first 20 minutes (de Toro *et al.*, 2010; Engdahl, 1996; Sutton *et al.*, 1994). Moreover, Vinck *et al.* (1999) reported that the recovery pattern is frequency-specific. Such inter-subject differences in DPOAE patterns are of particular interest for this doctoral project and support the idea of providing a personal hearing health monitoring device to each worker in order to establish their individual susceptibility to noise.

Despite the various studies to find the dose-response relationship, only a few have assessed the noise-induced changes in the DPOAE growth functions for humans (Bharadwaj *et al.*, 2015;

Engdahl & Kemp, 1996). One study assessed the short-term effects of noise on DPOAE growth functions, but the restricted frequency range, number of subjects and noise duration tested have limited the conclusions of this study (Engdahl & Kemp, 1996). Hence, testing DPOAE growth functions *in situ* should provide a more elaborate dataset to model the effects of noise exposure on growth functions for humans. Such model will be helpful in this doctoral research to estimate the most significant predictors of NIHL based on DPOAE growth functions. A literature review on the statistical methods to identify such a model is presented in the following Section 1.5.

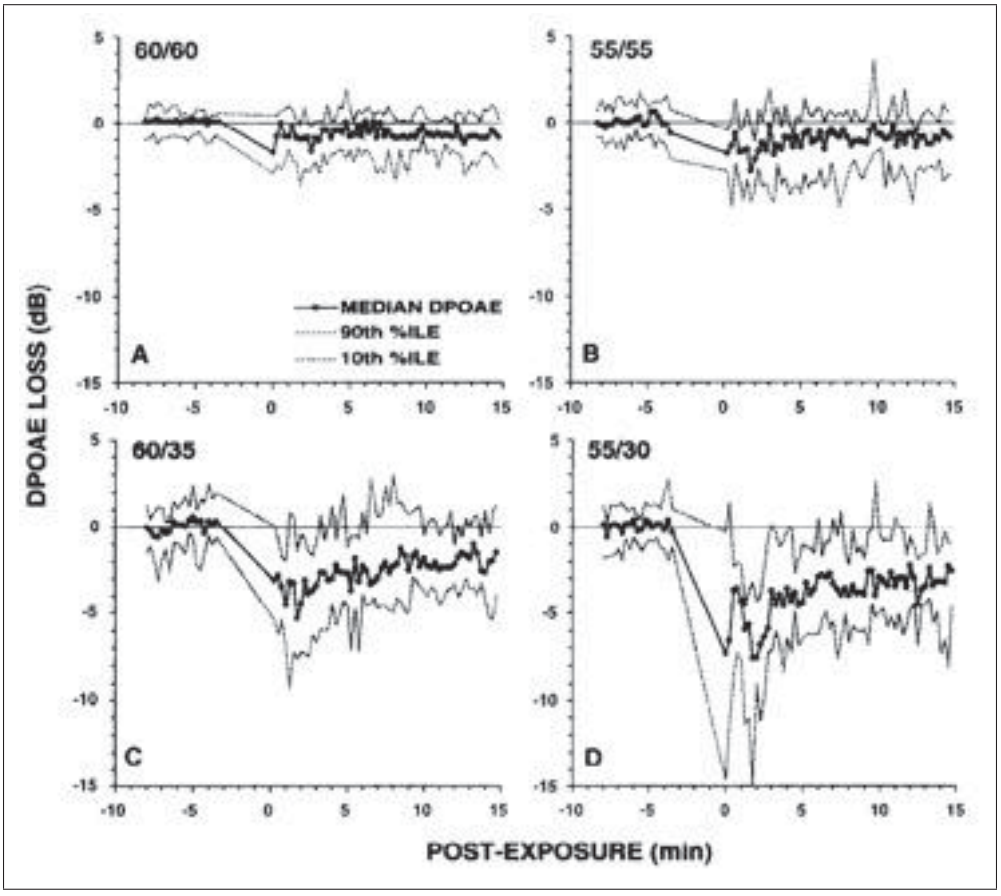

Figure 1.10 Median DPOAE-loss functions beginning at 0 min following tonal (noise) over-exposure, for each tested stimuli magnitude ratio. Fine dotted lines indicate the 10^{th} and 90^{th} percentiles for each condition. Reproduced from Sutton *et al.* (1994)

1.5 Statistical methods to assess changes in hearing status

Several statistical methods are available and required to establish the relationship between the noise exposure conditions over the day and the variations in DPOAE levels or any other hearing tests for close monitoring. In order to start the analysis for this doctoral thesis with the correct tools, a literature review of statistical methods previously used in other studies is detailed below.

First, to verify if there are changes in measured levels, for example in PTA HTLs or DPOAE levels, throughout the day it is possible to use a repeated measures ANalysis Of VAriance (ANOVA) and observe whether the difference between conditions (days) is significant or not. However, the ANOVA doesn't output the mean of differences and it is complicated to use in the case of the evaluation of each DPOAE frequency, therefore Venet *et al.* (2014) used a simpler Student t-test over each DPOAE frequencies individually. In the case where the data comes from the same group of participants for different conditions, i.e. paired data, a paired t-test must be used. The t-test assumes normality of the data, which is not always the case. To analyze data which does not respect the normality constraint, a non-parametric test is required. An example would be the Wilcoxon test, which is similar to the t-test and is used in Attias, J., Bresloff, I., Reshef, I., Horowitz, G. & Furman, V. (1998)'s study to calculate the mean of differences and the significance (p-value) between the group with a history of noise exposure and the group without history of noise exposure, for each tested frequency. For multiple comparisons to find relationships between subgroups, the post-hoc Bonferroni procedure can be used to verify if results in different conditions are significantly different. It uses a correction factor on the α value based on the number of hypotheses to make sure that the changes are definitely true changes, it is less likely to have a type I error than a simple t-test.

Multilevel models

Nonetheless, finding a statistically significant change in DPOAE levels with a t-test does not give much information on how this change was induced. The noise exposure level is one factor amongst many others that can influence the discrete DPOAE levels. In order to find the most

significant predictors of NIHL, a lot of information on the noise conditions and its induced effects on hearing health is necessary. This information needs to be encoded with time to model the progress of the changes in predictor values on the dependent variable. Multilevel models , also known as mixed models, can fit a variety of linear models to the data and allows to use these fitted models to make statistical inferences about the data (SAS, 2016; Singer, J. D., Willett, J. B., Willett, J. B. et al., 2003). The multilevel model provides the flexibility of modelling not only the means of the data, as in the standard linear model, but with their variances and covariances as well (SAS, 2016; Singer *et al.*, 2003). Multilevel models allow to observe the effects of predictors across time within subjects (level-1) and between subjects (level-2). For example, the equation for the level-1 of the multilevel model can look as follows:

$$Y_{ij} = \pi_{0i} + \pi_{1i}\text{TIME}_{ij} + \varepsilon_{ij}, \tag{1.7}$$

- where π_{0i} represents individual i's true initial status (intercept), that is the value of the outcome variable (for example the DPOAE level) when $\text{TIME}_{ij} = 0$.
- π_{1i} represents individual i's true rate of change during the period under study.
- ε_{ij} represents the portion of individual i's outcome that is unpredicted on occasion j (random error).

The level-2 equation can look as follows:

$$\pi_{0i} = \gamma_{00} + \gamma_{01}\text{EXPOSED}_i + \zeta_{0i} \tag{1.8}$$

$$\pi_{1i} = \gamma_{10} + \gamma_{11}\text{EXPOSED}_i + \zeta_{1i}, \tag{1.9}$$

- where γ_{00} and γ_{10} are the level-2 intercepts which represent the population average initial status and rate of change respectively, with the predictor EXPOSED = 0 which corresponds to the non-exposed group in this example. If both parameters are 0, the average individual who is in the non-exposed group has a normal DPOAE level and does not have a DPOAE shift.

- γ_{01} and γ_{11} are the level-2 slopes which represent the effect of EXPOSED (fixed effect coefficient) on the change of trajectories, providing increments or decrements to initial status and rates of change respectively for the exposed group.

- ζ_{0i} and ζ_{1i} are the level-2 residuals which represent the portions of initial status (ζ_{0i}) or rate of change (ζ_{1i}) which are unexplained at level-2. They represent the deviations of the individual change trajectories around their respective group average trends.

It is also possible to represent the equations of these two levels in a single equation:

$$\begin{aligned} Y_{ij} =&[\gamma_{00} + \gamma_{10}\text{TIME}_{ij} + \gamma_{01}\text{EXPOSED}_i + \gamma_{11}(\text{EXPOSED}_i \text{ x } \text{TIME}_{ij})] \\ &+ [\zeta_{0i} + \zeta_{1i}\text{TIME}_{ij} + \varepsilon_{ij}], \end{aligned} \tag{1.10}$$

where the brackets help to distinguish the model's structural and stochastic components (Singer *et al.*, 2003). To evaluate the statistical significance for each coefficient, the p-value is based on the mean, that is the fixed effect coefficient, and its standard error.

In order to find the relationship between noise exposure and its effects on hearing health, multilevel models can therefore be developed using various noise metrics as time-varying predictors , as used for Chapter 5. An example of code for the models with such time-varying predictors is presented in Appendix IV. Based on these predictors, multilevel models are built sequentially by including one predictor at a time. The best model is selected based on the most optimal goodness-of-fit which is usually found with the lowest log-likelihood, Akaike Information Criterion (AIC) and Bayesian Information Criterion (BIC) (Singer *et al.*, 2003). The predictors included need to significantly improve the goodness-of-fit of the model. This can also be assessed with an ANOVA between the reference and improved models. In order to simplify the models' parameters and analysis, one univariate (i.e. one outcome) model is recommended per f_2 stimulus frequency. A similar multilevel model approach was used to find the relationship between noise exposure and its induced hearing loss in previous studies (Lutman *et al.*, 2008; Rabinowitz *et al.*, 2013). These models are therefore of particular interest for the current doctoral project. Based on the experimental measurements, they help to find the most

significant predictors of change in hearing health. In addition, it is possible to use the identified optimal model to predict the combined effects of all significant predictors on hearing health, therefore estimating the risk of NIHL.

1.6 Partial conclusion

In summary, NIHL is still an important occupational issue although hearing conservation programs are integrated in the workplace with annual hearing health follow-up and noise dosimetry. Studies suggest that temporal noise metrics, such as the noise impulsiveness, are important and the equal energy hypothesis is not sufficient to characterize complex industrial noise. Noise can have effects on different parts of the auditory system such as OHC, IHC-synapses and the auditory nerve. This explains the various hearing health assessment methods, ranging from audiometry to ABR, that were developed to test each hearing mechanism separately. From these hearing tests, DPOAE measurements appear as a suitable indicator of hearing health changes which could also help to monitor of the onset of synaptopathy *in situ*. High frequency DPOAE growth functions at regular time intervals should provide optimal time sensitive information on an individual's auditory system health. Finally, according to the literature, continuous monitoring of the noise-induced effects on hearing health should be evaluated with multilevel models.

CHAPTER 2

DEVELOPED MATERIALS AND METHODS

Available clinical DPOAE devices are not robust against noise interference in high ambient SPL environments and do not give the possibility to add new functionalities. Hence, a portable system has been developed to conduct the in-field experiments. The system's developed hardware and software are presented in Section 2.1. This system's earpieces must be calibrated to compensate for the miniature loudspeakers response in the earcanal to obtain reliable results with the designed earpieces. Various calibration methods exist, and two approaches have been explored during this doctoral project. The first approach also integrates a fit-test procedure to assess if the eartip of the earpiece is correctly positioned in the earcanal to ensure the users are correctly protected from the exposure and the calibration gives reliable results before the individuals are exposed to ambient noise. The second approach uses the Thevenin equivalent of the miniature loudspeaker to estimate the sound pressure level at the eardrum position with the forward pressure level. These calibration methods are presented in Section 2.2.

2.1 Development of the noise exposure and OAE measurement system

In order to continuously monitor hearing health during noise exposure, there is no commercial system currently available that is able to perform DPOAE measurements in high noise level environments. Hence, a portable OAE measurement device has been designed in the laboratory. This system includes DPOAE probes with custom fit or generic foam eartips to provide passive attenuation for optimal DPOAE measurements and hearing protection. These earpieces are attached to an embedded system to process and record the data. This system has been developed and improved over 6 years from the end of the masters degree (Nadon, 2014) until the end of this doctorate project. Two versions of the device, referred to as ARP1DPOAE and ARP3DPOAE respectively, have been designed with success and are presented below. Each of them has been used in different experiments (see Chapter 3 to 5) to observe changes in hearing health on human

participants and test the system's performance in noisy conditions (Nadon, 2014; Nadon *et al.*, 2015a,1).

2.1.1 First generation of the OAE system - ARP1DPOAE

The first generation of the OAE system (ARP1DPOAE shown in Fig. 3.1) has two DPOAE earpieces which are each equipped with two high-quality Wide-Band FK miniature loudspeakers (Knowles, FK series) to send the two pure-tone stimuli without any sound distortion in each of the probes' PVC tubing. The earpieces also included a miniature microphone (Knowles, GA38 series) connected to a separate PVC tube to measure the OAE response and physiological noise. A second miniature microphone (Sonion, 66AF31) is placed in the probe earpiece facing outward, i.e. pinna side, to measure the external ambient noise. A custom-molded ear tip has been designed to slide on the probe's electronic components core. This way, the custom-molded ear tips could simply be interchanged for each participant while using the same probe electronics, ensuring consistent electroacoustic responses across all the experiments and a comfortable fit for everyone. This earpiece design is further detailed in Nadon (2014).

To record and process the data, the choice of DPOAE hardware electronics was based on the first Auditory Research Platform (CRITIAS, 2019) developed by Kuba Mazur (2016). The components have been designed specifically to record DPOAE levels in noisy conditions. The system integrated a signal conditioning amplifier to optimize the signal-to-noise ratio (SNR) of the IEM, a digital signal processor (DSP) to implement the designed DPOAE measurement algorithms, a micro-controller and a Bluetooth communication dongle to transmit the calculated DPOAE levels and background noise levels to a smartphone, as detailed in Chapter 3. An Android smartphone application, shown in Fig. 3.2, has been designed to display the DPOAE data received from the device and to transmit various commands to the device, such as switching DPOAE stimulus frequencies. The box of the designed system measures approximately 8.0 x 7.5 x 4.0 cm and is therefore small enough to be worn by a worker, clipped on his or her belt during the entire work shift for instance. The two DPOAE earpieces are required to extract the DPOAE signal using an adaptive filtering algorithm as presented briefly in Appendix I and

detailed in (Nadon *et al.*, 2017a). The earpieces also serve as custom-molded hearing protectors, providing high passive attenuation of the ambient noise. This system was used in the study presented in Chapter 3. However, it had a few limitations as detailed in Section 2.1.1.

Advances and limitations of the ARP1DPOAE

This first generation of the DPOAE system has been tested in laboratory conditions. Its performance is sufficient to carry the measurements in controlled conditions and yielded publishable results as demonstrated in Chapter 3. However, this system depends on other devices such as a sound level meter as well as a smartphone or tablet to control and save the data from the device through Bluetooth. A portable recorder is also necessary to record the raw audio from the earpieces since the DSPs audiostream limitations with the micro-controller and the maximum compatible capacity limited to a 2 GB micro SD card is not sufficient for an entire day recording 3 channels at a sampling frequency of 44100 Hz. The system is therefore not easy to carry around for the purpose of the research with its multiple devices and connections.

Moreover, various Bluetooth communication problems caused data dropouts and electrical noises in the earpieces signals, hence it is difficult to post-process the data and it possibly reduced the statistical significance of the results. Additional problems with the electronics, the DSP's instructions memory limitations and micro-controller integration problems did not allow the development of new features such as noise exposure level measurements. The library of pre-programmed algorithms on the DSP limited the implementation of more complex algorithms.

The designed ARP1DPOAE earpieces are robust against acoustical and electrical noise interference, but they are heavy for a daily use. Besides, the earpiece can slip out of the participants' ear during the experiment when the custom molded tip fit is not holding in the second bend of the earcanal.

Figure 2.1 Picture of the developed system (ARP3DPOAE) with the additional external battery supply, touch screen stylus and earpieces showing measured OEM and IEM sound pressure levels. The external battery provided enough energy for 8 hours

2.1.2 Second generation of the OAE system - ARP3DPOAE

In order to solve the problems of ARP1DPOAE highlighted above, the system has been completely redesigned. The second generation of the DPOAE system (see Fig. 2.1) is based on a miniature computer, here called Auditory Research Platform 3 (ARP3). This computer allows : more processing power with its Intel® processor, more elaborate algorithms and more storage capacity. This gives the possibility to record the in-ear and outer-ear sound pressure levels of both earpieces simultaneously while recording the raw audio signals in the 128 GB micro SD card and performing DPOAE measurements.

To perform the DPOAE measurements in noisy environments, the second generation of earpiece uses comply foam eartips, since these are easy to fit in participants' ears and provided sufficient passive attenuation. Yet, this HPD's comfort in the ear is not personalized and may have been compromised for some individuals. The miniature loudspeakers of the DPOAE probe have been replaced with the Knowles RAB32063 for their availability, minimal distortion and small form factor to fit in the earpiece underbody. The OEM has also been replaced by the Sonion 50PC32 since the 66AF31 used previously has been discontinued. For the IEM, the Knowles GA38 has been kept, since its SNR performance is still the most optimal compared to other Sonion models tested.

Figure 2.2 Picture of the developed system in its carrying fanny pack pouch

To connect the two earpieces to the ARP3, a sound card here referred as the SoundBoard has been designed for a direct interface of the earpieces signals with any computer through USB 2.0 interface, as shown in Fig. 2.3. The internal sound card of the ARP3 did not provide enough inputs and outputs for the requirements of the project. Hence, the SoundBoard was designed

since there was no DSP or codec solution available on the market during the design phase that had 24 bit resolution and 4-channel for inputs plus 4-channel for outputs. The SoundBoard is a 24 bit audio interface inspired by the Super Audio Board by William Hollender (2019) with a few hardware and firmware modifications such as the support of 4-channel inputs and 4-channel outputs, inspired by a Teensy project (PJRC store, 2019). The SoundBoard also integrates microphone signal conditioning pre-amplifiers. These conditioning pre-amplifiers (see schematics in Appendix II) were designed during the masters project (Nadon, 2014). The 24-bit resolution is practical to detect the low magnitude DPOAE signal and the 44100 Hz sampling frequency is sufficient for the acoustical requirements of the project. The schematics of the SoundBoard integrating final improvements are available in Appendix II.

Figure 2.3 Picture of the developed SoundBoard with the designed metal tubing earpiece

The SoundBoard is designed with many practical features such as the ability to switch the miniature loudspeakers as a stereo pair using serial commands through the USB interface, enabling either the left or the right earpiece at a time with the software. The IEM-I and IEM-C,

OEM-I and OEM-C microphones are also interchangeable when selecting the earpiece, to ensure that the adaptive filters , as presented in Appendix I, and other processing are using the proper signals. A pre-calibrated white noise signal can also be generated using a serial command to enable contralateral ear stimulation for CAS DPOAE measurements.

For the subsequent *in situ* experiments, new features are implemented in the designed software such as: built-in outer-ear and in-ear sound level meters (see Fig. 2.4), 4-channel audio recording, DPOAE growth function and CAS DPOAE measurements (see Fig. 2.6), selection of the tested ear, in silence fit-test and DPOAE calibration, as well as a FPL calibration method that is under test (see steps of cavity pressure measurements in Fig. 2.5). A timer is set at 20 minutes to notify the users with an alarm sound in their earpiece that it is time to do a DPOAE measurement (see Fig. 2.6). When continuous noise exposure levels exceed 80 dBA at the OEM, the system does not allow the user to start the DPOAE measurement to ensure that measurements are conducted in conditions within the known noise rejection limitations of the system and that levels behind the earplug does not trigger the MEM reflex.

The software used for the algorithms' processing, graphical user interface (GUI) and audio recording is developed in C language using Visual Studio and QT. This gives the programmers more flexibility as the algorithms can also run on regular desktop computers to test them in the laboratory before testing them *in situ*. This way, the software is easier to debug during the development phase and is directly usable for the portable ARP3 system. The developed software's GUI is controllable with a touch screen and stylus as shown in Fig. 2.1. Smartphones are therefore no longer needed with the DPOAE system.

The ARP3DPOAE is a practical all-in-one device integrating dosimeter, DPOAE measurement and audio recorder features and that fits in a fanny pack as shown in Fig. 2.2. Four complete systems have been assembled in order to test 4 individuals simultaneously during the *in situ* experiments.

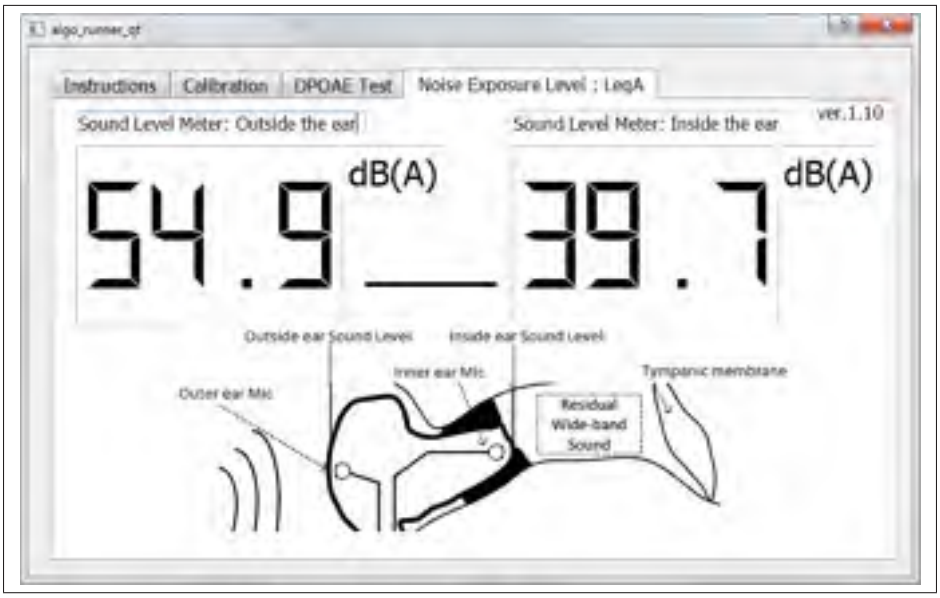

Figure 2.4 Screenshot of the built-in sound level meter screen showing sound levels outside the ear on the left and inside the ear on the right. A small schematic of the earpiece in the earcanal is shown in the software so that users can understand the use of the two values

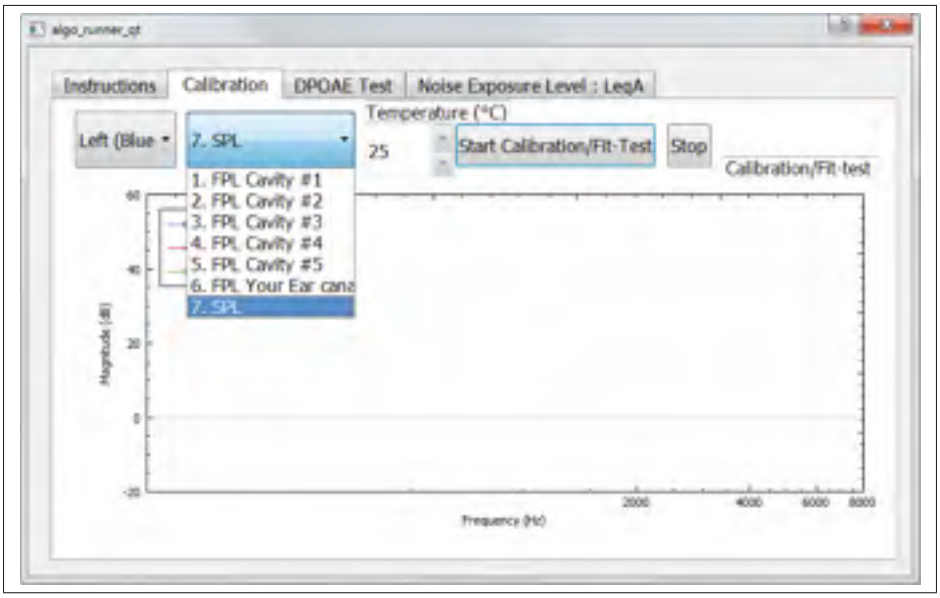

Figure 2.5 Screenshot of the calibration method selection in the Calibration tab. Users normally keep the default parameter, which is set at sound pressure level calibration 'SPL' for in-field calibration of the selected earpiece. The forward pressure level 'FPL' calibration method, presented in Section 2.2.2, is under development

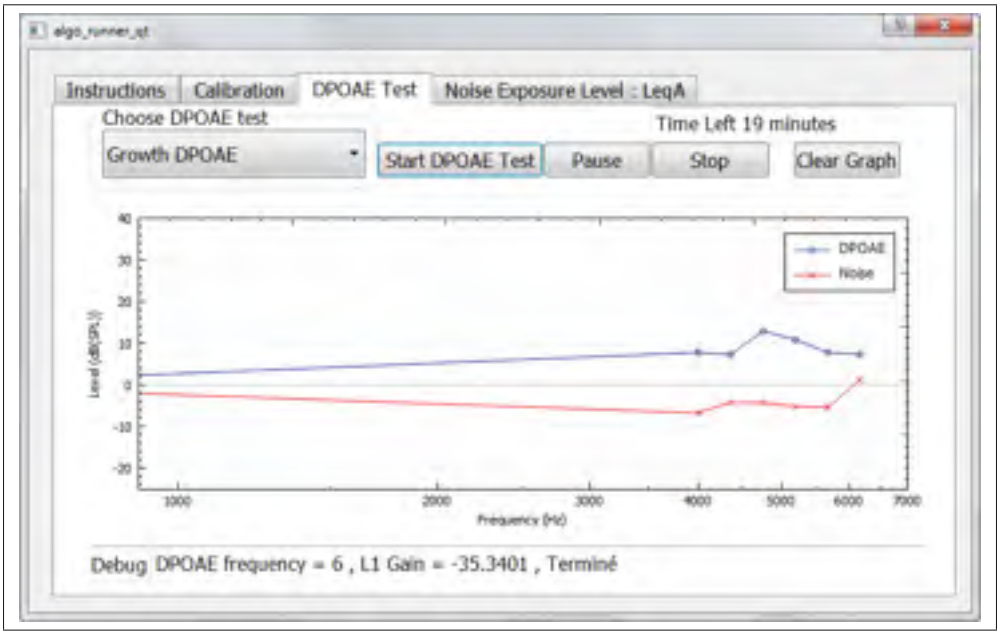

Figure 2.6 Example of DPOAE measurement shown in the software. Three stimuli levels are tested and the DPOAE levels are shown per f_2 frequency between 4000 and 6169 Hz for one stimulus level at a time. The DPOAE growth function can be analyzed afterwards from the saved data. Growth DPOAE measurement is set as the default so that users can easily start these measurements when the timer notifies them every 20 minutes

Limitations

In spite of the major improvements over the previous generation of the system. The second generation of the DPOAE system still has a few limitations that can be improved in the near future. These limitations are presented below:

1. The dynamic range of the SoundBoard is restricted due to the power supply rails that are shared with a chip that needs ± 2.75 V rails for proper operation. This can be fixed with a new version of the SoundBoard with separate 5 V rails and 2.75 V rails (see Appendix II). At the same time, the size of the SoundBoard could be optimized by removing the OEM's conditioning amplifier stage to use the SoundBoard specifically in the DPOAE and sound level meter configurations.

2. The implementation of the 4-channel inputs (IEM-I, IEM-C, OEM-I, OEM-C) at 24-bit and the selected 2-channel outputs at 44100kHz sampling rate was challenging since the USB2.0 interface represented a bottleneck for all the data.This required to develop a firmware patch that re-synchronizes all buffered USB streams, thus losing one sample approximately every 20 minutes. This implementation could be improved in the future with some help of audio driver experts.

3. The developed software contained a priority scheduling problem between the different processing threads which occasioned short discontinuities in the audio data (.dat) file recorded on the SD card. This has been discovered while post-processing the raw audio signals for the experiment presented in Chapter 4. The problem has been solved by containing the problematic code in a "critical section" (Microsoft, 2019) to ensure the threads priority does not overwrite the buffers in the software while it is copying on the SD card.

4. The miniature computer (Yuntab, 2019) used in the ARP3DPOAE has several problems such as the battery discharging too fast, although the internal battery is supposed to last approximately 2 hours and there is an external battery connected through the micro-USB charging port of the computer. This makes the system shut down quite often during experiments. This problem occurs regularly with 2 systems out of the 4 systems built. Moreover, the computer needs to be in its original aluminum casing for heat dissipation otherwise it shuts down due to overheating. Hence the system cannot be integrated in a smaller box with other components. Besides, the miniature computer is discontinued by the manufacturer and cannot be replaced with new ones. More expensive miniature computers are now available on the market (Ockel, 2019) with integrated touch screens. These new computers are a good replacement solution, but building four new systems will substantially increase the costs of the project as well as the time necessary to test the integration of the software and electronics in one box.

2.1.3 Partial conclusion

A portable DPOAE measurement device has been designed for the *in situ* hearing health monitoring during noise exposure. Two versions of this system have been developed and used in different experiments throughout the doctoral project. These systems allow to record DPOAE measurements, noise exposure levels and raw audio signals for further post-processing. The results obtained with both systems have been used for publications as shown in Chapters 3 to 5.

2.2 Earpiece Calibration methods

2.2.1 In-silence fit-test and calibration method

Probe fit-test

To ensure the DPOAE probe is well positioned in the earcanal for proper hearing protection and DPOAE measurement before being exposed to ambient noise the fit is tested "in-silence", i.e. without external sound source. This is achieved by comparing the magnitude at 150 Hz with the reference magnitude at 1000 Hz of the secondary transfer function which identifies the path between the loudspeaker and in-ear microphone (see Fig. 2.7). As shown in Fig. 2.8, the magnitude at 150 Hz is sensitive to earplug leaks, which is explained with acoustical modeling in Appendix III. This low frequency is selected since it is known to be less affected by Helmholtz resonances caused by the narrow air leak in the mechanical coupling between the probe and the earcanal. The earpiece position is considered a good fit, as shown in Fig. 2.9, when the magnitude at 150 Hz is within 2 to 8 dB below the reference magnitude. On the other hand, a leak is detected and the system notifies the user to re-fit when the magnitude at 150 Hz is 9 dB below the reference magnitude . A re-fit is also required if the two miniature loudspeaker calibrations are different (>5 dB) within the high frequency range, i.e. when the f_1 = 5057 Hz stimulus frequency is more than 5 dB above the f_2 = 5187 Hz stimulus frequency , as this indicates that the probe tubes are too close to the walls of the external auditory meatus. The system also notifies to re-fit if the f_1 = 5057 Hz stimulus frequency is more than 10 dB above

the reference magnitude as this is another indicator of an air leak. The in-silence fit-test results have been previously verified experimentally by comparing the loudspeaker response at 150 Hz with the passive attenuation of the probe, i.e. the primary transfer function $G(z)$ shown in Fig. 2.7a, measured with an external loudspeaker (see Appendix III).

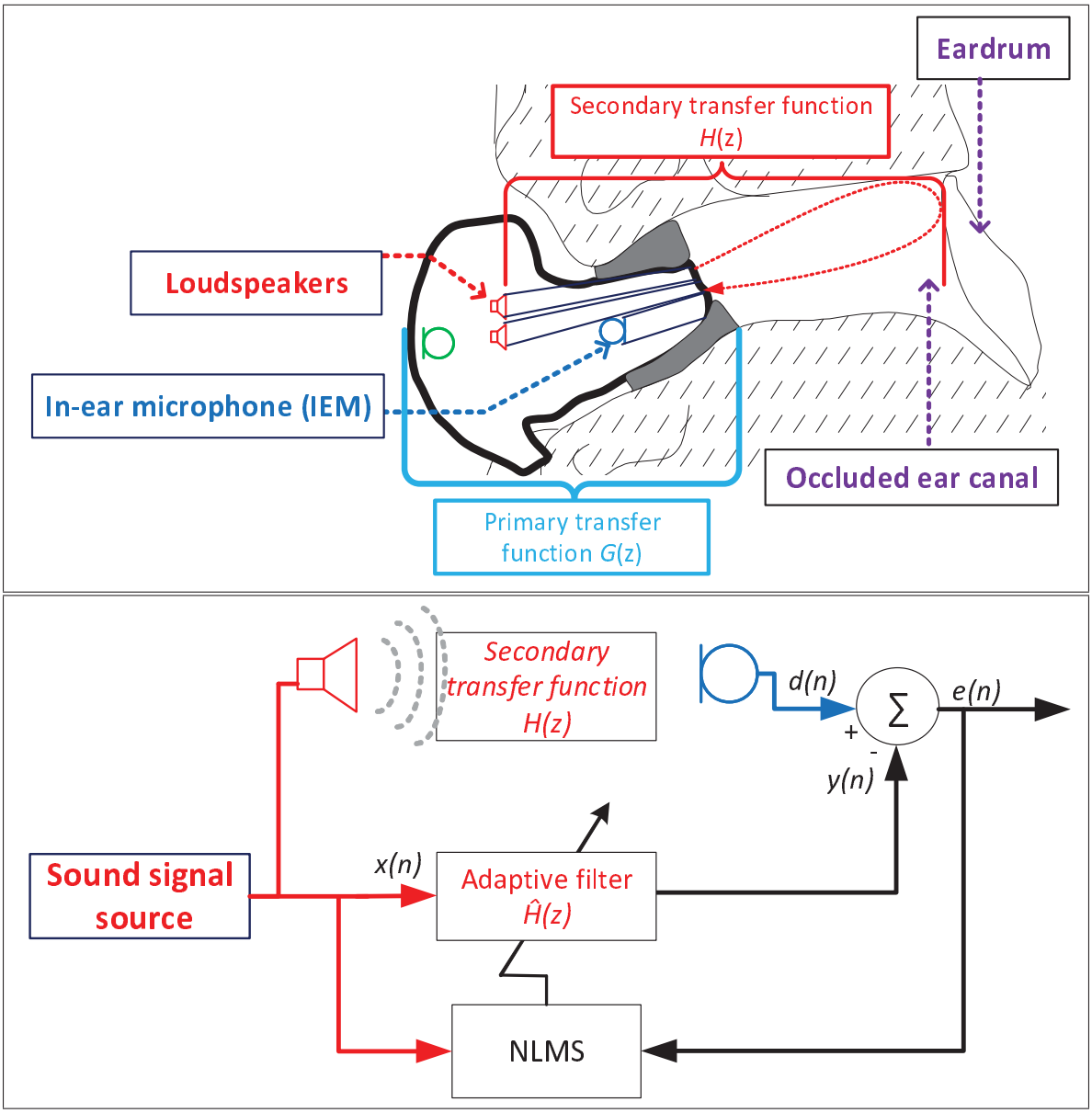

Figure 2.7 Schematic of the in-silence fit-test and calibration method showing the probe components and transfer functions (top) and the adaptive filtering signal processing for the identification of the secondary transfer function (bottom)

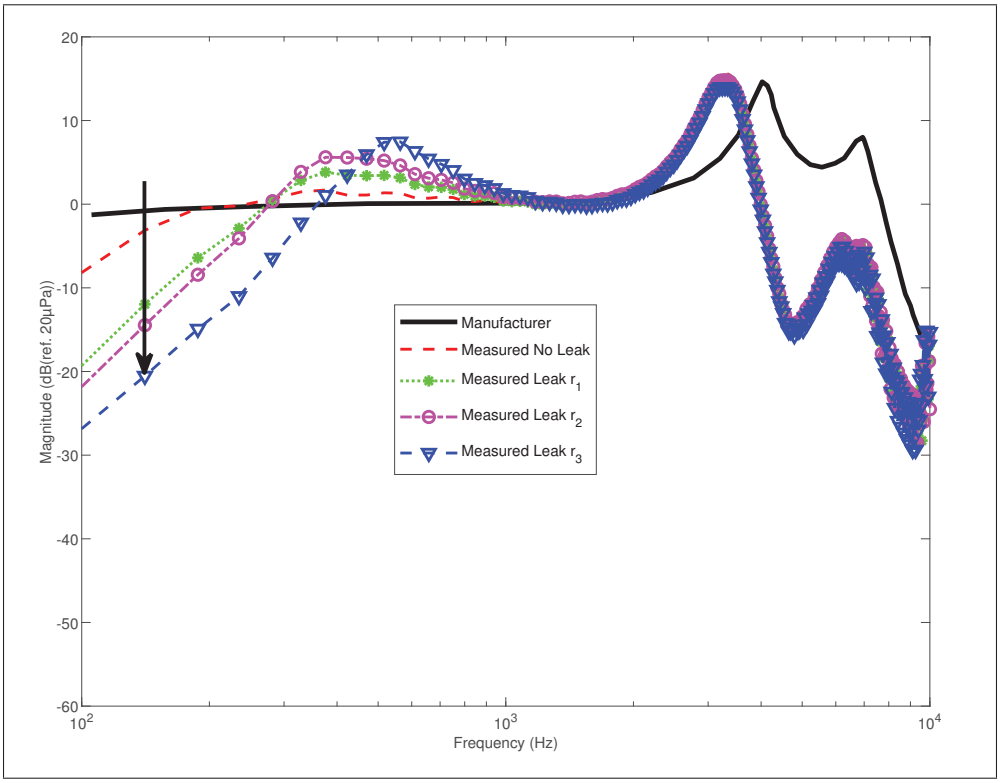

Figure 2.8 Loudspeaker's transfer function for in-silence fit-test assessment and DPOAE probe calibration, showing the typical magnitude reduction effect of leakage at 150 Hz with the black arrow

DPOAE stimuli calibration

The in situ stimuli calibration is performed at least once after the earpiece is fitted in the ear to ensure the DPOAE stimuli levels are well adjusted for the individual's earcanal acoustics at the moment a DPOAE level is measured. In addition to this calibration, the magnitudes at the discrete DPOAE stimuli (f_1 and f_2) and response (f_{dp}) frequencies are first compensated for the differences between the in-ear microphone response with the probe tubing and the reference microphone in the artificial ear of a head and torso simulator (HATS). This is achieved by identifying the transfer function between the probe and HATS microphones and then calculating the differences between the magnitudes at 1000 Hz and at the discrete frequencies f_1, f_2 and f_{dp}. Using this method, the stimuli levels are corrected to get the same level across all discrete frequencies at the HATS eardrum position . Then, the following *in situ* calibration ,

in the individual's ear, compensates for differences between individuals' earcanal acoustics in reference to the initial calibration in the HATS. An example of the correction values for the stimuli and DPOAE levels in the HATS is shown in Table 2.1. This correction is only calculated once in the laboratory and does not need to be adjusted *in situ*.

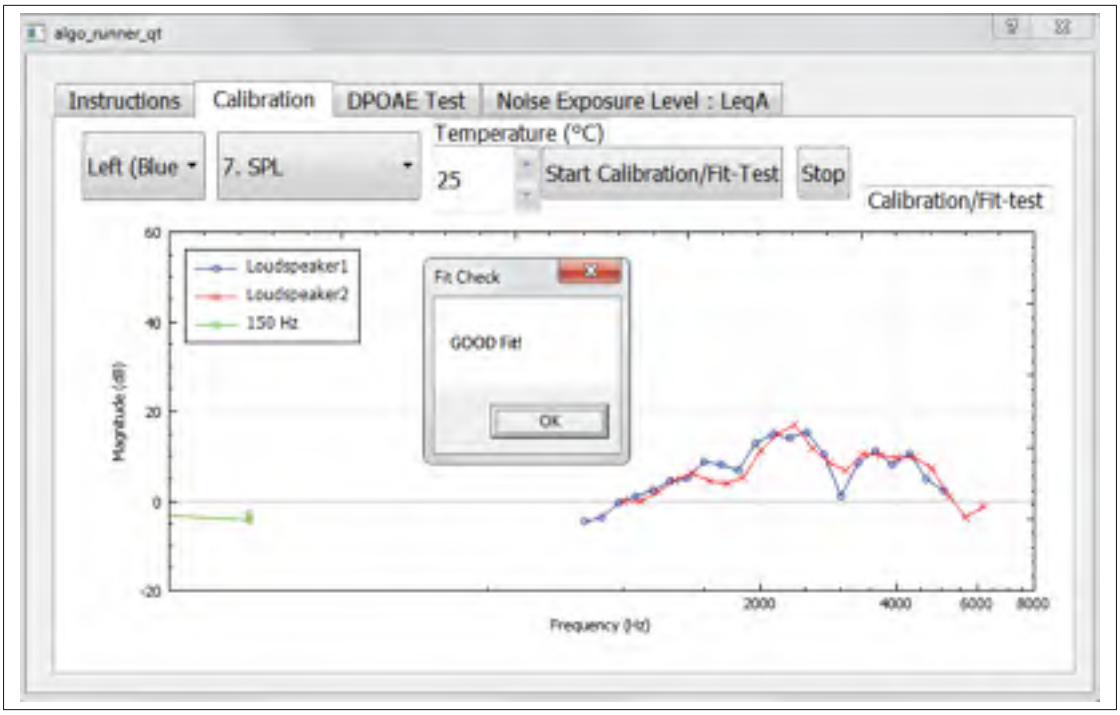

Figure 2.9 ARP3DPOAE's GUI showing a good earpiece fit in a human ear

The *in situ* DPOAE stimuli calibration is a basic method used simultaneously with the in-silence fit-test which consists in adjusting gains at discrete frequencies to compensate the emitted sound level. First, a wideband (e.g. white noise) stimulus signal is sent to the loudspeaker in order to characterize the full acoustical frequency range, i.e. frequencies from 20 to 20000 Hz. Then, the loudspeaker and earcanal acoustics transfer function, i.e. the secondary transfer function $H(z)$, is identified using an adaptive filter with the digital signal sent to the loudspeaker as the reference signal (x) and the in-ear microphone as the desired signal (d), see Fig. 2.7. Finally, the gains for L_1 and L_2 stimuli levels are adjusted by calculating the difference between the magnitudes at the discrete stimuli frequencies and the reference magnitude in the identified transfer function. This method is a quick and easy way to calibrate all stimuli signals within 30 seconds.

Table 2.1 DPOAE stimuli (f_1 and f_2) and response (f_{dp}) calibration values referenced at 1000 Hz used to compensate for earpiece tubing and ideal earcanal acoustics. Note: a 4 dB offset is integrated in the correction values for f_1 and f_2 to adjust stimuli levels L_1 = 65 dB(SPL) and L_2 = 55 dB(SPL)

f_1 (Hz)	Correction (dB)	f_2 (Hz)	Correction (dB)	f_{dp} (Hz)	Correction (dB)
5057	-2.7	6169	-4.5	3943	-2.0
4637	0.8	5657	1.0	3620	-4.7
4252	0.4	5187	-2.6	3319	-8.2
3899	3.0	4757	-3.2	3043	-11.6
3575	5.0	4362	-2.0	2791	-12.1
3279	7.8	4000	1.0	2560	-9.7
3007	11.6	3668	4.0	2342	-7.4
2757	9.0	3364	6.0	2147	-6.0
2528	5.0	3084	8.0	1967	-4.5
2318	4.0	2828	10.0	1808	-3.4
2126	4.0	2594	7.0	1655	-2.5
1949	4.0	2378	3.0	1518	-1.9
1788	6.0	2181	2.0	1396	-1.5
1639	6.0	2000	4.0	1279	1.0
1503	4.0	1834	5.0	1174	0.7
1379	3.0	1682	7.0	1071	0.3
1264	3.0	1542	6.0	985	0.0
1159	3.0	1414	5.0	905	0.4
1063	4.0	1297	4.0	825	0.7
975	4.0	1189	3.0	761	1.0
894	4.0	1091	4.0	696	1.2
820	5.0	1000	4.0	641	1.4

This *in situ* calibration method is practical for in-field experiments . Nonetheless, to estimate the stimuli and DPOAE response levels that would be measured at the eardrum position with a probe microphone and obtain more precise DPOAE measurements in future experiments with the developed DPOAE system, an approach based on the forward pressure level is proposed in the following section.

2.2.2 Forward Pressure Level calibration method

The in-silence fit-test and calibration previously described is well adapted for in-field tests for its ease of use and fast execution. However, this basic method does not compensate precisely for

the differences in sound pressure levels between the position at the earpiece tip ($SPL_{entrance}$ in Fig. 1.3) and the eardrum ($SPL_{terminal}$) which can be up to 20 dB due to interference between forward and reverse waves at frequencies near the quarter -wave nulls of the occluded earcanal. These differences mainly affect the sound pressures when the OAE stimulus (f_1 or f_2) and the OAE response are at the same frequency with stimulus-frequency OAE (SFOAE), which is not the case for DPOAEs. Therefore, the interpretation of the effects of quarter-wave nulls on DPOAEs is more complicated as the impact of calibration errors are less predictable (Charaziak & Shera, 2017).

Considering the various earcanal shapes (between-subject variations) and insertion depth of the earpiece (within-subject variations), a robust calibration method could help to minimize systematic differences in DPOAE levels. Therefore $SPL_{terminal}$ should be estimated in individuals using a non-invasive method as this sound pressure level is a more stable reference between- and within-subjects than $SPL_{entrance}$. To estimate this $SPL_{terminal}$ the emitted sound pressure component from the loudspeaker, known as the forward pressure level (Scheperle *et al.*, 2011), can be estimated from the sound pressure level measured at the earpiece position using the Thevenin equivalent of the loudspeaker . This removes the reflected sound pressure component from the total sound pressure level for an accurate estimate of the sound pressure level that would be measured close to the eardrum position. This method has been used lately for otoacoustic emission stimuli calibration and improved the precision in high frequencies, that is f> 5 kHz (Charaziak & Shera, 2017). The technique can also be applied in the opposite direction to correct the levels of the DPOAE response (Charaziak & Shera, 2017). However, this method requires high-end earpieces and acquisition cards to record the sound pressure responses with minimal distortion for the Thevenin estimate. In order to make this calibration method more accessible, an approach to condition the wideband calibration stimulus, such as a chirp or logarithmic chirp, is proposed to reduce the dynamic range necessary for the acquisition system. This allows to calibrate the earpiece frequency response relative to $SPL_{terminal}$ using a low resolution or high latency system, therefore reducing the cost. This proposed approach also gives the possibility to use analog conditioning amplifiers, generally included in DPOAE

systems, that can potentially clip or saturate the recorded IEM signal due to the resonance peaks in the occluded cavity. The use and integration of the FPL calibration and the proposed pre-conditioning method in this PhD project are detailed in Section 2.2.2.1.

2.2.2.1 Implementation of the FPL calibration method in the designed DPOAE system

2.2.2.1.1 Hardware

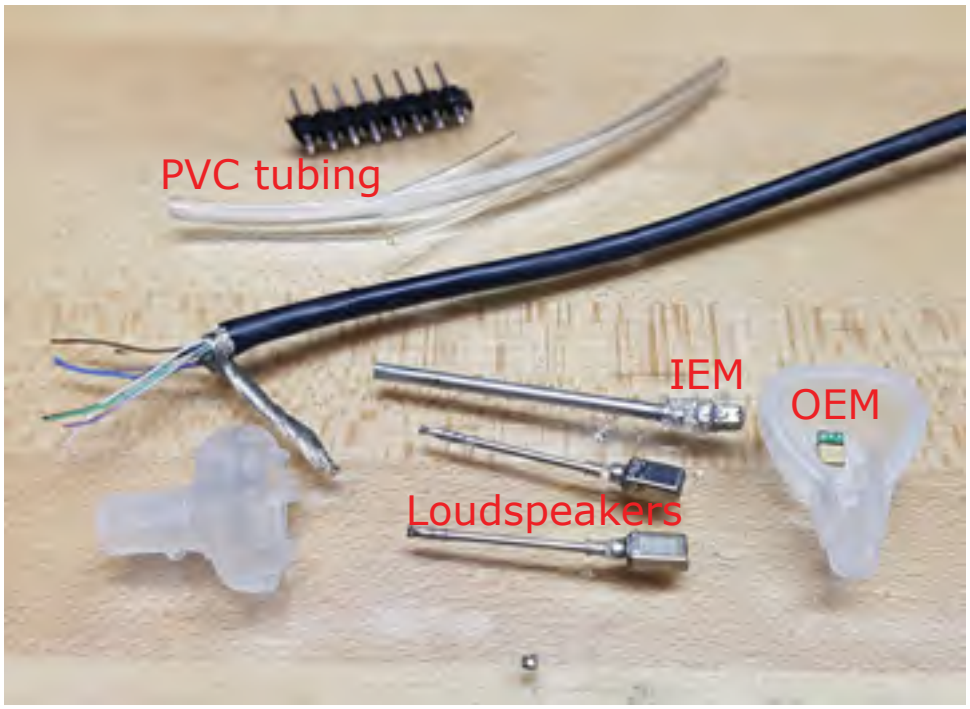

Figure 2.10 Metal tubing attached to the earpiece components for the specific design of the forward pressure level probe shown at the bottom in comparison to the PVC tubing are shown at the top

According to the "calibration error" (Charaziak & Shera, 2017) obtained with the forward pressure level calibration experiments conducted with the PVC tubing in the DPOAE probe in comparison to a reference ER-10B probe (Etymotic Research, Il, USA), a new DPOAE probe design was needed to minimize the system distortion (Charaziak & Shera, 2017; Richmond, S. A., Kopun, J. G., Neely, S. T., Tan, H. & Gorga, M. P., 2011). An earpiece has therefore been

designed with metal tubing for all in-ear components such as microphones and loudspeakers, these metal tubes are shown in Fig. 2.10 & 2.11. The hard walls of the metal tubing helped to maximize the reflections and thus minimize the distortion that can be caused by the transmission losses in adjacent tubing (Siegel, J. H., 1995).

Figure 2.11 Earpiece for FPL calibration with loudspeakers' metal tubes cut flush with the plastic underbody shown with the green silicone eartip . The IEM metal tube protruding by 4 mm compared to the loudspeakers' tubes helps to minimize evanescent waves

Table 2.2 Table of the cavity lengths measured physically with a digital caliper and estimated acoustically based on the resonance frequency peaks measured with the DPOAE probe in the cavity. A difference of approximately 6 mm is observed between the measured and estimated lengths, possibly due to the eartip insertion depth and the 4 mm length of the IEM tubing used to minimize the effects of the evanescent waves

Cavity	Physical length (cm)	Acoustical length (cm)
1	8.74	8.08
2	7.92	7.22
3	7.08	6.45
4	6.41	5.83
5	5.04	4.47

In order to identify the sound source's Thevenin equivalent, the choice of the cavity lengths is important for the FPL calibration to minimize the overlap between the different cavities'

resonance peaks and troughs as mentioned earlier in Section 1.3.2.2.1. To cover a higher frequency range for the DPOAE measurements (i.e. frequencies ranging from approximately 500 Hz to 8 kHz), cavity lengths have been selected between 1 and 9 cm. The cavities' acoustical lengths chosen for the designed probe are shown in Table 2.2.

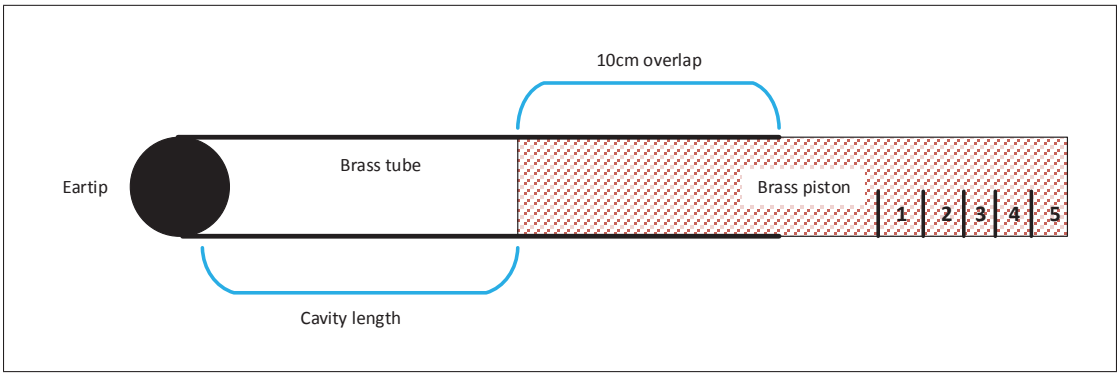

Figure 2.12 Schematic of the cavity with variable lengths achieved with the sliding piston with a very precise outer diameter that fits snuggly in the inner diameter of the brass tube. The piston needs to be at least approximately 10 cm in the tube to allow sufficient acoustical seal for FPL calibrations

Figure 2.13 Picture of the cavity with variable lengths achieved with the sliding piston with a very precise outer diameter that fits snuggly in the inner diameter of the brass tube. The piston needs to be at least approximately 10 cm in the tube to allow sufficient acoustical seal for FPL calibrations

To optimize the decay of evanescent modes and minimize the effects of the evanescent waves on the measured IEM pressure (Huang, G. T., Rosowski, J. J., Puria, S. & Peake, W. T., 2000), brass tubing with precise dimensions and a small inner diameter is used for the cavities, e.g. 7.9mm inner diameter is the closest to the earcanal dimensions (Charaziak & Shera, 2017; Scheperle *et al.*, 2011). The cavity lengths are then adjusted by sliding a piston in the brass tube as shown

in Fig. 2.12 & 2.13. This keeps the probe positioned in the same tube and helps the Thevenin estimation since the insertion depth and seal are unchanged, resulting in more accurate acoustical length estimation.

To minimize the error in the estimated acoustical length further, the green silicone eartip shown in Fig. 2.11 & 2.13 is mounted flush with the probe for a snug fit with the calibration cavities, therefore minimizing the leakage and volume behind the IEM tube end. A foam eartip can be used afterwards for the FPL calibration in the human earcanal for a comfortable fit. To ensure that the stimulus does not generate distortion when identifying the cavity pressure responses for the Thevenin equivalent estimation, special signal processing techniques are used and detailed in Section 2.2.2.1.2.

2.2.2.1.2 Signal processing

The stimulus signal to identify the cavity pressure responses consists in 12 cycles of 2048 samples. The first two cycles are used for synchronization of the acoustical and digital waveforms, since there is a small delay between the generation of the signal through the miniature loudspeakers and the IEM recorded signal. These two synchronization cycles use a 3 kHz sine wave windowed with Envelope 1, as shown in Fig. 2.14. The envelope helps to reduce the generation of harmonics, i.e. ringing, caused by a fast zero-crossing and also to enhance the latency estimation. This sine wave frequency is chosen for all cavity lengths to minimize possible constructive interference due to the reflected wave in the occluded cavity. The precise estimate of the system's latency is obtained with a cross-correlation between the generated sine wave signal and the captured signal with the IEM. This latency is compensated using a delay (D) in the time averaging algorithm, shown in Fig. 2.14, for the cavity frequency response estimation. The following 10 cycles to identify the response in the cavities use a logarithmic chirp to minimize the distortion in the wideband frequency response, maximize the high frequency response and compensate for the loudspeaker roll-off (Scheperle *et al.*, 2011). This chirp signal is enhanced to minimize the saturation of the IEM signal using a pre-conditioning algorithm detailed in Section 2.2.2.1.2.

Signal pre-conditioning

The signal pre-conditioning method consists in filtering and windowing the chirp signal $S_2(n)$ emitted by the loudspeaker to ensure the acoustical signal magnitude of the occluded cavity resonance's peaks do not saturate the recorded IEM signal, and ensure the resonance's nulls are above the recording system's noise floor for optimal dynamic range. This is achieved by filtering the chirp signal with one or two Infinite Impulse Response (IIR) notch filters in series with central frequencies at the first harmonics of the selected cavities' resonance frequencies, which are estimated with the acoustical lengths of wavelength λ, as shown in Fig. 2.14. For example, the central frequency is set at $f_{c1a} \approx 2$ kHz for the first notch filter and $f_{c1b} \approx 4.2$ kHz for the second notch filter of the first cavity as shown in the emitted response in Fig. 2.15. Afterwards, to minimize the ringing caused by the discontinuities since the signal is generated in a loop, while not compromising the frequency range of the pressure response, the chirp signal is windowed with a fade-in/fade-out function envelope (Envelope 2) over the first and last ≈50 samples.

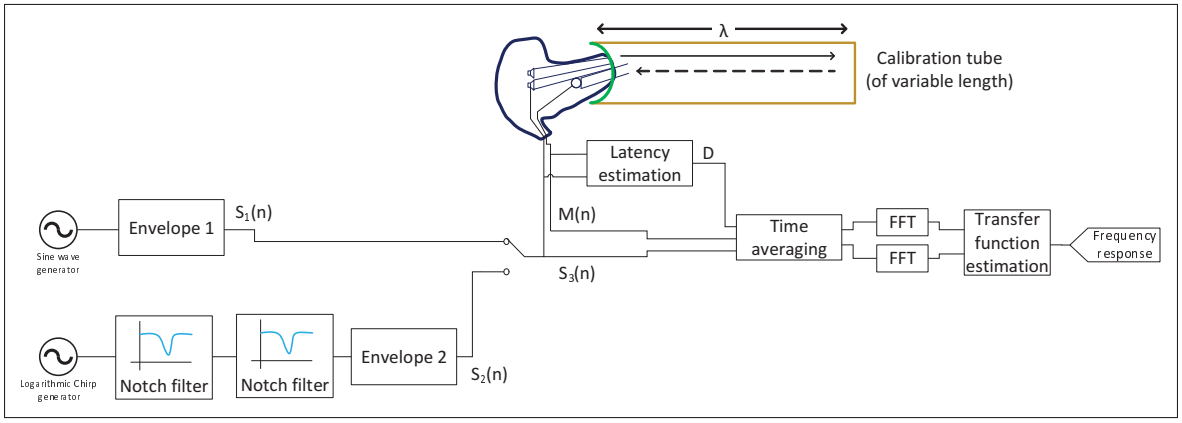

Figure 2.14 Schematic of the FPL calibration pre-conditioning method

The signal processing for the 12 recorded cycles shown in Fig. 2.14 is done offline in the designed software. The temporal averaging starts at the sample index indicated by the latency D plus two 2048-sample cycles in order to average only the logarithmic chirps. A Fast Fourier Transform (FFT) is then computed on both the digital signal sent to the loudspeakers $S_3(n)$ and the captured IEM signal $M(n)$. The sound pressure frequency response for the selected cavity, e.g. P_1 shown

in Fig. 2.15, is then calculated on the ratio of the two FFTs using a transfer function, as shown in Fig. 2.14. The pre-conditioning method has been tested in MATLAB (Mathworks, 2018) prior to the integration in the designed DPOAE system, the results of the FPL calibration using this method are presented below.

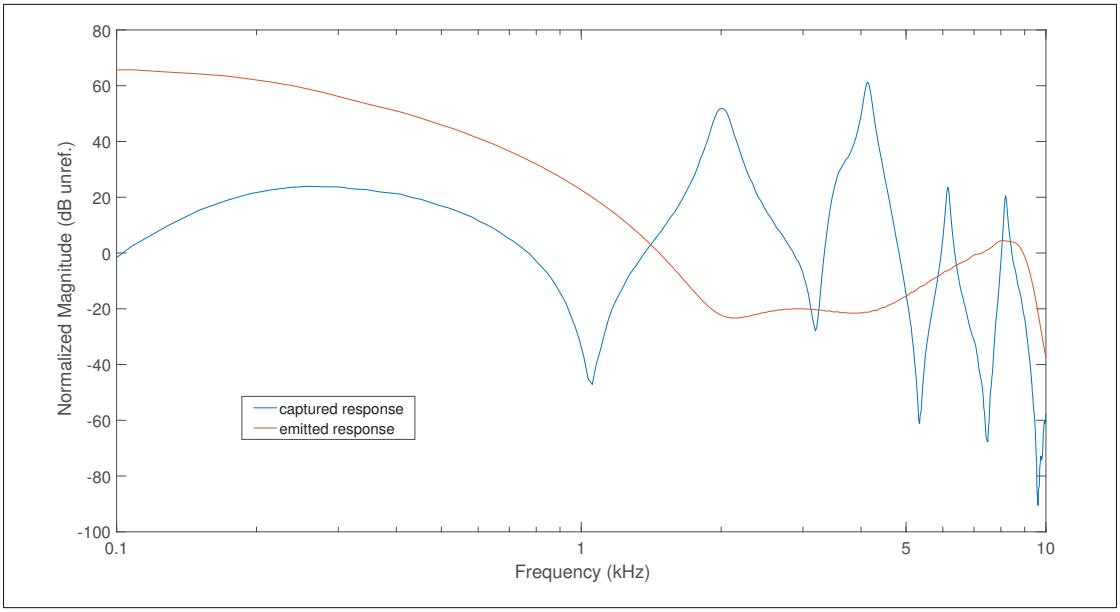

Figure 2.15 Frequency response emitted and captured to show the minimal distortion up to 9 kHz and the notch of the filters and roll-off of the ramp window in the emitted response

2.2.2.2 Practical use of the FPL calibration with the designed pre-conditioning method and OAE probe

The goal of the FPL calibration method is to estimate the sound pressure level at the eardrum position ($SPL_{terminal}$) without using a probe microphone with its tube touching the eardrum. So the FPL calibration has been tested in a short cavity of 17.8 mm long with an inner diameter of 9.9 mm, shown in Fig. 2.16, to simulate an eardrum with a probe microphone connected at the eardrum position to measure $SPL_{terminal}$. The forward pressure level is then compared to $SPL_{terminal}$ and the uncorrected $SPL_{entrance}$ measured at the cavity entrance with the DPOAE earpiece in Fig. 2.17. The effects of the DPOAE probe's IEM tubing are calculated with a transfer function between the earpiece microphone and a second microphone without tube positioned

within a millimetre. These effects are applied on $SPL_{terminal}$ to show the good agreement of '$SPL_{terminal}$ with tube correction' with the FPL, which includes this tube response. This close match between responses indicates that the DPOAE frequency range could be extended up to approximately 8 kHz with the FPL calibration method. The $SPL_{entrance}$ response differs from the FPL above approximately 2 kHz for the cylindrical cavity tested. However, earcanals do not have an ideal cylindrical shape, hence further experiments are required in human ears to confirm the robustness of FPL calibration compared to $SPL_{entrance}$.

Figure 2.16 Setup used to compare the different sound pressure response measured in a test cavity simulating an earcanal with the DPOAE earpiece at the entrance and the probe microphone at the eardrum position

2.2.3 Partial conclusion

The in-silence fit-test method is a complementary method to the FPL calibration. Integrating these methods in the DPOAE system would allow users to assess the DPOAE probe fit for proper hearing protection before being exposed to noise and calibrate the DPOAE stimuli signals precisely at frequencies up to approximately 8 kHz. Further fine-tuning of the pre-conditioning algorithm parameters is necessary to minimize the distortion and to finalize the integration of the FPL calibration in the portable DPOAE system to test it in industrial conditions. Although this would allow more accurate baseline DPOAE measurements in high frequencies where more important cochlear damage can be observed and this would also allow to compare the absolute results between various studies. The FPL calibration is not essential to conduct the *in situ* measurements in this project since the repeated DPOAE measurement results are differential as

they are compared to the daily reference measurement and between the stimulation levels in the growth DPOAE measurement. Moreover, using a calibration tube to calibrate the probes each time the user needs to re-fit the probe may actually complicate the measurement procedure for non-expert users and cause more calibration problems. In addition, the tested DPOAE frequency range in the PhD project is limited below f_2 = 6200 Hz and might not substantially benefit from the improvements in high frequency accuracy according to the specific frequency range affected by the method as mentioned in the literature. Hence, further testing of the FPL calibration method with the designed DPOAE system is needed before using the method in the workplace for continuous DPOAE measurements.

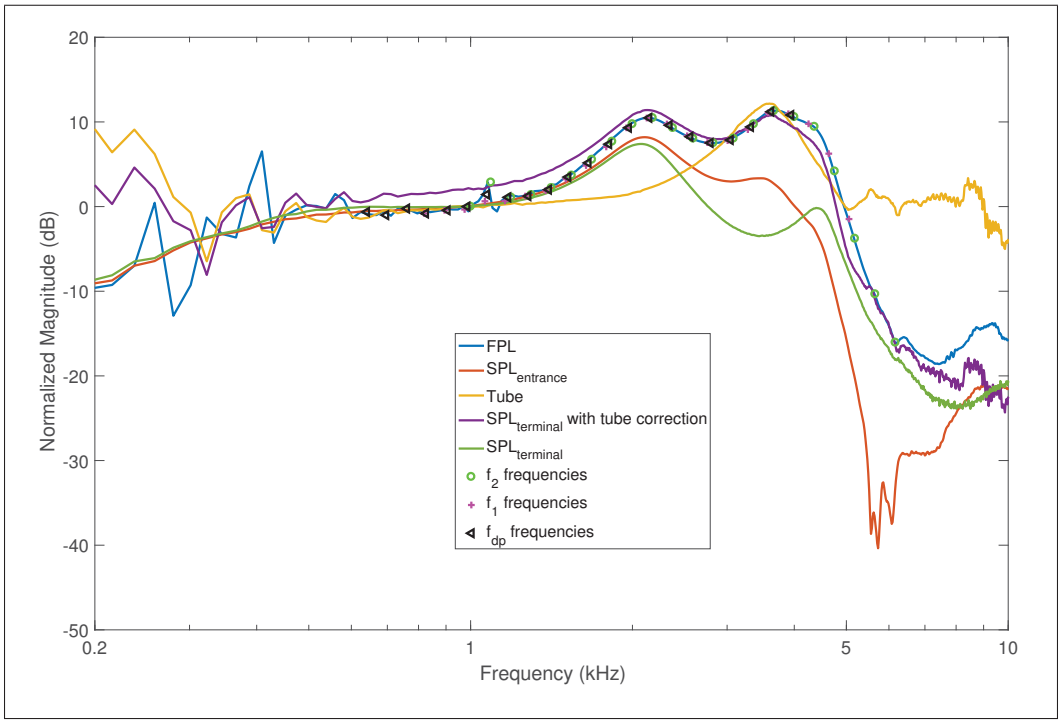

Figure 2.17 Frequency responses from 200 Hz to 10 kHz obtained with the different sound pressure estimates presented in Table 1.1, showing a good agreement between the FPL and $SPL_{terminal}$ with tube correction

CHAPTER 3

FIELD MONITORING OF OTOACOUSTIC EMISSIONS DURING NOISE EXPOSURE: PILOT STUDY IN CONTROLLED ENVIRONMENT

Vincent Nadon[1], Annelies Bockstael [2], Dick Botteldooren[3], Jérémie Voix[1]

[1] École de technologie supérieure, Mechanical Engineering department,
1100 Notre-Dame Ouest, Montréal, Québec, Canada H3C 1K3
[2] Université de Montréal,
7077 avenue du Parc, Montreal, Quebec, Canada, H3N 1X7
[3] Ghent University, WAVES research group,
Technologiepark, Zwijnaarde 15, B-9052, Ghent, Belgium

Article published in American Journal of Audiology in October 2017.

3.1 Abstract

Purpose: In spite of all the efforts to implement workplace hearing conservation programs, noise-induced hearing loss remains the leading cause of disability for North American workers. Nonetheless, an individual's susceptibility to noise-induced hearing loss can be estimated by monitoring changes in hearing status in relation to the level of ambient noise exposure.

The purpose of this study was to validate an approach that could improve workplace hearing conservation practices. The approach was developed using a portable and robust system designed for noisy environments and consisted of taking continuous measurements with high temporal resolution of the health status of the inner ear using otoacoustic emissions (OAEs).

Method: A pilot study was conducted in a laboratory, exposing human subjects to industrial noise recordings at realistic levels. In parallel, OAEs were measured periodically using the designed OAE system as well as with a commercially available OAE system, used as a reference.

Results: Variations in OAE levels were analyzed and discussed along with the limitations of the reference and designed systems.

Conclusions: This study demonstrates that the monitoring of an individual's OAEs could be useful in monitoring temporary changes in hearing status induced by exposure to ambient noise and could be considered as a new tool for effective hearing conservation programs in the workplace.

3.2 Introduction

Over 22 million North American workers are exposed daily to noise doses that may induce hearing loss (NIOSH, 2016), and despite efforts for workplace hearing conservation programs (Canetto, P., 2009), occupational hearing loss remains the most reported work related disability. In an attempt to solve this problem, current practices in hearing conservation usually involve the use of hearing protection devices as an easy solution against high-noise-level exposure and periodic hearing tests to monitor the workers' hearing health. On the basis of ambient noise exposure levels and local noise regulations, the workers' hearing levels are monitored regularly, usually yearly, with audiograms. However, the intervals between each test are generally too long because between appointments, hearing damage can gradually increase before it is detected and before actions can be taken to remediate the situation. Therefore, shorter intervals could be required between audiograms depending on a worker's susceptibility to noise exposure. For practical reasons, however, the shortest measurement interval is about 8-hr because tonal audiometry is time consuming, and audiometry requires a low-noise test environment because it is difficult for subjects to hear the tones in noisy environments, making it quite disruptive for the worker's routine.

In addition, at the moment, there is no way to determine if the maximum noise dose on the basis of an 8-hr work shift, as is recommended by legislation, is suitable for a given individual, because of the individual's own susceptibility to noise-induced hearing loss (NIHL). As a result, even with the current legislation in Europe and North America, 18% of workers run the risk of developing NIHL over the course of their work life (ISO, 2013). The assessment of the risk of incurring hearing trauma by the current legislation takes into account neither the frequency spectrum nor the temporal fluctuations in noise exposure for individual workers. Moreover, the

passive attenuation provided by hearing protectors can vary over time and between individuals, resulting in differences in noise exposure levels under the protector. Therefore, to identify the characteristics of the kinds of noise that cause hearing loss and quantify the maximum dose allowed for a given worker's own susceptibility to ultimately take appropriate actions at the right time to prevent further damage, it would be of clear benefit to have a system that is able to simultaneously record and process the noise frequency spectrum to calculate the cumulative dose and also to continuously measure the outer hair cells' (OHCs') response, enabling true prevention of NIHL.

To achieve this type of inner ear health measurement system, it is possible to use otoacoustic emissions (OAEs). Excessive noise exposure damages hair cells in the cochlea and other structures, and OAEs can be an early indicator of these changes in ear health (Sliwinska-Kowalska *et al.*, 2001). OAE measurements are an objective, and the fastest way, to test and assess the health of OHCs, because the active participation of the worker is not needed. This eliminates issues found in some subjective tests such as classic audiometry, for instance, in which results can be affected by the learning process and sensitivity to test conditions, and are time-consuming. However, as mentioned, the clinical devices available at the moment and the test duration make it impossible to monitor the cumulated hair cell harm continuously in an industrial workplace due to the devices' sensitivity to ambient noise. As a consequence, very few experiments using available systems (Zare *et al.*, 2015) have been conducted in a noisy industrial work environment, as it is difficult to obtain a reliable measurement due to the noise interference disturbing the recorded signal.

As a solution for the noise interference in OAE measurements, a robust system that is able to evaluate the variations in workers' OHC health during a daily work shift was designed. For the proposed approach, this system uses distortion product OAE (DPOAE) to test the OHCs' health status with an adaptive filtering noise rejection algorithm to reduce the interference of noise. DPOAEs are frequency specific, enabling easy comparison with results from other hearing tests such as audiograms. Continuous DPOAE measurements eventually will be used, in addition to noise dose measurements, to establish the relationship between the changes in OHC activity

and the noise dose to which each individual worker was exposed. This type of dose– response relationship provides a direct measurement of the effects of noise on OHCs with high temporal resolution, giving the opportunity to take appropriate action at the right moment. Moreover, the relationship could provide personalized information on an individual's susceptibility to noise and his or her risk of developing NIHL over time. Such a hearing assessment tool and method to detect early changes in hearing status could definitely benefit translational researchers and clinicians and could hopefully stimulate new research and result in greater knowledge about hearing mechanisms.

This study is original compared with previous studies because the DPOAE signals are processed here with adaptive filtering noise rejection in real time on the system's processor to provide faster and more reliable DPOAE measurements in higher ambient noise levels. Moreover, for the purpose of this study, DPOAEs were measured in sound pressure levels of LAeq-4h = 85 dBA, which are noise conditions in which DPOAE measurements have not previously been reported (Nadon *et al.*, 2015a) on the basis of the authors' present knowledge of the literature.

The main objective of this study is to validate that the inner ear health monitoring approach using the recently designed system is able to detect OHC changes by observing variations in DPOAE levels during noise exposure. Other audiological measurements such as pure-tone audiometry (PTA) and acoustic reflex threshold (ART) tests were also conducted pre-exposure and post-exposure to acquire reference data about other possible mechanisms involved with the DPOAE shift.

To make sure the designed DPOAE system was measuring true physiological DPOAE changes, its variability between consecutive measurements in noisy conditions was calculated. The designed system was also compared with the commercial device used here as a reference system using two metrics: (a) deviation from the pre-exposure measurement and (b) measurement duration. The deviation from the pre-exposure, that is, baseline, measurement gives information on the system's performance in loud environments for eventual continuous monitoring of OHCs. The measurement duration to cover the DPOAEs' frequency range for the reference system was

compared with the designed system, bearing in mind that measurements with high temporal resolution are needed for early detection and intervention, such that measurements had to be as short as possible.

3.3 Method

3.3.1 Screening

The study was approved by the Research Ethics Office of Ghent University, an institutional review board. Convenience sampling was used to find participants for the experiment, that is, an invitation was sent to university students. The nine test volunteers (six men, three women) went through a screening test, starting with an otoscopic examination to make sure that no cerumen could potentially clog the DPOAE probes and that the molding of the custom-fit ear tips would not clog the earcanal. A standard DPOAE test in each ear was recorded with the reference system to verify that the subject had DPOAEs present for most of the tested frequencies. If DPOAE levels were detected over 5 dB SPL for about 80% of the tested frequencies, on the basis of normative data (Keppler, H., Dhooge, I., Maes, L., D'haenens, W., Bockstael, A., Philips, B., Swinnen, F. & Vinck, B., 2010a), the subject was then screened with a classic PTA test in each ear with a -10 dB/+5 dB step. Subjects were retained for the study if their hearing thresholds were below 25 dB HL for about 85% of the tested frequencies from 250 to 8000 Hz, bearing in mind that frequencies $\leq$ 4 kHz are expected to be less vulnerable to permanent threshold shifts. The ear tested for continuous DPOAE measurements was randomized unless a problem was detected with one ear during the screening.

For the subjects tested using the designed system, the probe tips were custom molded in the subjects' ears using the proprietary SonoFit (Sonomax, 2016) automated self-fit process. The probe tips were then adapted to the DPOAE probe's electronics core. The DPOAE probes also served as hearing protectors during ambient noise exposure in this study. Therefore, the DPOAE probe passive attenuation was measured, using the field microphone-in-real-ear (F-MIRE) method (Voix, J. & Laville, F., 2009), by sending wideband noise in front of the subject with the

DPOAE probes fitted in the subject's ears, and by calculating the transfer function between the external and internal microphone signals for both ears. A simplified probe fit test method, on the basis of the magnitude of the frequency response at low frequencies (Nadon *et al.*, 2015a), was also integrated in the designed device. The initial F-MIRE and probe fit test data were kept for reference for the subsequent probe fit test in the field using the simplified approach.

3.3.2 Experimental setup

The pure-tone hearing threshold levels (HTLs) were measured manually using the Hughson–Westlake method on a commercial AC5 audiometer (Interacoustics) with TDH-39 audiometric headphones (Telephonics). The threshold levels were evaluated on seven octave bands: 250, 500, 1000, 2000, 4000, 6000, and 8000 Hz for the screening test; for daily monitoring, 250 Hz was replaced with the intermediate 3000-Hz octave band, which is better for detecting changes caused by noise exposure.

To test the stapedial reflex threshold known as the ART, a Titan (Interacoustics) otoadmittance system was used. Before each ART measurement, a standard tympanometry was performed automatically by the system to remove any static pressure on both sides of the eardrum. The reflex was measured by sending narrowband noise, centered at three different test frequencies of 1, 2, and 4 kHz, into the ipsilateral ear. While the noise level was increased from 70 to 90 dBA, the probe simultaneously measured changes in earcanal impedance to detect when the change in acoustic immittance exceeded the deflection criteria of 0.03, set by default with the otoadmittance system, and then recorded this noise level as the ART.

The reference DPOAE system was an ER-10B+ probe and amplifier system (Etymotic Research) connected to a laptop computer with a Fireface 802 soundcard (RME). The laptop used the EMAV software (Neely & Liu, 1994) to measure the DPOAEs. The ER-10B+ microphone amplifier was set at a gain of +20 dB. Premolded silicone ear tips were used on the probe during the experiment, and the contralateral ear was blocked with a disposable foam earplug during noise exposure. Before conducting the experiment, the probe system parameters were calibrated

in EMAV, according to the instructions provided in the software's manual (Neely & Liu, 1994). The software used a sampling frequency of 44.1 kHz with a window of 8192 samples and used a noise threshold limit (NTL) of 8 mPa as default. The NTL is used in EMAV to reject a DPOAE sample when an artifact is detected, that is, when the calculated noise level is higher than this threshold. Increasing the NTL therefore results in a less restrictive artifact rejection, potentially leading to the calculation of the DPOAE level on a recorded signal with noise interference.

The 22 selected DPOAE frequencies corresponded to f_2 frequencies ranging from 1000 to 6200 Hz with eight frequencies per octave, with an f_2/f_1 ratio of 1.22. Stimuli levels were set to L_1 = 65 and L_2 = 55 dB SPL. The DPOAE signal-to-noise ratio (SNR) criterion was set at 5 dB; therefore, any DPOAE level not respecting this criterion was not accepted, and the system remeasured that DPOAE frequency until the criterion was met at least twice and then averaged the two results. To reduce the measurement time duration, which was already extended in noisy conditions to fulfill the 5-dB SNR criterion, only one complete scan was measured when the subjects were exposed to noise, whereas two complete scans of the 22 DPOAE frequencies were measured for the screening. To complete the measurements during noise exposure with this system, the 8-mPa NTL had to be adjusted at the beginning of each measurement, resulting in greater disturbance recorded in the DPOAE measurement, because the level measured in the DPOAE frequency bin could consist of the sum of the ambient noise disturbance and the DPOAE itself. This results in an artificial increase of the DPOAE level. The software calculated the noise level on adjacent bins, which could be lower than this DPOAE frequency bin containing artifacts, thereby satisfying the 5-dB SNR criterion of the software but resulting in a greater deviation from the baseline measurement. When the NTL was not adjusted, the EMAV software would not pursue the measurement and would repeat the measurements on the same frequencies indefinitely.

A DPOAE measurement device designed in a laboratory, consisting of DPOAE probe earpieces and a DPOAE hardware box (shown in Figure 3.1), was used in the present study and is later referred to as the designed system (Nadon *et al.*, 2015a). Each of the two DPOAE probe earpieces contained two high-quality miniature balanced armature receivers (Knowles, FK series) to send

the two pure-tone stimuli without any sound distortion and one miniature microphone to measure the OAE response and physiological noise. A miniature microphone was placed in the probe earpiece facing outward, that is, pinnade, to measure the external ambient noise (probe details can be found in Nadon *et al.* (2015a)). A custom-molded ear tip, fitted to each subject's ear canals, was designed, into which could be slid the probe's electronic components core. This way, the custom-molded ear tips could simply be interchanged for each subject while using the same probe electronics, ensuring consistent electroacoustic responses across all the experiments.

Figure 3.1 The distortion product otoacoustic emission measurement device designed in a laboratory with its electronic hardware box and its two measurement probes featuring custom-molded ear tips

The choice of DPOAE hardware electronics was based on the Auditory Research Platform (CRITIAS, 2019), and the components were designed specifically to record DPOAE levels in noisy conditions. They integrated a signal conditioner, a digital signal processor (DSP), and a Bluetooth communication dongle to transmit the calculated DPOAE levels and background noise

levels to a smartphone. An Android smartphone application, shown in Figure 3.2, was designed to display the DPOAE data received from the device and to transmit various commands to the device, such as to switch frequencies. The box of the designed system measures approximately 8.0 x 7.5 x 4.0 cm and is therefore small enough to be worn by a worker, for instance, clipped on his or her belt, during the entire work shift. The system's two custom-molded DPOAE probes, required to extract the DPOAE signal using an adaptive filtering algorithm proposed earlier by the authors (Nadon *et al.*, 2017a), also served as custom-molded hearing protectors, as they provide high passive acoustic attenuation of the ambient noise.

The adaptive filtering noise rejection algorithm previously developed (Nadon *et al.*, 2015a) was implemented in the DSP together with the DPOAE and the noise level extraction algorithm previously developed (Nadon, V., Voix, J., Bockstael, A. & Botteldooren, D., 2014). While the ability of the system's algorithms to extract DPOAE levels in noisy conditions was already validated (Nadon *et al.*, 2015a), it was previously tested in noise levels lower than those here, which exceeded 85 dBA. The performance of the noise rejection algorithm assessed in previous works (Nadon *et al.*, 2015a,1) showed that the measured noise levels remained below the DPOAE levels, respecting the SNR criterion, when noise rejection is activated for moderate noise exposure levels, but a slight artificial increase in absolute DPOAE levels can result from the artifacts of the algorithms for higher noise exposure levels. Because an artificial increase in DPOAE levels can occur, especially for the higher noise exposure levels tested here, the evaluation of the designed and reference system performance is based on the deviation from the baseline DPOAE measurement.

In the present study, most of the algorithms ran in real time as opposed to off-line, and the DPOAE level output was processed, displayed, and saved "live" during the measurement, making it possible to repeat a measurement when necessary. To maintain a level of consistency across the two DPOAE devices tested, the f_2 frequency range was set at 1000-6169 Hz with eight tested frequencies per octave band for a total of 22 frequencies. The primary-tone frequency ratio f_2/f_1 was kept at 1.22. Stimuli levels were set at L_1 = 65 dB and L_2 = 55 dB. Each frequency was tested for approximately 2 s, during which the samples were averaged, for a total of 45 s for

a complete scan of the 22 frequencies. This sequence was repeated at least twice, and usually three times, when the measurement was disturbed by unpredicted events, such as coughing.

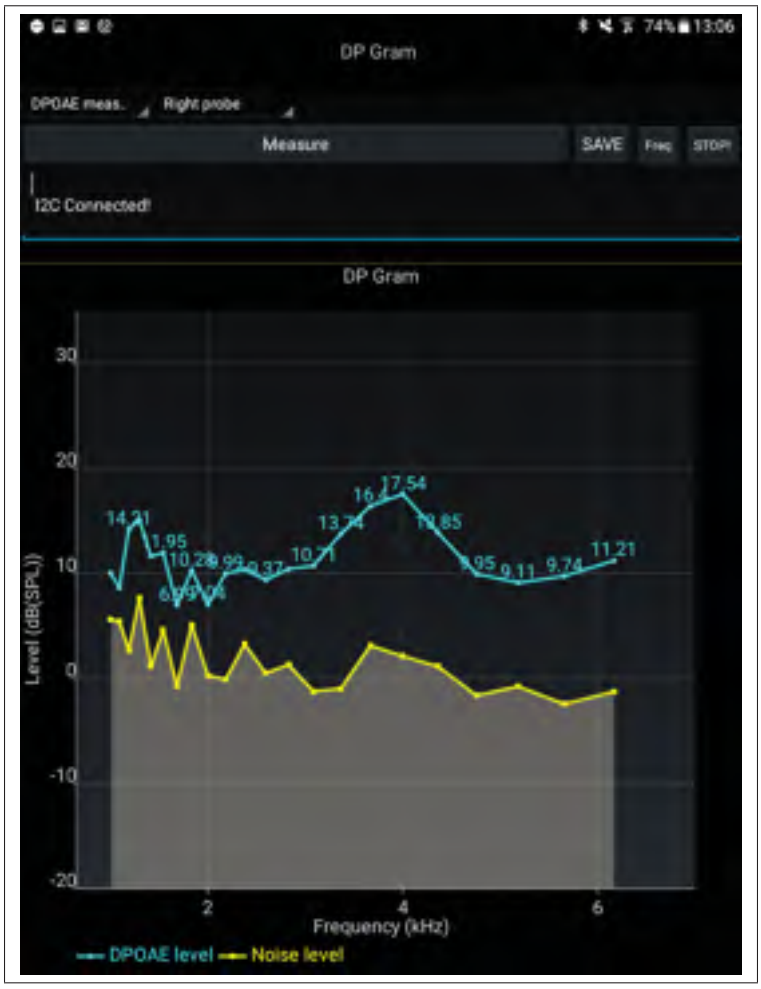

Figure 3.2 Screenshot of the designed Android smartphone application showing the distortion product otoacoustic emission (DPOAE) measurement data received over Bluetooth from the DPOAE device designed in a laboratory

3.3.3 Physical Experimental Test Setup

For optimal isolation from ambient noise disturbances, the measurements for screening, pre-exposure, and post-exposure were all conducted in a semi-anechoic room separated from

the noisy environment. For a more diffused and louder sound field, DPOAE measurements during noise exposure were carried out in a semi-reverberant room. The sound system used to simulate a noisy environment using noise recordings consisted of an amplifier connected to a laptop computer playing back industrial noise from the NOISEX-92 database (Carnegie Mellon University, 1992) and pink noise recordings. Two loudspeakers were positioned at a distance of 2.4 m from the test subjects, one on the left and one on the right, as seen in Figure 3.3. Noise levels were calibrated using the pink noise recordings at 87 dBA in the room with the SVAN 959 sound level meter (Svantek) placed approximately at the height of the subject's ears and in the middle, between the two seats, approximately 50 cm from the seats, without the subjects being present. Industrial and pink noise recordings were created at a high noise level of 87 dBA and were emitted at a constant level for the first 20 min, followed by a reduced level at 67 dBA and then held at a constant level for the next 10 min. These levels were determined in such a way as to take into account the passive attenuation of the ear tips and earplugs, so that the residual sound pressure level in the occluded ear canal would not trigger the acoustic reflex, at least during the 67-dBA exposure, when the DPOAE measurements were less disturbed by the high ambient noise levels, given that the noise levels usually required to trigger the acoustic reflex range from 70 to 100 dB SPL, with the average being at 85 dB SPL according to Sun (2008). As seen in detail in Figure 3.4 and at the top of Figure 3.5, this sequence was looped for 4 hr for the daily noise exposure with an L_{Aeq-4h} of approximately 85 dBA. To obtain the reference for quiet conditions, no noise recording was played through the loudspeakers during the 4 hr of the experiment.

3.3.4 Pre-Exposure Tests

Once the subjects were retained for the experiment, they were exposed on three different days to the following noise conditions: industrial noise, pink noise, and no noise. This last condition, referred to as quiet, corresponds to background noise of approximately 45 dBA. On the day of the DPOAE monitoring measurements, the subjects first went through the pre-exposure tests, shown as block "A" in Figure 3.4, which consist of a manual PTA test and stapedial reflex measurement

with tympanometry. Prior to the DPOAE measurements with the designed DPOAE monitoring system, the probe fit test (Nadon, V., Bockstael, A., Botteldooren, D. & Voix, J., 2015c) was executed, and the result shown on the smartphone was saved. The probe was refitted if the measured $R_{A/D}$ ratio (Nadon *et al.*, 2015c) differed by more than two times the reference value measured after the first fit. Afterward, the DPOAE primary-tone stimuli were calibrated for proper DPOAE recording. As a final note, adaptation was switched on, so that the adaptive filters could reject the ambient noise from the DPOAE measurements, and a pre-exposure DPOAE measurement was recorded. The adaptation feature stayed on for all noise conditions, including quiet conditions.

To save time, two subjects were tested simultaneously: Subject A was tested with the designed system, whereas subject B was tested with the reference DPOAE system, as seen in Figure 3.3. A total of five subjects were tested with the designed system and four with the reference system.

3.3.5 Tests During Exposure

After the calibration of the DPOAE stimuli signals and probe fit measurement (block "B" in Figure 3.4), the noise exposure started, and every 15 min, a new DPOAE measurement (block "C") was performed at least twice with the designed system, with a complete measurement of the DPOAE frequency range, f_{dp} from approximately 600 to 4000 Hz, corresponding to f_2 from 1000 to 6169 Hz.

During the ambient noise exposure, one complete scan was recorded with the reference system on test subject B, while the software averaged at discrete DPOAE frequencies on the basis of two consecutive measurements passing the 5-dB criterion. To perform an average on a similar number of consecutive measurements with the designed system, at least two complete scans were recorded, because each discrete DPOAE frequency was only repeated once per scan with this system, compared with at least twice per scan with the reference system.

Noise exposure was monitored and recorded during the experiment with the sound level meter positioned in the room, as shown in Figure 3.3. Subject A was protected from the noise exposure

with the passive attenuation of the two DPOAE probes necessary for the measurements, whereas subject B was protected with the DPOAE probe on one side and by a disposable foam earplug on the other. Raw signals from the designed system's external and internal microphones were recorded via an analog audio output of the DPOAE system with a Zoom H5 (Zoom) portable audio recorder equipped with an EXH-6 TRS capsule (Zoom, 2019) to record the four audio outputs simultaneously.

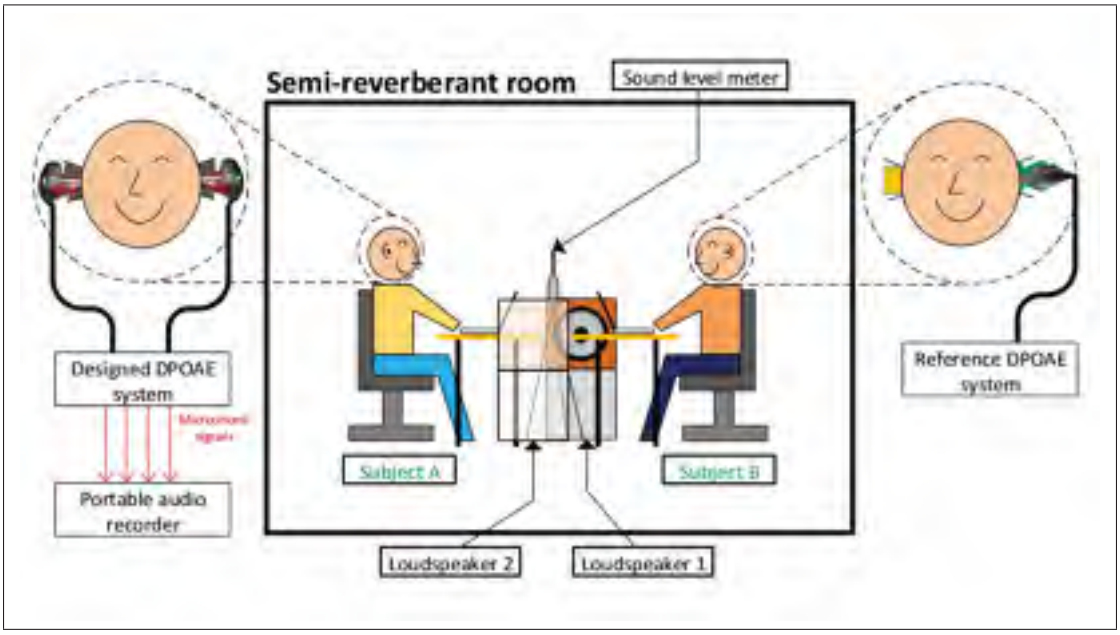

Figure 3.3 Physical setup used for the tests during the ambient noise exposure. The schematic shows the sound level meter in the middle between the test subjects to record the ambient noise sound pressure levels, with subject A tested by the designed system and subject B tested by the reference system. Both subjects were sitting still in one spot, facing each other, for the entire testing session. They were allowed to move out of the room only during the planned breaks and for emergencies after raising their hand. The subjects were allowed to read and to bring their laptops to work on during the experiment. The loudspeakers used for the ambient noise exposure are shown on each side of the tables. The portable audio recorder records the ipsilateral in-ear microphone (IEM-I), ipsilateral outer ear microphone (OEM-I), contralateral IEM (IEM-C), and contralateral OEM (OEM-C) signals of the designed system. DPOAE = distortion product otoacoustic emission

These raw signals could be used later to calculate the in-ear noise exposure, the outer ear exposure, the hearing protection provided by the probe, and post-process DPOAE signals if necessary.

After about 2 hr of noise exposure, a break of 30 min to 1 hr was allowed for subjects to rest and eat. This break occurred at the same time for both test subjects, as shown in Figure 3.4, so that the probes could be refitted and calibrated before exposing the subjects to noise once again.

3.3.6 Post-Exposure Tests

After being exposed to 4 hr of noise, the subjects went through the post-exposure tests, which are similar to the pre-exposure tests ("A" in Figure 3.4), except that the post-exposure test sequence begins with a DPOAE test once the noise exposure has stopped. Therefore, DPOAEs were measured twice in post-exposure, once immediately after the noise exposure, and once at the very end of the post-exposure tests. The post-exposure tests will make it possible to evaluate whether the noise exposure had an effect on the pure-tone auditory thresholds and to observe the recovery mechanisms of the inner ear by comparing the first post-exposure DPOAE measurements with the very last post-exposure measurements.

3.3.7 Post-processing on the OAE Data

Audio artifacts, such as those resulting from the subject coughing, sneezing, and talking, and probe fit changes could lead to DPOAE measurement outliers. These outliers were rejected in post-processing using a thresholding method. The threshold was based on the accepted tolerance on repeated DPOAE measurements (Keppler, H., Dhooge, I., Corthals, P., Maes, L., D'haenens, W., Bockstael, A., Philips, B., Swinnen, F. & Vinck, B., 2010b) and was set to 7 dB, corresponding to double the 3-dB tolerance plus 1 dB. Any DPOAE measurement greater by 7 dB from the previous one was rejected. Such outlier rejection was applied in post-processing but could eventually be included in the real-time processing of the data.

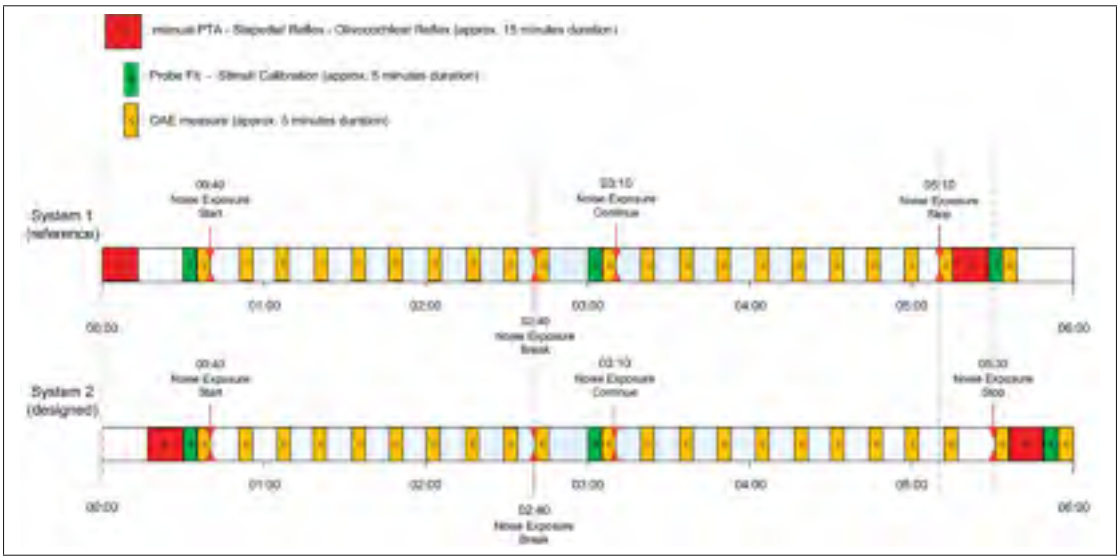

Figure 3.4 Timeline of the experiment protocol for subjects A and B, periodically tested using two otoacoustic emission systems, the designed system and the reference system, while continuously exposed to noise. PTA = pure-tone audiometry. OAE = otoacoustic emission

When audio artifacts interfered with the measurement, the measurement on the 22 DPOAE frequencies was still saved, and a following attempt was started. All consecutive measurements within a 5-min interval were then averaged in post-processing after passing through the thresholding procedure.

3.3.8 Statistical Analysis

To verify if the changes in PTA HTLs and ART between pre-exposure and post-exposure were statistically significant, a paired t test or a nonparametric paired Wilcoxon test was used, on the basis of the Shapiro test and Q-Q plots. The paired t tests, or Wilcoxon tests, were calculated per frequency point and per noise condition. The output of interest was the mean of differences, and p values indicated if the results were statistically significant. A significance level of $\alpha = 0.05$ was chosen for these tests.

A multilevel analysis of variance (ANOVA) was conducted separately on the designed system's DPOAE data and the reference system's DPOAE data. It used the participants as a random

variable and the test frequency, time of measurement, and noise levels as fixed factors. To satisfy the model assumptions for the ANOVA, the linear model needed normally distributed residuals for both systems on the basis of a one-sample Kolmogorov–Smirnov test. Therefore, residuals were discarded from the full data set, that is, without the 7-dB DPOAE variation threshold post-processing. For both systems, these residuals consisted mostly of extreme DPOAE values at either approximately +35 dB for the upper range or -20 dB SPL for the lower range. Removing these residuals, 324 observations out of 1265 for the designed system, did not notably alter the coefficients obtained for the model.

3.4 Results

3.4.1 PTA

The PTA tests were conducted to screen the participants and to monitor hearing status. In the latter case, PTA was conducted for pre-exposure and post-exposure measurements. To calculate the differences in HTLs, the results for post-exposure were subtracted from the pre-exposure results. Therefore, positive values indicate lower thresholds, that is, better hearing, in post-exposure results. According to the paired data Wilcoxon signed-ranks test with continuity correction, only a positive HTL change was statistically significant (p = .05) at 3 kHz with a mean of differences of 4.4 dB HL for industrial noise conditions. Therefore, HTLs did not seem affected by the noise because, in general, subjects had slightly better auditory thresholds after the noise exposure.

3.4.2 ARTs

The ART tests, also known as stapedial reflex thresholds, were conducted to monitor hearing status with the pre-exposure measurements at the beginning of the day and post-exposure at the end of the day. Positive values indicate lower thresholds in pre-exposure results; therefore, a positive difference might indicate an effect due to the noise exposure. The changes detected are relatively small, within a measurement step of 5 dB of the otoadmittance system, and are not statistically significant between post-exposure and pre-exposure within the same test conditions.

However, by evaluating the statistical difference across the test conditions, industrial and pink noise conditions each paired with quiet conditions, a statistically significant ($p < .05$) increase in ART was observed at 4 kHz for both industrial and pink noise conditions with the mean of differences of 0.0 and 1.1 dB SPL, respectively, versus a mean of difference of -3.1 dB SPL for the quiet conditions.

3.4.3 DPOAEs

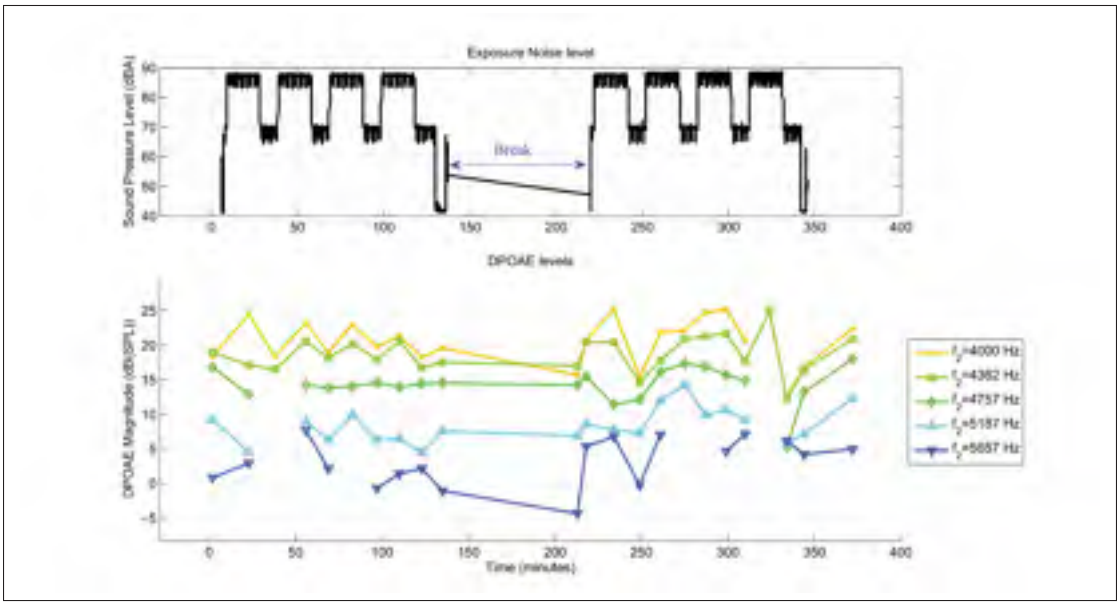

Figure 3.5 Typical timeline of exposure noise level (top) synchronized with distortion product otoacoustic emission variations (DPOAE) at five test frequencies during the experiment on a subject (bottom). Blank data points for certain frequencies result from the post-processing threshold method removing outliers

Noise exposure levels captured from the sound level meter were synchronized with DPOAE level measurements to facilitate analysis. An example of the noise exposure and DPOAE levels is presented for one subject in Figure 3.5. Results were analyzed per DPOAE frequency for each of the participants for the variations from their baseline measurement ($t = 0$ min) in Figures 3.6 and 3.7. This way, effects of noise exposure on DPOAE responses can be observed by comparing the progression of the DPOAE changes during noise exposure with the baseline. The first measurement, pre-exposure, is the baseline followed by measurements during noise exposure.

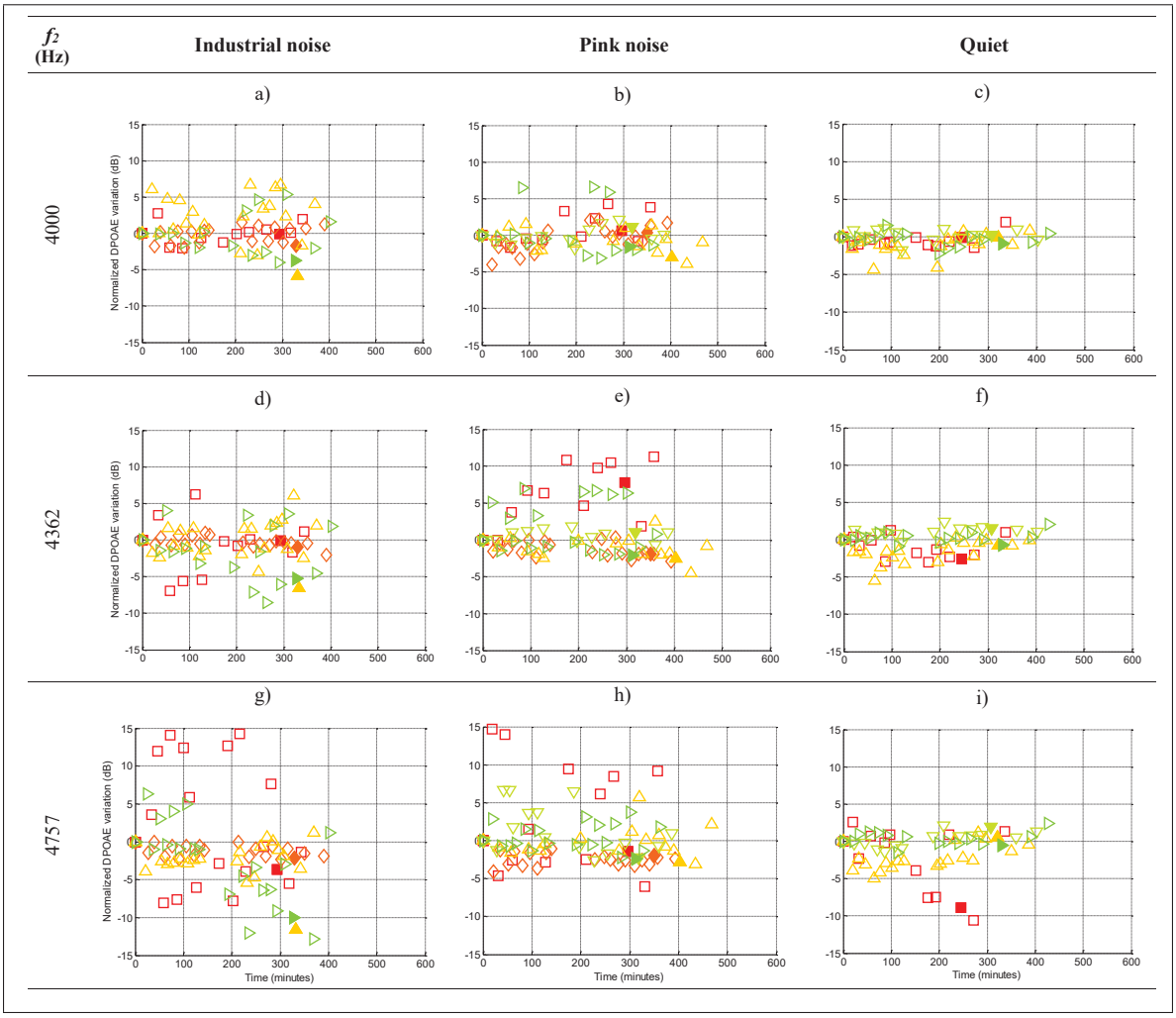

Figure 3.6 Comparison of distortion product otoacoustic emission (DPOAE) variations over time for the designed system between the three types of noise conditions; variations are normalized with the baseline (at t = 0 min) DPOAE level. The first point represents the baseline recorded pre-exposure; the following data points are during the noise exposure (67–87 dBA). The filled marker indicates the last measurement during noise exposure, which is followed by the two last DPOAE measurements measured after the noise exposure. The first post-exposure data points are usually below the baseline for industrial and pink noise conditions, indicating possible effects of noise exposure on outer hair cells. The last data point is usually closer to or above the baseline, possibly indicating that the inner ear status is back to normal

The markers in Figure 3.6 that are fully filled, as opposed to the other lighter markers, indicate the last measurement taken during the noise exposure, followed by two DPOAE measurements taken after the noise exposure. The DPOAE level recovery between the last two measurements

conducted in approximately 45 dBA could indicate potential effects of noise exposure on OHC. The measurements are displayed aligned with their time, in minutes, relative to their respective baseline. The figures are aligned for easy comparison of the effects of the various noise conditions, and the least changes are expected for the measurements in quiet conditions.

Results are then displayed in comparison with other subjects measured with the reference DPOAE system in Figure 3.7 to verify the consistency, or lack thereof, across the two systems and to observe the possible effects of noise on DPOAE levels on more subjects overall.

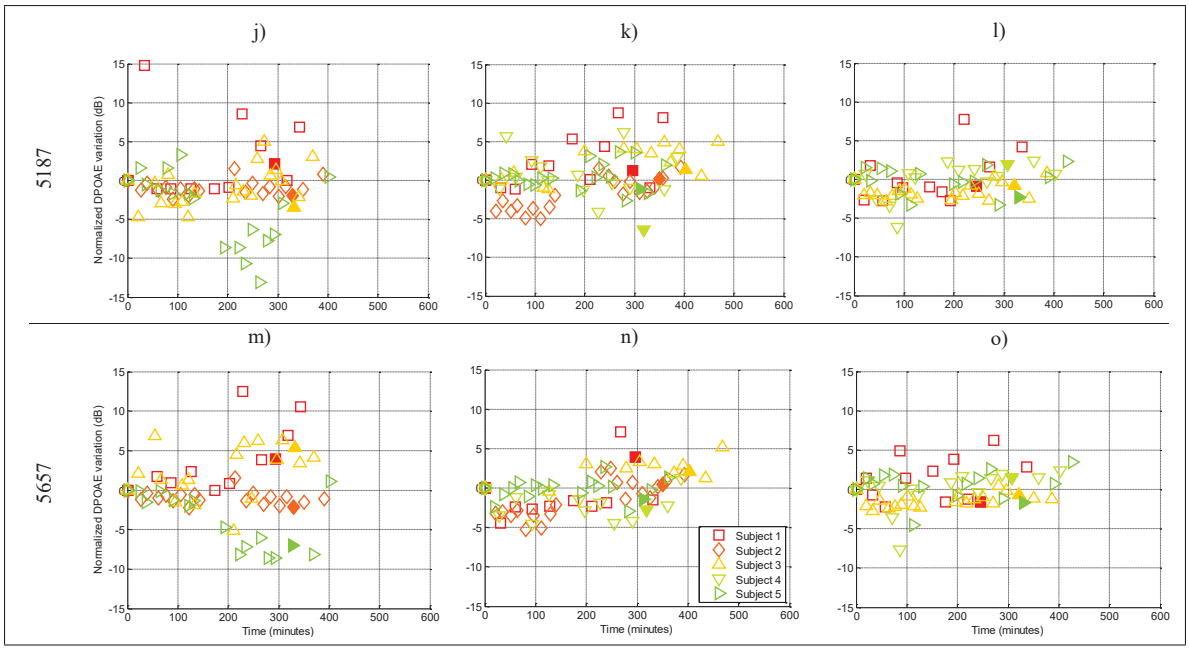

Figure 3.6 (Continued)

To validate that the designed system was able to detect OHC changes by observing variations in DPOAE levels during noise exposure (> 65 dBA), data points slightly before and after the fully filled markers are expected below the 0-dB normalized baseline for the noisy test conditions. The last DPOAE levels measured are expected to increase, because they are recorded during the recovery phase, that is, post-exposure. For most subjects using the designed system, results in industrial and pink noise do correspond to this trend (see Figure 3.6). On the other hand, the results are more scattered with the reference system (see Figure 3.7). For both the reference and

designed systems, it is possible that data points were affected by the ambient noise disturbance as is the case for subjects 5 and 6 in Figures 3.7(c) and 3.7(d), for example, when the ambient noise level measured with the sound level meter was approximately 87 dBA. This disturbance could potentially mask true changes in DPOAEs. The two last data points in the plots (see Figures 3.6 and 3.7) helped visualize whether OHC changes did occur during noise exposure, by observing the recovery curve.

3.4.4 Simulation of DPOAE Shifts Using the Obtained Linear Model

The multilevel ANOVA conducted on the data sets showed that the effects of the test frequency and the interaction between the noise level and the time of the measurement were statistically significant ($p < .001$). To observe the fixed effects on the DPOAE levels without the effects of random variables, the linear model for the designed system was tested with values generated at similar noise levels as the ones used during the experiment with corresponding measurement times.

According to the simulated data from the linear model shown in Figure 3.8, increasing the test frequency decreased the absolute DPOAE level, whereas the interaction of the measurement time with an increase in the noise level outside the ear also reduced the DPOAE level. Upper and lower confidence intervals are plotted in Figure 3.8 with error bars, above and below the average modeled response, to illustrate the possible range of DPOAE variation expected on individual test subjects. However, possibly due to the ambient noise disturbance with the reference system, positive DPOAE shifts are observed with the reference system's model fixed-effect coefficients for the interaction of the time of measurement and the noise level as shown in Table 3.1. The effect of the test frequency still decreased the absolute DPOAE level. To improve the fit of the model with experimental data, especially for the recovery period and the quiet conditions effects, a nonlinear model could have been used; however, modeling was not the main objective of the study.

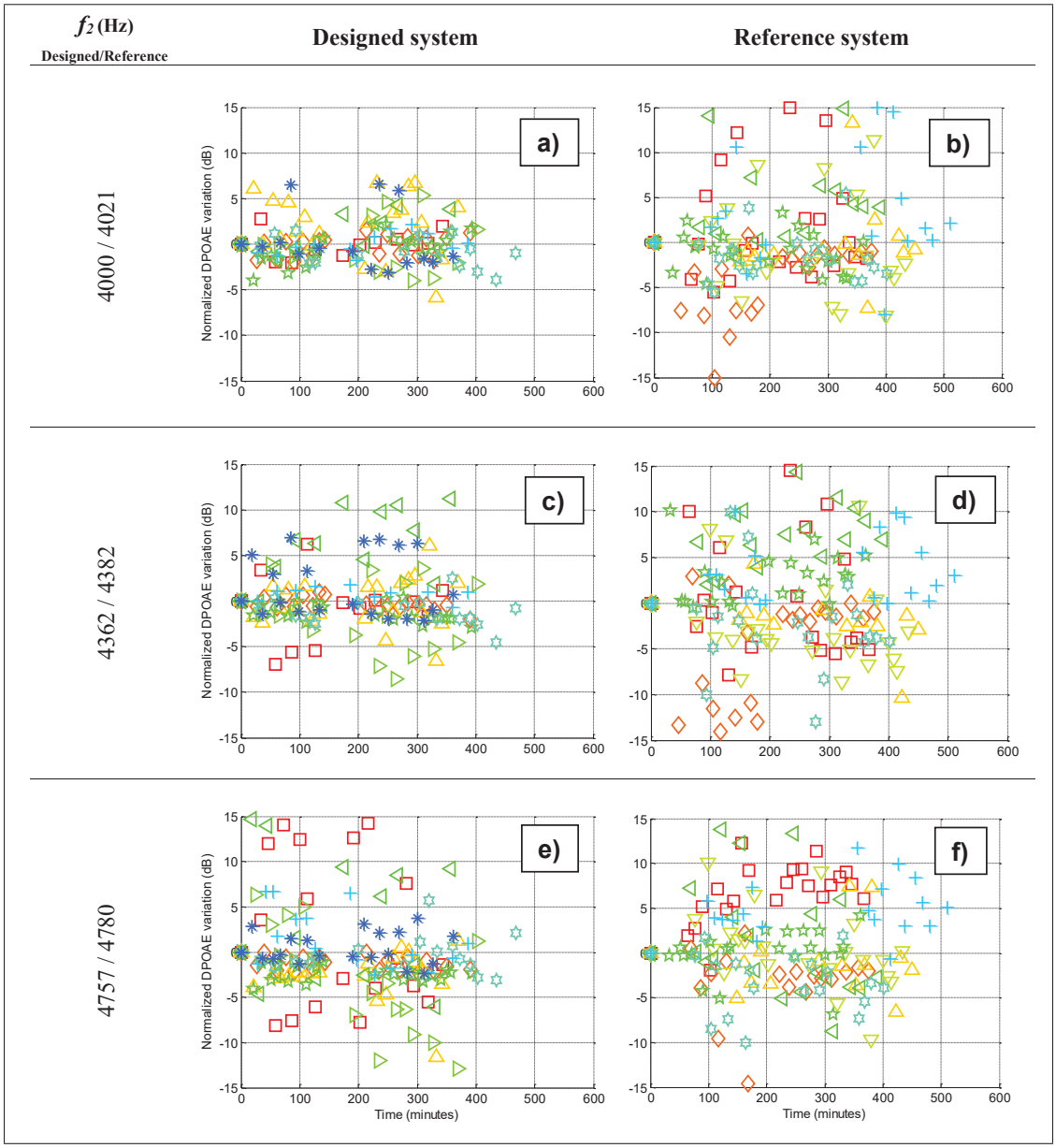

Figure 3.7 Comparison of distortion product otoacoustic emission (DPOAE) variations over time for the designed and reference systems; variations are normalized with the baseline DPOAE level at t = 0 min. The first point represents the baseline recorded pre-exposure, the following data points are during the noise exposure (67–87 dBA), and the last two points on the right are post-exposure measurements. Results with the reference system are more scattered than with the designed system, indicating that the reference system is probably less robust to test for DPOAE changes in high ambient noise levels

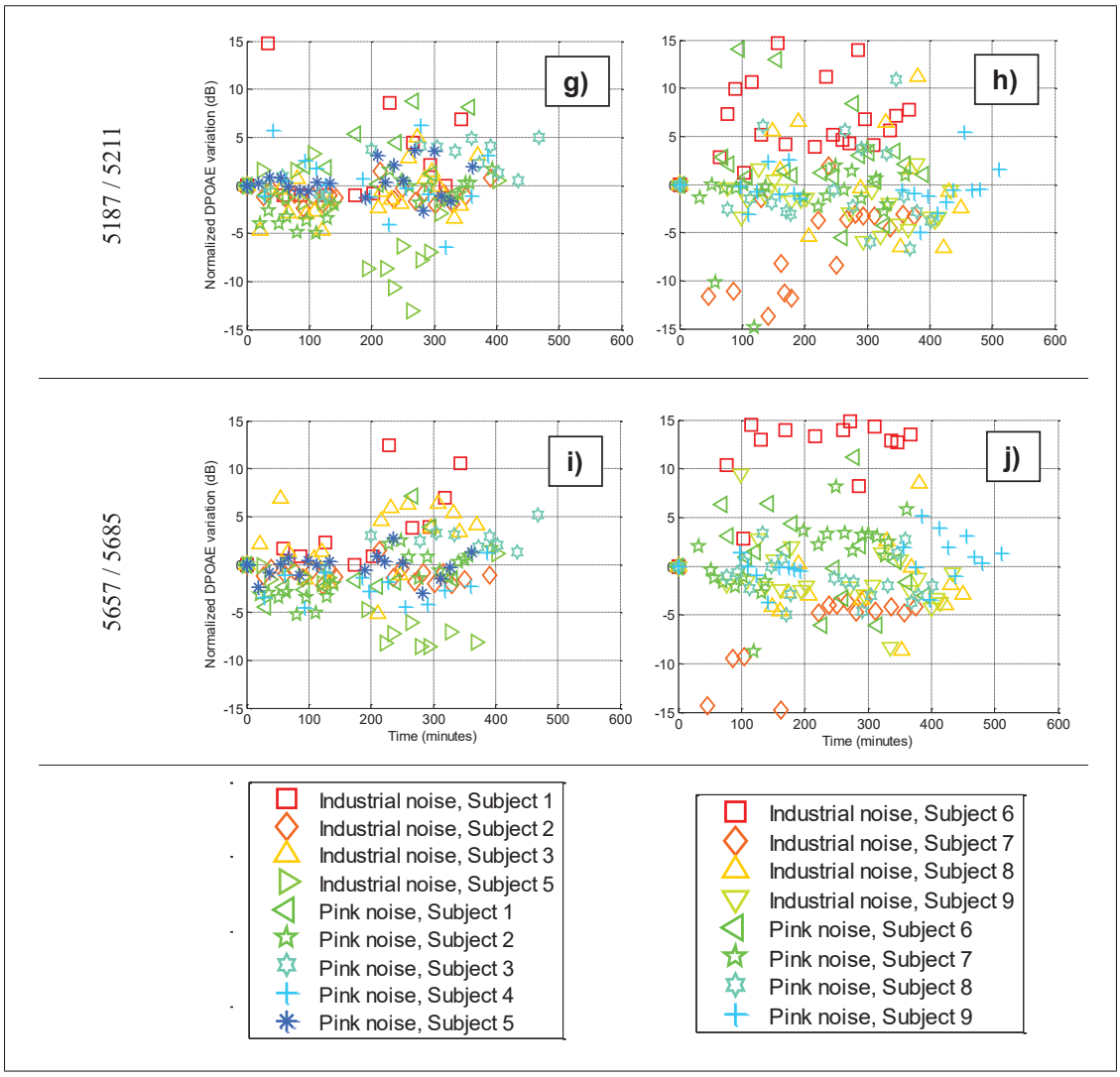

Figure 3.7 (Continued)

3.4.5 Performance of Systems in High Ambient Noise Levels

To evaluate the performance of the designed and reference systems in high levels of ambient noise, the effect of the disturbance on the DPOAE measurements was further assessed by computing the deviation from the baseline DPOAE level. Resulting deviations are compared between the two systems, in the three noise exposure levels, and are shown as normal probability plots in Figure 3.9.

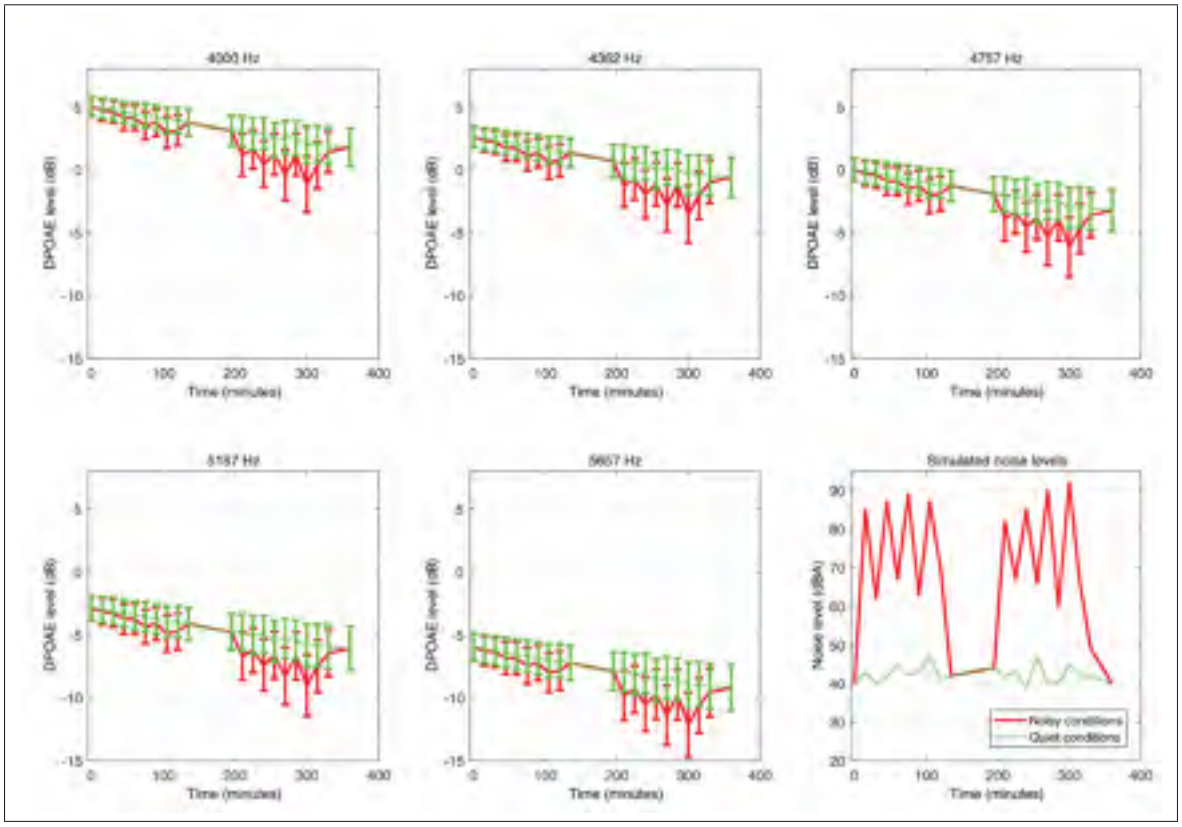

Figure 3.8 Simulated distortion product otoacoustic emission (DPOAE) levels on the basis of the linear model computed from the designed system data set. The DPOAE levels were calculated from noise levels similar to those recorded during the experiment for noisy (red) and quiet (green) conditions with approximate measurement times. The simulated data show that the absolute DPOAE level decreases with higher DPOAE test frequencies, with f_2 indicated on top of the figures. The interaction between the high noise levels and the time of measurement decreases the DPOAE level as observed with the experimental data. The confidence intervals on the simulated data are shown with the error bars. The noise levels used to simulate DPOAE levels with the model are shown on the bottom right

For the reference system in Figure 3.9(a), it can be seen that the intersection of the 87-dBA noise level plot with the 50% probability is at approximately 5.7 dB, and the plot has a lower slope than the 67- and 45-dBA noise levels, indicating a larger range of artificial shift in DPOAE levels due to the high noise level disturbance. For the designed system in Figure 3.9(b), a slightly greater effect is observed because there is no algorithm to block the measurement when the noise level is too high. However, in Figure 3.9(c), the normal probability plots are closer together between the different noise levels because the data were processed with the 7-dB threshold

method explained earlier, which can be compared with the NTL used by the EMAV software. The intersection of the 87-dBA noise level plot with the 50% probability is at approximately 2.9 dB, and the normality fit has a greater slope than with the reference system, indicating a smaller range of artificial shift in DPOAE levels caused by the high noise level disturbance. True physiological positive DPOAE changes can result from noise exposure; therefore, this metric should be interpreted as a comparison across systems relative to the measurements in lower noise exposure levels of 45 dBA, because the deviation from the baseline includes the noise interference inducing an artificial increase in DPOAE levels (Nadon *et al.*, 2015a), in addition to potential positive physiological changes in DPOAE levels. However, the positive physiological changes would be relatively smaller than the interference of the 87-dBA noise levels.

Table 3.1 Fixed-effect coefficients for the designed and reference systems' linear models

	Designed		**Reference**	
	Estimate	**Standard Error**	**Estimate**	**Standard Error**
Intercept	31.5	3.5	10.0	2.5
Frequency	-6.6e-03	1.9e-04	-1.0e-03	1.8e-04
Time	1.3e-02	3.1e-03	-6.3-03	3.0e-03
Noise level	1.8e-01	1.1e-02	-1.2e-02	1.3e-02
Time * Noise level	-2.2e-04	5.2e-05	1.6e-04	5.0e-05

To verify that the variations in DPOAE levels result from cochlear activity affected by noise exposure and are not simply caused by the system's variability between measurements, the test–retest variability of the designed DPOAE system was estimated using the standard deviations of the DPOAE levels, as measured from the consecutive measurements, saved within the 5-min interval usually needed to complete the several DPOAE measurements. The standard deviation results are plotted as box plots per noise levels in Figure 3.10. It was impossible to assess the test–retest variability for the reference system, as the EMAV software automatically repeated the measurement at problematic frequencies if certain criteria were not met and output only the average result, thereby not enabling the calculation of a standard deviation. Moreover, during noise exposure, only one measurement of the DPOAE frequency range was completed per 15 min. Between these measurements, the subjects were exposed to a different ambient noise

level (see Figure 3.5). Therefore, due to different test conditions, the standard deviations could not be calculated across the periodic DPOAE measurements for the reference system.

The NTL parameter was adjusted manually in the EMAV software until the reference system could proceed in taking the DPOAE measurement while in the presence of high ambient noise levels. The NTL parameters were in approximate ranges of 8–15 mPa for 45 dBA, 12–103 mPa for 67 dBA, and 8–150 mPa for 87 dBA of noise levels. As the NTL parameter is increased, a greater amount of ambient noise disturbance is captured by the DPOAE measurements. As observed in the greater deviation from the baseline, with more scattered data in Figure 3.7 and a greater DPOAE shift at the intersection with the 50% probability in Figure 3.9(a) for 87 dBA, the EMAV software no longer rejected noisy samples, as it would have when using more restrictive limits such as the default 8-mPa set for lower ambient noise levels such as 45 dBA.

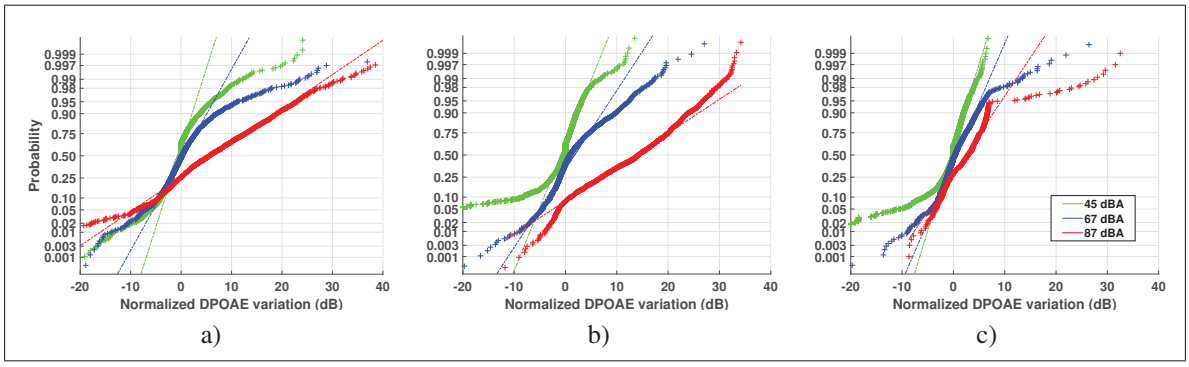

Figure 3.9 Normal probability plots of the distortion product otoacoustic emission (DPOAE) deviation from the baseline in ambient noise levels of 45, 67, and 87 dBA (all sources, i.e., industrial noise, pink noise, and quiet conditions, merged) for (a) the reference system, (b) the designed system without threshold processing, and (c) the designed system with the 7-dB threshold processing. Overall, better immunity, that is, a smaller deviation from the baseline (0 dB), to ambient noise levels is observed for the designed system with the threshold method than for the reference system

Due to the relatively fast recovery rate of DPOAE levels, that is, within a few minutes, the measurement duration can be a crucial factor in the detection of temporary cochlear activity changes (de Toro *et al.*, 2010; Engdahl, 1996; Sutton *et al.*, 1994; Vinck *et al.*, 1999). The measurement durations for the designed DPOAE system were compared with those obtained

with the reference system and are presented in Figure 3.11. It is important to note that only one measurement could be performed every 15 min for the reference system in noisy conditions and that the noise limit threshold had to be modified in order to proceed to the measurement. During that period, several complete measurements were performed with the designed system as one complete scan of the DPOAE frequencies takes only 45 s and no parameter needed to be adjusted. This results in test durations ranging approximately from 3 to 6 min for a single measurement with the reference system, compared with a much shorter duration ranging from 90 to 135 s (approximately 2 min) for two to three measurements with the designed system.

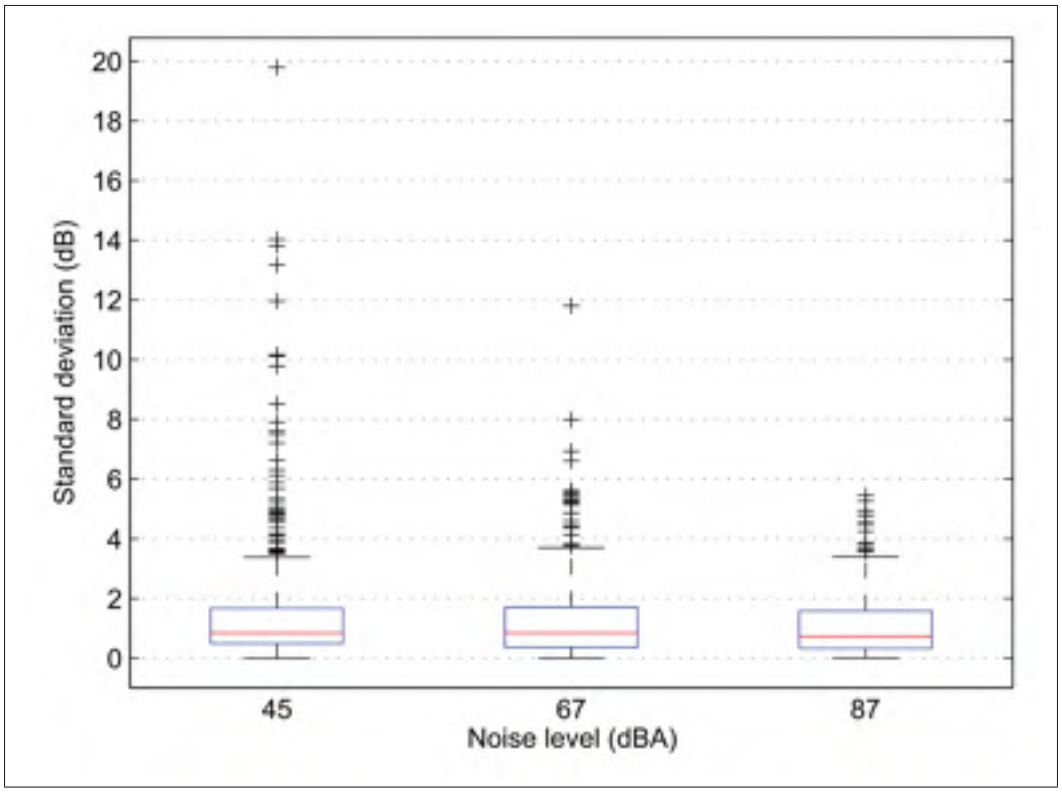

Figure 3.10 Test–retest variability between consecutive measurements for the designed DPOAE system in ambient noise levels of 45, 67, and 87 dBA (all sources, i.e., industrial noise, pink noise, and quiet conditions, merged). The (+) symbol represents outliers

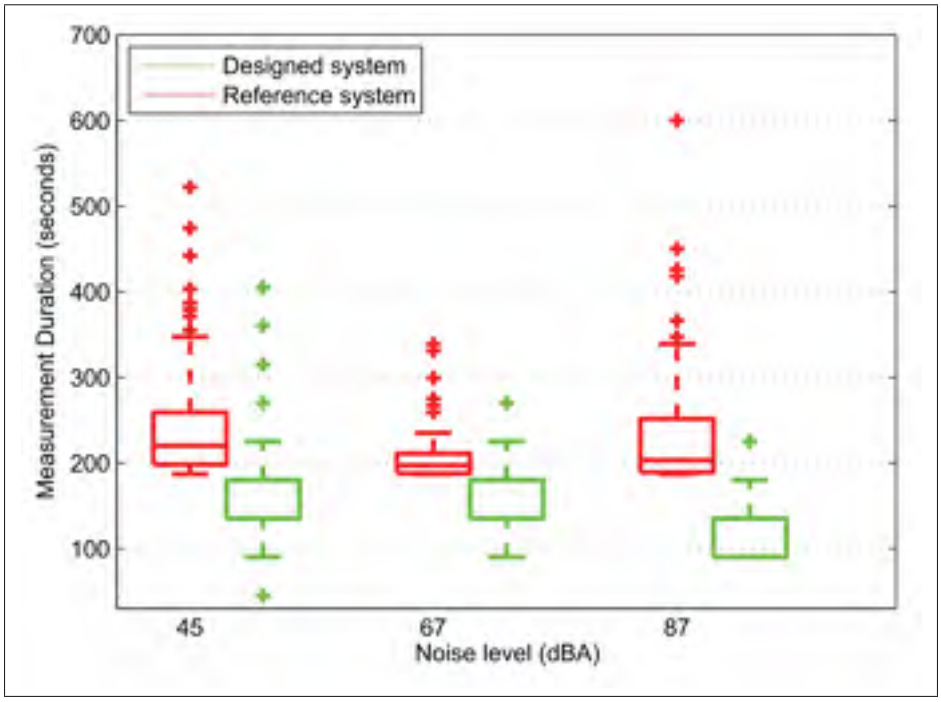

Figure 3.11 Comparison of the distortion product otoacoustic emission measurement duration for the reference system and the designed system in ambient noise levels of 45, 67, and 87 dBA (all sources, i.e., industrial noise, pink noise, and quiet conditions, merged). The (+) symbol represents outliers

3.5 Discussion

3.5.1 PTA

In this experiment, PTA was used as a reference in the screening test to verify that test subjects did not suffer from a permanent threshold shift. The participants were asked about their most recent noise exposure history prior to the screening PTA; therefore, a full recovery of past temporary changes was expected. PTA was also used to verify if any temporary inner ear status changes could be detected between pre-exposure and post-exposure. It was expected that PTA would be less sensitive, compared with DPOAEs, to detect early the onset of cochlear changes (Sliwinska-Kowalska *et al.*, 2001; Vinck *et al.*, 1999). According to the results presented in the previous section, the subjects' HTLs did not appear to be affected by the noise exposure.

3.5.2 ARTs

The ART differences between pre-exposure and post-exposure were analyzed to show the potential effect of the noise exposure on the middle ear muscle contraction, which could be used to detect early changes in hearing status, earlier than the NIHL measured by PTA (Venet *et al.*, 2014). The ART is lower in post-exposure measurements for the quiet condition, whereas for the industrial and pink noise conditions, the ART is slightly increased. This increase in the ART indicates a lack of response of the middle ear muscle to lower magnitude stimulus signals, which could be related to a decreased signal transmission resulting from OHC activity, which, in turn, could be caused by the noise exposure (Venet *et al.*, 2014). ART variations at 4 kHz for industrial and pink noise conditions are in agreement with the DPOAE shifts around 4 kHz.

3.5.3 OAEs

The DPOAE frequencies of interest analyzed for this study corresponded to f_2 ranging from 4000 to 5657 Hz because this range of frequencies is more susceptible to temporary hearing changes, and the passive attenuation of the probe and adaptive filtering in the DSP of the designed system both reduce the ambient noise disturbance in DPOAE signals more effectively at these frequencies. It is unfortunate, however, that the f_2 = 6169 Hz frequency could not be analyzed in the study, possibly because of communication latency issues in the system, which sometimes affect the selection of the correct bandpass filters, resulting in more noise interference for this first DPOAE frequency. Therefore, the f_2 = 6169 Hz frequency was discarded in this study.

Furthermore, some outlier data points are visible in Figure 3.6. For example, subject 1 had very low absolute OAE levels, less than –10 dB for $f_2 \geq 5657$ Hz and, therefore, closer to the noise floor of the DPOAE measurement system. In this case, DPOAE levels varied from inside to outside the range of normal system operation, and this caused DPOAE level changes compared with the baseline. This variation caused by absolute DPOAE levels outside the range of normal operation was also seen in quiet conditions, resulting in greater DPOAE changes than the expected changes of approximately 0 dB. Subject 4 was the very first to be tested

with the designed system, in industrial noise conditions, and some problems related to the connection between the DPOAE system and the portable audio recorder, affecting both the DPOAE level calculated by the DSP and the portable recorder signal, were noticed straightaway and immediately corrected for the following measurements. The faulty measurements for this subject were discarded.

For the reference system, according to DPOAE measurements in noise exposure (see Figure 3.7), DPOAE levels are higher than those recorded with the designed system. This suggests that the NTL selected to continue the measurement in noise did not reject the ambient noise that disturbed the DPOAE measurement. Although positive physiological DPOAE changes are possible, referring here to the 2-min bounce as mentioned in previous studies (Kemp, D., 1986; Kirk, D. & Patuzzi, R., 1997), these positive changes are expected to be relatively smaller for the $2f_1-f_2$ DPOAE frequency (Kirk & Patuzzi, 1997) than the noise interference masking this potential DPOAE change. This is particularly because the reference system was not designed to measure in high ambient noise levels. Moreover, results with the reference system are more scattered than those recorded with the designed system (see Figure 3.7) for which DPOAE levels are more concentrated below the baseline. According to these observations, the software processing and probe fit for the reference system appears to be more affected by the ambient noise disturbance than the designed system.

For the designed system, the last measurement post-exposure tends toward the baseline levels (see Figure 3.6) and is sometimes higher than the baseline, an observation also reported by de Toro *et al.* (2010). This positive shift is more noticeable in Figures 3.6(a) and 3.6(n). A greater negative change in DPOAE levels was detected for DPOAE measurements in industrial and pink noise than in quiet conditions, as shown with subjects 4 and 5 in Figure 3.6. Minor variations in DPOAE levels (approximately 1–2 dB) were observed for most subjects in quiet conditions as shown in Figure 3.6, as is expected when there is no noise exposure. The greater variations in DPOAE levels are visible for higher DPOAE frequencies. This effect can be observed by comparing Figures 3.6(a), 3.6(d), 3.6(g), 3.6(j), and 3.6(m). Maximum effects of noise exposure on DPOAEs were observed at 4757 and 5187 Hz in industrial noise conditions. The maximum

negative DPOAE shift from the baseline, calculated from the last valid measurement during noise exposure (filled marker) and the first measurement post-exposure, across frequencies (f_2 = 4000–5657 Hz) ranged from -5.9 to -22.3 dB (5187 Hz) in industrial noise, from -2.7 to -6.4 dB in pink noise conditions, and from -1.4 to -2.6 dB in quiet conditions, the latter possibly explained by some minor changes in the probe fit over the day or minor noise disturbance from the subject when he was working (Keppler, H., 2010). In comparison, de Toro *et al.* (2010) showed that across subjects and test frequencies, the DPOAE shift from the baseline ranged approximately from -10 to +2 dB after a 2-kHz monaural sound exposure. A similar DPOAE shift range can be observed from the simulated data on the basis of the linear model in Figure 3.8.

Fast DPOAE measurements following the noise exposure are more sensitive to measuring DPOAE changes, that is, before DPOAE levels go back to pre-exposure levels (de Toro *et al.*, 2010). Therefore, DPOAE measurements during the noise exposure, when possible, are of value with the designed system because the effect of noise exposure can be assessed directly before any restoration effects have taken place.

For the current study, the maximum noise level was set at around 87 dBA so that the resulting exposure in the earcanal protected under the hearing protection device was about 70–80 dBA. A review by Melnick, W. (1991) pointed out that the levels estimated to produce measurable temporary threshold shifts assessed with an audiogram ranged approximately from 74 dB SPL at 4000 Hz to 86 dB SPL at 250 Hz. In the current study, subjects were exposed to 4 hr (240 min) of ambient noise with an LAeq-4h of approximately 85 dBA, a sufficient noise exposure to trigger temporary DPOAE changes, as was demonstrated in Figure 3.6.

The median standard deviation (see Figure 3.8), calculated on the same consecutive measurements used for the mean DPOAE levels, is estimated at approximately 0.8 dB for all noise conditions. This indicates that results did not vary more across consecutive measurements when the subject was exposed to higher ambient noise levels. This can be explained by the performance of the adaptive filtering noise rejection. When the DPOAE level during or post-exposure is lower than the baseline, the negative DPOAE variation exceeding the test–retest variability could be

considered a real change in inner ear activity. This appeared to be the case with the designed system for industrial and pink noise conditions.

The greater number of outliers in the 45-dBA box plot (see Figure 3.10) can be explained by the number of DPOAE measurements recorded for the first probe fit. After a problem was noticed at one of the DPOAE frequencies, possibly caused by a primary-tone level that needed recalibration after the probe was dislodged, the probe was refitted, and a new calibration and DPOAE measurement was recorded. The primary tones were rarely recalibrated during higher ambient noise levels (67–87 dBA).

The test duration for the reference system was imposed by the selected EMAV software and was a minimum of about 3 min in 45 dBA and up to 6 min in 87 dBA of ambient noise levels. This duration is much longer than the 45 s required to perform one complete measurement with the designed system (see Figure 3.11). The reference system has similar measurement duration limitations as other commercial systems in noisy conditions (Smith, S., Kei, J., McPherson, B. & Smyth, V., 2001).

For the designed system, the variations in measurement duration for the 45-dBA noise conditions can be explained by the several fit/refitting of the probe at the beginning of the day to obtain the most stable and highest DPOAE levels. However, in higher noise levels, the duration of measurements was more consistent because the probes were already correctly fit after the measurement in quiet conditions, and no refitting was necessary between consecutive measurements. Regardless of the ambient noise levels, about two to three attempts were performed, with each attempt lasting about 45 s to cover the complete range of DPOAE frequencies for a total duration ranging from about 90 to 13 s (approximately 2 min). Overall, faster DPOAE measurements were performed with the designed system than with the reference system, as observed in Figure 3.11. This shorter measurement duration will definitely help detect the cochlear changes at the optimal moment, that is, within the first 5 min after a possible traumatic noise exposure event and preferably before the cochlear status goes back to normal (de Toro *et al.*, 2010). In an ideal scenario, as is the case in this study, DPOAE measurements

should be conducted while subjects are exposed to noise to detect maximal DPOAE changes. Shorter measurement duration also means that DPOAE levels do not have much time to come back to pre-exposure levels while other DPOAE frequencies are tested (de Toro *et al.*, 2010).

3.6 Conclusions

To improve the protection of workers against the risk of NIHL, continuous monitoring of workers' inner ear activity could give the opportunity to detect temporary changes in cochlear status and take the appropriate actions before the changes become irreversible. A robust system was designed to monitor OHC activity in high ambient noise levels using DPOAEs. The main objective of this study was to validate that the approach using an inner ear monitoring system designed in a laboratory is able to detect changes in OHC activity by observing variations in DPOAE levels during and after noise exposure. As demonstrated in the study, it is possible to measure DPOAEs in ambient noise exposure levels exceeding 85 dBA at high frequencies with the designed system, if subjects have high baseline OAE levels and a good DPOAE probe fit can be accomplished. Overall, it is possible to monitor DPOAEs in noise levels of at least 65 dBA regardless of the OAE probe fit and subjects' baseline DPOAE levels. The designed system is able to detect relatively small changes in DPOAE levels in noise exposure because of the system's relatively low test–retest variability. The temporary DPOAE level changes indicate that OHC activity is potentially affected by ambient noise exposure.

Future research shall consider a study of larger scale conducted with more test subjects and in-field noise exposure conditions, in addition to an improved version of the designed system's hardware and software, that should improve the detection of physiological DPOAE changes. Furthermore, by reducing the time spent on other audiological tests, more post-exposure DPOAE measurements could be measured closer to the possible traumatic noise events. For example, one DPOAE measurement could be conducted every 2 min in post-exposure and would help analyze more precisely the relationship between the noise dose received from the ambient noise and the shift in DPOAE levels. By monitoring the worker's inner ear activity and the noise exposure level, each worker's own susceptibility to NIHL could also be identified. The

approach presented in this study to detect early changes in hearing status could definitely benefit translational researchers and other field practitioners in hearing conservation and hopefully stimulate new research about hearing mechanisms.

3.7 Acknowledgments

Annelies Bockstael was a postdoctoral fellow of the Research Foundation—Flanders (FWO) up until January 2017; the support of this organization is gratefully acknowledged. The ETS-affiliated authors would like to acknowledge the Natural Sciences and Engineering Research Council (NSERC) Individual Discovery Grant Program and the Fond de Recherche Nature et Technologies Nouveau Chercheur award for its financial support, as well as for technical support provided by EERS Technologies 4.0 Inc. through the NSERC-EERS Industrial Research Chair in In-Ear Technology for prototyping the experimental otoacoustic emission probes. Vincent Nadon is grateful to the Institut de Recherche Robert- Sauvé en Santé et Sécurité du Travail for its financial support and would also like to thank Georges Hart at Lapperre for granting him access to the otoadmittance system.

CHAPTER 4

METHOD FOR PROTECTED NOISE EXPOSURE LEVEL ASSESSMENT UNDER AN IN-EAR HEARING PROTECTION DEVICE: A PILOT STUDY

Vincent Nadon[1,2], Fabien Bonnet [1,2], Rachel E. Bouserhal [1,2],
Antoine Bernier [1,2], Jérémie Voix[1,2]

[1] Université du Québec, École de technologie supérieure (ÉTS),
1100, Notre-Dame Ouest, Montreal, Quebec, Canada, H3C 1K3
[2] Centre for Interdisciplinary Research in Music Media and Technology,
527 Rue Sherbrooke Ouest, Montreal, Quebec, Canada, H3A 1E3

Article submitted to the International Journal of Audiology in September 2019.

4.1 Abstract

Objective: To properly measure the effective noise exposure level of workers protected by hearing protection devices (HPD), the use of in-ear noise dosimeters (IEND) is increasing. Commercial IENDs typically feature one in-ear microphone that captures all noises inside the ear and they do not discriminate residual ambient noise in the earcanal from wearer-induced disturbances (WID) to calculate the in-ear sound pressure levels (SPL). In this paper, a method to alleviate this particular issue with IENDs and calculate the hearing protection level on-site is proposed.

Design: The sound captured by an outer-ear microphone is filtered with an adaptive filter that models the HPD transfer function to estimate the in-ear SPL, this way part of the WIDs mostly captured by the in-ear microphone can be rejected from the SPL. The level of protection provided by the earplugs can then be estimated from the difference between in-ear and outer-ear SPLs. The proposed method is validated by comparing the outcome of the proposed WID rejection method to a reference method.

Study sample: The detailed methods are assessed on *in-situ* audio recordings obtained from 16 industrial workers monitored for up to 4 days.

Results: The merits of the proposed adaptive filter approach for the rejection of WIDs are discussed in terms of residual SPL and hearing protection level measurement accuracy.

Conclusions: Based on the findings, recommendations for the integration of the proposed WID rejection method in future in-ear dosimetry devices are suggested.

4.2 Introduction

Despite the efforts to integrate hearing conservation programs in the workplace and the use of HPDs (Rabinowitz *et al.*, 2013), noise-induced hearing loss (NIHL) remains the most common and expensive occupational disease (NIOSH, 2016). Although industrial workers do wear hearing protection (Feder, K., Michaud, D., McNamee, J., Fitzpatrick, E., Davies, H. & Leroux, T., 2017; Rabinowitz *et al.*, 2013; Tantranont, K. & Codchanak, N., 2017), it is difficult to evaluate the effective noise exposure using a standard sound level meter or a personal dosimeter placed on their shoulder, since the residual sound pressure level (SPL) in the earcanal, that is behind the hearing protector, coming from ambient noise is usually unknown (Berger *et al.*, 1998). Indeed, many factors need to be considered when estimating the effective residual noise exposure, such as the attenuation rating of the hearing protector, the quality of the HPD fit (Smith *et al.*, 2014), the duration the protector was removed during noise exposure (Groenewold *et al.*, 2014; HSE, 2019a), as well as how the human auditory mechanisms interact with changes in noise exposure levels (Borgh *et al.*, 2008; Creutzfeldt, O., Ojemann, G. & Lettich, E., 1989; Mukerji *et al.*, 2010).

The real-ear attenuation at threshold (REAT) (ANSI, 2008) is commonly used to measure the attenuation of the HPD in laboratory based on the hearing thresholds of human subjects with and without HPD. However, the *in situ* attenuation of the HPD can differ significantly from laboratory values (Neitzel, R., Somers, S. & Seixas, N., 2006; Nélisse *et al.*, 2011) and the REAT can be influenced by the hearing thresholds of tested individuals (Berger, E., 1985). For these reasons, objective methods like the field microphone in real ear (F-MIRE) technique were developed to measure the attenuation of HPDs in the field, also referred to as real-world

attenuation (Nélisse *et al.*, 2011; Voix, J., Smith, Pegeen & Berger, Elliott, 2019). The F-MIRE technique uses an outer-ear microphone (OEM) and an in-ear microphone (IEM) to calculate the attenuation of the HPD. Its popularization, and that of other quantitative methods for individual fit testing HPDs also known as Field Attenuation Estimation Systems (FAES) (3M, 2020; Voix *et al.*, 2019), revealed that testing HPD attenuation at regular intervals is important to estimate the real attenuation of the HPD on workers during their work shift. These FAES measurement techniques also feature the calculation of a single number personal attenuation rating (PAR) (Berger, E. H., 2010).

Another promising way of assessing adequate protection with HPDs is in-ear noise dosimetry (IEND) (Bonnet, F., Voix, J. & Nélisse, H., 2015; Davis, S. K., Calamia, P. T., Murphy, W. J. & Smalt, C. J., 2019; Rabinowitz *et al.*, 2013; Theis, M. A., Gallagher, H. L., McKinley, R. L. & Bjorn, V. S., 2012). Not only does IEND give a more accurate estimate of the residual noise level reaching the eardrum than regular noise dosimeters which monitor noise levels outside the earcanal (Smalt, C. J., Lacirignola, J., Davis, S. K., Calamia, P. T. & Collins, P. P., 2017) since IEND bypasses the need for assumptions and correction factors for microphone placement, such an approach has also recently proven to raise awareness among workers as the noise exposure feedback helped them reduce their noise dose through more appropriate HPD use (Trawick, J. A., Slagley, J. & Eninger, R. M., 2019). However, the SPL measured inside the earcanal may be affected by various wearer-induced disturbances (WID) (Bonnet, F., Nélisse, H., Nogarolli, M. A. & Voix, J., 2019a) such as talking, coughing or chewing, as well as microphonics, which are amplified by the occlusion effect when wearing an earplug (Berger, E. & Kerivan, J., 1983). As a result, the earplug can increase the in-ear noise dose instead of reducing it. Moreover, middle-ear mechanisms (Borgh *et al.*, 2008; Mukerji *et al.*, 2010), such as the stapedial reflex and nervous system mechanisms (Creutzfeldt *et al.*, 1989), are known to be triggered by self-generated noises, such as chewing or speaking . These mechanisms attenuate the intensity of these self-generated noises reaching the inner ear (Mukerji *et al.*, 2010). Hence, IENDs would benefit from a method to isolate the contribution of such WIDs from the calculated in-ear noise dose to reflect the real effects of noise exposure levels and duration on

the auditory system (Bonnet, 2019). Yet, to this day, commercial IENDs do not feature this option.

To isolate the contribution of WIDs from the in-ear cumulative noise exposure levels, a new approach is proposed in this study using an adaptive filtering method. This method is used for: 1) in-ear dosimetry and 2) as a field attenuation estimation system. To evaluate the method, it is compared to a reference algorithm (Bonnet, 2019) which uses the coherence variations (Bonnet, 2019; Randall, R. B. & Tech, B., 1987; Voix, J., 2006) in the HPD's transfer function , calculated between the OEM and IEM signals, to flag and reject WID noise events. The equivalent noise level (L_{eq}) is calculated from the output of both the proposed and reference WID rejection methods with a 3 dB exchange rate (Berger, 2003) for comparison. In addition, the proposed adaptive filter approach is used to estimate the hearing protection level provided by the HPD during the day. The protection level estimates are validated through comparisons with PAR estimates of a reference method based on cross-spectra and autospectra further detailed in Section 4.3.2. To estimate the impact of WID rejection on the actual in-ear equivalent SPL, a study is conducted in two industrial environments with 16 human participants exposed to machine noises in their daily routine for up to four days.

The proposed and reference WID rejection methods, as well as a new approach to calculate the PAR are presented in Section 4.3. Results comparing the reference and proposed algorithms for both PAR calculation and residual SPL estimation after WID rejection are presented in Section 4.4. Finally, the discussions and conclusions are presented in Section 4.5 and 4.6 respectively.

4.3 Methodology

4.3.1 Field data collection

4.3.1.1 Human subjects and tested environments

To collect sufficient data to compare the WID rejection algorithms presented in this study, 16 participants routinely exposed to noise levels fluctuating between 45 and approximately 100 dBA at their workplaces were selected for tests conducted over up to four days. These participants are divided into two groups. The first group, hereafter called Noise Group 1 (NG1), consists of 3 individuals working in a Computer Numerical Control (CNC) machining workshop and aged between 36 and 44 years old. The second group, hereafter called Noise Group 2 (NG2), is formed by 13 individuals in a woodworking school and aged between 18 and 44 years old, with a median age of 28. In their daily routine, NG1 participants were mainly exposed to background ventilation noise as well as the noise of machining metal parts coming from a CNC machine behind a window. NG2 participants were exposed to background ventilation noise as well as a variety of woodworking machinery noises produced, for example, by industrial wood jointers, planers and wood hammers. Therefore, NG2 participants were almost constantly exposed to noise for a maximum period of 5 hours, with a 30-minute lunch break for some, while NG1 participants were exposed more occasionally to loud noises as they entered and left the workshop during their 8-hour work shift. The approximate duration of the experiment per day is presented in Table 4.1. All participants were indoors in semi-reverberant rooms during the tests, thus eliminating other possible outdoor noise sources from wind, traffic, etc. The experiment with NG1 participants was approved by the Comité d'éthique pour la recherche, the internal review board (IRB) of the École de technologie supérieure. The participation of NG2 subjects was approved by the IRB of the woodworking school.

Table 4.1 Approximate duration of the experiment per day for each group of participants, numbered from #1 to #16 for a total of approximately 294 hours of recorded data, of which a subset of approximately 147 hours are used in the current study due to reasons detailed in Section 4.3.4.1

Group	Participants #	Days	Hours/day
NG1	1-3	4	8
NG2	4-7	4	5
NG2	8-10, 12-14, 16	4	6
NG2	11	2	6
NG2	15	1	6

4.3.1.2 Audio recording equipment

The raw audio data was recorded on-site with a recording device, dubbed the Auditory Research Platform (ARP), developed over the years at the NSERC-EERS Industrial Research Chair in In-Ear Technologies (CRITIAS, 2019), and shown in Fig. 4.1. This portable device specifically designed to perform measurements in high noise level environments features two high attenuation earplugs, each equipped with electronic components to perform the acoustical measurements: an IEM, an OEM and two miniature loudspeakers. A fit-test was performed before entering the noisy environment to ensure a proper fit quality and sufficient protection (Nadon, V., Bockstael, A., Botteldooren, D. & Voix, J., 2015b). The participants were wearing the portable device in a fanny pack for easier transportation, and the earpieces' wires were covered by their aprons or shirts and attached to their collar using a shirt clip to reduce the risk of microphonics and to ensure the wires would not hang out and risk getting stuck in machinery as shown on the right in Fig. 4.1. To verify the accuracy of the ambient SPLs measured with the designed portable system, the participants were also wearing a Spark 706RC reference dosimeter (Larson Davis, NY, USA) to measure the ambient SPL L_D (see Table 4.2 for definition of the variables used further on). The dosimeter's microphone was attached to their shoulder on the same side as the ear being tested.

Figure 4.1 The Auditory Research Platform (ARP) with hearing protection earpieces including electronic components for outer-ear and in-ear noise dosimetry (left), and a worker wearing the ARP during *in situ* measurements (right)

4.3.2 Personal attenuation rating

The PAR is a single number estimate that quantifies the noise attenuation achieved by an HPD on a given individual (Berger, 2010). A low PAR resulting from poor HPD fit can explain why a worker was overexposed.

In this study, the PAR is estimated using two different methods. The first method uses the passive attenuation of the earplug based on the $H_3[n]$ transfer function, shown in Fig. 4.2, estimated with the average of the ratios of the cross-spectra and autospectra of OEM and IEM signals (Voix, 2006). The PAR_{ref} is then calculated with this earplug attenuation per octave band. The second method uses the difference between $L_{\text{eq,OEM}}$ and the residual SPL, denoted L_{AF}, estimated from the adaptive filter output , where the adaptive filter identifies the earplug's

passive attenuation transfer function as detailed in Section 4.3.3. This method is developed and used in this study as it performs a less computationally exhaustive PAR assessment technique, since the identification of the transfer function with Fast Fourier Transform (FFT) is no longer needed. This gives the possibility to calculate the PAR and assess the fit quality for the whole duration that the protector is worn, whereas current FAES generally measure the PAR only once, before being exposed to noise. The proposed $\mathrm{PAR}_{\mathrm{AF}}$ is calculated as follows:

$$\mathrm{PAR}_{\mathrm{AF}} = L_{\mathrm{eq,OEM}} - L_{\mathrm{AF}}, \tag{4.1}$$

where the $L_{\mathrm{eq,OEM}}$ is the equivalent sound level calculated from the A-weighted OEM signal and L_{AF} is the A-weighted level of the adaptive filter output further explained in Section 4.3.3.

The $\mathrm{PAR}_{\mathrm{AF}}$ estimates are then compared with $\mathrm{PAR}_{\mathrm{ref}}$ to ensure that they give similar results so that eventually the $\mathrm{PAR}_{\mathrm{AF}}$ could be integrated in a portable IEND and provide information on hearing protection level to the user. In this work, the PAR can also be used to detect when the earplug transfer function is not correctly identified with the adaptive filter ; on the assumption that a) the passive attenuation of a given HPD should not vary over a short period of time if the earplug is fit correctly, and b) the estimation of the PAR should also remain constant and positive over a couple seconds. The continuous estimation of the PAR can therefore be used to reject incorrect estimates of the residual SPL when using the proposed WID rejection method later detailed in Section 4.3.3.

4.3.3 Proposed residual sound pressure level estimation using adaptive filtering

WIDs are more present in the IEM signal $i(n)$ than in the OEM due to the occlusion effect and the attenuation of the earplug. Hence, in order to reject the WIDs from the in-ear residual ambient SPL, the OEM signal denoted $o(n)$, is used to estimate the residual ambient SPL behind the earplug by filtering this signal with an estimate of the earplug transfer function $\hat{H}$ to obtain $i^*(n)$.

To estimate the earplug transfer function $\hat{H}$, the broadband ambient noise is captured using the OEM and IEM while the earpiece is worn. The earplug transfer function is then modeled

continuously by a finite impulse response (FIR) filter obtained using an adaptive Normalized Least-Mean Square (NLMS) method as follows:

$$\begin{aligned} i^*(n) &= \mathbf{w}^T(n)\mathbf{o}(n), \\ e(n) &= i(n) - i^*(n), \\ \mathbf{w}(n+1) &= \mathbf{w}(n) + \frac{\mu\, e(n)\mathbf{o}(n)}{\mathbf{o}^T(n)\mathbf{o}(n)} \end{aligned} \tag{4.2}$$

where $o(n)$ is the OEM signal and $i(n)$ the IEM signal. The filter coefficients $\mathbf{w}(\mathbf{n})$ converge towards the earplug transfer function by minimizing the error $e(n)$. The μ adaptation step size is set to 0.5, based on a previous study (Nadon *et al.*, 2017a), to correctly identify the transfer function within two seconds with an adaptive filter of $N = 200$ coefficients. The filtered output is then used as the in-ear sound pressure estimate $i^*(n)$, as shown in Fig. 4.2. This signal is then passed through an A-weighted filter and used to calculate the equivalent sound level L_{AF} in dBA.

In order to obtain a precise estimate of the earplug transfer function and ensure proper estimation of $\mathrm{PAR}_{\mathrm{AF}}$ and L_{AF}, an adaptation time of approximately 10 seconds is used. However, when a WID is present within the 0.33 s period of analysis during the adaptation of the filter and the ambient SPL is too low, the identified earplug transfer function is incorrect and results in a negative PAR. Part of the results obtained with an inadequate earplug transfer function estimate resulting from a WID are removed by using L_{AF} in the daily L_{eq} only when a valid $\mathrm{PAR}_{\mathrm{AF}}$ is estimated on 30 seconds, i.e. when $\mathrm{PAR}_{\mathrm{AF}} > 0$ dB. This criterion reduces the risk of overestimating L_{AF} past the 10-second adaptation period.

4.3.4 Reference WID detection and rejection method

The reference WID detection method is based on the calculation of the coherence between the IEM and OEM signals (Randall & Tech, 1987). The method is based on the fact that when the sound pressure level measured inside the ear is mostly due to surrounding external noise, a high coherence is observed between the two microphone signals as sound travels predominantly through the earplug. When the IEM is disturbed by WIDs, such as speech, this

coherence decreases within the frequency range of the disturbance signal. When such coherence is measured at regular time intervals and averaged across a predefined frequency range [f_{min} f_{max}], it is then possible to define an indicator, here referred to as Δ (dB), to detect WID events (Bonnet, 2019; Bonnet *et al.*, 2019a). A binary decision is taken by comparing this indicator to a predefined threshold parameter Δ_{th} above which it is assumed that WIDs are present and contributing to the noise level measured by the IEM. The L_{th} threshold level is selected to distinguish between high-level WIDs -like shouted speech- which have a substantial impact on the noise levels measured by the OEM, and low-level WIDs -like chewing- which should only affect the signal measured by the IEM. To estimate the in-ear noise dose while excluding the noise contribution from low-level WIDs, the earplug transfer function is subtracted from the noise level measured by the OEM. For high-level WIDs, the noise level at the IEM is assumed to be the same as the last recorded audio sample where no WIDs are detected (Bonnet, 2019; Bonnet *et al.*, 2019a). This approach isolates most of the noise contributions from the wearer, regardless of the WID's type Bonnet *et al.* (2019a,1). In the present work, the parameter values of Δ_{th}=0.75 found by Bonnet *et al.* (2019a) is used, but the SPL threshold L_{th} is set at 70 dB as recommended by a more recent study (Bonnet *et al.*, 2019b).

Table 4.2 Definition of L_{eq} and PAR variables

Variable	Definition
L_{AF}	In-ear L_{eq} calculated with the $i^*(n)$ output of the **a**daptive **f**ilter ('AF')
L_{TF}	In-ear L_{eq} calculated from the $i(n)$ signal where the noise contribution of WIDs are excluded using the coherence from the **t**ransfer **f**unction-based reference method ('TF')
L_D	Ambient L_{eq} calculated from the Larson Davis reference dosimeter with shoulder microphone
PAR_{ref}	personal attenuation rating estimated from the **ref**erence ('ref') method that uses the average of the autospectrum and cross-spectrum estimates of the $i(n)$ and $o(n)$ signals.
PAR_{AF}	personal attenuation rating estimated using the L_{eq} calculated from the estimated $i^*(n)$ **a**daptive **f**ilter ('AF') output and the $L_{\text{eq,OEM}}$

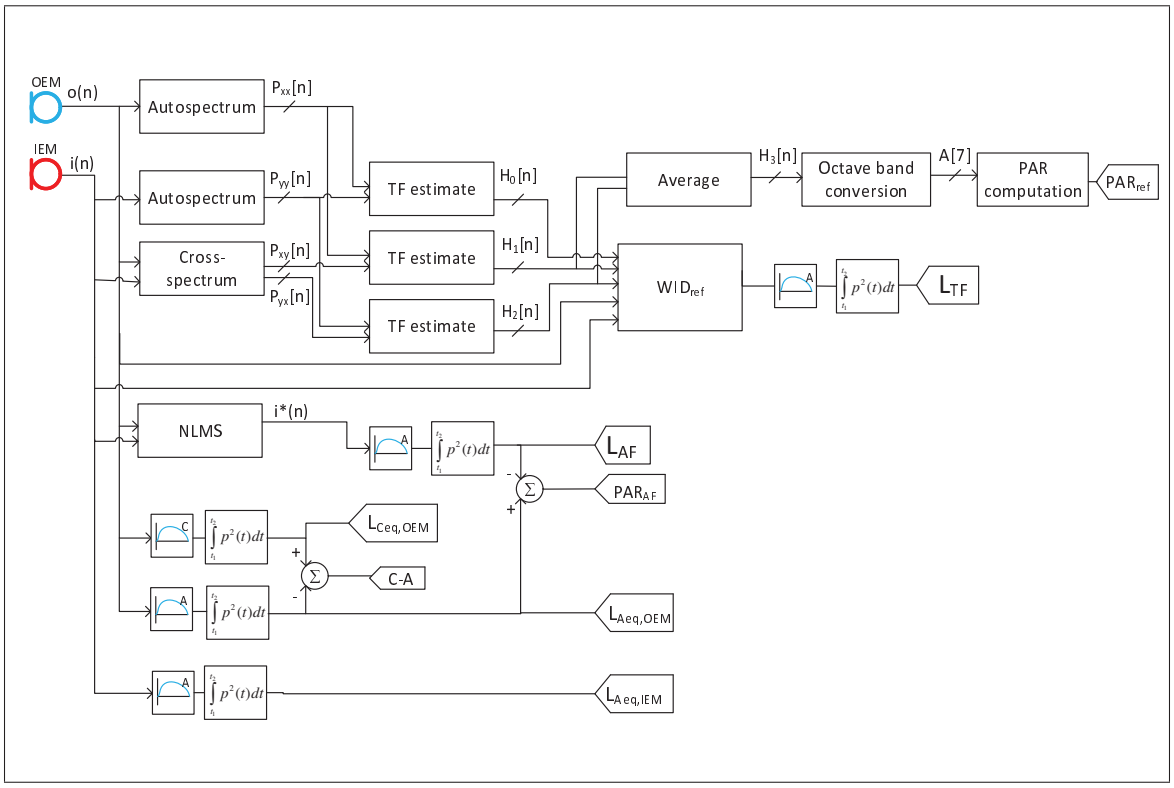

Figure 4.2 Schematic of the algorithm used to estimate the equivalent noise levels defined in Table 4.2 and other noise metrics

4.3.4.1 Artifact rejection in recorded audio signals

Due to a technical issue in the ARP software developed for this study, short discontinuities in the audio data recorded were found at random times, simultaneously on all audio channels. Such discontinuities were thoroughly investigated and attributed to a lack of proper interruption management resulting in overwriting part of the audio circular buffers. Since these discontinuities happen randomly but were in-sync on all acquired signals, partial recovery was possible and the *in situ* collected data was judged to be of sufficiently high-value to justify the development of an artifact rejection algorithm.

In order to clean the recorded audio data and remove the discontinuity artifacts, a comparison is made between the low-frequency coherence (Δ) and a higher-frequency coherence indicator (Δ_{HF}) defined here, the only difference between Δ_{HF} and Δ being that Δ_{HF} is calculated among

third-octave frequencies from 1500 to 8000 Hz instead of 200 to 1250 Hz. The audio signal is discarded from post-processing whenever Δ_{HF} exceeded Δ by at least 3 dB , during the 0.33 s period of analysis. This allowed rejecting the discontinuity artifacts while retaining the rest of the signal. In most situations, WIDs are not rejected by this approach as WIDs contribute mostly to lower frequencies (Bonnet, 2019), hence affecting Δ more than Δ_{HF}. An example of the proposed data correction is shown in Fig. 4.3 where the audio signals with the discontinuities recorded on a Head and Torso Simulator (HATS) are effectively rejected by the presented coherence-based approach. This artifact rejection algorithm is used to remove all discontinuities from the processed audio before the analysis presented in this study, which resulted in the removal of approximately half of the total useful audio data, but still retaining close to 147 h of reliable *in situ* recordings.

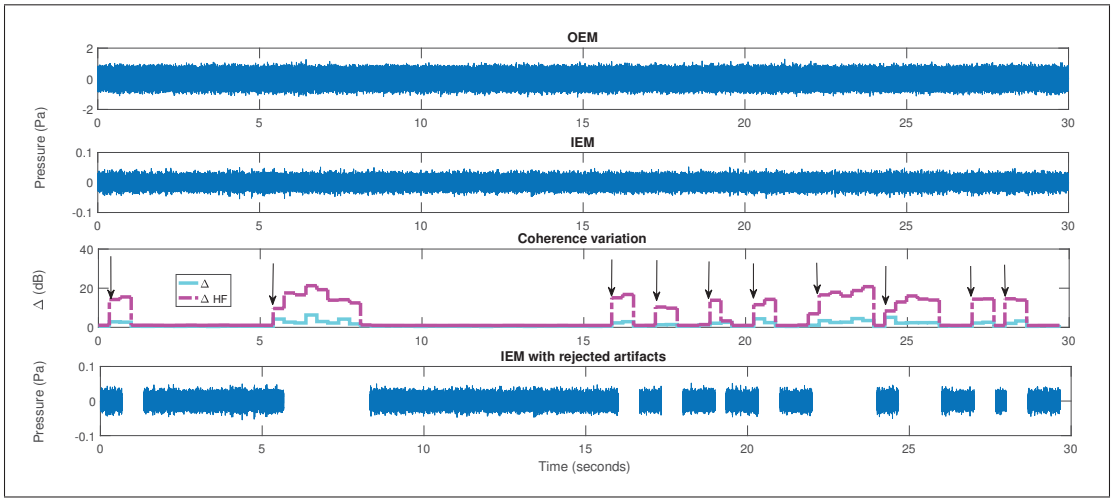

Figure 4.3 OEM and IEM signals, where no WIDs are present when the system is tested on a HATS. Discontinuities are not visible at first sight but caused erroneous values in the Δ The discontinuities are well detected, as pointed by the arrows, by comparing Δ_{HF} with Δ and are rejected both from the OEM and IEM signals (only the IEM is shown in the figure above)

4.4 Experimental results

4.4.1 Estimation of the PAR

To validate the proposed $\mathrm{PAR_{AF}}$, it is compared to $\mathrm{PAR_{ref}}$ in the Bland-Altman plot in Fig. 4.4. Such Bland-Altman plots are generally used to analyze the agreement between two different methods. As shown in the figure, the difference between the methods ranges from -8.3 to 6.6 dB at the 2.5^{th} and 97.5^{th} percentile (right graph).

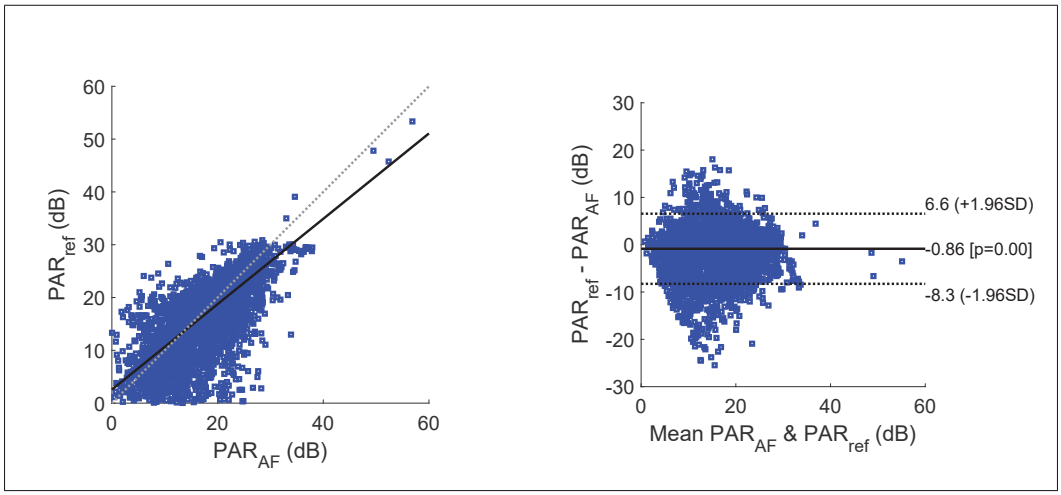

Figure 4.4 Bland-Altman plots showing the correlation of the $\mathrm{PAR_{AF}}$ approach and the reference $\mathrm{PAR_{ref}}$ approach used as a benchmark for all participants on all tested days (left) and the difference between the methods in function of the mean value of both methods (right)

4.4.2 Estimation of the residual sound pressure level

To calculate the difference between the estimated residual SPL and the original $L_{\mathrm{eq,IEM}}$, the OEM and IEM sound pressure levels of each individual participant are first calculated over 0.33 s and then accumulated each one second. As an example, these SPLs are shown at the top of Fig. 4.5a for one participant. These one-second equivalent sound pressure levels are compared between the different approaches (L_{AF}, L_{TF}, $L_{\mathrm{eq,IEM}}$ and $L_{\mathrm{eq,OEM}}$) and accumulated over 30 seconds, shown at the $L_{\mathrm{eq,30s}}$ mark at the bottom of Fig. 4.5a. These $L_{\mathrm{eq,30s}}$ levels are

then shown over a 10-minute period in Fig. 4.5b for that same participant. $L_{\text{eq, 1 day}}$ levels, shown in Fig. 4.6, are summed on the number of valid $L_{\text{eq, 10min}}$ data points for the work day. The graph in Fig. 4.5a shows the typical good agreement observed between L_{AF} and L_{TF}. It also illustrates the reduction in sound pressure level achieved with both methods rejecting WIDs when an accurate earplug transfer function is estimated. Fig. 4.6 shows that there are negligible differences between L_D and $L_{\text{eq,OEM}}$.

Results shown in Fig. 4.5 & 4.6 are illustrative of a typical measurement day and are further described to ease the interpretation of the results: during the experiment the participant may talk during low ambient noise levels, as shown with the higher $L_{\text{eq,IEM}}$ levels at the 0 and 10-minute mark in Fig. 4.6 . Such WIDs can occur at any moment during the 30-second period of analysis and causes the earplug transfer function to be incorrectly identified, thus resulting in a low L_{AF} level. On the other hand, an incorrect transfer function may also be identified when the participant generates a low-level WID during the 10 seconds used for the filter adaptation for L_{AF} , which occurs every 30 seconds in this study. In this case the identified transfer function overestimates the residual SPL L_{AF} when compared to $L_{\text{eq,IEM}}$ as shown at 20, 30, 100 and 200 minutes in Fig. 4.6. The variations in transfer function estimates are also visible in PAR_{AF} in Fig. 4.5b at approximately 106.3 minutes when the participant generated a WID, rejected by the reference method, but causing an incorrect filter adaptation for the proposed method. The PAR also decreases past 107.3 minutes due to the ambient noise level being too low, compared to the physiological noise behind the earplug, to correctly estimate the earplug transfer function. In these situations, the proposed method could benefit from a more robust PAR criterion than $\text{PAR}_{\text{AF}} > 0$ dB. This criterion must be optimized to better discriminate such artifacts and reject L_{AF} when the earplug transfer function is no longer adequate.

High-level disturbances are detected at 15, 18 to 20 and 27 to 28 seconds in the IEM signal in Fig. 4.5a, which are rejected in both L_{TF} and L_{AF}. In the illustrated case, these disturbances come from throat clearing, but also from audio notifications of the system triggered through participant interactions with the measurement software (e.g. waking up the device).

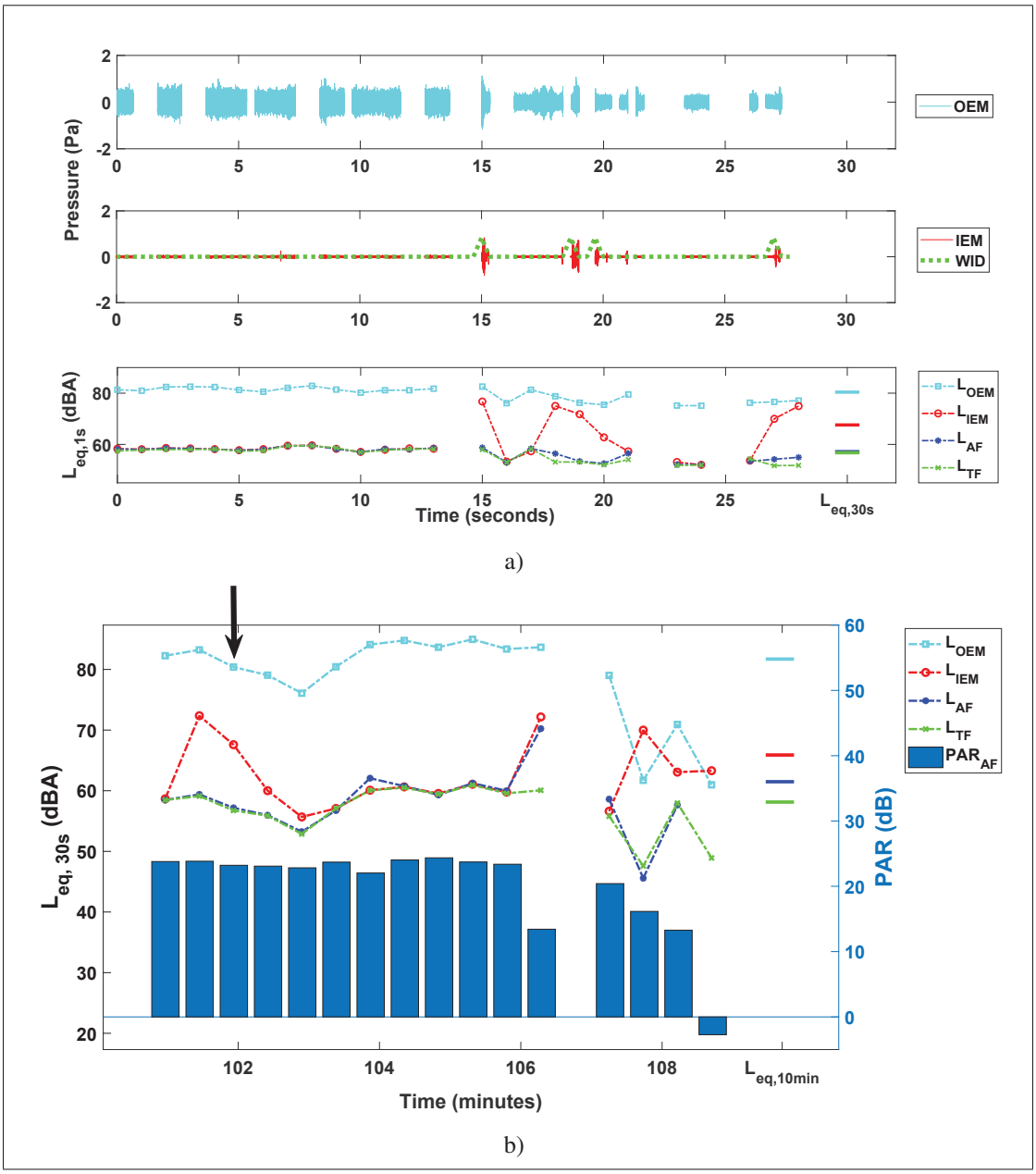

Figure 4.5 Example of typical cumulative equivalent noise levels for an individual. The figures show different steps of analysis: (a) over 30 s with the sound pressure expressed in Pascals at the top, (b) over 10 min and showing as well the proposed PAR estimate every 30 s. The accumulated L_{eq} levels for each microphone and different methods for the residual ambient SPL are shown at the right end of each plot. In (a) the WID detection flags of the reference algorithm indicate when the high level WID events have been isolated from the IEM signal to calculate L_{TF} . The arrow in (b) indicates the index of the 30 seconds of plot (a). The blank parts in waveform in (a) are the audio data rejected with the artifact rejection algorithm , whereas in (b) the 107^{th} minute is rejected due to the presence of stimuli from another in-ear measurement

To compare the performance of the proposed algorithm L_{AF} with the reference WID rejection method L_{TF} , the 1-day residual SPLs after WID rejection are compared to $L_{eq,IEM}$. These comparisons are displayed as a distribution for the different measurements (L_{AF}, L_{TF} and L_D) in the normal probability plot of Fig. 4.7. As shown in this figure, the intersection of the plots with the 0.5 probability, i.e. the mean difference, is at -3.4 dB for L_{AF} and -4.8 dB for L_{TF}. The proposed and reference WID rejection methods resulted in a similar ($p > 0.05$, paired *t-test*) mean difference, with approximately 0.3 dB overall between the two methods. The comparison of L_D with $L_{eq,IEM}$, ranging from -7.9 up to 22.7 dB with an average of 9.4 dB, shows the difference between the estimation of an individual's noise exposure level measured at the shoulder and an in-ear microphone behind an earplug. These differences account for the free-field to occluded earcanal correction (ISO, 2002), the attenuation provided by the earplug, and physiological noises measured exclusively by the IEM.

4.5 Discussion

4.5.1 PAR

The proposed PAR_{AF} between the $i^*(n)$ and $o(n)$ signals gives similar results to PAR_{ref} in most cases. However, large differences of approximately -8.3 and 6.6 dB, as shown in the Bland-Altman plots in Fig. 4.4, are caused due to the presence of WIDs during adaptation of the filter or the calculation of PAR_{ref}. Whereas the 6.6 dB difference is explained by incorrect earplug transfer function estimate, thus underestimating PAR_{AF}. Based on these assumptions, PAR_{ref} is expected to differ slightly from PAR_{AF} resulting in the correlation coefficient of $R^2 = 0.6$ (left graph). Such differences are acceptable for these *in situ* measurements considering the test conditions were not controlled, and could be improved by adapting the filter for the earplug transfer function and measuring PAR_{ref} at an optimal moment. Despite these possible improvements in PAR estimates, the proposed algorithm's PAR_{AF} did go up to approximately 30 dB, as shown on the left of Fig.4.4, and such high PAR suggests that the participants

were adequately protected during their work with the foam eartips provided with the designed earpieces.

To improve the earplug transfer function identification by avoiding filter adaptation when the PAR is low, the current PAR criterion of $\text{PAR}_{\text{AF}} > 0$ dB should be adjusted. For instance, the PAR criterion could be a function of the earplug fit quality in various situations, i.e. a criterion based on a threshold discriminating a good fit from a bad fit. For example, this criterion could be set at 25% below the PAR measured in an anechoic chamber. An adequate PAR criterion would also improve the proposed method's L_{AF} estimate. Moreover, the PAR should be estimated in high ambient noise settings when participants remain silent and do not generate WIDs. Following such improvements, the proposed PAR_{AF} could be used to estimate the protection level of workers in real time.

4.5.2 Residual sound pressure level

According to the results shown in Fig. 4.7 the mean difference between $L_{\text{eq,IEM}}$ and L_{AF}, for all participants over separate days, is approximately -3.4 dB for $L_{\text{eq,1 day}}$. The 1.4 dB difference between the proposed (-3.4 dB) and reference (-4.8 dB) WID rejection methods, is potentially caused by either: A) the adaptation of the filter during a WID which results in an incorrect transfer function estimate which also reduces the PAR, as shown for instance in Fig. 4.5b at the 106.3-minute mark; B) the reference method rejected more high-level WIDs during low ambient SPL than the proposed method due to the influence of these WIDs on the OEM signal which is used with the adaptive filter to estimate the residual SPL; or C) abrupt increases in the ambient SPL occurred during high-level WIDs, causing the reference algorithm to underestimate the in-ear noise exposure compared to the proposed algorithm. This hypothesis in C) is attributed to the reference algorithm using the last L_{eq} measured prior to WID detection (Bonnet, 2019), whereas the proposed method relies on the adaptive filter output which might be a better representation of the ambient SPL variations that occurred during high-level WIDs.

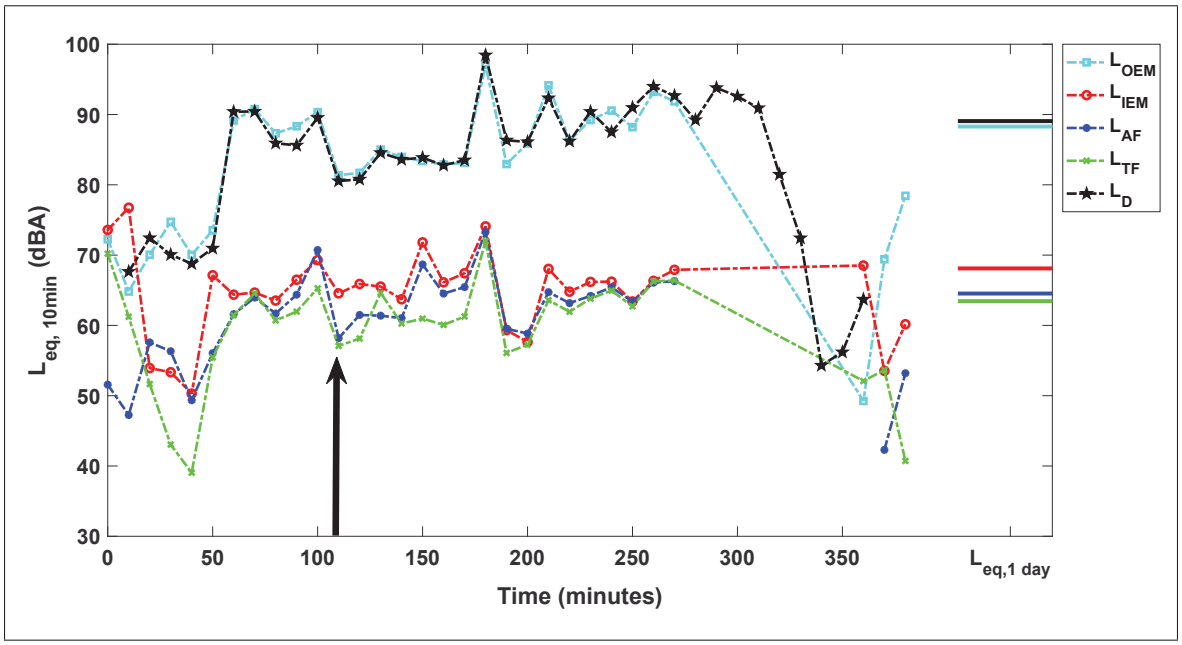

Figure 4.6 Example of typical cumulative equivalent noise levels, for the same individual as in Fig. 4.5, over one work day excluding L_{AF} when PAR_{AF} <0. The arrow indicates the index of the 10 minutes of the plot in Fig. 4.5b. Gaps in L_{eq} are explained by the device that was switched off, which was not the case of the reference dosimeter (L_D)

According to the experimental results, the proposed adaptive filter method appears as an efficient way to reject the WID noise events from the measured in-ear L_{eq}. When a proper earplug attenuation transfer function is estimated, as shown with PAR_{AF} higher than 23 dB in Fig. 4.5b, the proposed adaptive filtering method leads to lower residual SPL by rejecting the WIDs. As previously discussed, the comparison with the reference WID rejection method (Fig. 4.6 & 4.7) shows that a more efficient WID rejection is nonetheless possible by improving the proposed method to reduce the impact of high-level WIDs captured by the OEM and avoid overestimating the residual SPLs because of improper earplug transfer function estimates. The distinction between low-level and high-level WIDs is not present in the proposed approach, which uses $o(n)$ combined with the earplug's transfer function identified through the adaptive filter, to estimate the WID-free residual SPL in any given situation. Indeed high-level WIDs, e.g. raised speech or shocks on the earpiece, may affect the noise levels measured by the OEM, therefore L_{AF} does

not fully exclude WIDs, especially in low to moderate ambient SPLs. Hence, minor differences in the daily residual SPLs between the two methods are expected.

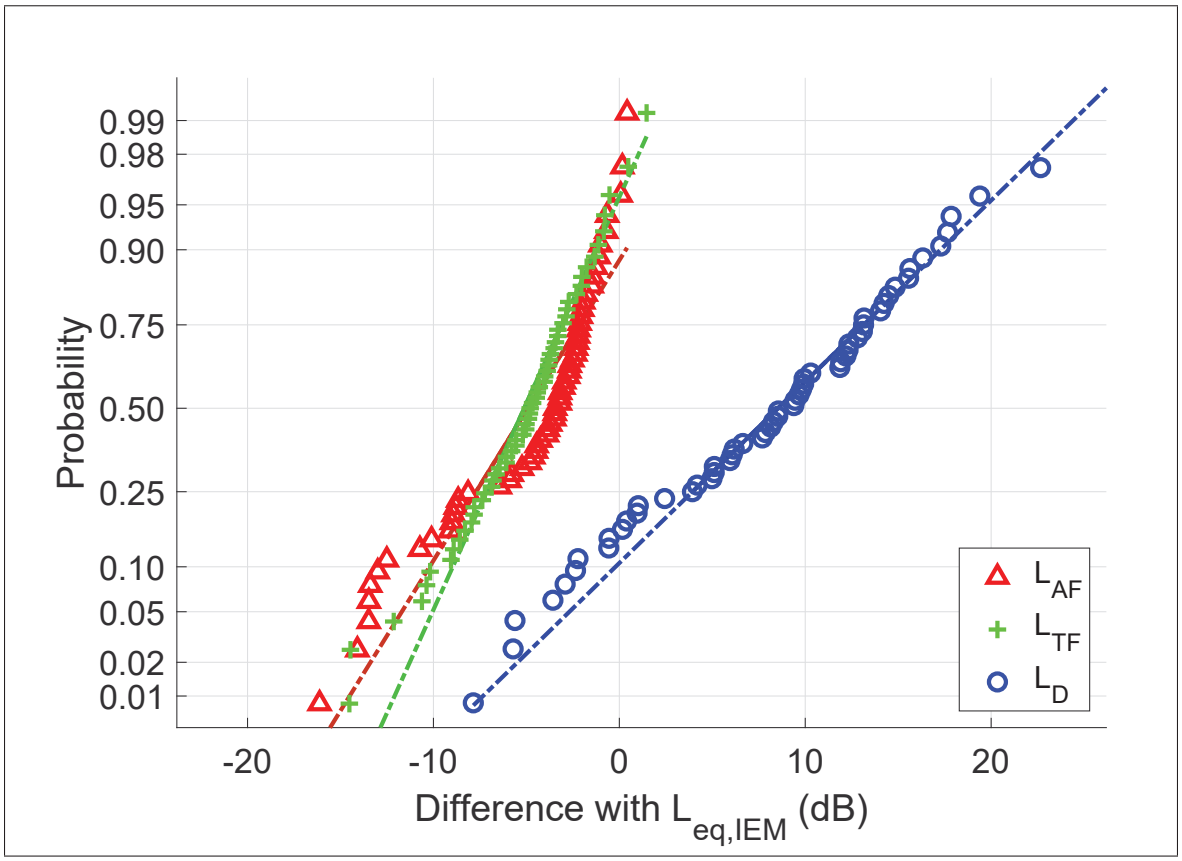

Figure 4.7 Normal probability plots showing the distribution of the IEM Equivalent sound level ($L_{eq,IEM}$) differences accumulated on each day with the first proposed approach (L_{AF}) and the reference algorithm output (L_{TF}), where each data point is a test day, for every participant. The reference Larson Davis dosimeter L_{eq} level (L_D) differences from the IEM are also included to show the important difference in daily accumulated levels between a microphone placed on the shoulder and a microphone placed in the earcanal

Another aspect to consider before using the proposed approach in commercial IENDs is the effects of the incoming noise directivity on the earplug transfer function. Preliminary measurements involving a subject wearing the earpieces used in this study showed that such transfer function could vary depending on the incidence angle of the sound source, especially at high frequencies. Up to 15.3 dB variations are observed between transfer function magnitudes estimated at 0, 90, 180 and 270° for frequencies above 4500 Hz in a 10 m^2 sound booth with the source placed

within 0.5 m from the subject's head. The impact of such variations on the estimated L_{eq} should be assessed before using the proposed algorithm in free-field or when machinery with very localized noise sources are used in small rooms with low reverberation time. Such differences in transfer functions could result in errors in the estimated L_{eq} and the PAR. However, the participants in the current study were only tested indoors where the effects of directivity are assumed to be minimal due to reverberation in the tested conditions. Moreover, the workers are moving continuously and noise sources can come from various tools surrounding them, hence logically the sum of the variations in the transfer function should result in a relatively small estimation error in the daily L_{eq}.

The adaptive filtering approach proposed in this paper is an interesting alternative to the reference method used for comparison (Bonnet, 2019; Bonnet *et al.*, 2019a). Although this new method may occasionally overestimate the in-ear noise exposure due to the influence of high-level WIDs (e.g. raised speech) on the OEM, it would allow to better account for the ambient SPL variations occurring during such WIDs and hence be more adapted to highly fluctuating noise environments. The low complexity of the proposed algorithm also requires less computational power , this results in a computation time of approximately 0.3 and 0.005 s faster to calculate the residual SPL and PAR respectively, compared to the reference methods as measured using MATLAB. These differences are mostly explained by the elaborate code for the decision process of the reference WID rejection algorithm and the extra calculation step to calculate the PAR. Hence, the proposed algorithm is a good option for implementation in future commercial IEND devices. Nevertheless, this method may be less adapted to low noise environments as it requires a good identification of the earplug's transfer function in the individual's ear, before WIDs are detected, and a sufficiently high ambient noise level to correctly reject the WIDs and estimate the PAR.

As mentioned earlier, to prevent the proposed approach's filter of adapting during WIDs, which leads to an underestimation of the earplug transfer function and an overestimation of the residual SPL, the earplug transfer function can also be identified at an optimal moment during the day . For example, when the noise level is sufficiently high and the wearer is quiet , since even

swallowing can generate an in-ear SPL of approximately 65 dBA and could lead to a negative PAR (Bonnet *et al.*, 2019a). Using the data collected in this study, this scenario was simulated on a typical subject and lead to an additional residual SPL reduction of approximately 1.3 dB when compared to the 30-second filter coefficients update, matching the reference algorithm's L_{TF} more closely. Changing the filter adaptation interval to 2-minute and 10-minute resulted in negligible changes compared to the residual SPLs obtained with the 30 s interval. Hence, adapting the filter every 30 s is a good compromise between continuously adapting the filter to track changes in the transfer function due to head movement and reducing the risk of adapting the filter while a WID is present in the signal. Ideally, the earplug transfer function should be updated regularly at a short-time interval, to ensure that potential changes in the earplug's fit are considered in the estimated in-ear noise level. For instance, the user could trigger an adaptation at regular time intervals whenever the dosimeter displays ambient noise levels higher than a certain threshold value to be defined. The user would have to remain quiet during the adaptation to obtain an accurate earplug transfer function. As a further verification step, the estimate could be discarded if too much variation is found in the PAR during adaptation.

The two algorithms were found to lower the estimated in-ear noise exposure due to WID rejection by 3.4 and 4.8 dB for the proposed and reference algorithms respectively, as shown in Fig. 4.7, when most participants were exposed to daily ambient SPLs varying from approximately 80 to 90 dBA. Less reduction in residual SPL would be expected from WID rejection in higher ambient noise levels as the WIDs would have less impact on the residual SPL.

The reduction of the WIDs' impact in the accumulated noise exposure levels can be important for occupational health purposes as the inclusion or rejection of WIDs could double or halve an individual's daily dose over the same time duration, when an exchange rate of 3 dB is considered. Moreover, it is clear that a shoulder microphone (L_D) overestimates (9.4 dB) the actual noise exposure that can affect the hearing health of a protected individual. Whereas the negative L_{D} differences shown in Fig. 4.7, such as -7.9 dB, are obtained from participants exposed to low ambient noise levels (ranging from approximately 60 to 70 dBA at the OEM) on specific days. At such levels, physiological noises (breathing, swallowing, chewing, etc.) and low-level

speech contribute to the in-ear SPLs while having a negligible effect on the shoulder microphone. Therefore, the in-ear residual ambient SPL estimated with proper earplug transfer function, microphone-to-eardrum corrections and WID rejection (Bonnet, 2019; Bonnet *et al.*, 2019a; Bonnet, F., Nélisse, H., Nogarolli, M. A. & Voix, J., 2020) should be considered to assess the risk of NIHL with the effective noise dose at the eardrum position in future studies.

4.6 Conclusions

A low-complexity method using adaptive filtering is proposed to detect wearer-induced disturbances and reject them from the residual SPL in the ear. This method is able to subtract the impact of WIDs in moderate and high ambient SPLs and performs well with quick changes in ambient noise levels during WIDs. The performance of the algorithm in low ambient SPLs requires a good earplug transfer function identified *a-priori*, otherwise an incorrect residual SPL is estimated. This method could eventually be integrated in IEND systems to run in real-time to estimate the residual SPL behind the earplug and the hearing protection level instantaneously using the proposed PAR estimate to provide users important information on their level of protection and daily in-field noise levels.

The performance of the proposed method is compared to a reference algorithm which achieves more WID rejection in residual SPL for low ambient SPL conditions. Both the proposed and reference methods could lead to a lower 1-day cumulative noise level by rejecting the WIDs and such reduction could more than double the allowed noise exposure duration for an exchange rate of 3 dB. The integration of such methods in a portable system could eventually help understand the relationship between the noise levels inside the ear and their effects on hearing health, especially if it is combined with otoacoustic emission measurements (Nadon, V., Bockstael, A., Botteldooren, D. & Voix, J., 2017b). In the long run, it may also help assess the effects of WIDS, e.g. speech, on hearing health.

Acknowledgment

The authors would like to acknowledge the financial support received from the Natural Sciences and Engineering Research Council (NSERC) through the NSERC-EERS Industrial Research Chair in In-Ear Technology (CRITIAS), as well as for technical support provided by EERS Global Technologies Inc. The authors would also like to thank the Centre for Interdisciplinary Research in Music Media and Technology (CIRMMT) for project funding opportunities. The first author is grateful to the Institut de recherche Robert-Sauvé en santé et sécurité du travail (IRSST) for the financial support received during his doctoral program and to the École nationale du meuble et d'ébénisterie (ENME) and its students for their participation in the field data collection.

CHAPTER 5

IN SITU OTOACOUSTIC EMISSION MONITORING TO ASSESS THE EFFECTS OF NOISE EXPOSURE ON HEARING HEALTH

Vincent Nadon[1,2], Jérémie Voix[1,2]

[1] Université du Québec, École de technologie supérieure (ÉTS),
1100, Notre-Dame West, Montreal, Quebec, Canada, H3C 1K3
[2] Centre for Interdisciplinary Research in Music Media and Technology,
527, Rue Sherbrooke Ouest, Montreal, Quebec, Canada, H3A 1E3

Article submitted to the Annals of Work Exposures and Health journal in November 2019.

5.1 Abstract

Many industrial workers are exposed on a daily basis to noise exposure levels that put them at risk of Noise-Induced Hearing Loss (NIHL). This occupational health problem remains the largest cause of indemnity in North American industries despite hearing conservation programs. These programs involve hearing assessment tests, but the measurements are generally conducted on too long intervals and are not sufficiently sensitive to prevent permanent hearing damage. Moreover, current noise regulations may be too permissive towards the maximum noise levels allowed. Short-interval hearing assessment is thus necessary to observe the temporary hearing health changes and prevent permanent damage. The short-term effects of noise exposure characteristics are therefore investigated using repeated measurements of otoacoustic emission (OAE) growth functions. This paper presents the most significant predictors of hearing health changes in sixteen individuals equipped with the OAE system's earpieces.

The experimental results of this study show that the noise level, impulsiveness and frequency spectrum can explain the decline in OAE levels. As a consequence, hearing conservation programs should take these noise metrics into account for proper NIHL risk assessment. Such noise exposure and hearing health monitoring should improve hearing conservation practices in the workplace and eventually mitigate occupational hearing loss.

5.2 Introduction

More than 22 million North-American workers (NIOSH, 2016) are exposed to excessive noise levels that put them at risk of developing Noise-Induced Hearing Loss (NIHL). Despite the efforts for hearing conservation programs in the workplace (Canetto, 2009), occupational hearing loss remains the most reported work-related disability. In an attempt to solve this problem, current hearing conservation practices usually involve the use of hearing protection devices as an easy solution against high noise exposure levels (Feder *et al.*, 2017; Rabinowitz *et al.*, 2013; Tantranont & Codchanak, 2017). However, these hearing protectors are generally not correctly fitted (Smith *et al.*, 2014) nor worn for the entire noise exposure duration (Groenewold *et al.*, 2014; HSE, 2019a). As a result, the estimated noise level underneath the hearing protector remains inaccurate and workers are exposed to noise levels above the recommended Permissible Exposure Levels (PEL). In order to measure this residual noise exposure level correctly, In-Ear Noise Dosimeters (IENDs) have been recently developed to measure underneath the protector using a microphone positioned in the earcanal. These IENDs currently do not remove the wearer-induced disturbances (WID) which are amplified by the occlusion effect (Bonnet *et al.*, 2019b; Nadon, V., Bonnet, F., E. Bouserhal, R., Bernier, A. & Voix, J., 2019) and do not compensate for earcanal transfer functions. Hence, current IENDs possibly overestimate the effective noise exposure level.

Furthermore, there is no way to validate that the PEL currently based on 8-hours as recommended by noise regulations is suitable given that the susceptibility to NIHL varies with each individual. Studies (Davis *et al.*, 2012; Qiu *et al.*, 2013; Vinck *et al.*, 1999) have shown that noise frequency spectrum and temporal variations can have different effects on hearing mechanisms. And yet, these metrics are currently not being taken into account in the ISO1999 standard (ISO, 2013) to estimate the risks of NIHL.

Risks of hidden hearing loss

Recent advances in auditory science show that moderate noise exposure levels are not without any risks (Bharadwaj *et al.*, 2015). Although such moderate noise levels may not induce changes in auditory thresholds in quiet conditions in the short term, they may induce damage to the cochlea's inner hair cell synapses (i.e. synaptopathy) and to the auditory nerve fibres (i.e. neuropathy). These types of hearing damage are therefore "hidden" since they are not detected with pure-tone audiometry, but usually impede speech intelligibility in noisy conditions (Kujawa & Liberman, 2015; Liberman, 2016). Current techniques to assess hidden hearing loss on humans with Auditory Brainstem Responses (ABR), for example, only detect the symptoms once the damage is irreversible and therefore do not prevent the onset of hearing damage.

Proposed hearing health monitoring approach

In order to potentially prevent this irreversible hidden damage, otoacoustic emissions (OAE) can be measured to detect temporary changes in the cochlea's outer-hair cell activity within a few minutes post-exposure. The cochlea is the organ responsible for the amplification and conversion of an acoustical stimulus to electrical nerve signal through its outer and inner-hair cells respectively. These signals are transmitted to the auditory cortex by the auditory nerve, but once the outer-hair cells are damaged the nerve signal loses amplitude and frequency resolution. This damage eventually leads to a loss of hearing sensitivity and an increase in Hearing Threshold Levels (HTL).

The measurement of Distortion Product OtoAcoustic Emissions (DPOAEs) is achieved by emitting two pure-tone acoustic stimulation signals at frequencies f_1 and f_2 in the earcanal using two miniature loudspeakers (Whitehead *et al.*, 1994). These stimuli signals are amplified or compressed by the non-linear cochlear amplification process, which results in the distortion product otoacoustic emission response found at frequency $f_{dp} = 2f_1 - f_2$. The DPOAE response is captured using an in-ear microphone (IEM) positioned in the earcanal. The stimuli (input) levels, denoted L_1 and L_2, modify the level of the DPOAE response (output) through the

non-linear cochlear amplification process. The DPOAE input/output function, referred here as the growth function, can be altered by excessive noise exposure due to damage in the cochlea's mechanics. The measurement of these growth functions can help to differentiate between two types of noise-induced hearing changes: 1) cochlear dysfunctions visible through changes in the DPOAE growth function slope and 2) other sources of changes in DPOAE levels like stimuli calibration, stapedial reflex or middle-ear dysfunctions which are visible through changes in DPOAE levels at all stimulation levels (Gehr *et al.*, 2004; Keefe, 2002).

DPOAE measurements are ideal to monitor hearing health in industrial environments since they are objective, fast and do not require an active participation of the worker. Yet, clinical DPOAE measurement devices available at the moment are not able to continuously monitor the onset of hearing damage in high ambient noise levels because the noise interference disturbs the recorded DPOAE signal. As a result, very few experiments were previously conducted with DPOAEs in industrial environments during noise exposure. Hence, a robust system was developed to measure DPOAEs in high ambient noise levels (Nadon, 2014; Nadon *et al.*, 2015a,1,1).

The current study is designed to monitor the short-term effects of noise exposure on hearing health through close monitoring of DPOAE growth functions during noise exposure using the developed system. The main objectives of this study are to:

1. Find the most significant predictors of NIHL.
2. Build mathematical models that estimate the relationship between these predictors and DPOAE levels.
3. Use the models to observe how noise exposure affects the DPOAE growth functions.

5.3 Material and methods

5.3.1 Subjects

To collect the data in this study, 16 subjects exposed daily to moderate noise levels at their workplace were selected and divided into two groups. The first group, referred to here as Noise Group 1 (NG1), consists of 3 individuals working in a Computer Numerical Control (CNC) machining workshop and aged between 36 and 44. The second group, referred to here as Noise Group 2 (NG2), consists of 13 individuals in a woodworking school and aged between 18 and 44. The experiment with NG1 participants was approved by the internal review board (IRB) of the École de technologie supérieure (ÉTS) (École de technologie supérieure, 2019). The participation of NG2 subjects was approved by both the IRB of the woodworking school and ÉTS.

The subjects were screened based on their best ear's pure-tone audiometry screening test conducted with an MA41 portable audiometer (MAICO, MN, USA) calibrated with TDH-49 headphones (Telephonics, NY, USA) according to the ISO 389:1991(E) standard (ISO, 1991). The headphones provided sufficient attenuation to perform the screening tests in a regular quiet room without acoustical treatment. Audiological measurements were conducted with the participants sitting on a chair facing the wall. Pure-tone audiometry was tested at [250, 500, 1000, 2000, 3000, 4000, 6000, 8000] Hz using the Hughson-Westlake method with a 5 dB step adjustment (Katz *et al.*, 2009).

The participants were then tested with the Auditory Research Platform (ARP) (CRITIAS, 2019), shown in Fig. 5.1a, a portable DPOAE system designed specifically for in-field measurements equipped with advanced noise-rejection algorithms (Nadon *et al.*, 2017a). Participants were asked to remain quiet during all DPOAE measurements. In order to pass the test, their DPOAE levels for their best ear had to be higher than the system's noise floor, measured approximately at -10 dB(SPL). DPOAE growth functions were measured twice, covering six f_2 frequencies from 4000 to 6169 Hz, then linearly averaged to confirm the participants' inclusion in the test groups.

Figure 5.1 a) Designed system with DPOAE earpieces also used as hearing protection with foam eartips. b) Each earpiece includes in-ear/outer-ear microphones and two-miniature loudspeakers for DPOAE stimuli generation

5.3.2 Noise exposure

In their daily routine, NG1 participants were mainly exposed to noise from background ventilation as well as CNC machines. They were occasionally exposed to high noise levels as they entered and exited the workshop during their 8-hour work shift. NG2 participants were exposed to background ventilation noise as well as a variety of woodworking machinery noises produced, for example, by industrial wood jointers, planers or wood hammers. They were exposed to noise for periods of up to 5 hours. Each participant was tested during a period of up to four days in their working environment, that is, in semi-reverberant rooms to eliminate other possible ambient noise sources such as wind, traffic, etc.

The outer-ear (OEM) and in-ear (IEM) microphone signals of the ARP earpieces recorded the noise exposure continuously. These earpieces, shown in Fig. 5.1b, are also equipped with two miniature loudspeakers (Knowles, IL, USA) to generate the stimuli required for the DPOAE measurements. The A-weighted ambient noise level ($L_{\mathrm{Aeq,O}}$) is calculated on the effective exposure duration (T) using a 30 second sample duration (T_i) of the OEM signal with a 3 dB exchange rate. This equivalent noise level is used for most of the statistical analyses detailed in

Section 5.3.4. The residual ambient noise level behind the earplug ($L_{Aeq,I}$) is calculated using the IEM signal, but with all the wearer-induced disturbances (WID) removed. These WIDs, such as throat sounds, speech, coughing, footstep noises, etc. are removed from the IEM signal using a previously developed WID rejection algorithm (Nadon *et al.*, 2019). The output of this WID rejection algorithm is A-weighted to calculate the $L_{Aeq,I}$ on the effective exposure duration with a 30 second time resolution.

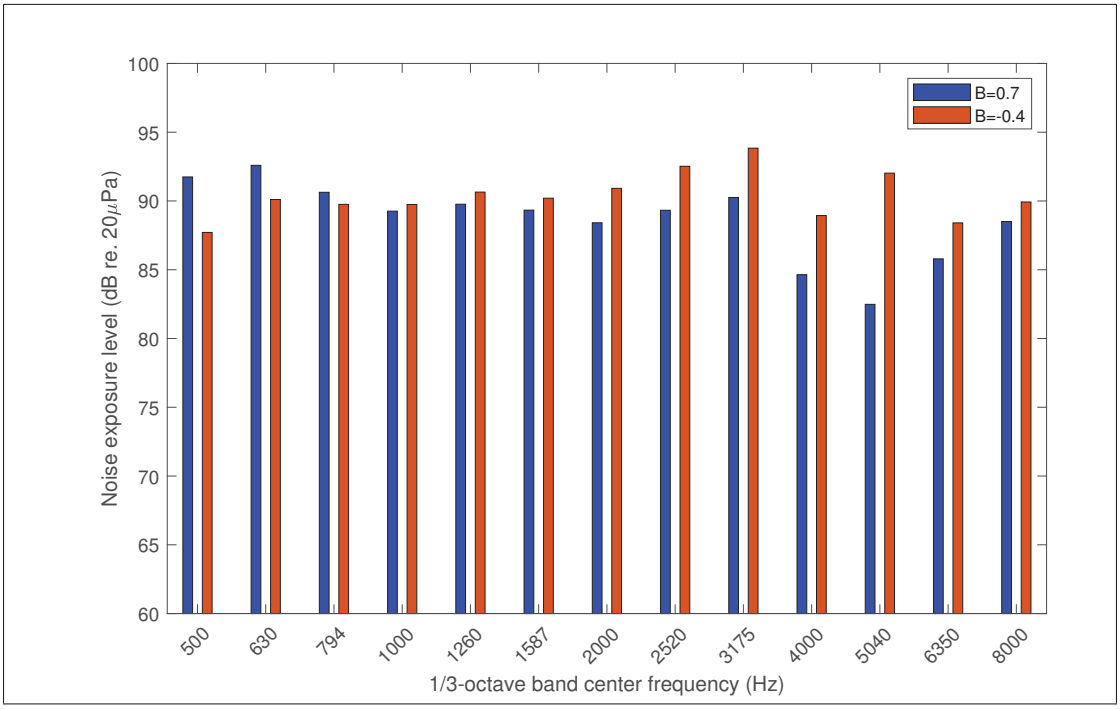

Figure 5.2 Noise frequency spectrum per 1/3-octave band for typical spectral balance (B) values in the tested noise conditions, showing more low frequency content for B=0.7 dB and more high-frequency content for B=-0.4 dB

The ARP also recorded raw audio signals to compute, in a post-processing phase, the following noise metrics:

A) The noise frequency spectrum balance (B) is the difference, in dB, between the C- and A-weighted cumulative ambient sound pressure levels. A spectral balance superior to +1 dB indicates that the ambient noise has more low-frequency energy (ANSI, 2007;

Nélisse *et al.*, 2011). An example of noise frequency spectrum for typical spectral balance values is shown in Fig. 5.2.

B) The crest factor, expressed in dB, estimates the impulsiveness of the noise signal as the ratio of the peak magnitude on the root-mean square (RMS) average (Starck *et al.*, 2003). The crest factor is calculated first on 30 second samples. The 30 second crest factors are then time-weighted averaged on the effective exposure duration. A noise exposure with a crest factor ≥ 15 dB is considered impulsive (Starck *et al.*, 2003).

C) Kurtosis ($\beta(t)$) is defined as the ratio of the fourth-order central moment to the squared second-order moment of the amplitude distribution (Davis *et al.*, 2012; Qiu *et al.*, 2013). The 30 second-sample kurtosis is estimated using the OEM signal and the Sound and Vibration Tools (Zechmann, E., 2019). The cumulative kurtosis is calculated on the effective exposure duration using the time-weighted average of the 30 second kurtoses. This metric is used to quantify the normality or non-normality of a noise signal distribution. A signal with a Gaussian distribution has a $\beta(t) = 3$ whereas non-Gaussian noises, such as impulsive industrial noises and speech, have a $\beta(t) \geq 3$ (Davis *et al.*, 2012). All noise metrics that characterize a non-Gaussian noise e.g. transient peaks, inter-transient intervals, transient period and crest factor have different effects on the kurtosis value (Davis *et al.*, 2012).

5.3.3 *In situ* DPOAE growth function measurements

5.3.3.1 DPOAE parameters

DPOAE levels are time-sensitive (de Toro *et al.*, 2010), therefore measurements should be efficient by reducing the frequency range and the amount of stimuli levels. To reduce the frequency range, measurements are restricted to f_2 from 4000 to 6169 Hz since the greatest noise-induced DPOAE shifts are expected in high frequencies, a 1/2-octave band above the ambient noise frequency range with maximum energy (Cody & Johnstone, 1981; de Toro *et al.*, 2010; Maison *et al.*, 2013). Moreover, the L_1 stimuli levels are set from 60 dB(SPL) to

70 dB(SPL) using a 5 dB step with L_2 set 10 dB lower than L_1 (Engdahl & Kemp, 1996), since the cochlear compression in humans is at its maximum at these levels (Bharadwaj *et al.*, 2015; Engdahl & Kemp, 1996). These L_2 levels also show the greatest DPOAE amplitude loss in chinchillas (Eddins, A. C., Zuskov, M. & Salvi, R. J., 1999). Besides, high stimuli levels ($L_2 \geq$ 50 dB(SPL)) make it possible to measure DPOAE responses in higher noise levels (Gates *et al.*, 2002).

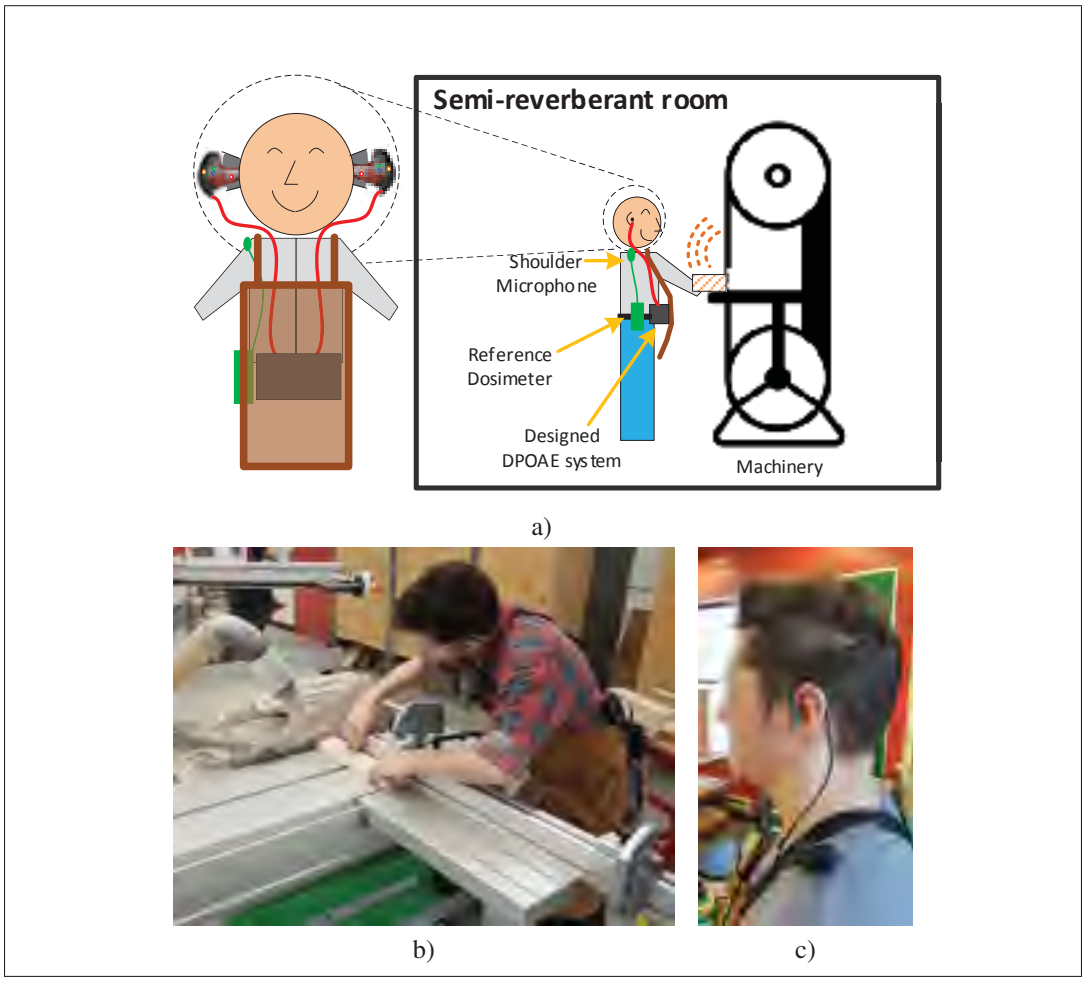

Figure 5.3 a) Schematic of a typical participant in his work environment wearing the designed DPOAE system and the reference dosimeter. Machinery icon from Björn Grundström on Noun Project (Grundström, 2019). b) and c) Pictures of participants wearing the designed DPOAE system with hearing protection provided by the earpieces while working. Reference dosimeter microphone shown attached to the subject's shoulder in picture c)

5.3.3.2 Experimental protocol

To test DPOAEs during work, the subjects carried the ARP in a fanny pack as shown in Fig. 5.3. The earpiece's ear hook and wires were placed under the apron and helped to secure the earpiece position in the ear and reduce the risk of pulling on the earpiece. The microphone of the Larson Davis Spark 706RC reference dosimeter (Larson Davis, NY, USA) was attached to the subject's shoulder on the side of the tested ear. This reference dosimeter was used to verify the ambient noise levels measured with the ARP.

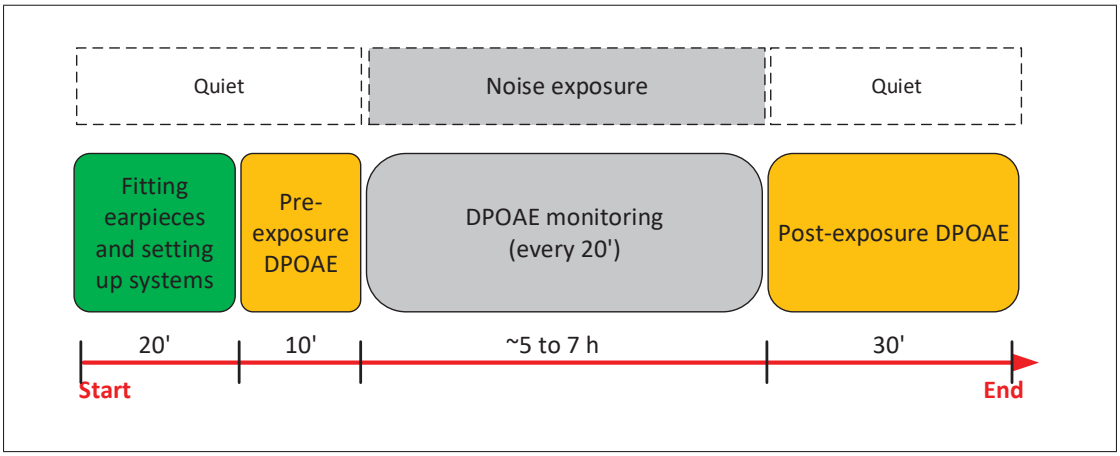

Figure 5.4 Daily experiment timeline with noise conditions (top) and measurements recorded (bottom)

The subjects tested their earpiece fit and calibrated the DPOAE stimuli during the first 20 minutes before entering the workshop (see Fig. 5.4). Once in the workshop, the fit-test and calibration was done every time the user re-fitted the earpiece or restarted the designed DPOAE system. The identified earcanal response is therefore always up-to-date to detect possible leaks in the earplug fit (Nadon *et al.*, 2015c) and compensate the DPOAE stimuli levels. After calibration, the subjects recorded their pre-exposure DPOAE growth functions for a reference baseline.

During the work shift, a timer is set to notify the subjects every 20 minutes to start a growth function measurement, as shown in Fig. 5.4. This allows sufficient time to observe the induced effects of noise exposure considering the possible lag (Singer *et al.*, 2003) between the dose and

the response (de Toro *et al.*, 2010; Engdahl, 1996). At the end of their work day, participants measured DPOAE growth functions every 3 minutes post-exposure to detect a possible recovery of DPOAE levels over approximately 30 minutes.

5.3.4 Multilevel model analysis

Multilevel models allow to observe the effects of predictors across time within subjects (level 1) and between subjects (level 2). In order to find the relationship between noise exposure and its effects on otoacoustic emissions, multilevel models are therefore developed using the noise metrics presented in Section 5.3.2 as time-varying predictors. These time-varying predictors are grand mean centered (Singer *et al.*, 2003) on the average (e.g. average $L_{\mathrm{Aeq,O}}$ is 78.1 dBA and average crest factor is 23.3 dB) calculated across all subjects. The time is reported in hours to facilitate the interpretation of the results and improve the precision of the coefficient estimates. The subjects' age and gender are included in the models as time-invariant predictors. All models included a random intercept for each day per participants to control for the non-independence of their repeated measurements (Rabinowitz *et al.*, 2013; Singer *et al.*, 2003). The models are built using the *nlme* package in R (José Pinheiro, Douglas Bates, Saikat DebRoy, Deepayan Sarkar, EISPACK authors, Siem Heisterkamp, Bert Van Willigen, R-core, 2019) with maximum likelihood and a first-order autoregressive covariance structure. Hence, any variability in measurement is constant regardless when the measurement is taken (Bolger, N. & Laurenceau, J.-P., 2013; Yakunina *et al.*, 2018). The predictors are added one at a time to select the optimal model that minimizes the log-likelihood and Akaike information criterion (AIC), thus improving the goodness-of-fit.

5.4 Results

5.4.1 Noise metric estimates

Fig. 5.5 shows the distribution of the cumulative noise metric values for approximately 294 hours of noise exposure. According to the distribution shown in Fig. 5.5a, the spectral balance *B*

varies mostly between -1.5 dB and 3 dB. The mode of the distribution is centered between 0 dB and approximately -0.5 dB indicating that the noise frequency content is balanced across the various test conditions with slightly more high-frequency noise (ANSI, 2007; Nélisse *et al.*, 2011). An example of the noise frequency spectrum for B = -0.4 dB is shown in Fig. 5.2.

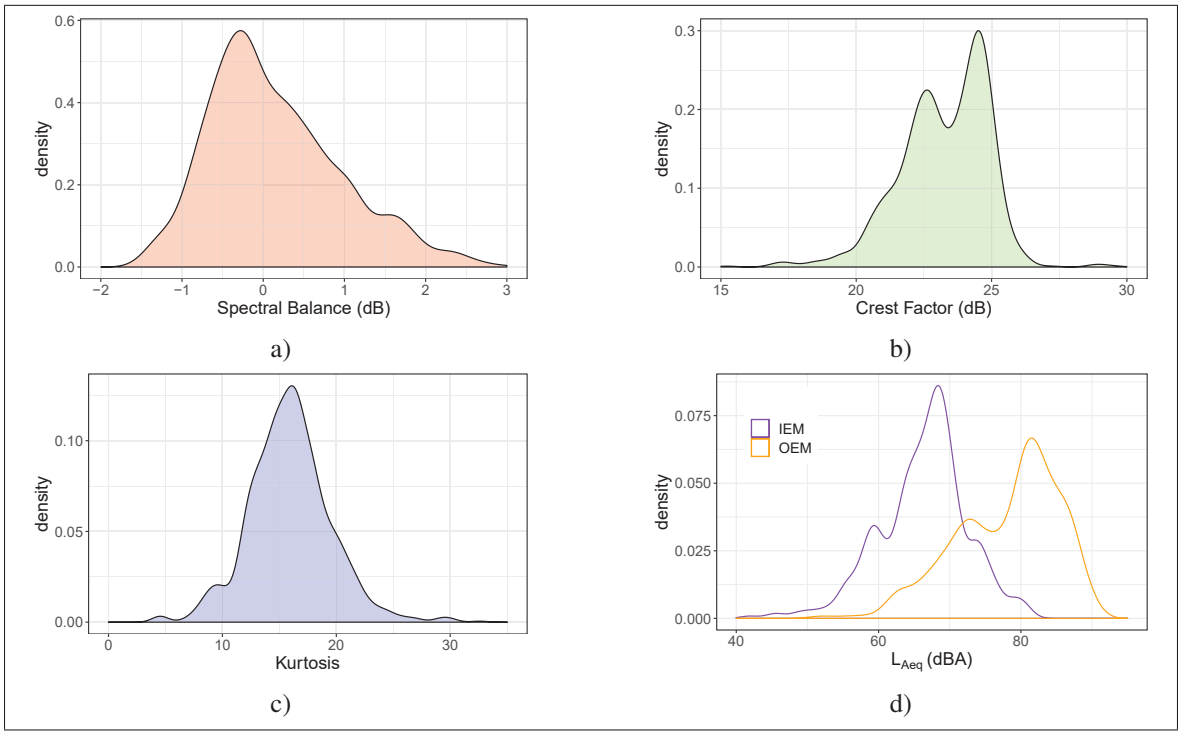

Figure 5.5 Distributions of the cumulative (a) spectral balance, (b) crest factor, (c) kurtosis and (d) $L_{\mathrm{Aeq,O}}$ compared to $L_{\mathrm{Aeq,I}}$ for approximately 294 hours of recorded audio

The crest factor distribution in Fig. 5.5b is bimodal with the first mode occurring at approximately 22.5 dB and the second mode at approximately 24.7 dB; most crest factor values range between 20 and 25 dB. These crest factor values indicate that the noise is impulsive according to the 15 dB criterion (Starck *et al.*, 2003; Starck, J. & Pekkarinen, J., 1987). The noise impulsiveness is also confirmed with the kurtosis shown in Fig. 5.5c that is mostly above the 3 dB criterion for Gaussian noises (Qiu *et al.*, 2013). Ambient noise levels captured by the OEM ($L_{\mathrm{Aeq,O}}$) mostly range from 60 to 90 dBA in Fig. 5.5d, indicating moderate to high noise exposure levels. The residual ambient noise levels captured by the IEM ($L_{\mathrm{Aeq,I}}$) range from 55 to 80 dBA with the mode of the distribution at approximately 67 dBA. The difference between $L_{\mathrm{Aeq,O}}$ and

$L_{\text{Aeq,I}}$ indicates that the earpieces with foam eartips provided enough attenuation for the tested noise conditions, but some subjects may not have a good seal on some occasions. An example of the noise metrics measured over time on a typical subject from NG2 is presented in Fig. 5.6.

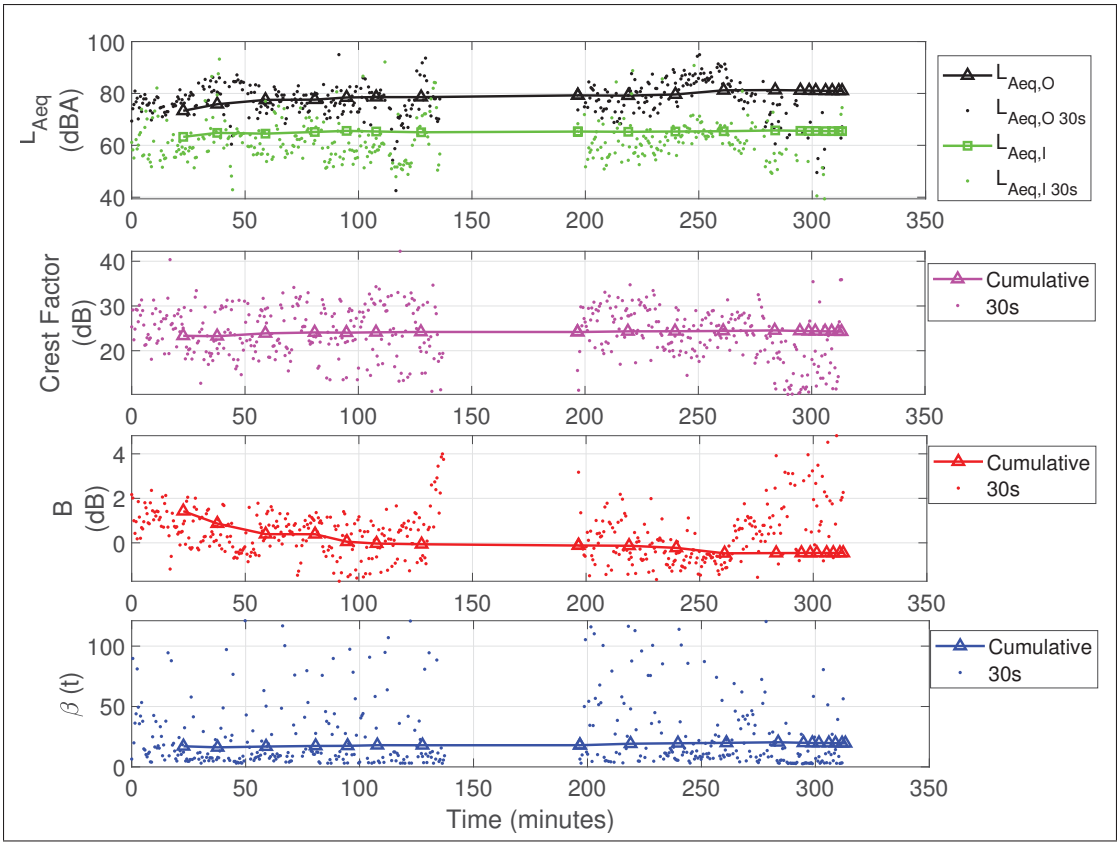

Figure 5.6 In-ear ($L_{\text{Aeq,I}}$) and Outer-ear ($L_{\text{Aeq,O}}$) noise exposure levels, crest factor, spectral balance (B) and kurtosis (β(t)) cumulative average corresponding to each moment a DPOAE is measured over the accumulated time for a typical subject from NG2. The dots ('.') represent the metrics at each 30 s sample

5.4.2 Otoacoustic emission growth functions

Fig. 5.7 shows the DPOAE shifts over time for each L_1 stimulus level for a typical participant from NG2. These shifts correspond to the effects of noise exposure metrics shown in Fig. 5.6. The shifts are calculated as the difference with the first valid DPOAE measurement of the day, referred to as the baseline. According to these results, the DPOAE growth function slope gets steeper as time progresses with the effects of the cumulative ambient noise levels. Minimal

recovery of DPOAE shifts is observed post-exposure (solid lines) in the last 30 minutes. The noise exposure and DPOAE shift measurements are further analyzed on all tested participants using the multilevel models and simulations.

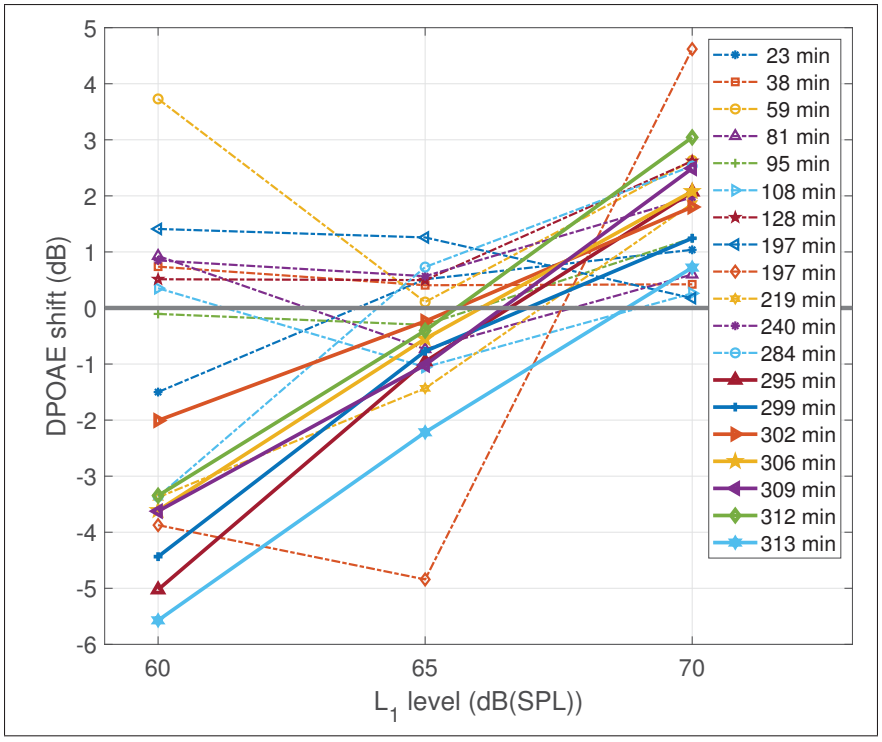

Figure 5.7 DPOAE shifts at f_2 = 4000 Hz as a function of L_1 stimulus levels on a typical subject from NG2. Solid lines indicate the DPOAE levels measured post-exposure. These plots show a linearization of the DPOAE growth functions caused by the noise exposure and time presented in Fig. 5.6

According to the models' AIC for the goodness-of-fit, the most significant predictors for DPOAE shifts are the crest factor and noise level $L_{\text{Aeq,O}}$ or $L_{\text{Aeq,I}}$. The latter is analyzed in a separate model than $L_{\text{Aeq,O}}$ since these two predictors are collinear. A separate univariate model is designed with the significant predictors for each stimulus L_1 ranging from 60 to 70 dB(SPL) and for each f_2 frequency from 4000 to 6169 Hz. The coefficient estimates of these models are presented in Tables 5.1 to 5.3. Each coefficient describes the size and direction of the relationship between the predictor and the DPOAE level.

Table 5.1 Coefficients of mixed models per f_2 stimulus frequency for L_1 = 60 dB(SPL) showing that the most significant combined effects of crest factor and ambient noise level $L_{\mathrm{Aex,O}}$ with time on DPOAE shifts are at f_2 = 4362 Hz

	f_2 frequency (Hz)					
	4000	4362	4757	5187	5657	6169
Time	−0.296***	−0.276***	−0.230***	0.014	−0.149**	−0.137**
	(0.062)	(0.057)	(0.053)	(0.060)	(0.060)	(0.054)
Noise level	0.151***	0.140***	0.167***	0.051	0.091***	0.093***
	(0.036)	(0.033)	(0.031)	(0.034)	(0.034)	(0.032)
Crest Factor	0.361**	0.413***	0.221*	0.308**	0.276*	0.527***
	(0.143)	(0.133)	(0.124)	(0.143)	(0.153)	(0.137)
Time : Noise level	−0.019**	−0.038***	−0.032***	−0.015*	−0.018**	−0.024***
	(0.008)	(0.007)	(0.007)	(0.008)	(0.008)	(0.007)
Time : Crest Factor	−0.085**	−0.096***	−0.030	−0.048	−0.041	−0.111***
	(0.036)	(0.033)	(0.031)	(0.036)	(0.036)	(0.033)
Intercept	1.835***	1.478***	1.293***	0.506	1.117***	0.937***
	(0.358)	(0.310)	(0.313)	(0.348)	(0.330)	(0.294)
Observations	722	711	702	684	673	751
Note: (standard error)						*p<0.1; **p<0.05; ***p<0.01

Table 5.1 shows that the combination of time and $L_{\mathrm{Aeq,O}}$ (*Time : Noise level*) has significant effects (p<0.05) on the reduction of DPOAE levels across the tested f_2 range for L_1 =60 dB(SPL), the strongest effects (-0.038 and -0.032) appearing at 4362 and 4757 Hz. The combination of time and crest factor (*Time : Crest Factor*) also has a strong effect on the DPOAE level, with the strongest effects at 4000, 4362 and 6169 Hz. Table 5.2 shows that *Time : Noise level* still has significant (p<0.05) effects on the DPOAE levels for L_1 = 65 dB(SPL) for most of the tested frequencies. *Time : Crest Factor* has the strongest effects at f_2=4000 Hz. Table 5.3 shows that *Time : Noise level* has the most significant (p<0.05) effects for L_1 = 70 dB(SPL) at f_2 frequencies from 4000 to 5187 Hz. However, *Time : Crest Factor* has significant (p<0.1) effects only at f_2=4757 Hz.

Table 5.2 Coefficients of mixed models per f_2 stimulus frequency for L_1 = 65 dB(SPL) showing that the most significant combined effects of crest factor and ambient noise level $L_{\text{Aex,O}}$ with time on DPOAE shifts are at f_2 = 4000 Hz

	f_2 frequency (Hz)					
	4000	4362	4757	5187	5657	6169
Time	−0.246***	−0.147***	−0.115*	−0.103*	−0.149***	−0.080
	(0.069)	(0.055)	(0.062)	(0.061)	(0.057)	(0.064)
Noise level	0.111***	0.092***	0.126***	0.072**	0.120***	0.081**
	(0.038)	(0.032)	(0.035)	(0.034)	(0.033)	(0.034)
Crest Factor	0.180	0.197	0.330**	0.472***	0.217	0.181
	(0.146)	(0.129)	(0.140)	(0.140)	(0.134)	(0.144)
Time : Noise level	−0.016*	−0.018**	−0.022***	−0.012	−0.026***	−0.020**
	(0.009)	(0.007)	(0.008)	(0.008)	(0.007)	(0.008)
Time : Crest Factor	−0.078**	−0.062*	−0.076**	−0.048	0.016	−0.051
	(0.038)	(0.032)	(0.036)	(0.035)	(0.034)	(0.038)
Intercept	1.275***	1.252***	1.037***	0.618*	1.100***	0.952***
	(0.360)	(0.307)	(0.384)	(0.325)	(0.308)	(0.351)
Observations	681	717	692	709	698	718
Note: (standard error)						*p<0.1; **p<0.05; ***p<0.01

The coefficient estimates for *Time : Noise level* using $L_{\text{Aeq,I}}$ have moderate effects (most effects at 4757 Hz with -0.021, p<0.05) on DPOAE levels. Moreover, based on the Bayesian Information Criterion (BIC) the models using $L_{\text{Aeq,I}}$ (BIC = 3855) did not show any improvements in the goodness-of-fit compared to the models using $L_{\text{Aeq,O}}$ (BIC = 3847). As a result, the models using $L_{\text{Aeq,I}}$ are not analyzed further, but are discussed in Section 5.5.

In order to facilitate the visualization of the combined effects of the coefficients, a test vector of typical noise levels shown in Fig. 5.8a is used as an input for the models. This vector is normalized before calculating the DPOAE shift, since the model coefficients were previously calculated on grand mean centered levels. These noise levels and time values are multiplied with the corresponding coefficients, then summed and the output DPOAE shift for f_2 ranging

from 4000 to 4757 Hz is shown in Fig. 5.8. The same procedure is used to show the effects of the crest factor (Fig. 5.9a) on the DPOAE shift at f_2 = 4362 Hz in Fig. 5.9b. Fig. 5.10 shows the sum of the effects of time, noise level and crest factor. This sum indicates that the crest factor and time have stronger effects on DPOAE shifts than the effects of noise level on its own (Fig. 5.8). The simulation results indicate a linearization of the DPOAE growth function at f_2=4362 Hz. This observation is further discussed in Section 5.5.

Table 5.3 Coefficients of mixed models per f_2 stimulus frequency for L_1 = 70 dB(SPL) showing the significant combined effects of ambient noise level $L_{\text{Aex,O}}$ with time on DPOAE shifts

	f_2 frequency (Hz)					
	4000	4362	4757	5187	5657	6169
Time	−0.179**	−0.158***	−0.230***	−0.194***	−0.036	−0.084
	(0.079)	(0.059)	(0.058)	(0.049)	(0.061)	(0.056)
Noise level	0.106**	0.078**	0.159***	0.115***	0.046	0.060**
	(0.042)	(0.034)	(0.034)	(0.031)	(0.036)	(0.030)
Crest Factor	0.189	0.216	0.328**	0.226*	0.086	0.186
	(0.164)	(0.134)	(0.134)	(0.124)	(0.140)	(0.126)
Time : Noise level	−0.030***	−0.023***	−0.037***	−0.022***	−0.006	−0.007
	(0.010)	(0.008)	(0.008)	(0.006)	(0.008)	(0.007)
Time : Crest Factor	−0.060	−0.025	−0.067*	−0.017	−0.001	−0.031
	(0.044)	(0.035)	(0.035)	(0.029)	(0.038)	(0.033)
Intercept	1.205***	1.093***	1.499***	1.099***	0.893**	1.202***
	(0.398)	(0.322)	(0.322)	(0.329)	(0.366)	(0.320)
Observations	517	661	669	712	700	730
Note: (standard error)					*p<0.1; **p<0.05; ***p<0.01	

5.5 Discussion

As illustrated in Fig. 5.10 the DPOAE shifts suggest that the lower L_1 stimulation levels are, in general, the most sensitive to long noise exposure. The shifts observed at f_2= 4362 Hz result in

the linearization of the cochlear gain with a steeper slope and indicate changes in OHC activity. These results are in agreement with the DPOAE shifts using similar stimuli parameters found in (Engdahl & Kemp, 1996; Sutton *et al.*, 1994). The models' coefficients for noise levels presented in Table 5.2 are also within a similar range as the results obtained in a previous experiment (Nadon *et al.*, 2017b). Considering the predictors in the current study are grand mean centered and the time is converted from minutes to hours, these adjustments are taken into account in the comparison.

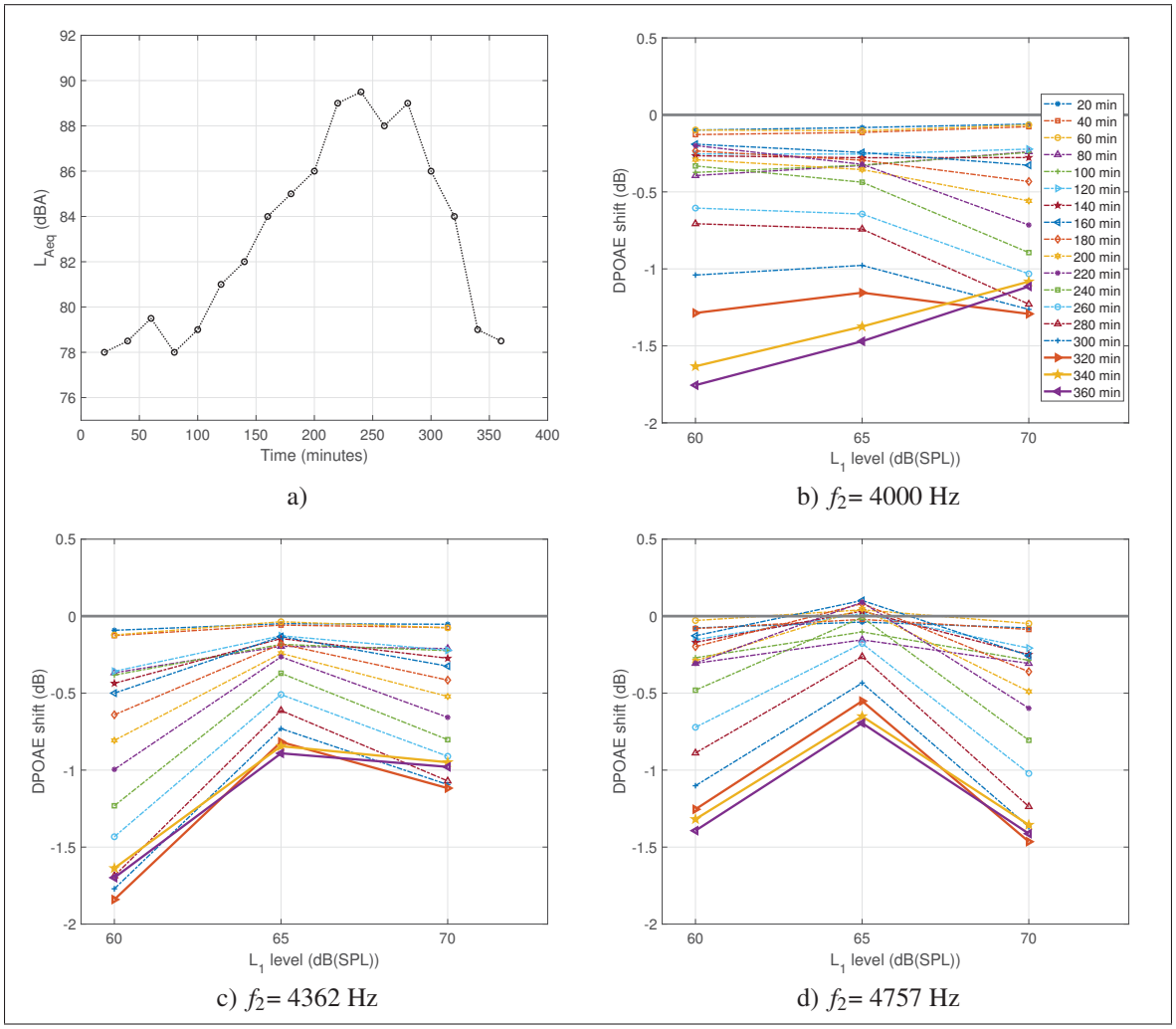

Figure 5.8 Noise level test vector shown in a). b), c) and d) show the effects of noise on the simulated DPOAE shifts at 4000, 4362 and 4757 Hz respectively using the vector in a) and the model coefficient estimates presented in Tables 5.1 to 5.3

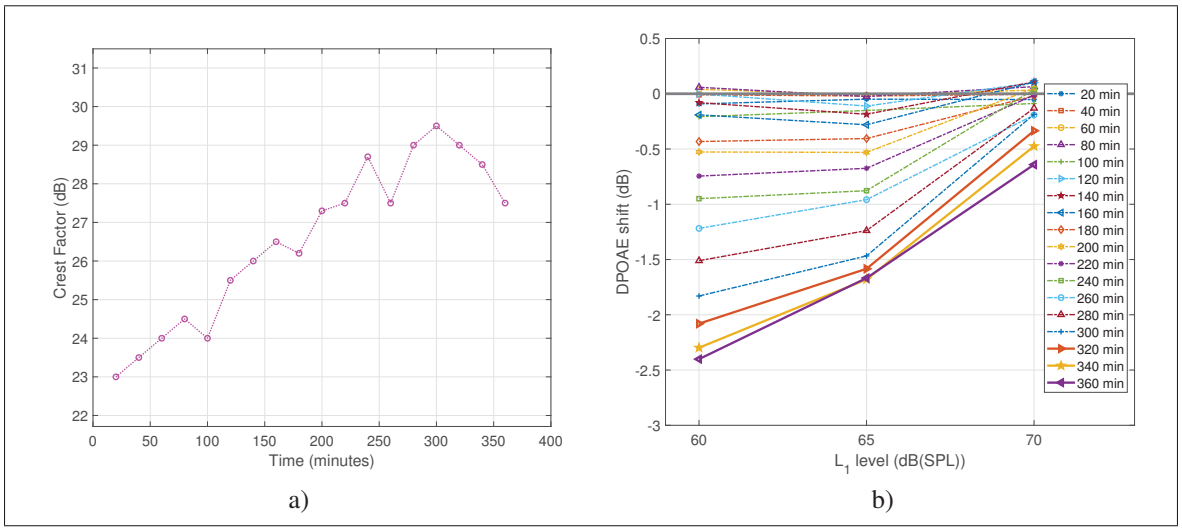

Figure 5.9 Simulations using a) the test vector for crest factor to observe in b) the effects on simulated DPOAE shifts at f_2 = 4362 Hz with the model coefficient estimates presented in Tables 5.1 to 5.3

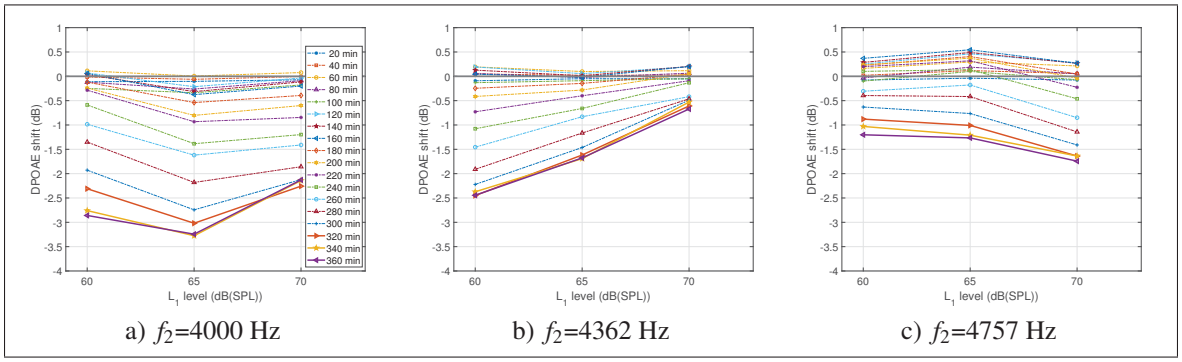

Figure 5.10 Sum of the effects of the noise levels shown in Fig. 5.8a and crest factor in Fig. 5.9a on simulated DPOAE shifts using model coefficient estimates presented in Tables 5.1 to 5.3

Fig. 5.9b & 5.10 show that the crest factor induced additional DPOAE shifts at lower L_1 stimulus levels. These results support the importance of impulsiveness metrics in NIHL assessment (Davis *et al.*, 2012; Qiu *et al.*, 2013; Starck *et al.*, 2003; Starck & Pekkarinen, 1987). Despite the fact that some subjects show a clear linearization of the growth function at f_2 = 4000 Hz as shown with a steeper slope of DPOAE shifts in Fig. 5.7. The average of noise-induced shifts at f_2 = 4000 and 4757 Hz estimated with the models (Fig.5.10) results in a slope close to zero,

hence a growth function slope that remains generally unchanged. These shifts could potentially be explained by the effects of temporary changes in the middle-ear (Gehr *et al.*, 2004) on the DPOAE levels. However, further research is needed to confirm the source of these DPOAE shifts. The results therefore suggest that the noise exposure has mostly induced damage in the outer hair cells responding to f_2=4362 Hz. According to the coefficients in Tables 5.1 to 5.3 and the simulations presented in Fig. 5.10, the greatest noise-induced changes are mostly at f_2 frequencies ranging from 4000 to 4757 Hz. This is in agreement with the 1/2-octave shift theory (Cody & Johnstone, 1981; de Toro *et al.*, 2010; Eddins *et al.*, 1999; Engdahl & Kemp, 1996; Maison *et al.*, 2013), since most of the energy in the noise signal is concentrated around or below the 3175 Hz 1/3-octave band for the tested noise conditions (see Fig 5.2 & 5.5a). However, the noise frequency spectrum balance did not improve the goodness-of-fit of the multilevel models, hence they are not included in the following models. This is possibly due to the homogeneity of the noise frequency spectrum across the tested conditions. A more thorough analysis of the noise frequency spectrum could help to explain changes in DPOAE levels at specific frequencies. Yet, this would require either a complex metric or keeping the entire frequency spectrum in memory.

Based on the AIC for goodness-of-fit, the kurtosis did not improve the tested models. This can be explained by the kurtosis average, using a time-weighted average of the kurtosis calculated on 30-second samples. This averaging method can reduce the impact of high kurtosis values. Besides, participants were only exposed to impulsive noises, as shown with $\beta(t) > 3$ in Fig. 5.5a. Consequently, the range of kurtosis values measured might not have an additional effect on the DPOAE shifts.

According to the models tested, $L_{\text{Aeq,I}}$ did not improve the model predictions. To improve these predictions, a calibration of the earcanal to eardrum transfer function should be included in the system to compensate for the differences in frequency response in the IEM signal (Bonnet *et al.*, 2020). This calibration would help to achieve a better estimate of noise levels at the eardrum location, closer to the inner-ear. Hence, this noise level would give a more accurate estimate of the noise that actually reaches the inner ear and that could possibly cause hearing damage.

The effects of parameters such as gender and age did not improve the goodness-of-fit of the models, possibly since the selected participants were a relatively young and homogeneous group, the oldest participants being 44 years of age. Older participants would be needed to observe the effects of aging. However, older participants with normal hearing thresholds and who are still active in the workplace are hard to find.

According to the results presented in this study, future IENDs should definitely include the crest factor as a noise impulsiveness metric and a noise-frequency spectrum balance metric. This would allow to properly assess the workers' risk of hearing health deterioration in industrial environments. Considering that $L_{\mathrm{Aeq,O}}$ remained mostly below 90 dBA in the tested noise conditions (see Fig. 5.5d), more noise-induced changes in cochlear mechanics are expected with the higher noise levels normally found in industrial environments (Eddins *et al.*, 1999).

5.6 Conclusions

The current study shows that even when surrounded by ambient noise levels that are higher than those normally found in clinical environments to measure DPOAEs, it is possible to monitor noise metrics and their short-term effects on otoacoustic emissions during noise exposure. According to the DPOAE growth function measurements, moderate levels of impulsive noise exposure can have detrimental effects on an individual's cochlear mechanisms. The risk of noise-induced hearing loss is still present in spite of the hearing protection provided by the earpieces, which reduce the ambient sound pressure levels to approximately 50 to 80 dBA. This risk is higher at f_2 frequencies within half of an octave band above the noise frequency range having the most energy.

Recommendations

To mitigate these risks, hearing conservation programs should start to integrate the measurements of noise impulsiveness and spectral balance metrics in the workplace. These best practices will help to define a new permissible exposure limit which should be personalized based on

individual's age and daily DPOAE shift. The maximum limit should remain below 75 dBA, underneath the hearing protector, according to the most conservative studies (Neitzel, R. & Fligor, B., 2017). These recommendations, once properly integrated in the workplace on a large scale, should be standardized to prevent occupational hearing loss more effectively.

Acknowledgment

The authors would like to acknowledge the financial support received from the Natural Sciences and Engineering Research Council (NSERC) through the NSERC-EERS Industrial Research Chair in In-Ear Technology (CRITIAS), as well as the technical support provided by EERS Global Technologies Inc. The authors would also like to thank the Centre for Interdisciplinary Research in Music Media and Technology (CIRMMT) for project funding opportunities. The first author is grateful to the Institut de recherche Robert-Sauvé en santé et sécurité du travail (IRSST) for the financial support received during his doctoral program and to the École nationale du meuble et d'ébénisterie (ENME) and its students for their participation in the field data collection.

.

CHAPTER 6

EXPERIMENTAL RESULTS: PERMANENT HEARING HEALTH CHANGES

As described in Section 1.3.2.2.3, the Contralateral Acoustic Stimulation (CAS) DPOAE suppression can be reduced due to long-term effects of noise exposure. This change in suppression is thought to arise from accumulated noise-induced damage to low spontaneous rate - high threshold auditory nerve fibres and is considered as a hidden hearing loss. The DPOAE measurement component without CAS can also be used to analyze the permanent changes in OHC activity.

To observe the potential effects of noise exposure on CAS DPOAE suppression, a pilot experiment was conducted with individuals in a simulated industrial environment (see Chapter 3 for a description of the experiment setup). However, the CAS DPOAE suppression effects were not statistically significant due to the small changes in DPOAE levels which are masked by the inter- and intra-subject variability. The statistical methods used to observe the effects of CAS DPOAE suppression per stimulus frequency were not robust enough to differentiate the small differences in suppression magnitude. CAS DPOAE measurements were therefore tested again in the second experiment (see Chapter 5 for a description of the experiment setup) with a wideband contralateral stimulus set at 65 dB(SPL). More participants have been included in that second study as well to increase the statistical power. A brief description of the pilot experiment is detailed in Section 6.1 and followed by the second experiment's description, statistical methods, results and discussion in Section 6.2.

6.1 Pilot experiment

The pilot experiment in controlled conditions, also described in Nadon, V. (2016)'s study and presented briefly in Chapter 3, was conducted on 9 human subjects (6 males and 3 females). Their CAS DPOAE suppression was assessed with a reference otoacoustic emission system (Etymotic Research, Il, USA) (Etymotic Research, 2019a). The 60 dBA wideband CAS was

generated in the contralateral ear using regular in-ear earphones through a laptop computer sound card while the EMAV (Neely & Liu, 1994) software was used to measure the DPOAEs.

The effects of DPOAE suppression are calculated as the differences between the DPOAE levels without CAS and with CAS. The average difference between pre- and post-exposure measurements of DPOAE suppression obtained in the pilot study ranged between -1.28 and +1.70 dB for industrial noise, -0.57 and +1.66 for constant noise and -1.65 and +0.62 dB for quiet conditions for the 22 tested f_2 frequencies. The effects were not statistically significant according to the *t*-test for the noisy conditions tested (Nadon, 2016).

These inconclusive results might be explained by the time interval between measurements during this pilot experiment. The measurements were conducted only a few days apart, hence it did not allow sufficient time to observe the effects of noise exposure on the MOC reflex mechanisms since MOC reflex fatigue is usually detected in the long term, a well-known limitation already mentioned in other studies (Müller & Janssen, 2008). Therefore, CAS DPOAE measurements should be conducted first during initial participant screening and second a few months later. Another limitation of this pilot study is the 9 participants that have been tested on three days. This sample size and the number of observations might not be sufficient to detect small DPOAE suppression effects. The protocol for the second experiment, presented below, was therefore adjusted based on these observations.

6.2 Second experiment

To improve the assessment of CAS DPOAEs, 20 participants were selected of which 16 were part of the regularly exposed noise group, referred to as NG1 and NG2 as described in Chapter 4 & 5. The additional 4 participants , 3 females and 1 male between 21 and 32 years of age, were selected particularly for this experiment and they were not exposed to noise in their office space, they are referred to as the quiet group (QG1). The time span between the initial screening CAS DPOAE measurement and the follow-up CAS DPOAE measurement ranged from 18 to 189 days with an average of 92 days.

For this experiment, the CAS DPOAE suppression was measured during the screening, pre- and post-exposure on 4 days, as well as the follow-up a few months later to ensure the progression of changes in suppression could be monitored. Only pre-exposure measurements are kept for the following analysis to ensure the changes are due to long-term damages instead of the temporary effects of noise exposure each day. An example of CAS DPOAE suppression is shown for a typical individual in Fig. 6.1. These measurements were achieved with the designed DPOAE system (see Chapter 2.1), with the contralateral earpiece generating white noise at a level of 65 dBA, a value often used in literature (Guinan Jr, J. J., Backus, B. C., Lilaonitkul, W. & Aharonson, V., 2003; Stuart, A. & Cobb, K. M., 2015; Yakunina *et al.*, 2018). Meanwhile the ipsi-lateral earpiece was simultaneously stimulating the DPOAE primary tones and recording the response. The white noise CAS level (65 dBA) was selected in order to increase the suppression effects compared to the pilot experiment and thereby improve the detection of noise-induced effects on hearing mechanisms.

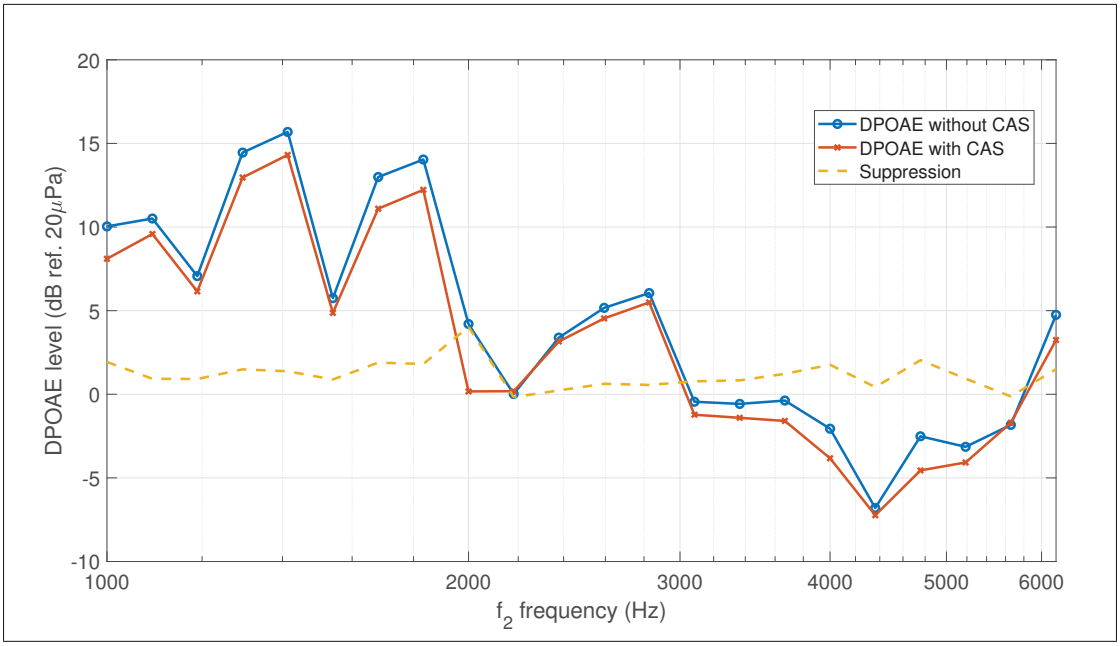

Figure 6.1 CAS DPOAE levels, without and then with the contralateral wideband noise, at the 22 f_2 stimuli frequencies measured on one typical subject using the ARP3DPOAE system showing the suppression effects between the two measurements (dashed line). The measurements are approximately three seconds apart

To measure CAS DPOAEs with the designed system's software, the second stage of adaptive filtering using the contralateral IEM (IEM-C) (Nadon, 2014; Nadon, V., Voix, J., Bockstael, A., Botteldooren, D. & Jean-Marc, L., 2015d) presented briefly in Appendix I was turned off to ensure the filter would not adapt on the contralateral wideband stimulus. When the filter adapts during contralateral stimulation, it does not identify the transfer function between the two earpieces' IEMs correctly since the ipsi-lateral ear is not stimulated with the same signal simultaneously. This incorrect transfer function identification modifies the processed DPOAE level, thus reducing the effect of the CAS DPOAE suppression.

Multilevel models are used in this second experiment to analyze the results. The selection of these robust statistical methods and the optimization of the parameters are described in Section 6.2.1.

6.2.1 Statistical Methods - Multilevel Models

After a first analysis of the CAS DPOAE suppression obtained in the second study with a simple *t*-test per f_2 stimulus frequency, no effects of noise exposure and time were found. However, the DPOAE shifts between the initial screening and the follow-up tests for NG1&2 and QG1 revealed that the groups exposed to occupational noise had a greater DPOAE shift for f_2 stimuli ranging from approximately 3000 to 4500 Hz. Therefore CAS DPOAE results have been analyzed further using multilevel models (Singer *et al.*, 2003) with the Maximum Likelihood (ML) and autoregressive correlation structure. These models allow to find the within-subject, such as the effects of time (*Session*), and between-subject differences between the groups (*Exposed1*), as well as individuals' *Age* and gender (*Gender1*). The coefficients for categorical predictors with only two statuses are always estimated using the predictor equal to one, e.g.*Gender1*: gives the fixed effect for Gender = 1 which represents males. When Gender = 0 the coefficient gives the fixed effects for females. In order to calculate the coefficient considering the females, it is possible to invert the coding, hence Gender = 0 would be attributed to males (Singer *et al.*, 2003).

Based on the predictors that might have an effect on changes in hearing health, the statistical models are built sequentially by including one predictor at a time. The model with optimal goodness-of-fit is then selected based on the lowest log-likelihood, Akaike Information Criterion (AIC) and Bayesian Information Criterion (BIC) (Singer *et al.*, 2003) as shown at the bottom of Table 6.1 & 6.2. The predictors need to significantly improve the fit of the model, this can also be evaluated with an ANOVA (analysis of variance) between the reference and improved models. In order to simplify the models' parameters and analysis, one univariate (i.e. one outcome) model is used per f_2 stimulus frequency.

6.2.2 Results

6.2.2.1 CAS DPOAE suppression

In order to find the most important predictors for CAS DPOAE suppression changes the model with the optimal goodness-of-fit, shown in blue in Table. 6.1, is selected based on the lowest AIC and BIC values. This optimal fit is obtained on a dataset including all tested frequencies to observe the global effects on the dependent variable. The optimal model includes the predictors *Exposed1*, indicating the fixed effect coefficient applied to groups exposed to noise, and *Gender1* indicating the fixed effects of male participants.

According to the models presented in Table. 6.1, effects of *Session* are small and not statistically significant, therefore the suppression magnitude did not change significantly during the time of the longitudinal study. This suggests that there is no short-term effect of noise on the DPOAE suppression. Random effects of session are estimated null, as explained by the non-convergence of models tested *a-priori* and visual inspection of the individuals' plots of suppression over time. Therefore, the intercept for Session has been set to 0 for the models presented in Table V-1 found in Appendix V.

The optimal model predictors are applied for each tested f_2 frequency as shown in Table V-1. In this table, the fixed effects coefficients indicate by how much the DPOAE suppression at the f_2

frequency changes for 1-unit of the predictor. For example, the group exposed to occupational noise has a CAS DPOAE suppression at f_2 = 1091 Hz that is 1.3 dB lower than the non-exposed group. The standard error shown between parenthesis can be used to calculate the confidence interval of these coefficient estimates.

Table 6.1 Fixed effects coefficients of models for the CAS DPOAE suppression. Lower values of log-likelihood, Akaike Information Criterion and Bayesian Information Criterion correspond to better models

	Dependent variable:						
	Suppression						
	(1)	(2)	(3)	(4)	(5)	**(6)**	(7)
Session		0.008		0.008			
		(0.019)		(0.019)			
Exposed1			−0.169	−0.169	−0.205	−0.337**	−0.177
			(0.132)	(0.132)	(0.133)	(0.121)	(0.136)
Age					0.006		
					(0.008)		
Gender1						0.288***	0.632***
						(0.099)	(0.215)
Exposed1:Gender1							−0.434*
							(0.238)
Intercept	0.381***	0.360***	0.510***	0.495***	0.540***	0.477***	0.379***
	(0.058)	(0.063)	(0.118)	(0.123)	(0.118)	(0.103)	(0.107)
Observations	2,266	2,266	2,266	2,266	2,266	2,266	2,266
Log Likelihood	−3,762.038	−3,759.763	−3,759.144	−3,759.062	−3,758.831	−3,756.032	−3,754.535
Akaike Inf. Crit.	7,532.077	7,533.526	7,532.287	7,534.124	7,533.662	7,528.063	7,527.069
Bayesian Inf. Crit.	7,554.980	7,573.606	7,572.368	7,579.930	7,579.469	7,573.869	7,578.601
Note: (standard error)							*p<0.1; **p<0.05; ***p<0.01

Fixed effect coefficients for *Exposed1* and *Gender1* are presented per f_2 DPOAE stimulus frequency in Fig. 6.2 to easily distinguish the frequencies with the most changes. The thresholds shown in orange and red are selected empirically to observe the fixed effects coefficients that appear to stand out from other tested f_2 frequencies. Some coefficient estimates, highlighted in orange and red, appear to have great effects on the suppression at frequencies mostly found between 1091 and 1834 Hz, a frequency range reported to have the most CAS suppression according to the literature (Sun, 2008; Yakunina *et al.*, 2018). However, they are not all statistically significant ($p > 0.1$) due to their large standard error. Additional data is needed to find significant effects at these frequencies where the effects are smaller. The most significant effects of *Exposed1* are found at 1091**, 1189**, 1584* and 1682** Hz, where the exposed groups

have less CAS DPOAE suppression by 0.5 dB and more. Male participants have in general more CAS DPOAE suppression effects, for this same frequency range (1189 to 1682 Hz), by over 0.5 dB compared to the females tested.

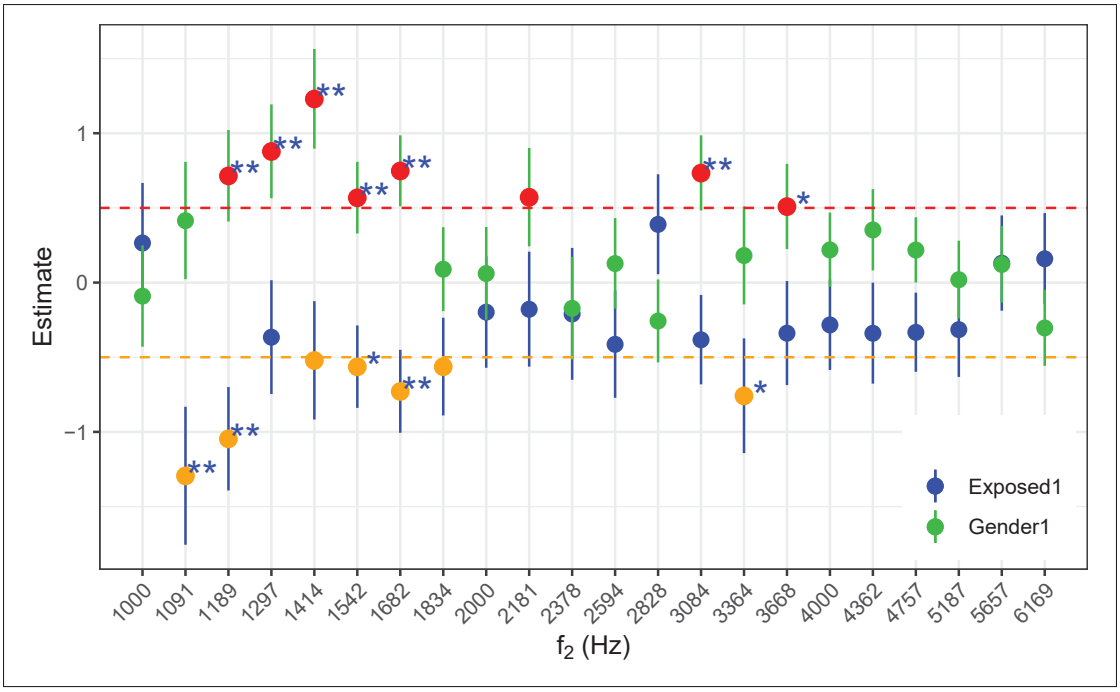

Figure 6.2 Fixed effect coefficient estimates per f_2 stimulus frequency explaining the DPOAE suppression (dB) with error bars showing the standard error. Orange and red dots indicate greater fixed effects
Note: '*' = $p < 0.1$ '**' = $p < 0.05$

All models with fixed effects greater than the thresholds set and in the frequency range of interest (1091 to 1834 Hz) have been tested for normality assumptions with the Shapiro-Wilk and Kolmogorov-Smirnov tests (Singer *et al.*, 2003), in addition to visual inspection of the residuals. The null hypothesis of these tests is that the residuals are normally distributed. Thus if the p value is greater than the chosen alpha level of 0.05, the null hypothesis that the residuals are normally distributed cannot be rejected. According to these normality tests, the residuals for all tested models are normally distributed. The CAS DPOAE suppression at f_2 = 1682 Hz did not pass the Shapiro-Wilk test ($p < 0.05$), but passed the non-parametric Kolmogorov-Smirnov

test ($p > 0.05$). Visual inspection of this model's residuals in a Quantile-Quantile (Q-Q) plot showed no major deviance from normality (see Fig. VI-1 in Appendix).

6.2.2.2 DPOAE shift

In order to find the predictors which have the most effects on long-term DPOAE shifts, the model with the most optimal goodness-of-fit is selected. The 4^{th} model shown in blue in Table. 6.2 is selected since it has one of the lowest log-likelihood and AIC considering the number of predictors included. Moreover, the coefficient estimates of the separate models at each f_2 frequency (shown in Fig. V-2) are more statistically significant than if the other predictors are included. According to this optimal model, the predictors *Exposed1* and its crossed effects with session (*Session:Exposed1*), which indicates the fixed effects of time, are the most interesting.

Table 6.2 Fixed effects coefficients of models for DPOAE shifts. Lower values of log-likelihood, Akaike Information Criterion and Bayesian Information Criterion correspond to better models

	Dependent variable:						
	DPOAE level						
	(1)	(2)	(3)	**(4)**	(5)	(6)	(7)
Session		−0.124	−0.124	0.063	−0.124	−0.124	−0.124
		(0.078)	(0.078)	(0.168)	(0.078)	(0.078)	(0.078)
Exposed1			−1.356	−0.088			
			(1.349)	(1.691)			
Session:Exposed1				−0.234			
				(0.188)			
Age					−0.096		0.034
					(0.074)		(0.099)
Gender1:Age							−0.250*
							(0.141)
Gender1						−1.034	−0.706
						(1.104)	(1.032)
Intercept	2.618***	2.950***	4.035***	3.021**	2.950***	3.571***	3.574***
	(0.582)	(0.676)	(1.279)	(1.513)	(0.696)	(0.934)	(0.928)
Observations	1,319	1,319	1,319	1,319	1,319	1,319	1,319
Log Likelihood	−3,906.523	−3,895.542	−3,895.084	−3,894.337	−3,894.840	−3,895.119	−3,893.218
Akaike Inf. Crit.	7,821.047	7,805.084	7,806.167	7,806.675	7,805.680	7,806.238	7,806.435
Bayesian Inf. Crit.	7,841.785	7,841.377	7,847.644	7,853.336	7,847.157	7,847.715	7,858.282
Note: (standard error)							*p<0.1; **p<0.05; ***p<0.01

These predictors are applied for all tested f_2 frequencies as shown in Table V-2 found in Appendix. In this table, the fixed effects coefficients indicate by how much the dependent variable, i.e. the DPOAE level at the f_2 frequency, changes for 1-unit of the predictor.

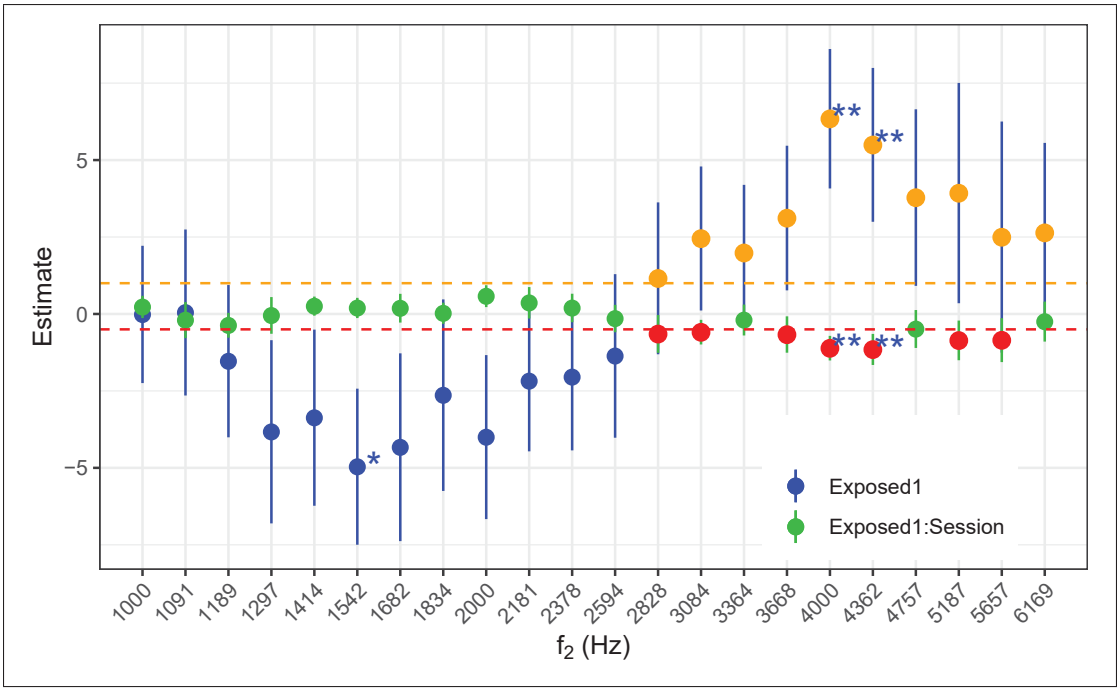

Figure 6.3 Fixed effect coefficient estimates per f_2 stimulus frequency explaining the changes in absolute DPOAE level (dB) without CAS, with error bars showing the standard error. Orange and red dots indicate greater fixed effects
Note: '*' = $p < 0.1$ '**' = $p < 0.05$

The fixed effect coefficient estimates for *Exposed1* and crossed effects *Exposed1:Session* are presented per f_2 DPOAE stimulus frequency in Fig. 6.3 to facilitate the analysis and observe frequencies with the most significant changes. The thresholds at 1 and -0.5 dB shown in orange and red respectively are selected empirically to observe the coefficients that stand out from other tested f_2 frequencies. Coefficient estimates highlighted in orange and red appear to have great effects on the DPOAE shift at frequencies between 2828 and 6169 Hz, a frequency range known to have the most DPOAE shift induced by noise exposure according to the literature (Marshall, L., Miller, J. A. L., Heller, L. M. et al., 2001; Müller & Janssen, 2008; Rosati, M. V., Tomei, F., Loreti, B., Casale, T., Cianfrone, G., Altissimi, G., Tomei, G., Bernardini, A., Di Marzio,

A., Sacco, C. et al., 2018) due to the noise exposure frequency content and the 1/2-octave band shift (Cody & Johnstone, 1981). However, some coefficient estimates are not statistically significant ($p > 0.1$) due to their large standard error. More data is therefore needed again to find significant effects at these frequencies where the effects are smaller. The most significant effects of *Exposed1* are found at 4000** and 4362** Hz where the exposed group has higher DPOAE levels in general compared to the non-exposed group, and their DPOAE shift over time (at 4000** and 4362** Hz) is also greater than the non-exposed group.

All models with fixed effects greater than the thresholds set and in the frequency range of interest (2828 to 6169 Hz) have been tested for normality assumptions with the Shapiro-Wilk and Kolmogorov-Smirnov tests, in addition to visual inspection of the residuals. All models' residuals are normally distributed.

6.2.3 Discussion

6.2.3.1 Findings

CAS DPOAE suppression

According to the CAS DPOAE suppression results presented in this experiment, individuals exposed to noise in their workplace have less suppression. This indicates that the MOC reflex inhibiting the cochlea's DPOAE levels is somewhat affected by noise exposure in the long term. This reduction in inhibition could potentially explain the higher DPOAE levels found in the exposed groups (see Table V-2). In the current study, the initial CAS DPOAE suppression is also found to be greater for males than for females, results reported in similar studies as well (Yakunina *et al.*, 2018).

Previous studies suggest that the MOC reflex may have many functions, such as 1) a protective role against moderate and high noise exposure levels (Maison & Liberman, 2000; Müller & Janssen, 2008). 2) The MOC reflex is also involved in the ability to listen to someone's voice in high

background noise levels (Kim *et al.*, 2006), also known as the cocktail party effect. In addition, the small changes detected in the MOC reflex suggest that the central gain feedback may be altered due to noise-induced damages in either peripheral, e.g. IHC-synapses or auditory nerve fibres, or central auditory systems. This change in central gain has already been reported in previous studies as a possible explanation for the onset of tinnitus (Schaette & McAlpine, 2011). Hence, individuals exposed to moderate-high noise exposure levels on a daily basis would be more susceptible to develop NIHL, could potentially have more difficulty to discriminate speech from high background noise levels and could develop tinnitus in the long term. These symptoms are generally associated with noise-induced hearing loss and hidden hearing loss.

Long-term DPOAE shifts

These hypotheses are further supported by the DPOAE shifts over time found at f_2 = 4000 Hz and 4362 Hz for the individuals in groups regularly exposed to noise. These permanent DPOAE shifts are in agreement with the temporary DPOAE growth function changes induced by noise exposure as detailed in Chapter 5. Considering that the permanent DPOAE shifts are measured pre-exposure, discarding the effects of daily noise exposure, and the growth functions indicate a cochlear dysfunction. The detected long-term DPOAE shifts are likely attributable to progressive noise-induced OHC dysfunction (Fernandez *et al.*, 2015), not middle-ear dysfunctions.

Despite the small magnitude of the DPOAE shifts detected over the relatively short time span of this longitudinal study (approximately 6 months). The robust statistical methods used for the second experiment to analyze the data allowed to find changes in cochlear health for individuals exposed to occupational noise. Greater effects of noise exposure on the auditory system's health are expected in larger epidemiological studies with measurements over several years.

According to the models' statistics, age is not a significant predictor for changes in CAS suppression and DPOAE shift in the tested groups, contrary to what is found in the literature (Gates *et al.*, 2002; Kim *et al.*, 2006; Sergeyenko *et al.*, 2013). This can be explained by the selection process that required subjects with normal hearing which resulted in a relatively

homogeneous group of young adults. Moreover, the experiment was conducted within one year and was definitely not long enough to monitor the effects of aging. Hence, it is somehow expected that age is not a predictor for changes in hearing health in this study. A group with older subjects and a wider age range would probably have exhibited more age-related hearing loss.

The results obtained in this second experiment show that the improvements in the stimuli parameters, the protocol and statistical tests lead to more meaningful conclusions compared to the first pilot experiment where only very small changes were observed at $f_2 < 2500$ Hz. However, these results obtained in the second experiment need to be considered with the limitations presented below.

6.2.3.2 Limitations

Time span

The time span of the study, limited to a few months, allowed to monitor very small permanent changes in DPOAE levels ($\approx$ 1-2 dB). However, no progress in time is found in the CAS DPOAE suppression over the 6 sessions. A longer longitudinal study would possibly allow to monitor greater DPOAE shifts and a greater reduction in suppression in noise-exposed individuals.

Intervals between measurements

Another limitation is the irregular time interval between the first and last sessions which may not have allowed enough time for changes in some individuals. A longer and more regular interval may allow to detect more statistically significant changes. Moreover, to minimize the effects of close proximity between each test sessions and the variability due to systematic errors on specific test days, only three sessions out of six are analyzed for the DPOAE shifts. More measurements with larger time intervals would again increase the significance of the changes detected in long-term DPOAE shifts.

Balanced groups

The number of participants included in the study may not be sufficient to generalize the models for a larger population. The groups should also be more balanced between the non-exposed and exposed individuals, as well as between genders for future experiments to draw more robust conclusions.

Noise exposure history

Workers' noise exposure from leisure activities and other exposures right before the experiment are not included in the present analysis of the occupational noise's effective long term effects. Therefore, the current results should be interpreted with caution.

6.3 Partial conclusion

According to the results presented in the second experiment, males exposed to noise are the most susceptible to the onset of permanent changes in their auditory system's health. The long-term effects observed in the DPOAE shifts also suggest that moderate ly high noise exposure levels could potentially have a permanent detrimental effect on the auditory system. Age is not a significant predictor of hearing loss in the experiment possibly due to the relatively homogeneous group of young adults. Considering the relatively short time span of approximately 6 months for this second longitudinal study, greater DPOAE shifts and reduction of CAS DPOAE suppression are expected over several years of accumulated noise exposure. More definitive and conclusive results could be obtained in the case that the workers' long term noise exposure history had been thoroughly assessed.

CHAPTER 7

SUMMARY AND OUTCOMES

A summary of this thesis's advances, limitations and recommendations are presented for each objective in Section 7.1 below. The possible outcomes of this research are then presented in Section 7.2.

7.1 Summary

This section presents an overview of the main findings and scientific advances answering the doctorate objectives presented in the Introduction's Section 0.3.1. Each advance is followed by its limitations and recommendations for future research.

7.1.1 Assessing individual's hearing health in controlled conditions

This scientific development meets the first objective of the doctoral project, which is to evaluate the designed portable DPOAE system's performance in high noise levels to monitor hearing health.

7.1.1.1 Advances

As presented in Chapter 3, the hearing health of nine human subjects was assessed in controlled conditions with the first prototype of the designed DPOAE system and a clinical DPOAE device used as a reference. According to the results obtained, the designed DPOAE system is able to monitor the changes in OHC activity in ambient sound pressure levels exceeding 85 dBA, which is not possible with the clinical device. These changes detected in OHC activity support the recent statements made by other researchers that moderate noise exposure levels behind the earplug (below approximately 70 dBA) might trigger a pathophysiological process which has measurable and detrimental effects on the auditory system.

7.1.1.2 Limitations and recommendations for future work

The developed system has been tested in controlled conditions at ambient SPLs of approximately 87 dBA with custom fitted eartips on only 9 participants. A larger study with more participants, in their own working environment with ambient SPLs exceeding 87 dBA would definitely be a good test for the designed system to see if it is possible to detect changes in OHC activity on workers. To conduct the suggested *in situ* experiments, the time spent on other audiological tests should be minimized to allow more time for DPOAE measurements and to also minimize the interference with the participants' work and other activities.

7.1.2 Monitoring sound pressure levels behind the hearing protector

This scientific development addresses the second objective of the doctoral project, which is to monitor the residual ambient sound pressure level behind the earplug to estimate the hearing protection level *in situ* and find the relationship between this noise level and changes induced in hearing health.

7.1.2.1 Advances

As presented in Chapter 4, the ambient sound pressure levels were measured outside and inside the protected ear of 16 human subjects using earpieces of the second system developed and these SPLs were compared against the ambient SPLs measured with a reference dosimeter. To remove the Wearer Induced Disturbances (WID) from the in-ear SPL, the proposed approach uses an adaptive filter to estimate the in-ear SPL using the outer-ear microphone. This approach was then validated by comparing the daily equivalent levels (L_{eq}) with a reference WID rejection method. According to the results, the proposed WID rejection method can lead to a lower daily L_{eq} by approximately 3.4 dB compared to the unprocessed residual ambient SPL. Considering an exchange rate of 3 dB, or equal energy principle, this substantial reduction in daily L_{eq} under the hearing protector could double a worker's permissible noise exposure duration.

7.1.2.2 Limitations and recommendations for future work

The proposed method does not reject WIDs completely when the disturbance captured by the IEM is also captured by the OEM in low to moderate ambient noise SPL conditions. This is either caused by a) the adaptive filter which cannot identify the earplug transfer function correctly when the ambient SPL is not sufficiently high to mask the in-ear physiological noise or b) because the WID SPL captured by the OEM is higher than the ambient noise SPL and therefore the algorithm cannot completely filter out the WID signal. To use the proposed WID rejection method in future experiments, the filter should only adapt at specific time intervals while the user remains silent and does not move. The identified earplug transfer function should, as well, be updated regularly to ensure that any changes in earplug fit are taken into account. Further research is also necessary to find a complimentary algorithm to reject high-level WIDs from the OEM signal , potentially leading to a lower daily L_{eq}. Moreover, estimates of the residual ambient SPL should include a microphone-to-eardrum correction. Although the precise assessment of this correction is now possible thanks to the work of close collaborators (Bonnet *et al.*, 2020), this correction is not included in the current project since it would require a specific earpiece configuration. This configuration is not compatible with the current design of the DPOAE probe. New DPOAE probes should therefore be developed to include these modifications in order to assess these individual corrections.

7.1.3 Estimation of the noise dose-response relationship with hearing health

This scientific development addresses the third objective of the doctoral project, which is to estimate the dose-response relationship between noise exposure characteristics and how they induce changes in hearing health measured on individuals in their noisy industrial environment.

7.1.3.1 Advances

As presented in Chapters 5 & 6, the noise exposure levels outside and inside the protected ear as well as the hearing health was monitored on 16 subjects exposed to moderate levels of noise at

their work as well as on 4 subjects not exposed to noise. The participants' hearing health was first tested during an initial screening and then their DPOAE levels were monitored regularly at short time intervals on 4 days during noise exposure with the designed DPOAE system to observe the short-term effects of noise. A few weeks to a couple of months after these measurements, their DPOAEs were measured again to follow up on any onset of permanent changes in their hearing health. According to the results, the temporary changes in the DPOAE growth function slope, which suggest a cochlear dysfunction, are attributable to the cumulative ambient noise level and impulsiveness over time. In addition, these temporary noise-induced changes are reflected in permanent changes in OHC activity, within the same frequency range, and MOC reflex as shown with DPOAE levels and CAS DPOAE suppression in Chapter 6. These results also confirmed the relationship between the noise's frequency spectrum and the frequency range with most damage occurring in the cochlea.

7.1.3.2 Limitations and recommendations for future work

To improve the robustness of the *in situ* DPOAE measurements the adaptive filtering noise rejection method briefly presented in Appendix I could be enhanced with more complex algorithms such as adaptive infinite impulse response (IIR) filters and beamforming with multiple microphones, for example. Further research is necessary to fine-tune and implement these algorithms on the actual hardware. Furthermore, the passive attenuation of the earpiece could be improved by using longer or custom-fitted eartips. However, this requires a special design of the earpiece and eartip to fit the three sound tubes required for the in-ear loudspeakers and microphone. To reduce the variability in the DPOAE calibration and therefore possibly reduce the variability for DPOAE measurements in higher frequency ranges, a Forward Pressure Level (FPL) calibration should be integrated in the designed DPOAE system . This could be achieved with the pre-conditioning method presented in Chapter 2 in addition to ARP3 DPOAE hardware improvements as well as the implementation of a simple calibration procedure, like the integrated FPL Calibrator in the ER-10X (Etymotic Research, 2019b).

In order to accurately detect changes in hearing health caused by the long-term effects of noise exposure, DPOAE measurements should also be measured with a longer time interval, either monthly or yearly. This should allow enough time for permanent hearing changes to become significant for most subjects, to easily detect them with the developed DPOAE system and statistical tests.

To validate the results of the short-term and long-term effects of noise exposure, the models' fixed-effect coefficients need to be tested on data collected in other experiments on a larger population and in various noise environments. This requires several duplicates of the designed DPOAE systems and a significant amount of time to collect sufficient data. Support from occupational health&safety research organizations such as the CNESST, IRSST, OSHA or NIOSH shall be sought to conduct these experiments on a larger scale. Great interest and commitment will also be required to convince equipment manufacturers to improve and mass market the prototype system developed during this doctoral project. Once the methods are validated on a larger scale and possibly standardized, these standards may eventually lead to new noise regulations that would require employers to properly monitor and effectively limit their workers' noise exposure.

Ultimately to minimize the risk of NIHL, workers may be asked to wear HPDs in moderate ambient noise levels to ensure the L_{eq} estimated under their protector remains below approximately 75 dBA (Neitzel & Fligor, 2017). Such protection may reduce speech intelligibility and restrict communication. Hence, advanced technologies may be required to maintain communication while wearing HPDs, such as digital earplugs that can let the ambient sounds get to the protected ear at reasonable levels. This would ensure that individuals remain both adequately protected against noise exposure and able to communicate, thereby avoiding issues of overprotection (HSE, 2019b). The developed OAE and noise metric measurement methods should be used in conjunction with such communication technologies. In this way, the system can also keep monitoring the noise exposure metrics in addition to their effects on hearing health for proper hearing conservation. By collecting information on the individuals' hearing health, a Permissible Exposure Limit (PEL) could be customized based, for example, on a maximum permissible

daily DPOAE shift instead of a maximum noise level (Czyżewski *et al.*, 2007). Eventually, the integration of these methods in the workplace should tangibly help to reduce and hopefully eliminate the cases of occupational hearing loss.

7.2 Outcomes

7.2.1 Scientific outcomes

Through *in situ* otoacoustic emission measurements and noise exposure assessment in the workplace, this doctoral project provided evidence on the effects of noise exposure on various hearing mechanisms that are supported by the scientific literature (Bharadwaj *et al.*, 2015; Cody & Johnstone, 1981; Fernandez *et al.*, 2015; Gehr *et al.*, 2004; Maison *et al.*, 2013). According to the multilevel models and the frequency range of the cochlear damage presented in Chapter 5 the most significant predictors of temporary hearing health changes are the noise's level, impulsiveness and frequency spectrum. These temporary hearing health changes can eventually translate into permanent hearing damage as detailed in Chapter 6. The evidence of these noise metric effects on hearing health are detailed as follows:

1. Results of this research project showed that noise exposure level and impulsiveness are significant predictors of short-term changes in DPOAE growth function slopes. This suggests that outer-hair cell damage occurred at the most affected cochlear frequencies. Noise exposure can also induce DPOAE shifts that do not alter the growth function slope at frequencies adjacent to the OHC damage, which according to some studies could suggest a middle-ear dysfunction (Gehr *et al.*, 2004). Further research is needed to confirm the nature of these DPOAE shifts.

2. The temporary noise-induced changes measured with otoacoustic emissions can reveal that other hearing mechanisms are being affected by noise exposure. These more subtle effects of noise exposure can be detected over the long term following cumulative damage. In this project, the subtle noise-induced damages resulted in a reduction of CAS DPOAE suppression in the exposed groups. This indicates a weaker medial olivocochlear reflex

which, in turn, suggests accumulated noise-induced damage in either the IHC-synapses, auditory nerve fibres or central auditory systems.

3. The long-term DPOAE shifts measured in this research suggest that the short-term damages in outer-hair cells can eventually translate into permanent damage. This indicates that frequent noise exposure can induce an accumulated damage in the cochlea's OHC.

4. The largest, short-term and long-term, DPOAE shifts are measured at frequencies within or above half an octave band of the noise's frequency range with the most energy (Cody & Johnstone, 1981), as estimated with the spectral balance. Hence, this research also suggests that cochlear damages are related to the noise's frequency spectrum.

7.2.2 Technological outcomes

This research project required many technological developments to finally monitor the workers' noise exposure and their DPOAE levels in their own working environment. Two versions of portable systems were designed by the candidate to measure DPOAEs in the presence of high noise levels, where clinical DPOAE equipment typically cannot function properly. To achieve reliable measurements of the low amplitude DPOAE signal, 3 microphone inputs were used simultaneously to reject noise in real-time with the adaptive filtering algorithm. The second version of this portable DPOAE system includes a sound card developed by the candidate as well as software coded by the candidate. This system is designed to:

1. Calculate and record sound levels outside and inside the occluded ear, to enable workers to monitor their exposure levels in real-time and verify that their hearing protection provides enough attenuation.

2. Record raw audio signals from up to 4 channels simultaneously to enable post-processing of all the earpieces' outer and inner-ear microphone signals in MATLAB (Mathworks, 2018) using scripts developed by the candidate. This also enables the calculation of additional noise metrics such as kurtosis, crest factor, dynamic range and spectral balance and the rejection of Wearer Induced Disturbances such as speech, coughing and footstep sounds

from the in-ear L_{eq}. The WIDs tend to significantly increase the daily noise dose measured with the in-ear microphone. Hence, the option to remove them from the L_{eq} can help to find a more significant relationship between the noise exposure level and the induced hearing damage. All these noise metrics were used in the multilevel models to find the most significant predictors of NIHL.

3. Integrate the in-silence fit-test algorithm. This algorithm is used to quickly assess whether the earplugs need to be re-fitted before the workers are actually exposed to ambient noise. Thus the test verifies that the earpiece is correctly positioned in the earcanal, that it provides enough attenuation to conduct the DPOAE measurements in noise and ultimately, that users are sufficiently protected against excessive noise exposure levels.

4. Integrate the real-time adaptive filtering algorithm and DPOAE extraction algorithm to perform the DPOAE growth function measurements in high ambient noise levels. The 24-bit sound card and its conditioning circuit ensured an optimal dynamic range for DPOAE measurements. This sound card can also stimulate the contralateral ear with wide-band noise to measure CAS DPOAEs pre- and post-exposure. These DPOAE measurements helped to find the relationship between noise exposure and its short-term as well as long-term effects on hearing health.

The second version of the portable system can be used with the new DPOAE probe designed by the candidate for the Forward Pressure Level (FPL) calibration method. This should eventually minimize the variability in the DPOAE measurements and improve the statistical significance of the predictors in the models.

7.2.3 Occupational Health and Safety outcomes

The developed device and methods are essential tools that will allow occupational hygienists and other hearing health professionals to:

1. Sensitize employers and employees to the role and benefits of hearing conservation programs. This is critical to enhance the adoption of these programs by the population by changing the culture concerning hearing protection to truly improve NIHL prevention.

2. Integrate the measurements of important noise metrics and otoacoustic emission measurements in the workplace to use the most significant predictors for NIHL risk assessment and properly prevent occupational hearing loss.

3. Evaluate the individual's susceptibility and actual risk of developing noise-induced hearing loss through changes in DPOAE levels to concentrate the efforts of occupational health and safety professionals on the individuals who are most at risk.

CONCLUSION AND RECOMMENDATIONS

To detect the onset of NIHL with current hearing conservation programs, industrial hygienists and other practitioners in the workplace often rely solely on annual audiometric tests. However, the time lapse between these audiometric measurements are often far too long, often conducted after the hearing damage has appeared and thus, they do not prevent NIHL. To actively reduce the risk of NIHL, it is desirable to monitor otoacoustic emission (OAE) levels in the workplace to detect when slight changes in hearing health occur, before these hearing damages become irreversible. These OAE measurements in noisy work environments, where clinical devices do not perform well, have been conducted with the designed system as it is able to extract the OAE signal from the background noise using adaptive filtering noise rejection.

In order to properly model the dose-response relationship, this doctoral project proposes methods to monitor noise exposure and its induced changes in hearing health in industrial environments. The developed methods and portable systems are able to:

1. Measure DPOAEs in moderate to high ambient noise level environments;

2. Monitor noise exposure levels outside as well as inside the protected ear, calculating the in-ear equivalent sound level without Wearer-Induced Disturbances;

3. Perform different types of DPOAE measurements such as CAS DPOAE and DPOAE growth functions, to observe other possible noise-induced changes in the auditory system;

4. Record raw audio to post-process additional noise metrics such as the noise's frequency spectrum and temporal variations to find other predictors of NIHL.

The measurement methods developed and the designed portable OAE systems do fulfill both the research and doctoral projects' objectives.

The results presented in this doctoral thesis show that moderate to high impulsive noise levels can induce short-term changes in cochlear mechanisms. These short-term changes could possibly translate into permanent damages in outer hair cells and fatigue in the medial olivocochlear reflex. This reduction in DPOAE suppression is a symptom of potential damages to peripheral and central auditory systems. These symptoms are often related to hidden hearing loss and tinnitus. The damages occur mostly in outer hair cells responding to frequencies within or half an octave band above the noise's frequency range with most energy. These findings support the hypothesis that moderate noise levels are not without risks. Once validated on a larger population, the methods and devices developed in this research project should be implemented in the workplace through hearing conservation programs as best practices to prevent noise-induced hearing loss. To keep consistency in the procedures and the results, the methods should eventually be standardized. This would ultimately lead to a change in noise regulations to reflect these recent findings in hearing conservation research, ultimately requiring that employers use these methods to minimize the risks of noise-induced hearing loss in occupational settings.

APPENDIX I

ADAPTIVE FILTERING NOISE REJECTION AND DPOAE LEVEL EXTRACTION ALGORITHMS FOR DPOAE MEASUREMENTS

Adaptive filtering noise rejection

The adaptive filtering noise rejection algorithm used to measure DPOAEs in noisy conditions for this doctoral project is based on the algorithm presented in the candidate's master thesis and shown in Figure I-1. In this algorithm, a Finite Impulse Response (FIR) band-pass filter with centre frequency at $2f_1 - f_2$ is used to filter out the desired signal from the tested ear's IEM signal. The filter is also used on the other microphone signals (see OAE enhancer in the block diagram of the proposed noise rejection algorithm in Fig. I-1) for homogeneity in the subsequent signal processing.

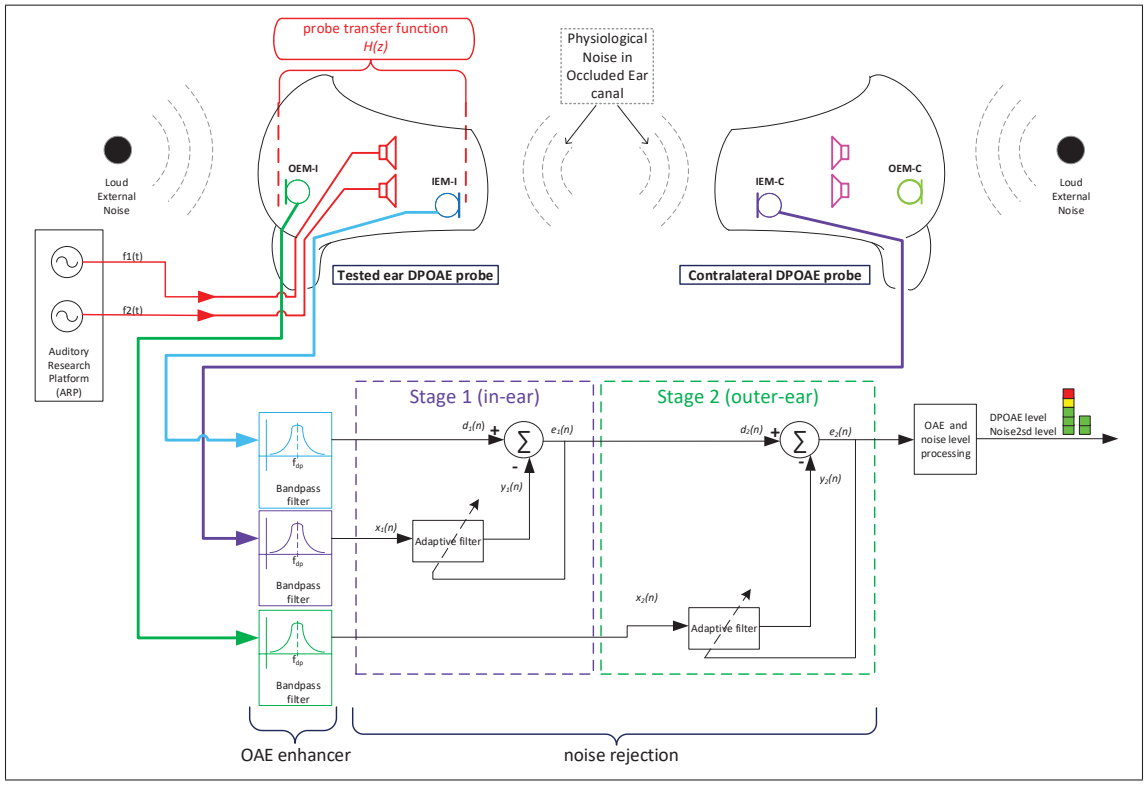

Figure-A I-1 Block diagram of the proposed Adaptive Filtering Noise Rejection algorithm

The Normalized Least-Mean Squares (NLMS) (Vijay K., M. & Douglas B., W., 1999) adaptive filter in *Stage 1* (Fig. I-1), using the adaptive filter's Eq. A I-3 with $i = 1$, models the transfer function between the contralateral IEM $x_1(n)$ and the tested ear IEM $d_1(n)$, where n represents the samples, which represents acoustical differences between the two ear canals:

$$y_1(n) = \hat{\mathbf{w}}_\mathbf{1}^{\,T}(n)\mathbf{x_1}(n) \tag{A I-1}$$

$$e_1(n) = d_1(n) - y_1(n) \tag{A I-2}$$

$$\hat{\mathbf{w}}_{\mathbf{i|i=1,2}}(n+1) = \hat{\mathbf{w}}_\mathbf{i}(n) + \frac{\mu\, e_i(n)\mathbf{x_i}(n)}{\mathbf{x_i}^T(n)\mathbf{x_i}(n)} \tag{A I-3}$$

In Eq. A I-3 with $i = 1$, the error signal $e_1(n)$ is used to correct the adaptive filter's coefficients represented by the vector $\hat{\mathbf{w}}_\mathbf{1}$ in order to model accurately the residual noise disturbance in the tested ear's IEM. The noise disturbance considered here for *Stage 1* is mainly caused by physiological noise arising from vital functions like breathing and heartbeats. In Eq. A I-3, where $\mathbf{x}^T(n)$ is the transposed form of the noise reference signal $\mathbf{x}(n)$, $i = 1$ represents *Stage 1* (Fig. I-1).

In *Stage 2* ($i = 2$ in Eq. A I-3) of the dual adaptive filter topology, the filter models the physical transfer function $H(z)$ of the probe in an occluded ear canal. In Eq. A I-3 with $i = 2$, the error signal $e_2(n)$ is used to correct the adaptive filter's coefficients ($\hat{\mathbf{w}}_\mathbf{2}$) in order to model the ambient noise disturbance captured by the tested ear's IEM. The error signal $e_2(n)$ calculated from the difference between the desired $d_2(n)$ and the adaptive filter $y_2(n)$ output signals in Eq. A I-4, is also used as the output of the noise rejection algorithm since it mainly consists of the DPOAE signal without the noise signals (physiological noise rejected with *Stage 1* and ambient noise with *Stage 2*):

$$e_2(n) = d_2(n) - y_2(n) \tag{A I-4}$$

$$y_2(n) = \hat{\mathbf{w}}_\mathbf{2}^{\,T}(n)\mathbf{x_2}(n) \tag{A I-5}$$

Here $y_2(n)$ is the ambient noise $x_2(n)$ filtered with the adaptive filter. The proposed adaptive filtering approach implies that the OAE response is not picked up by the OEM or contralateral IEM, which is normally the case since the DPOAE responses are unilaterally generated and the probes provide high passive attenuation, therefore they seal the low level DPOAE responses within the tested ear.

Otoacoustic emission level extraction algorithm

The DPOAE level extraction algorithm (Nadon *et al.*, 2014, 2015d) was developed during the candidate's master thesis (Nadon, 2014) to estimate the DPOAE signal from the recorded in-ear microphone signal without being affected by spectral leakage, which occurs when the stimuli are not an integer multiple of the FFT frequency resolution (Δf). This algorithm based on Amplitude Modulation (AM), shown in Figure I-2, has an automatic normalization process that adjusts the modulating carrier signal ($c(n)$) level to match the DPOAE level. Cross-correlation can be used to evaluate phase drifts, i.e. slight frequency variations, to sync the carrier ($c'(n)$) with the DPOAE signal to extract. The normalization process maximizes the modulation index h (National Association of Broadcasters, 1986) which corresponds to the ratio between the DPOAE signal magnitude and the carrier signal.

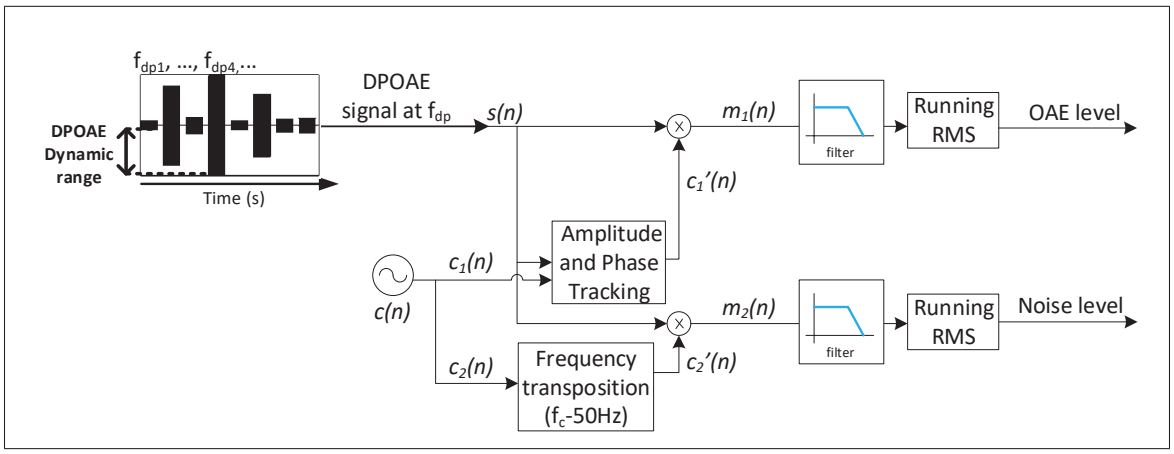

Figure-A I-2 Schematic of the DPOAE signal extraction algorithm

The AM modulation algorithm is presented in the equations shown in Eq. A I-6 to A I-12. The DPOAE signal (see Eq. A I-6) is modulated with a carrier signal (see Eq. A I-7) in order to estimate the magnitude of the DPOAE as a constant value (0 Hz). A band-pass FIR filter with a high order is centered around the DPOAE frequency f_{dp} to remove the stimuli signals from the temporal signal prior to the modulation (also shown before the adaptive filter stages in Figure I-1).

Eq. A I-6 to A I-12 are executed on a frame of sample size M. This frame size can be set manually, for example $M = 8000$, or adjusted automatically based on the DPOAE frequency (f_{dp}) in order to reduce the DPOAE stimulation and signal extraction time, especially with higher DPOAE frequencies.

In order to extract the DPOAE signal accurately, the frequency f_c of the modulating carrier $c(n)$ must be the same as f_{dp} the frequency of the DPOAE response signal.

$$s(n) = A_{dp}\sin(2\pi f_{dp} n t_s) \tag{A I-6}$$

$$c(n) = A_c\sin(2\pi f_c n t_s + \phi) \tag{A I-7}$$

To synchronize the carrier signal $c[n]$ with the DPOAE signal $s[n]$, the phase ϕ starts at $\frac{\pi}{2}$ rad and is increased by an additional delay within a loop until the cross-correlation (Eq. A I-8) gives the closest result to unity. The cross-correlation is used as a measure of similarity between the DPOAE signal and the carrier signal as a function of the time difference between the signals.

$$(c_1' \star s)(n) = \sum_{m=0}^{M/2-n} c_1'^{*}(m)s(m+n) \tag{A I-8}$$

A running Root-Mean Square (RMS) value gives the magnitude of the signal over a certain amount of cycles of the sinusoid signal. The RMS value of the signal is calculated with a rectangular window $w(n)$ with length W (Eq. A I-9).

$$\mathrm{rms}(s(n), w(n)) = \sqrt{\frac{s^2(n) * w(n)}{\sum_{n=0}^{W} w(n)}} \tag{A I-9}$$

$$c_1'(n) = \frac{\sum_{n=0}^{M} \mathrm{rms}(s(n), w(n))}{\sum_{n=0}^{M} \mathrm{rms}(c_1(n), w(n))} * c_1(n) \tag{A I-10}$$

The modulating carrier signal is then normalized ($c_1'[n]$) based on the RMS value of the DPOAE signal (see Eq. A I-10). The normalization process maximizes the result of the cross-correlation and the modulation index h. When this modulation index is maximum , that is $h = 1$ National Association of Broadcasters (1986), the modulated DPOAE signal has an optimal dynamic range. This also means that the DPOAE signal estimation error is minimized.

$$m_1(n) = s[n] \cdot c_1'[n] \tag{A I-11}$$

$$m_1(n) = \frac{A_{dp} A_{c_1'}}{2} \sin(2\pi(f_{dp} - f_{c_1'})nt_s - \phi) \tag{A I-12}$$

The constant (0 Hz) DPOAE signal obtained in $m_1(n)$ (see Eq. A I-11 and A I-12) is then filtered with a low-pass filter to remove the undesired signals such as the residual stimuli signal, noise and the $\sin(2\pi(f_{dp} + f_{c_1'})nt_s + \phi)$ component of the modulated DPOAE signal. The DPOAE level is then estimated by calculating the running RMS value of the filtered $m_1(n)$ signal.

The signal-to-noise ratio of the extracted DPOAE is evaluated from the ratio between the DPOAE level and the noise magnitude estimated with modulation technique briefly presented below and detailed in (Nadon *et al.*, 2014,1).

Noise estimator

The amplitude modulation, presented in the DPOAE level extraction algorithm, can also be used to estimate the noise around the DPOAE frequency. The noise estimator output $m_2(n) = s[n] \cdot c_2'[n]$, see Figure I-2, consists in the modulation of the DPOAE signal $s[n]$ with the modulating carrier $c_2'[n]$. The output $m_2(n)$ then goes through a filter to remove the modulated DPOAE signal and the residual modulated stimuli signals to finally estimate the noise level using a running RMS average.

Validation of the adaptive filtering noise rejection and DPOAE extraction algorithms

The developed algorithms have been thoroughly studied in controlled conditions during the candidate's master thesis (Nadon, 2014) prior to its use with the ARP in the pilot study and in the workplace for this doctoral project.

According to the experiments in controlled quiet conditions with a first experimental setup to test the algorithms, the DPOAE level estimated with the proposed algorithm follows the same trend as the ILO system over different test frequencies in quiet conditions (Nadon *et al.*, 2015a). Hence, the adaptive filter does not alter the DPOAE level in normal conditions of use. In terms of clinical relevance, third quartile values calculated per frequency confirms that, except around 4000 Hz, clinical test-retest variability (Keppler *et al.*, 2010a) is respected for the majority of observations with the first experimental setup (Nadon *et al.*, 2015a).

In controlled noise conditions, when the adaptive filters are switched off, DPOAE signal amplitude increases significantly ($p < 0.05$) with an increased background noise level from 65 to 75 dBA. If the adaptive filters are activated, the DPOAE signal amplitude is no longer systematically affected by the background noise. The DPOAE noise level with adaptive filtering noise rejection (ANR) off clearly varies for the different test conditions ($p < 0.0001$). For all conditions of background noise, the DPOAE noise levels are significantly lower with ANR activated ($p < 0.05$), as for ANR off, the DPOAE noise levels systematically increase with higher levels of background noise ($p < 0.05$). In contrast, no significant difference in DPOAE

noise level is found between test conditions with the ANR algorithm activated (Nadon *et al.*, 2015a).

Moreover, the stability of the obtained DPOAE signals is assessed by comparing DPOAE signal amplitudes in noise with the baseline DPOAE signal measured in quiet reference conditions. A pairwise non-parametric Wilcoxon test with Bonferroni correction shows that DPOAE levels do not differ significantly in noise compared to baseline if the ANR is active. When the ANR is off, however, the DPOAE level significantly deviates from the baseline conditions and this deviation increases with increasing background noise levels.

Finally, regardless of elevated background noise and the application of ANR algorithms, from clinical experience DPOAE measurements are expected to exhibit some test-retest variability even without re-fit of the DPOAE probe (Keppler *et al.*, 2010a). To quantify this variation in this first experimental setup, the average of the first and second measurement is compared to the average of the third and fourth measurement (within a few minutes). A paired comparison between DPOAE signal in averaged measurements 1-2, and measurements 3-4 is made across frequencies per test condition i.e. with the ANR algorithm on and off in the different conditions of background noise. The comparison showed that for all test conditions the averaged DPOAE amplitudes do not change significantly from one pair of measurements to another (paired Student's t-test, $p > 0.1$). The interquartile range of test-retest differences in DPOAE magnitude appears to be slightly higher for ANR off compared to ANR on (respectively 3.6 dB and 2.8 dB for white noise 70 dBA and 3.6 dB versus 2.9 dB for industrial noise at 75 dBA).

Despite poor passive noise reduction obtained with the first prototype of DPOAE probes (Nadon, 2014), experiments with the ANR algorithm clearly showed that DPOAE signal levels obtained in noisy conditions could be brought back to the DPOAE signal levels measured in quiet conditions. As a result, the DPOAE signal level measured in noisy conditions falls within the test-retest variability observed in quiet conditions. In addition, the noise level was reduced considerably, although for some frequencies the noise levels were not brought back completely to the level found in quiet conditions.

In summary, even in absence of good passive noise reduction from the hearing protector, the proposed ANR algorithm allows to reduce both white and industrial noise sufficiently to obtain high quality DPOAE signals even if DPOAE noise levels are not brought back exactly to the levels observed in quiet. Further details on the performance of the adaptive filtering noise rejection and DPOAE level extraction algorithms can be found in Chapter 4 and (Nadon *et al.*, 2014, 2015a, 2017a).

APPENDIX II

SOUNDBOARD SCHEMATIC INCLUDING THE FINAL IMPROVEMENTS

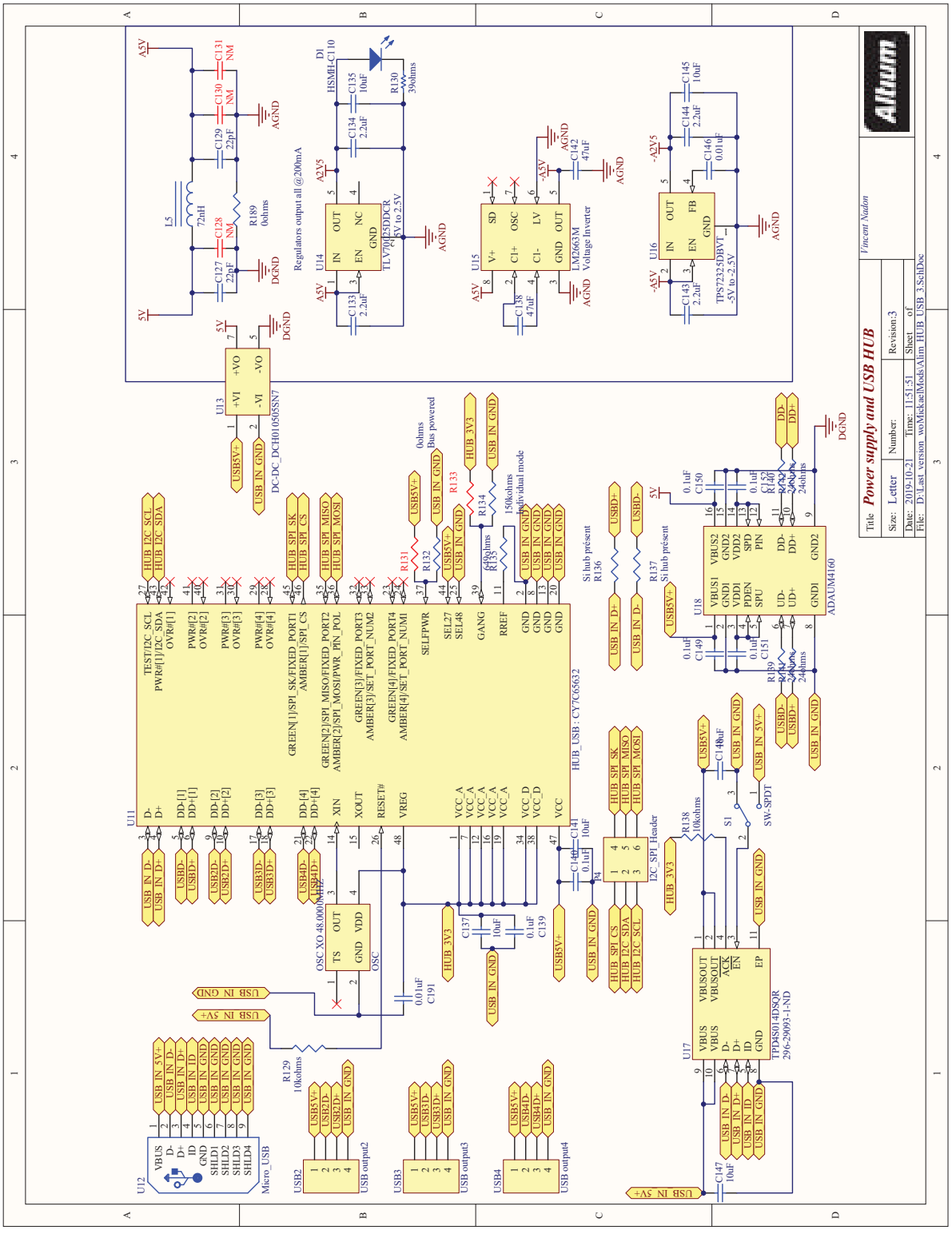
Power supply and USB HUB
Vincent Nadon
Title
Size: Letter
Number:
Revision:3
Date: 2019-10-21
Time: 11:51:51
Sheet of
File: D:\Last version wo\Mekse\Mods\Altm_HUB_USB_3.SchDoc
Altium
Regulators output all @200mA
DC-DC_DCH010505SN7
LM2663M Voltage Inverter
TPS72325DBVT -5V to -2.5V
TLV70025DDCR 5V to 2.5V
HSMH-C110
HUB_USB : CY7C65632
ADAUM4160
TPDS5014DSQR 296-29093-1-ND
Micro_USB
I2C_SPI_Header
OSC XO 48.000MHZ
Si hub présent
Bus powered
Individual mode
SW-SPDT
USB output2
USB output3
USB output4

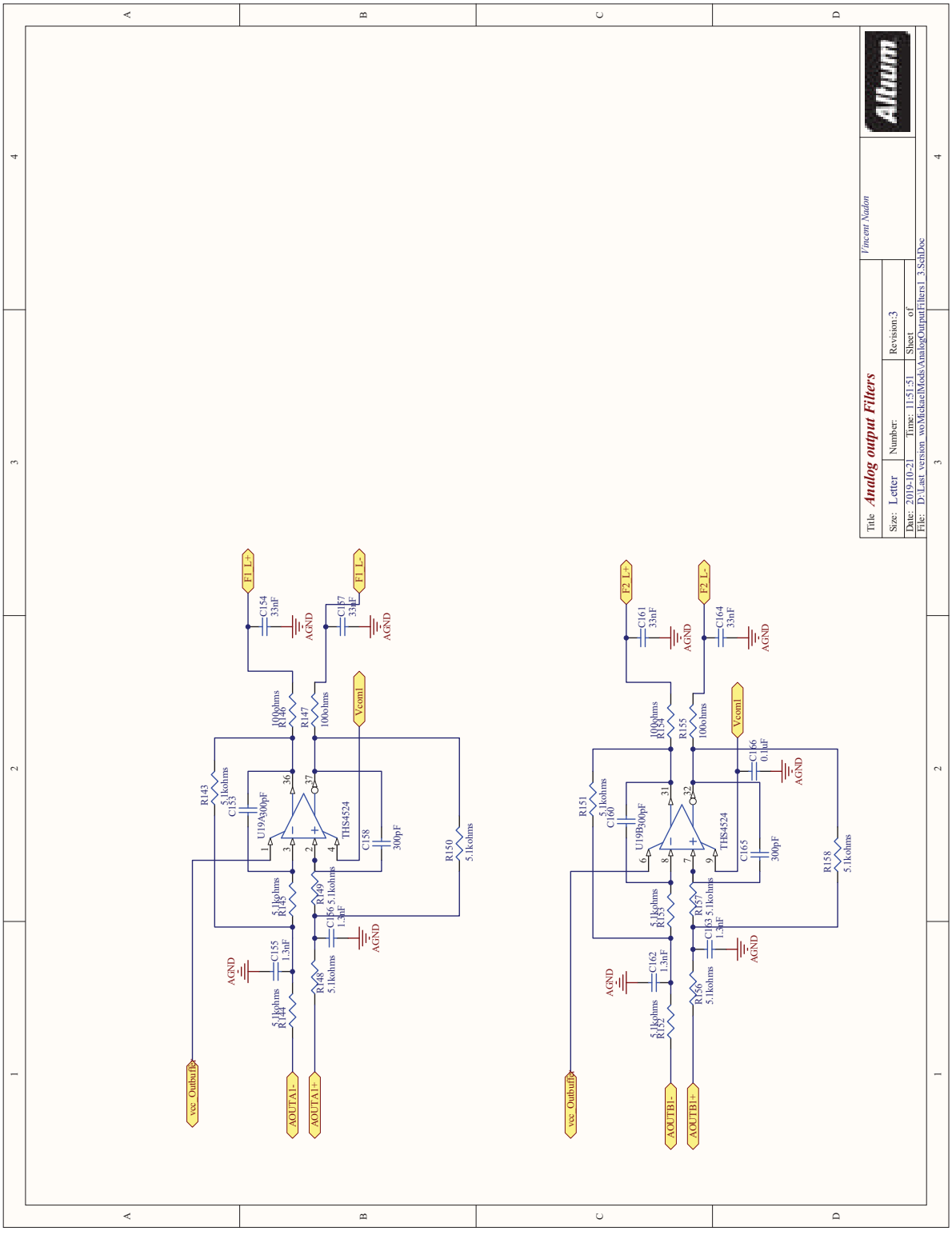
Title Analog output Filters
Size: Letter
Number:
Revision:3
Date: 2019-10-21
Time: 11:51:51
Sheet of
File: D:\Last version wo\MickaelMods\AnalogOutputFilters1 3.SchDoc
Vincent Nadon
Altium
F1 L+
F1 L-
F2 L+
F2 L-
AGND
Vcom1
vcc_Outbuff
AOUTA1-
AOUTA1+
AOUTB1-
AOUTB1+
U19A
U19B
THS4524
R143 5.1kohms
R144 5.1kohms
R145 5.1kohms
R146 100ohms
R147 100ohms
R148 5.1kohms
R149 5.1kohms
R150 5.1kohms
C153 300pF
C154 33nF
C155 1.3nF
C156 1.3nF
C157 33nF
C158 300pF
R151 5.1kohms
R152 5.1kohms
R153 5.1kohms
R154 100ohms
R155 100ohms
R156 5.1kohms
R157 5.1kohms
R158 5.1kohms
C160 300pF
C161 33nF
C162 1.3nF
C163 1.3nF
C164 33nF
C165 300pF
C166 0.1uF

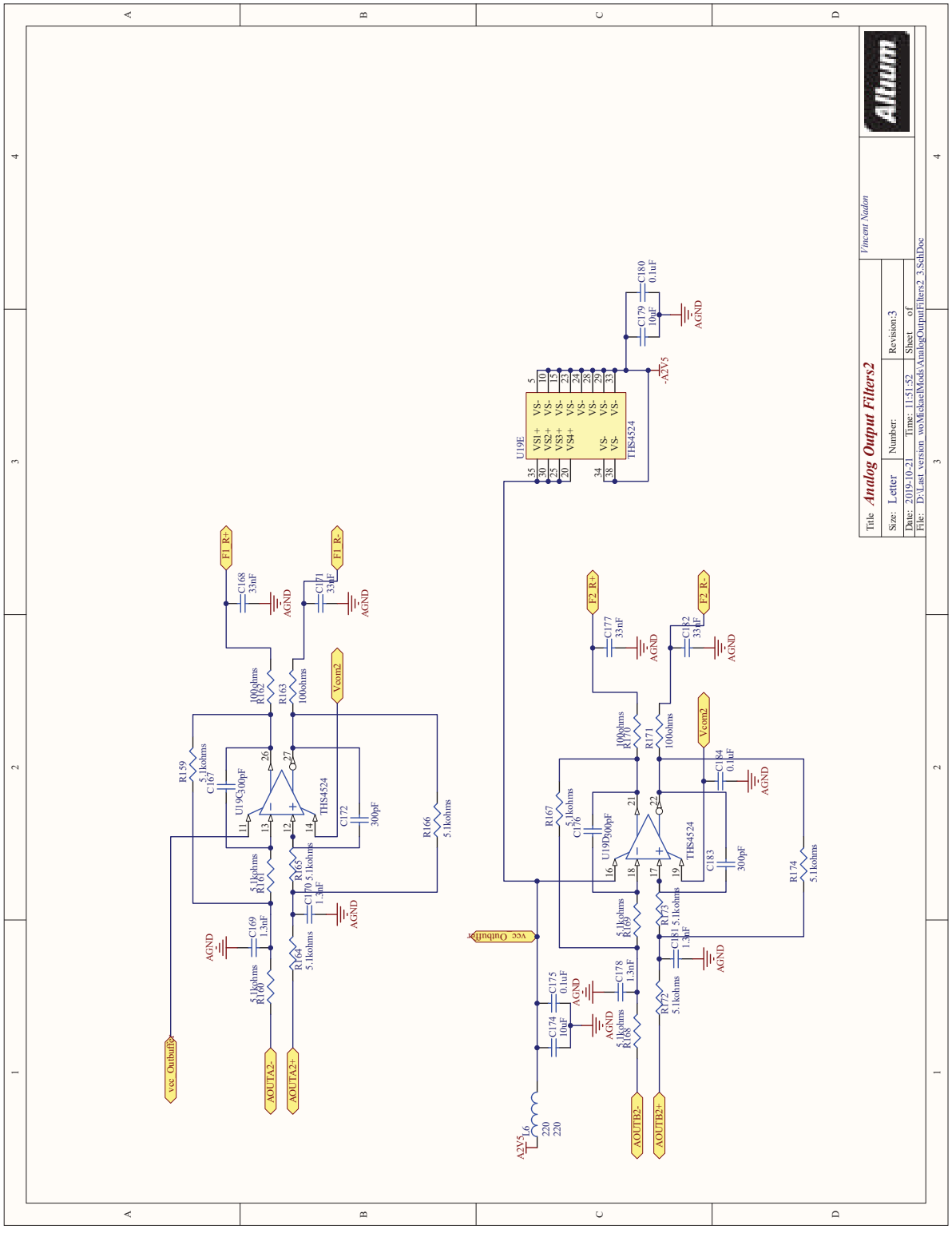
Title Analog Output Filters2
Size: Letter
Number:
Revision:3
Date: 2019-10-21
Time: 11:51:52
Sheet of
File: D:\Last version two\Meckae\Mods\AnalogOutputFilters2_3.SchDoc
Vincent Nadon
Altium
F1 R+
F1 R-
F2 R+
F2 R-
Vcom2
AGND
-A2V5
A2V5
VCC_Output1
VCC_Output2
AOUTA2-
AOUTA2+
AOUTB2-
AOUTB2+
U19C
U19D
U19E
THS4524
R159
R160
R161
R162
R163
R164
R165
R166
R167
R168
R169
R170
R171
R172
R173
R174
C167
C168
C169
C170
C171
C172
C176
C177
C178
C181
C182
C183
C184
C174
C175
C179
C180
L6

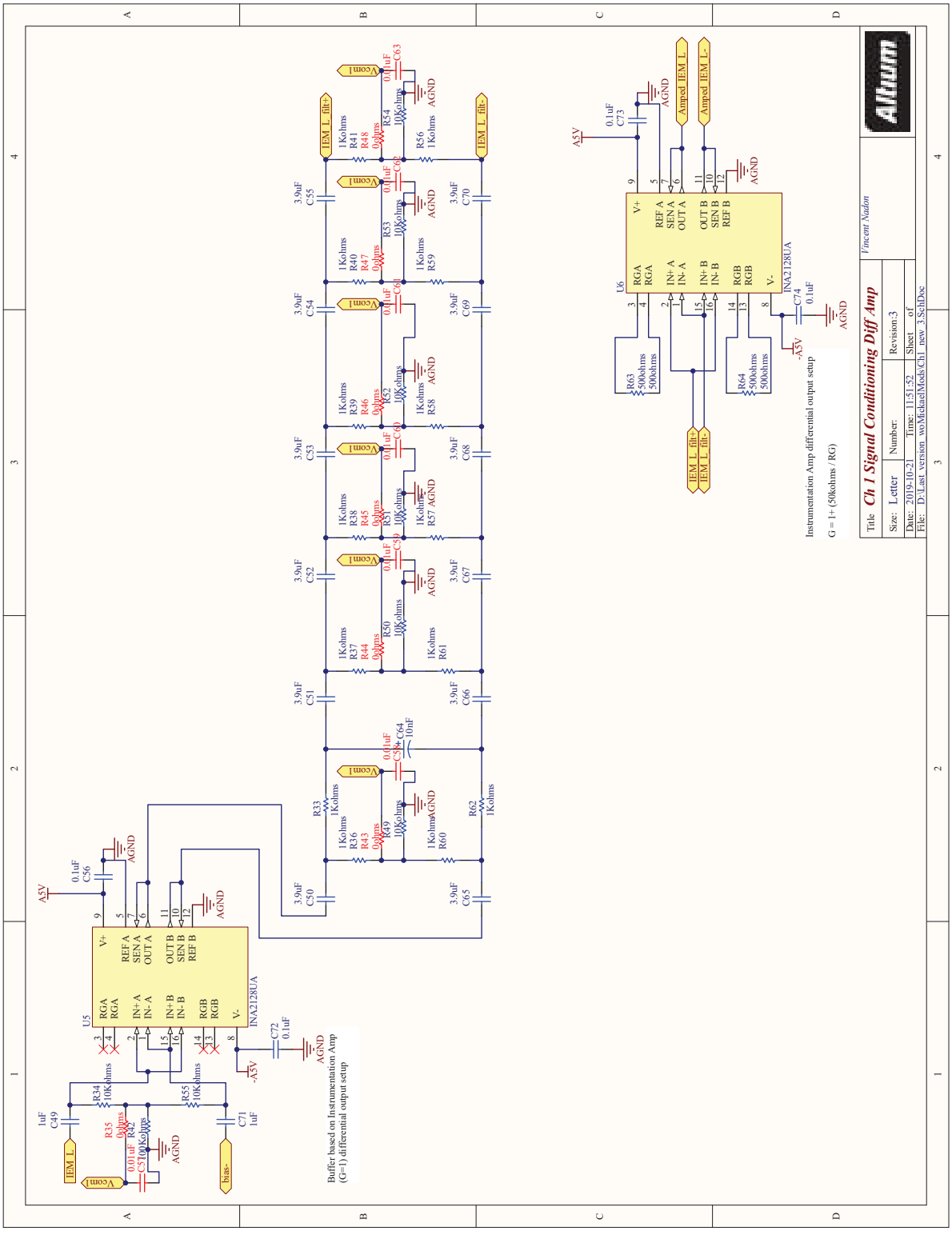
Ch 1 Signal Conditioning Diff Amp
Vincent Nadon
Altium
Title
Size: Letter
Number:
Revision:3
Date: 2019-10-21
Time: 11:51:52
Sheet of
File: D:\Last version wo\MickaelMods\Ch1 new 3.SchDoc
IEM L
bias-
Vcom1
U5
INA2128UA
U6
INA2128UA
A5V
-A5V
AGND
Buffer based on Instrumentation Amp
(G=1) differential output setup
Instrumentation Amp differential output setup
G = 1+ (50kohms / RG)
Amped IEM L+
Amped IEM L-
IEM L filt+
IEM L filt-

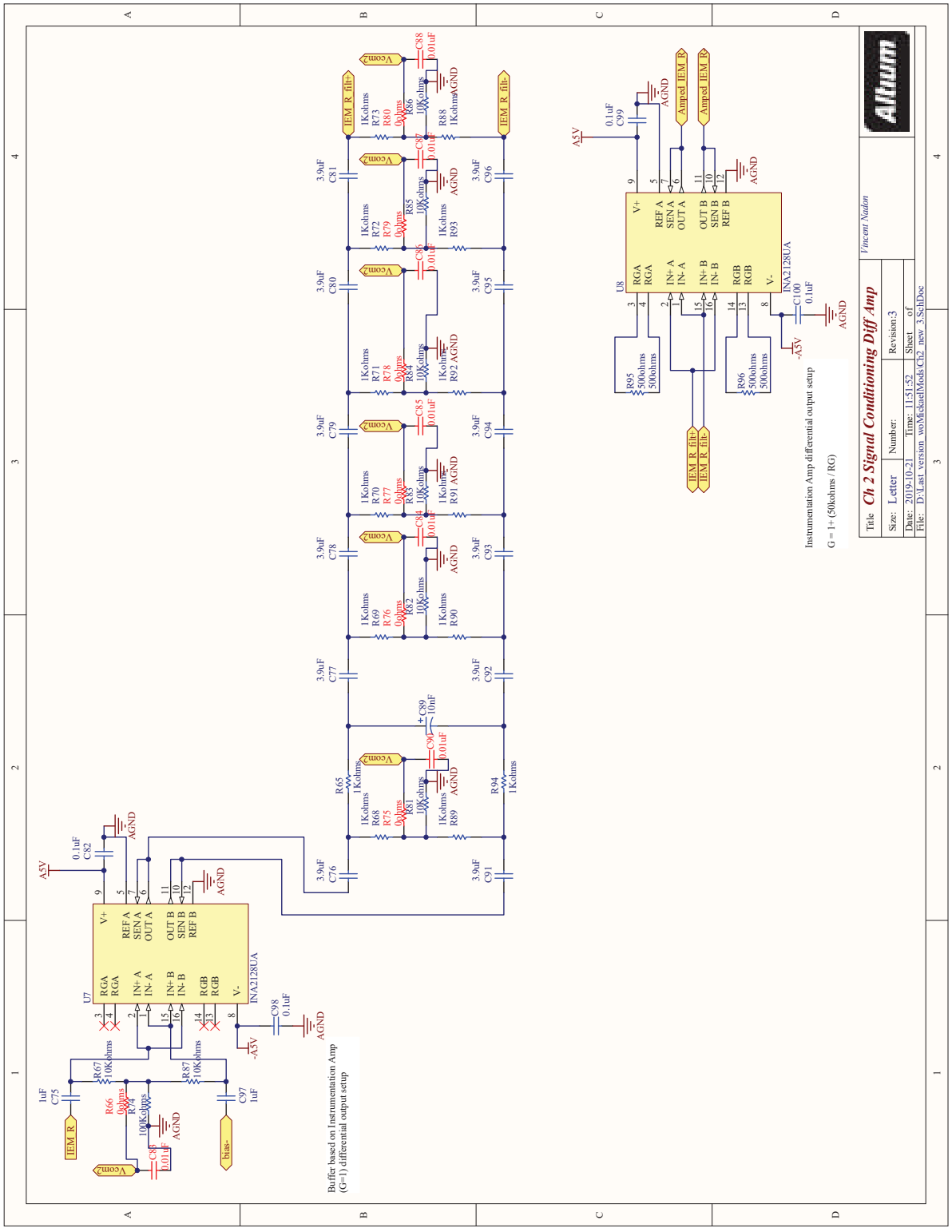
Ch 2 Signal Conditioning Diff Amp
Vincent Nadon
Allium
Size: Letter
Number:
Revision:3
Date: 2019-10-21
Time: 11:51:52
Sheet of
File: D:\Last version two\Meckael\Mods\Ch2_new 3.SchDoc
Buffer based on Instrumentation Amp (G=1) differential output setup
Instrumentation Amp differential output setup
G = 1+ (50kohms / RG)
INA2128UA
IEM_R
IEM_R_filt+
IEM_R_filt-
Amped IEM_R
bias-
Vcom2
A5V
-A5V
AGND

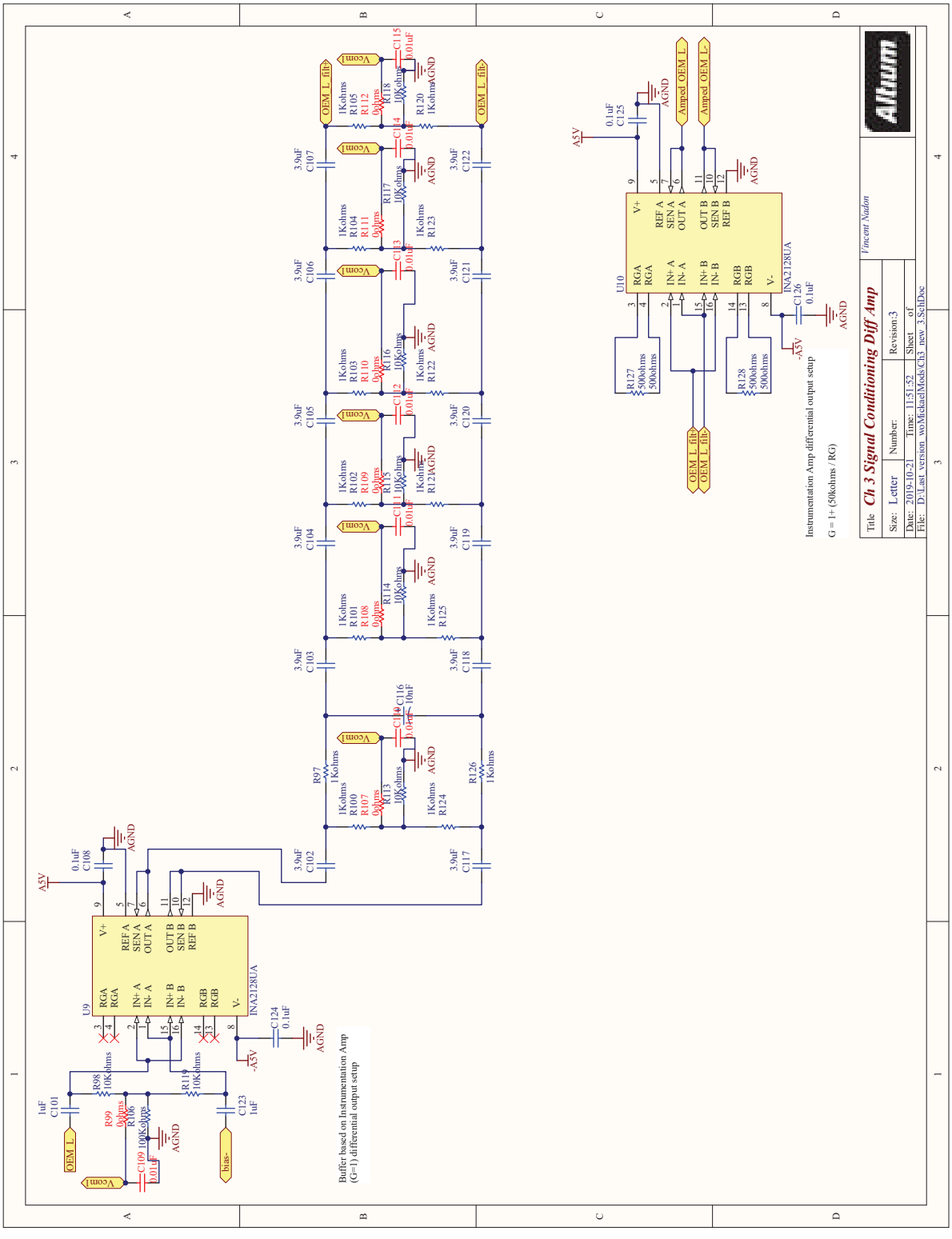
Ch 3 Signal Conditioning Diff Amp
Vincent Nadon
Title
Size: Letter
Number:
Revision:3
Date: 2019-10-21
Time: 11:51:52
Sheet of
File: D:\Last version wo\MickaelMods\Ch3 new 3.SchDoc
Buffer based on Instrumentation Amp (G=1) differential output setup
Instrumentation Amp differential output setup
G = 1+ (50kohms / RG)
INA2128UA
OEM L
OEM L_fib
Vcom1
bias-
Amped OEM L
Amped OEM L-
A5V
-A5V
AGND

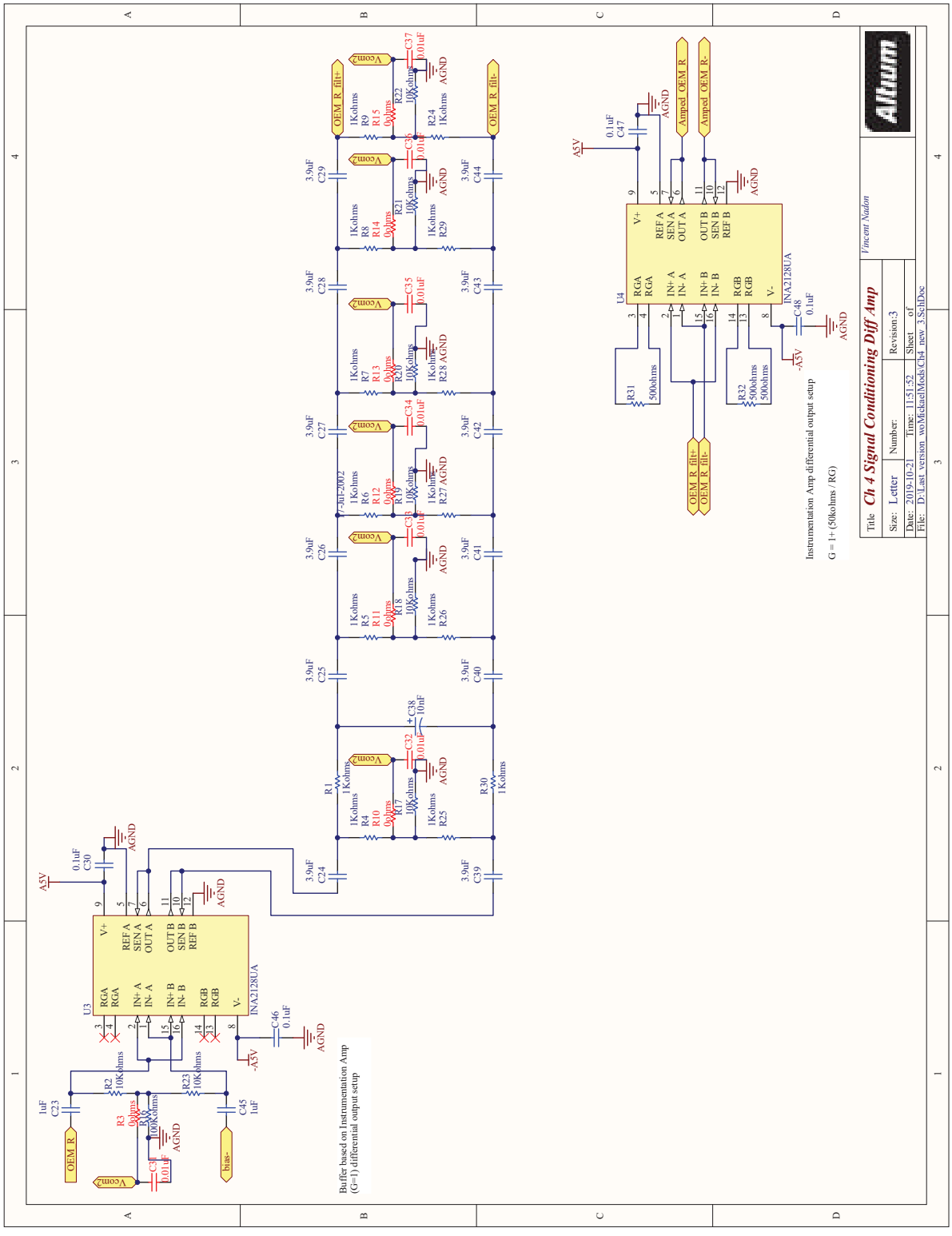
Ch 4 Signal Conditioning Diff Amp
Vincent Nadon
Altium
Size: Letter
Number:
Revision:3
Date: 2019-10-21
Time: 11:51:52
Sheet of
File: D:\Last version two\Meckael\Mods\Ch4 new 3.SchDoc
INA2128UA
Buffer based on Instrumentation Amp
(G=1) differential output setup
Instrumentation Amp differential output setup
G = 1+ (50kohms / RG)
OEM R
bias-
Amped OEM R
Amped OEM R-
OEM R filt+
OEM R filt-
A5V
-A5V
AGND
Vcom2

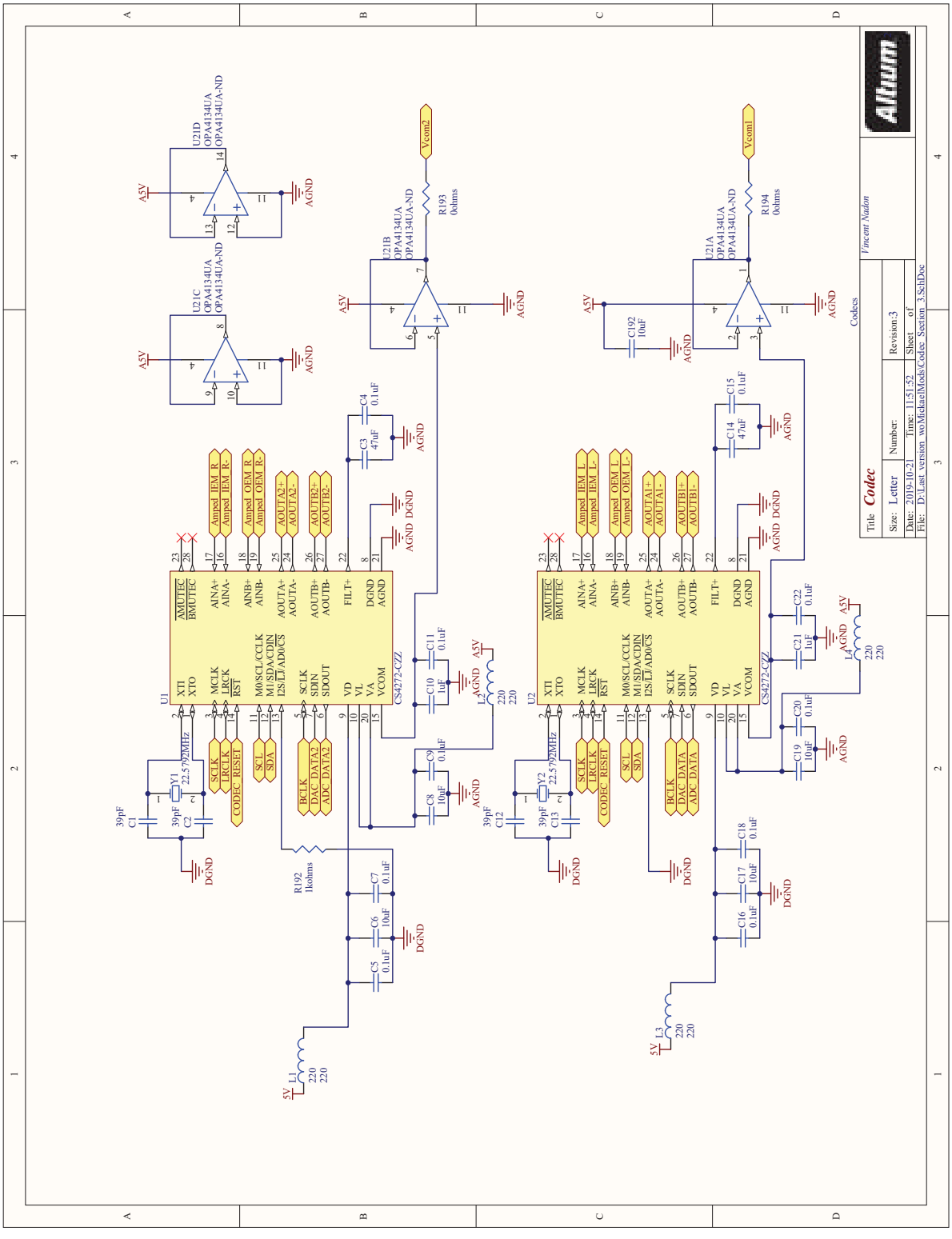
Codec
Vincent Nadon
Size: Letter
Number:
Revision:3
Date: 2019-10-21
Time: 11:51:52
Sheet of
File: D:\Last version wo\MickaelMods\Codec Section 3.SchDoc
U1
U2
CS4272-CZZ
XTI
XTO
MCLK
LRCK
SCLK
SDIN
SDOUT
RST
M0/SCL/CCLK
M1/SDA/CDIN
I2S/LJ/AD0/CS
FILT+
VD
VL
VA
VCOM
AMUTEC
BMUTEC
AINA+
AINA-
AINB+
AINB-
AOUTA+
AOUTA-
AOUTB+
AOUTB-
DGND
AGND
A5V
5V
Y1
Y2
22.5792MHz
39pF
C1
C2
C12
C13
CODEC_RESET
SCL
SDA
BCLK
DAC_DATA2
ADC_DATA2
DAC_DATA
ADC_DATA
Amped_HEM_R
Amped_HEM_R-
Amped_OEM_R
Amped_OEM_R-
Amped_HEM_L
Amped_HEM_L-
Amped_OEM_L
Amped_OEM_L-
AOUTA2+
AOUTA2-
AOUTB2+
AOUTB2-
AOUTA1+
AOUTA1-
AOUTB1+
AOUTB1-
R192
1kohms
R193
0ohms
R194
0ohms
Vcom2
Vcom1
U21A
U21B
U21C
U21D
OPA4134UA
OPA4134UA-ND
C192
10uF
L1
L2
L3
L4
220
C3
47uF
C4
0.1uF
C5
0.1uF
C6
10uF
C7
0.1uF
C8
10uF
C9
0.1uF
C10
1uF
C11
0.1uF
C14
47uF
C15
0.1uF
C16
0.1uF
C17
10uF
C18
0.1uF
C19
10uF
C20
0.1uF
C21
1uF
C22
0.1uF
Codecs
Section 3.SchDoc

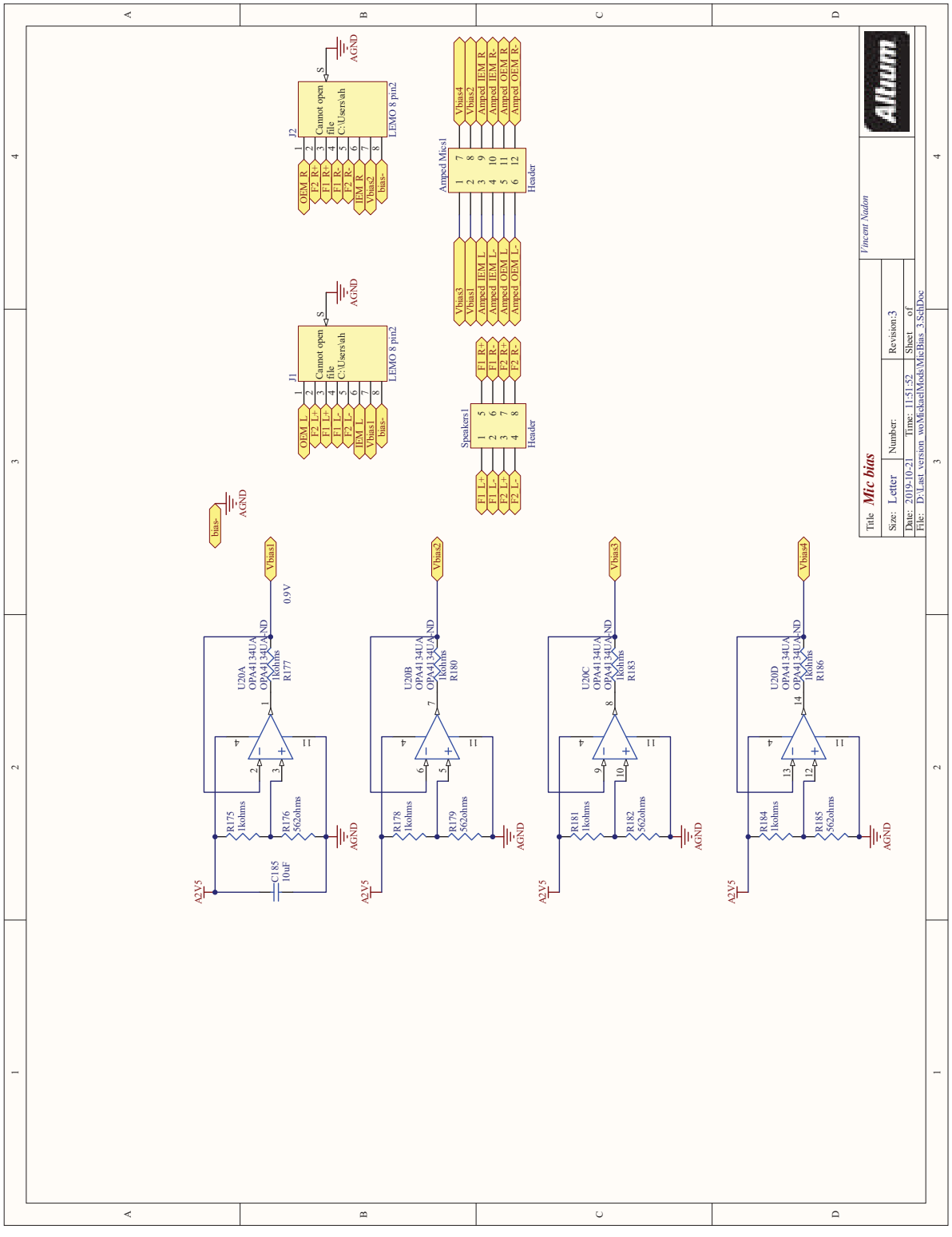
Title Mic bias
Size: Letter
Number:
Revision:3
Date: 2019-10-21
Time: 11:51:52
Sheet of
File: D:\Last version two\Meckael\Mods\MicBias 3.SchDoc
Vincent Nadon
Allium
J1
J2
OEM L
F2 L+
F1 L+
F1 L-
F2 L-
IEM L
Vbias1
bias-
OEM R
F2 R+
F1 R+
F1 R-
F2 R-
IEM R
Vbias2
Cannot open file
C:\Users\ah
LEMO 8 pin2
AGND
Speakers1
Header
Amped Miss1
Vbias3
Vbias1
Amped IEM L
Amped IEM L-
Amped OEM L
Amped OEM L-
Vbias4
Vbias2
Amped IEM R
Amped IEM R-
Amped OEM R
Amped OEM R-
U20A
U20B
U20C
U20D
OPA4134UA
R177
R180
R183
R186
1kohms
R175
R176
R178
R179
R181
R182
R184
R185
562ohms
C185
10uF
A2V5
0.9V
Vbias1
Vbias2
Vbias3
Vbias4

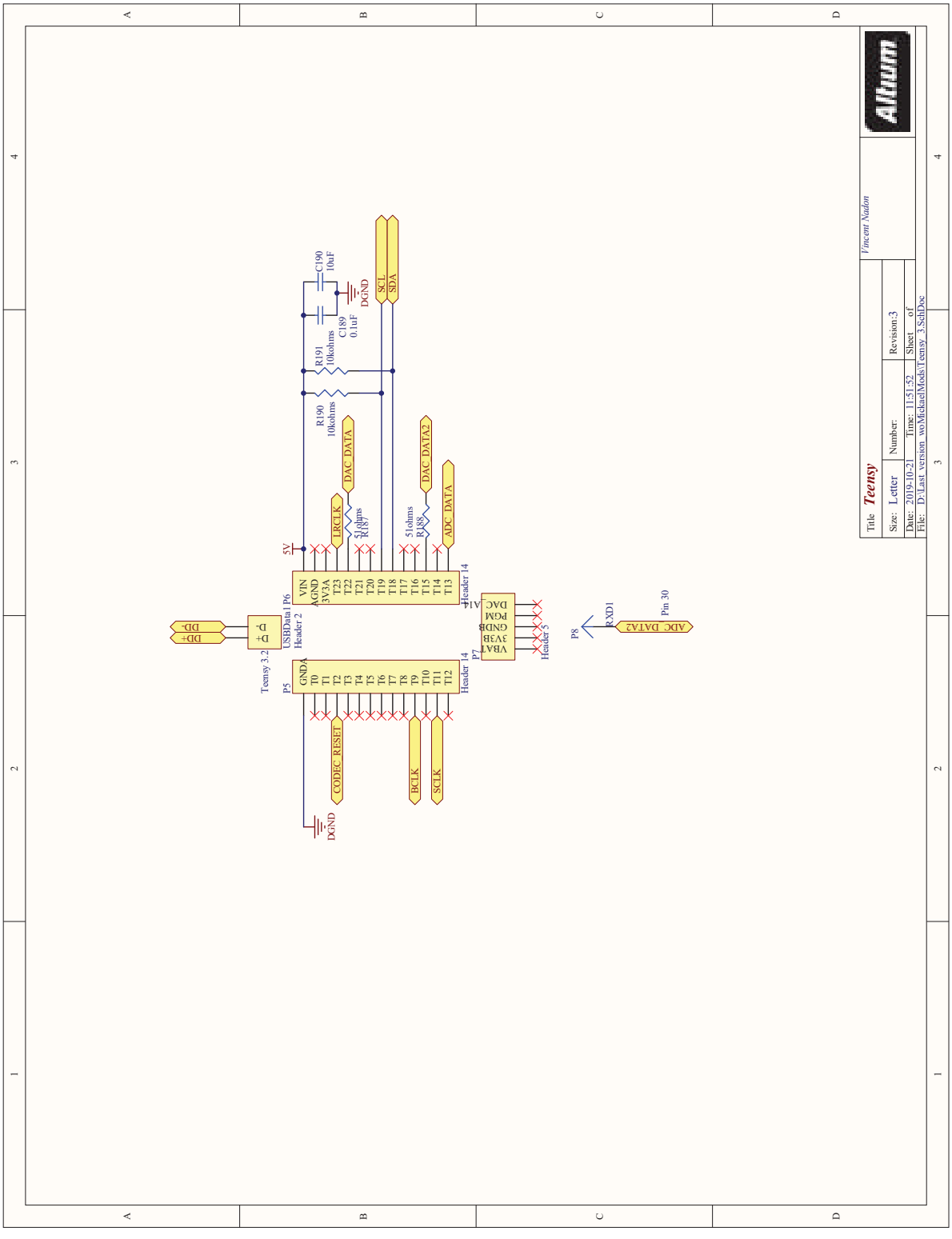
Title Teensy
Size: Letter
Number:
Revision:3
Date: 2019-10-21
Time: 11:51:52
Sheet of
File: D:\Last version wo\MickaelMods\Teensy 3.SchDoc
Vincent Nadon
Altium
Teensy 3.2
USBData1 P6
Header 2
D+
D-
P5
Header 14
P7
Header 14
Header 5
P8
RXD1
Pin 30
ADC_DATA2
VIN
AGND
3V3A
GNDA
T0
T1
T2
T3
T4
T5
T6
T7
T8
T9
T10
T11
T12
T13
T14
T15
T16
T17
T18
T19
T20
T21
T22
T23
VBAT
3V3B
GNDB
PGM
DAC
A1
5V
LRCLK
DAC_DATA
DAC_DATA2
ADC_DATA
R190
10kohms
R191
10kohms
C189
0.1uF
C190
10uF
DGND
SCL
SDA
51ohms
R188
R187
R189
CODEC_RESET
BCLK
SCLK

APPENDIX III

ASSESSMENT OF OTOACOUSTIC EMISSION PROBE FIT AT THE WORKFLOOR

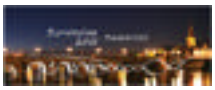

Assessment of otoacoustic emission probe fit at the workfloor

Vincent Nadon, Annelies Bockstael, Dick Botteldooren
INTEC, Acoustics Research group, Ghent University, Sint-Pietersnieuwstraat 41, B-9000 Ghent, Belgium

Jeremie Voix
École de technologie supérieure, 1100, Notre-Dame Ouest, Montreal, Quebec, H3C 1K3, Canada

Summary
In the workplace, practices in occupational health to prevent noise-induced hearing loss (NIHL) are currently based on a group average of exposure/damage relationships. These practices do not take into account the individual susceptibility to NIHL which is an important factor in a worker's actual risk of hearing loss. To evaluate and improve the effectiveness of personal hearing protection at the workfloor, an in-field measurement procedure of otoacoustic emissions (OAE) has been developed and validated. Unsupervised evaluation of OAE probe placement during the work shift is an important challenge for in-field OAE measurement. In this regard, proper OAE probe fit in the ear canal is a major concern in order to provide optimal passive noise attenuation to ensure that the worker's hearing is protected and improve signal-to-noise ratio of OAE measurements. In the following study, a lumped elements model of an occluded ear canal is used; first, to analyze the effects of probe fit leakage on the loudspeaker transfer function. Second, to validate the proposed method by comparing the model's transfer functions with those estimated during experiments with an OAE probe and tube setup. Afterwards, the probe's passive noise attenuation is calculated for different leaks by measuring sound pressure level inside and outside the occluded tube. Finally, the relationship between the probe's passive attenuation, miniature loudspeaker response and leakage is established. This proposed approach could assess the probe fit *in situ* and solve problems of unsupervised evaluation of probe placement by automatically warning the wearer of an improper fit after the loudspeaker response measurement.

PACS no. 43.58.+z, 43.60.+d, 43.64.Jb

1. Introduction

In noisy workplace environments, risk of noise-induced hearing loss (NIHL) due to occupational noise exposure is reduced using personal hearing protection devices (HPD). Even though different methods are available to assess passive noise attenuation individually [1, 2], one factor of uncertainty is the exposure level under the hearing protector and the susceptibility to NIHL which varies between individuals [3].

These problems could be solved by providing a special type of HPD to workers assessing the individual's auditory fatigue induced by daily noise exposure. Such a device would warn the worker or his superior in real-time when a (temporary) change in the worker's inner ear dynamics is detected. To monitor the diurnal effect of noise exposure, and thus prevent permanent changes in hearing sensitivity, an in-ear hearing protection device featuring otoacoustic emission (OAE) monitoring is a promising solution.

Distortion product OAEs (DPOAEs) are measured by sending two pure tone stimuli to the ear, f_1 and f_2 with a f_2/f_1 ratio of 1.22, generated by the two miniature loudspeakers within the OAE probe. Low-level cubic distortion signals (i.e. $f_{dp} = 2f_1 - f_2$) are generated by the active non-linear process of the outer hair cells (OHC), taking place inside the inner ear. The distortion product responses travel back from the inner ear to the outer ear where they can be recorded by an in-ear microphone (IEM) placed inside the ear canal. If the OHC inside the inner ear are fatigued or damaged —for instance due to previous excessive noise exposure— the amplitude of DPOAEs is found to be lower than if they were healthy. While the measured DPOAE signals are not directly related to the individual *absolute* hearing thresholds as assessed with a traditional audiogram, scientific evidences suggests that

these individual's DPOAEs can be used to track the *relative* change in hearing sensitivity [4]. Measuring DPOAEs outside a controlled environment —i.e. in-field hearing screening— is currently strongly hampered by their susceptibility to interfering environmental noise [5]. As typical DPOAE sound pressure levels (SPL) fall between -20 dB to 20 dB depending on stimuli levels and health of OHC [6].

The authors have designed a new type of DPOAE probe suitable for in-field measurements [7]. This probe includes two miniature loudspeakers with an in-ear microphone (IEM-I), as normally found in standard DPOAE probes, with an additional outer ear reference microphone (OEM-I) mounted flush on the outer faceplate of the earpiece embedded OAE probe. The probe was designed to use interchangeable custom fitted eartips, therefore providing optimal passive attenuation for every individual worker. To further improve the signal-to-noise ratio (SNR), the authors have developed a noise rejection algorithm topology designed for DPOAE measurements in-field [7]. Two DPOAE probes, one in each ear, are necessary for such algorithm and therefore the probes would be worn by workers at all times during their work shift. Wearing the two probes simultaneously would also protect the worker's hearing against environmental noise with the probe's passive attenuation. For optimal performance of such algorithm scheme, a proper fit of the DPOAE probe, is required in order to acoustically seal the ear canal from external sounds and isolate the in-ear microphones. Ensuring proper fit of the DPOAE probe would also improve the workers' effective hearing protection level.

The aim of the current paper is to develop a method for proper assessment of DPOAE probe fit *in-situ* without assistance of an occupational hygienist. The envisioned method would be integrated in the DPOAE system's [7] measurement routine. In this paper, effects of different sizes of leaks on the probe's miniature loudspeaker frequency response were simulated using a lumped element model of the loudspeaker in a 2cc cavity; bearing in mind that a leak, or improper fit, would affect the frequency response measured by the IEM. The simulated model was experimentally verified by fitting a DPOAE probe with mounting putty in a 2cc cavity. Leaks of different diameter were created in the probe and tube setup. The frequency response of the loudspeaker in the four leak conditions was measured using the IEM and compared with the simulated response. In addition, a 250 Hz pure tone was measured with the probe's IEM and was compared to a reference tone inside the Auditory Research Platform's (ARP) [8] DSPs to establish a comparison parameter for automatic evaluation of probe fit.

2. Materials and Methods

To measure the acoustic signals inside the tube the prototype earpiece-embedded OAE probe was used [7]. The DPOAE measurement system incorporating microphone conditioning amplifier and the ARP, developed within the Sonomax-ETS Industrial Chair in In-Ear Technologies (CRITIAS)[8], was used to generate logarithmic sine frequency sweep and pure tones inside the tube and to evaluate differences in SPL at 250 Hz between a leaky and non-leaky system. In usual DPOAE measurement operations, the system is used to generate primary tones with the miniature loudspeakers and process as well as record the DPOAE response from the IEM using the ARP. A 6cc (max) plastic syringe, adjusted to 2cc residual volume with probe fit, was used as a cavity for DPOAE probe fit experiments as seen in Fig. 1. A portable recorder system was used to capture the signals from the IEM and OEM. An external loudspeaker was used to generate white noise in order to characterize the passive attenuation of the probe fitted inside the tube as shown in Fig. 2.

For the prototype DPOAE earpiece, two high-quality miniature balanced armature loudspeakers with a wide-band frequency range are used in order to generate acoustic signals with minimal sound distortion on the audio frequency range for proper DPOAE measurements. The probe's IEM is placed towards the inside of the tube usually to measure DPOAE's, but in this study it was used to measure the frequency response of the miniature loudspeaker and the residual noise during the identification of the passive attenuation transfer function. The OEM is used to measure the external noise for the identification of the probe's passive attenuation transfer function.

In order to seal the tube for the experiments, about 0.6 cm thick of mounting putty was placed on the probe to fit it in inside the tube. Needles of different radius r_1=0.025, r_2=0.04 and r_3=0.06 cm were used to make a hole of known length and diameter in the mounting putty to simulate a probe fit leak, they were removed right away to not clog the hole. The needle sizes were used in ascending order to increase the hole size after measurements for each condition. The length of the leak (l_l=0.6 cm) was realistic bearing in mind that the earplug section actually sealing the first bend of the ear canal is normally no longer than 1 cm [9].

In the designed DPOAE measurement system [7], the earpiece is connected to a signal conditioning amplifier designed by the authors [7] in order to maximize the dynamic range of the DSP's ADC and filter undesired electrical interference and the microphones' DC supply. Logarithmic sine frequency sweep and pure tone signals used to characterize the miniature loudspeaker response are generated by the ARP which was connected via USB port to a laptop PC in order to control the DSPs inside. The ARP was also used to

Figure 1. Picture of the measurement tube and probe setup

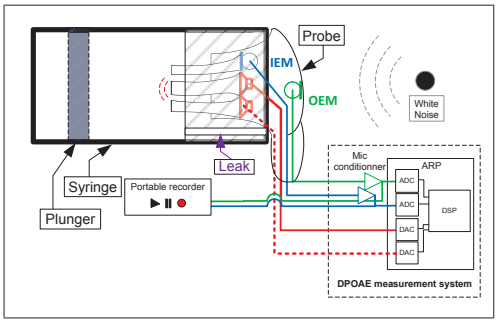

Figure 2. Schematic of tube and probe setup with portable recorder and DPOAE measurement system

calculate the $R_{A/D}$ ratio based on the probe's processed IEM signal input.

An audio recording system including a TASCAM DR-680 portable recorder (TEAC, CA, USA) was used for the acquisition of the IEM and OEM signals with a 24 bits ADC resolution (Fig. 2). The recording gain was adjusted to optimize input range for low levels with an upper limit at 94 dB (SPL) to ensure proper calibration of microphones initially. The DR-680 provided good synchronization between microphone signals with sampling frequency set at 48 kHz. Raw audio files were then transferred to a laptop computer equipped with MATLAB® (Mathworks, MA, USA) to post-process the signals. The simulations of the acoustical circuit model (Fig. 3) were also executed as a MATLAB script using Eq. 1 to 4. Measurements were carried in a quiet room without additional soundproofing materials.

2.1. Simulation of a probe fit leak

Since loudspeakers are electro-acoustic transducers, electrical parameters can be determined based on the acoustical parameters of a given loudspeaker and vice-versa. A two-port model established with Voltage (V) and Current (I) represents the electrical parameters, along with acoustical quantities Pressure (P) and Velocity (U). Z_e is the electrical impedance when $U = 0$, T_a is the transduction ratio and Z_a is the acoustical output impedance. Z_e, T_a and Z_a are also known as Hunt parameters [10, 11].

Hunt parameters can be used afterwards to model the miniature loudspeaker in the cavity as an

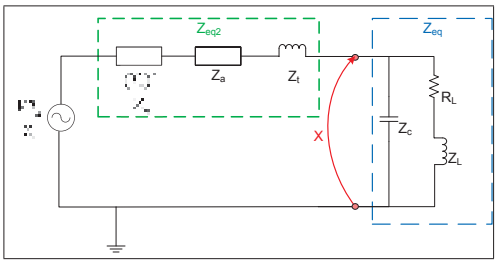

Figure 3. Lumped element, acoustical circuit model of a miniature loudspeaker with its port tube placed in a cavity with a leaky probe fit.

electronic lumped elements model through electro-acoustical analogies [12]. For the following paper, Hunt parameters for the miniature loudspeaker used in experiments were calculated beforehand [10]. Therefore, Z_e, T_a and Z_a are used as is in the simulated model. The circuit shown in Fig. 3 is an equivalent, simplified, circuit and therefore T_a^2/Z_e is actually the equivalent electrical impedance of the loudspeaker after removing the transduction ratio component of the circuit. The small tube glued to the miniature loudspeaker port, represented as Z_t, must be taken into account in the simulated acoustical circuit (see Fig. 3 and Eq. 4). Z_{eq2} represents the miniature loudspeaker with the tube glued on the port (Fig. 3).

The tube shaped leak shown in Fig. 2 can be modelled as an acoustic mass [12], here denoted as the inductance (Z_L), in series with the acoustic resistance (R_L) as in Fig. 3 , representing the friction of the air inside the small leak hole [13]. This resistor-inductance leak model is placed in parallel with the tube cavity's (Fig. 2) acoustic capacitance (Z_c). The leaky system acts as a high-pass filter with a resonance due to the presence of two reactive components, acoustic mass (Z_L) of the leak and acoustic capacitance (Z_c) of the cavity. The high-pass filter will cause a drop in lower frequency levels which can then be detected with a microphone. The resonance is also known as Helmholtz resonance and is normally used in bass reflex loudspeaker enclosures to boost the low frequency response [13, 14].

The acoustical analogy circuit's component values (Fig. 3) can be calculated out of the physical dimensions of the experimental setup (Fig. 2) with Eq. 1 to 4 . Eq. 1 and 2 represent the leak [13], Eq. 3 is the cavity compliance impedance and Eq. 4 is the miniature loudspeaker tubing impedance [12].

$$R_{L_i} = \frac{1}{\pi r_i^2}\rho_0\sqrt{2\omega\nu}\left(\frac{l_l}{r_i} + (1^*)\right) \tag{1}$$

$$Z_{L_i} = j\omega\rho_0\frac{(l_l + (1^*)l_l')}{\pi r_i^2} \tag{2}$$

$$Z_c = \frac{1}{j\omega C_{2cc}} \tag{3}$$

$$Z_t = \frac{j\rho_0 c_0}{S} \tan\left(\frac{\omega l_x}{c_0}\right) \quad (4)$$

In Eq. 1 to 4 variables are defined as ρ_0 : air density at $20^oC = 1.204kg/m^3$, c_0 : speed of sound at 20^oC = 343.2 m/s , ν : kinetic coefficient of viscosity at $20^oC = 1.56 * 10^{-5}m^2/s$, S : surface of the miniature loudspeaker tube = $\pi(0.08)^2 * 10^{-4}m^2$, l_x : length of the miniature loudspeaker tube = 0.0115 m , C_{2cc} : acoustic capacitance of the tube cavity in function of Volume $V_c = \frac{V_c}{\rho_0 c_0^2} = 1.41 * 10^{-11}m^5/N$, l_l : leak length = 0.006 m , l_l' : leak length end correction (if both tube ends are considered, replace 1^* by 2 in Eq. 1 and 2) = $0.85r_i$, f : frequency in Hertz , ω : angular speed = $2\pi f$, V_1 : voltage applied to the miniature loudspeaker's terminals in $Vrms$.

The circuit representing the miniature loudspeaker in the tube with/without leak (Fig. 3) was simulated using an input voltage $V_1 = 0.094Vrms$. To solve the acoustical circuit model, equivalent impedances and simple voltage divider were calculated as follows : $Z_{eq} = \left((R_{L_i} + Z_{L_i})^{-1} + Z_c^{-1}\right)^{-1}$, $Z_{eq2} = \frac{T_a^2}{Z_e} + Z_a + Z_t$, $|X| = \left|\frac{V_1 T_a}{Z_e} * \frac{Z_{eq}}{Z_{eq}+Z_{eq2}}\right|$. The SPL output ($|X|$) was then converted to dB in reference to 20μPa, this output represents the signal captured by the probe IEM inside the tube cavity in the experimental setup.

2.2. Experimental measurements

Measurements of the miniature loudspeaker frequency response, $R_{A/D}$ ratio inside the DSP and probe passive attenuation using the setup shown in Fig. 2 were repeated three times and levels were averaged for each leak condition. After each repetition, the probe was taken out of the tube cavity and refitted for the following measurement repetition.

The SPLs generated by the probe miniature loudspeaker were calibrated beforehand for 65 dB (SPL) at 250 Hz. This procedure was done by first measuring the level generated by a Svantek calibrator SV30A (Warsaw, Poland) set for 94 dB (SPL) at 1 kHz with the probe IEM recorded using the TASCAM portable recorder and then verifying if the correct level was observed in MATLAB, levels were matched using an adjustment factor. Secondly, the probe IEM was used to capture the 65 dB (SPL) 250 Hz pure tone generated by the miniature loudspeaker. The SPL was then observed in MATLAB and a small adjustment was made to the output gain of the DSP driving the miniature loudspeaker to match 65 dB (SPL).

2.2.1. Measurement of miniature loudspeaker frequency response with the DPOAE probe IEM

To measure the frequency response of the miniature loudspeaker, a logarithmic sine frequency sweep was generated using the DSP inside the ARP of the DPOAE measurement system. The SPL was captured by the probe's IEM.

2.2.2. Measurement of $R_{A/D}$ ratio in the DSP

Bearing in mind that the developed DPOAE system will be used in-field without expert supervision during otoacoustic emission measurements, the evaluation of the probe fit must be simple and quick without disturbing the user's activity. Therefore, an algorithm inside the DSP was designed to calculate differences in SPLs captured by the IEM used for measurements according to a reference pure tone signal (250 Hz) generated and measured solely inside the DSP while the probe is placed in the cavity. The analog (A) voltage output of the probe IEM measured by the DSP was averaged using a running Root Mean Square (RMS) averaging and then divided by the reference digital (D) signal averaged using running RMS in order to calculate a ratio, also referred here as $R_{A/D}$ ratio. Differences in such $R_{A/D}$ ratio can be used afterwards to automatically evaluate if the probe fit is good (baseline $R_{A/D}$ ratio) or leaky ($R_{A/D}$ ratio different from the baseline).

2.2.3. Measurement of the probe passive attenuation in the tube

To measure the passive attenuation provided by the DPOAE probe in the tube cavity, a small external loudspeaker was used to generate white noise (Fig.2). The level of white noise disturbance was set at 70 dB(A) at the probe's OEM position using a Svantek SVAN959 (Warsaw, Poland) sound level meter. The passive noise reduction provided by the probe sealing the tube cavity is evaluated using the difference between the probe's measured OEM and IEM SPLs per octave band.

3. Results

3.1. Simulated and measured frequency response

Magnitude of frequency responses were normalized throughout this paper in order to ease the comparison between the manufacturer's specifications, simulated and measured responses. The acoustical circuit model simulated in a non-leaky setup (Fig. 3), where R_L and Z_L are removed, gives a frequency response similar to the miniature loudspeaker's manufacturer specifications (Fig. 4). Considering that the length of tubing glued to the miniature loudspeaker's port used in experiments and reproduced in the simulations was different than specified in the manufacturer's datasheet, it is normal that the peak frequency is shifted slightly. The frequency response measured with the experimental setup shown in Fig. 2, shows that the minimum at 4885 Hz (between the two resonances) is lower in all measured conditions than simulated conditions (Fig. 4).

As shown in Fig. 4, there are very small differences in measured SPLs at 250 Hz between r_1 and r_2 (-3.29 vs -4.21 dB on average), especially considering

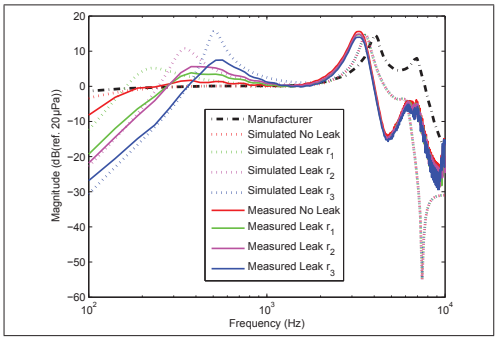

Figure 4. Simulation and single measurement frequency responses of a miniature loudspeaker for different leak sizes in a 2cc cavity.

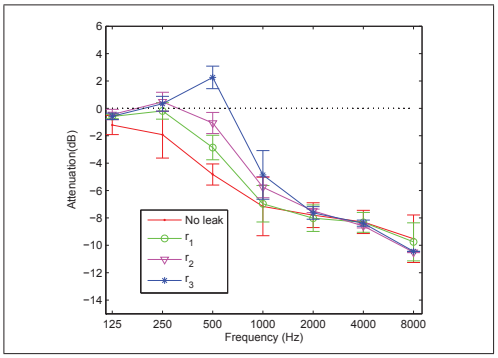

Figure 5. Attenuation measured between the probe's OEM and IEM.

the large standard deviations (3.17 and 3.40 dB respectively), this is mostly due to the very small radius difference between the two leaks. More leakage effect is seen when comparing the biggest leak (r_3) with the no leak condition (-10.43±3.45 vs -1.50±2.06 dB respectively). SPLs at 250 Hz in both simulation and experiments decrease as the leak radius increases. All leak conditions give higher SPLs than the no leak condition between 280 Hz and 1000 Hz, due to the Helmholtz resonance coming from the effect of the probe leak in the cavity. This effect is mimicked in the acoustic circuit model with R_L and Z_L which represent the leak (Fig. 3). This Helmholtz resonance is more visible for the r_3 leak at 526 Hz (Fig. 4). Bigger deviation between simulated and measured response in frequencies below 330 Hz for the r_1 leak condition might indicate some additional damping in the experimental setup which is more visible for smaller leaks, such damping is discussed in Section 4.

3.2. Measured $R_{A/D}$ ratio in DSP

$R_{A/D}$ ratios averaged over the three measurements for the no leak, r_1, r_2, r_3 leak conditions were respectively of 12.37±0.19, 14.62±3.26, 15.47±2.77, 20.52±2.72. These results show that as the leak radius increases the ratio also increases. The difference in $R_{A/D}$ ratio between the no leak and r_3 leak radius condition shows enough magnitude (8.15 dB) to be easily detected by an algorithm for automatic evaluation of probe fit quality in-field.

3.3. Measured passive attenuation of the probe in tube

The relationship between the loudspeaker response and the amount of passive attenuation provided by the DPOAE probe was assessed to eventually evaluate the probe fit in-field by solely measuring the $R_{A/D}$ ratio. The passive attenuation provided by the probe with mounting putty in the tube cavity is averaged over the three measurements and is shown in Fig. 5. Results indicate that the mounting putty and the syringe did not provide much passive attenuation (-4.83 dB at 500 Hz in the no leak condition), but was sufficient to show a realistic pattern for humans.

4. Discussion

As observed in Fig. 4, accuracy of the simulated model for frequencies over 4 kHz could be improved by modelling the cavity with a more complex cavity model such as the model from the B&K type 4195 (Brüel & Kjær, Nærum, Denmark) coupler [15].

Additional damping observed in the measured response when compared to the simulation results, especially for Helmholtz resonances and in frequencies below 330 Hz (Fig. 4), indicates that some physical properties of the experimental setup are not modelled. One possibility could be that the softness of the rubber material covering the syringe plunger is not modelled in the acoustical circuit (Fig. 3). Therefore, an additional acoustical impedance branch might be needed in parallel with the cavity's impedance Z_c in order to model this plunger surface which can be seen as an eardrum and modelled as an RLC circuit [16].

Although differences in measured SPL and $R_{A/D}$ ratios are subtle between r_1 and r_2 conditions (<1 dB) due to the size of the very small leak holes' radius which are also close to each other and that it is difficult to reproduce the hole perfectly for every manipulation. Overall, when looking at the no leak and r_3 leak conditions the differences in the $R_{A/D}$ ratio are sufficient to be detected. Since bigger leaks could be expected in tests with humans, more leak effect would be expected on the frequency response and could be automatically detected. The standard deviation could be decreased by doing more repetitions of the measurements.

The $R_{A/D}$ ratio is a relevant leak indicator (8.15 dB between no leak and r_3 leak conditions) which follows the measured SPL at 250 Hz and the probe's passive

attenuation. However, the ratios measured may not represent the exact value that would be measured in human ear canals. Therefore, the method must also be validated in humans in the future and new ratio criteria would be established.

To improve the passive attenuation of the setup, the syringe could be replaced by an adjustable thick brass cavity. Although such improvement could make the effects of the leak conditions more noticeable and closer to what would be expected in humans, the passive attenuation in the current study was sufficient to show leak effects.

The Helmholtz resonance effect could have an impact on the evaluation of a proper probe fit by misleading the user into thinking that a better seal is obtained since the $R_{A/D}$ ratio would decrease instead of normally increasing for bigger leaks. For smaller leak diameters, the resonance frequency will be lower (Fig. 4), but considering a known fixed eartip length sealing the ear canal [9] it is possible to detect a leak by first establishing a baseline with an optimal seal. $R_{A/D}$ ratios relative to this baseline should always increase if the ratio is measured at a frequency lower than the expected resonance. The $R_{A/D}$ ratio measured at 250 Hz is therefore an accurate indicator of a leak in the probe's seal for leak lengths shorter than 1 cm.

5. CONCLUSIONS

The scope of the study, i.e. visualize leak effects on the frequency response of the DPOAE probe miniature loudspeaker, was achieved. The simulated acoustic circuit model has shown sufficient similarities with the experimental setup to observe that the SPL around 250 Hz decreases as the leak radius increases and could be used to predict probe leak effects in humans. The $R_{A/D}$ ratio was shown to be a suitable indicator for automatic evaluation of probe fit leakage during in-field DPOAE measurements. Although a low frequency resonance due to the Helmholtz resonator effect might cause problems, by knowing the length of the eartip inserted in the ear canal the system can easily be tuned to only consider lower frequencies where the resonance has no effect on the $R_{A/D}$ ratio. As a result, the procedure detailed in this paper to measure the $R_{A/D}$ ratio can be integrated in the designed DPOAE system's measurement routine in an attempt to improve the reliability of in-field DPOAE measurements.

Acknowledgement

Annelies Bockstael is a postdoctoral fellow of the Research Foundation-Flanders (FWO); the support of this organization is gratefully acknowledged. The ETS-affiliated authors are thankful for the technical support from the *Sonomax-ETS Industrial Research Chair in In-Ear Technology* for prototyping the experimental DPOAE probes. Vincent Nadon is especially grateful to the Institut Robert-Sauvé en santé et sécurité au travail (IRSST) for its financial support for the project.

References

[1] Voix, J., and Laville, F.: The Objective Measurement of Earplug Field Performance. J. Acoust. Soc. Am., Vol. 125 (2009), 3722-3732.

[2] Bockstael, A., Van Renterghem, T., Botteldooren, D., Dhaenens, W., Keppler, H., Maes, L., Philips, B., Swinnen, F., and Vinck, B. : Verifying the attenuation of earplugs in situ: method validation on human subjects including individualized numerical simulations. J. Acoust. Soc. Am., USA Vol. 125 (2009), 1479-1489.

[3] Henderson, D., Subramaniam, M., and Boettcher, F. A.: Individual Susceptibility to Noise-Induced Hearing loss: An Old Topic Revisited. Ear Hearing, **14(3)** (1993).

[4] Marshall, L., Lapsley Miller, J., and Heller, L.: Distortion-product otoacoustic emissions as a screening tool for noise-induced hearing loss. Noise Health, **3** (2001), 43-60.

[5] Popelka, G. R., Karzon, R. K., Clary, R. A.: Identification of noise sources that influence distortion product otoacoustic emission measurements in human neonates. Ear and hearing, **19(4)** (1998), 319-328.

[6] Delgado, R. E., Ozdamar, O., Rahman, S., and Lopez, C. N.: Adaptive noise cancellation in a multimicrophone system for distortion product otoacoustic emission acquisition. IEEE Trans. Biomed. Eng., **47** (2000), 1154-64.

[7] Nadon V. : Développement d'une oreillette pour la mesure des émissions otoacoustiques, Master Thesis, École de technologie supérieure (2014).

[8] CRITIAS : Chaire de recherche industrielle en technologies intra-auriculaire Sonomax-ETS (CRITIAS), `http://critias.etsmtl.ca/the-technology/arp/` .

[9] Tufts, J. : Canal Segment Length of Custom Earplugs: Effects on Attenuation (and comfort). NHCA (2014).

[10] Bernier, A. : Development of an active hearing protection device for musicians, Technical Report, École de technologie supérieure (2014).

[11] Kim, N., Allen, J. B. : Two-port network analysis and modeling of a balanced armature receiver. Hearing Research, 301 (2013), 156-167.

[12] Kleiner, M. : Electroacoustics. CRC Press (2013).

[13] Beranek, L. L. : Acoustics. McGraw-Hill (1954) 137-138.

[14] Leach, W. M. Jr. : Computer Aided Electro-Acoustic Design with SPICE. Journal Audio Engineering Society, 39(7/8) (1991), 551-562.

[15] B&K. : Ear Simulator for Telephonometry B&K Type 4195 - Application Note (2014). p. 7.

[16] Hiipakka, M. : Measurement Apparatus and Modelling Techniques of Ear Canal Acoustics. Master Thesis, Helsinki University of Technology (2008). p.93.

APPENDIX IV

MULTILEVEL MODEL CODE DEVELOPED IN R : EXAMPLE FOR DPOAE GROWTH FUNCTIONS

Loading packages

```
library(R.matlab)
library(DescTools)
library(lme4)
library(nlme)
# library(MCMCglmm) library(glmmTMB) library(brms)
library(reshape2)
library(tidyr)
# library(tidyverse)
library(dplyr)
library(corrplot)
library(broom.mixed)
library(dotwhisker)
library(ggplot2)
theme_set(theme_bw())
library(plotly)
library(ggpubr)
library(stargazer)
library(sjPlot)
library(corrplot)
library(socviz)
library(rcompanion)
library(formatR)
```

Loading dataframe

```
setwd("L:/PhD_VincentNadon2014_2019/MATLAB_code/")
GrowthDPOAE.df <- read.csv(file = "dose_responseExperimentJune19.csv",
    header = TRUE, sep = ",")


# Clean NaN
GrowthDPOAE.df[GrowthDPOAE.df == "NaN"] <- NA

GrowthDPOAE.df2 <- GrowthDPOAE.df


GrowthDPOAE.df$timestamp[GrowthDPOAE.df$timestamp < 0] <- NA

colnames(GrowthDPOAE.df)[62] <- c("Gender")

GrowthDPOAE.df$Gender <- abs(GrowthDPOAE.df$Gender - 1)

GrowthDPOAE.df$timestamp <- (GrowthDPOAE.df$timestamp)/60
```

```
# Transform data to make residuals Normal Remove outliers
# from DPOAE levels
for (col_i in 5:22) {


    GrowthDPOAE.df[which((GrowthDPOAE.df[, col_i]) > 5.5), col_i] <- NA

    GrowthDPOAE.df[which((GrowthDPOAE.df[, col_i]) < -5.5), col_i] <- NA

    GrowthDPOAE.df[which(abs(GrowthDPOAE.df[, col_i]) == 0),
        col_i] <- NA


}

# Remove outliers from Leq + grand mean centering
for (col_i in 42:51) {
    mean_col2 = mean(GrowthDPOAE.df[, col_i], na.rm = TRUE)
    std_col2 = sd(GrowthDPOAE.df[, col_i], na.rm = TRUE)


    GrowthDPOAE.df[, col_i] <- GrowthDPOAE.df[, col_i] - mean_col2

    if (col_i == 44) {
        OEM_avg = mean_col2
    }

    if (col_i == 51) {
        crestF_avg = mean_col2
    }


}


DPshift_full <- GrowthDPOAE.df[, c(1:22, 44:45, 47, 48, 49, 51,
    61:63)]

Growth_full <- GrowthDPOAE.df[, c(1:4, 23:40, 44:45, 47, 48,
    49, 51, 61:63)]
```

Formatting Data

```
# DP_shift melt columns for LME4 univariate

# DP shift 65dB

DPshift_full2 <- DPshift_full

colnames(DPshift_full)[11:16] <- c("6169", "5657", "5187", "4757",
    "4362", "4000")

DP_shift_melt <- gather(DPshift_full, Frequency, DPOAE_level,
```

```
    11:16)

DP_shift_melt$Frequency <- as.numeric(DP_shift_melt$Frequency)/1000


DP_shift_melt <- (DP_shift_melt %>% drop_na())



# DP shift 60dB

DPshift_full60 <- DPshift_full2

colnames(DPshift_full60)[5:10] <- c("6169", "5657", "5187", "4757",
    "4362", "4000")

DP_shift_melt60 <- gather(DPshift_full60, Frequency, DPOAE_level,
    5:10)


DP_shift_melt60$Frequency <- as.numeric(DP_shift_melt60$Frequency)/1000


DP_shift_melt60 <- (DP_shift_melt60 %>% drop_na())



# DP shift 70dB

DPshift_full70 <- DPshift_full2

colnames(DPshift_full70)[17:22] <- c("6169", "5657", "5187",
    "4757", "4362", "4000")

DP_shift_melt70 <- gather(DPshift_full70, Frequency, DPOAE_level,
    17:22)


DP_shift_melt70$Frequency <- as.numeric(DP_shift_melt70$Frequency)/1000


DP_shift_melt70 <- (DP_shift_melt70 %>% drop_na())
```

Build up DPOAE LEVEL model with statistically significant predictors

```
# Unconditional means model
model.DPOAE.allf2 <- lme(DPOAE_level ~ 1, DP_shift_melt, random = ~1 |
    Participant, na.action = na.omit, method = "ML", correlation = corAR1())


# Unconditional growth model
model.DPOAE.allf2_time <- lme(DPOAE_level ~ timestamp, DP_shift_melt,
    random = ~1 | Participant, na.action = na.omit, method = "ML",
```

```
    correlation = corAR1())


# time with regular interval
model.DPOAE.allf2_time20 <- lme(DPOAE_level ~ timestamp20, DP_shift_melt,
    random = ~1 | Participant, na.action = na.omit, method = "ML",
    correlation = corAR1())


model.DPOAE.allf2_timeDay <- lme(DPOAE_level ~ timestamp, DP_shift_melt,
    random = ~1 | Participant/Day, na.action = na.omit, method = "ML",
    correlation = corAR1())

# including one time-varying predictor
model.DPOAE.allf2_OEM <- lme(DPOAE_level ~ timestamp * LeqAOEM,
    DP_shift_melt, random = ~1 | Participant/Day, na.action = na.omit,
    method = "ML", correlation = corAR1())

model.DPOAE.allf2_OEM2 <- lme(DPOAE_level ~ LeqAOEM, DP_shift_melt,
    random = ~1 | Participant/Day, na.action = na.omit, method = "ML",
    correlation = corAR1())

model.DPOAE.allf2_OEM3 <- lme(DPOAE_level ~ timestamp:LeqAOEM,
    DP_shift_melt, random = ~1 | Participant/Day, na.action = na.omit,
    method = "ML", correlation = corAR1())

model.DPOAE.allf2_C_A = update(model.DPOAE.allf2_OEM, . ~ . +
    timestamp * C_A)
print(summary(model.DPOAE.allf2_C_A))
print(anova(model.DPOAE.allf2_OEM, model.DPOAE.allf2_C_A))

model.DPOAE.allf2_Kurt = update(model.DPOAE.allf2_OEM, . ~ . +
    timestamp * Kurtosis)
print(summary(model.DPOAE.allf2_Kurt))
print(anova(model.DPOAE.allf2_OEM, model.DPOAE.allf2_Kurt))

model.DPOAE.allf2_CrestF = update(model.DPOAE.allf2_OEM, . ~
    . + timestamp * CrestF)
print(summary(model.DPOAE.allf2_CrestF))
print(anova(model.DPOAE.allf2_OEM, model.DPOAE.allf2_CrestF))

# Add time-invariant predictors Gender and Age

# Gender
model.DPOAE.allf2_Gender = update(model.DPOAE.allf2_OEM, . ~
    . + Gender)
print(summary(model.DPOAE.allf2_Gender))
print(anova(model.DPOAE.allf2_OEM, model.DPOAE.allf2_Gender))

# Age
model.DPOAE.allf2_Age = update(model.DPOAE.allf2_OEM, . ~ . +
    Age)
print(summary(model.DPOAE.allf2_Age))
print(anova(model.DPOAE.allf2_OEM, model.DPOAE.allf2_Age))

# Check Other Combination of noise metrics
```

```
# #Kurt*OEM
model.DPOAE.allf2_OEM_Kurt <- lme(DPOAE_level ~ timestamp * LeqAOEM *
    Kurtosis, DP_shift_melt, random = ~1 | Participant/Day, na.action = na.omit,
    method = "ML", correlation = corAR1())

# #CrestF*OEM
model.DPOAE.allf2_OEM_CrestF <- lme(DPOAE_level ~ timestamp *
    LeqAOEM * CrestF, DP_shift_melt, random = ~1 | Participant/Day,
    na.action = na.omit, method = "ML", correlation = corAR1())
```

Models for L1 = 65dB, DPOAE level per f2 frequency

```
# 6169

model.DPOAE_6169 = lme(L1_65_f2_6169 ~ timestamp * LeqAOEM +
    timestamp * CrestF, DPshift_full2, random = ~1 | Participant/Day,
    na.action = na.omit, method = "ML", correlation = corAR1())  #


# 5657

model.DPOAE_5657 = lme(L1_65_f2_5657 ~ timestamp * LeqAOEM +
    timestamp * CrestF, DPshift_full2, random = ~1 | Participant/Day,
    na.action = na.omit, method = "ML", correlation = corAR1())  #

# 5187

model.DPOAE_5187 = lme(L1_65_f2_5187 ~ timestamp * LeqAOEM +
    timestamp * CrestF, DPshift_full2, random = ~1 | Participant/Day,
    na.action = na.omit, method = "ML", correlation = corAR1())  #

# 4757

model.DPOAE_4757 = lme(L1_65_f2_4757 ~ timestamp * LeqAOEM +
    timestamp * CrestF, DPshift_full2, random = ~1 | Participant/Day,
    na.action = na.omit, method = "ML", correlation = corAR1())  #

# 4362

model.DPOAE_4362 = lme(L1_65_f2_4362 ~ timestamp * LeqAOEM +
    timestamp * CrestF, DPshift_full2, random = ~1 | Participant/Day,
    na.action = na.omit, method = "ML", correlation = corAR1())  #


# 4000

model.DPOAE_4000 = lme(L1_65_f2_4000 ~ timestamp * LeqAOEM +
    timestamp * CrestF, DPshift_full2, random = ~1 | Participant/Day,
    na.action = na.omit, method = "ML", correlation = corAR1())  #
```

APPENDIX V

COMPLIMENTARY MODEL TABLES FOR CHAPTER 6

Table-A V-1 Fixed effects coefficients of the optimal model for the CAS DPOAE suppression

	f_2 frequency (Hz)																					
	1000	1091	1189	1297	1414	1542	1682	1834	2000	2181	2378	2594	2828	3084	3364	3668	4000	4362	4757	5187	5657	6169
Exposed1	0.266	−1.294**	−1.046***	−0.365	−0.521	−0.563*	−0.728**	−0.563	−0.197	−0.178	−0.210	−0.413	0.391	−0.382	−0.758*	−0.338	−0.283	−0.339	−0.332	−0.314	0.130	0.160
	(0.401)	(0.462)	(0.346)	(0.381)	(0.396)	(0.276)	(0.278)	(0.327)	(0.373)	(0.385)	(0.442)	(0.359)	(0.335)	(0.299)	(0.384)	(0.348)	(0.303)	(0.338)	(0.265)	(0.318)	(0.319)	(0.305)
Gender1	−0.090	0.415	0.715**	0.879**	1.230***	0.569**	0.748***	0.090	0.061	0.572	−0.172	0.128	−0.257	0.734***	0.182	0.510*	0.219	0.353	0.219	0.020	0.122	−0.303
	(0.339)	(0.393)	(0.306)	(0.314)	(0.334)	(0.240)	(0.237)	(0.281)	(0.311)	(0.329)	(0.344)	(0.303)	(0.278)	(0.251)	(0.328)	(0.285)	(0.249)	(0.272)	(0.218)	(0.260)	(0.257)	(0.255)
Intercept	0.014	1.125***	0.513*	0.318	0.043	0.381	0.689***	0.755***	0.526*	0.173	0.539	0.852***	0.434	0.529**	0.901***	0.289	0.665**	0.391	0.450*	0.272	0.205	0.382
	(0.356)	(0.390)	(0.276)	(0.318)	(0.331)	(0.231)	(0.228)	(0.272)	(0.307)	(0.323)	(0.377)	(0.305)	(0.282)	(0.260)	(0.323)	(0.301)	(0.262)	(0.295)	(0.228)	(0.268)	(0.275)	(0.260)
Observations	84	93	92	101	101	97	99	107	100	100	95	101	106	99	104	109	111	116	115	113	111	112

Note: (standard error) *p<0.1; **p<0.05; ***p<0.01

Table-A V-2 Fixed effects coefficients of the optimal model for DPOAE shifts

	f_2 frequency (Hz)																					
	1000	1091	1189	1297	1414	1542	1682	1834	2000	2181	2378	2594	2828	3084	3364	3668	4000	4362	4757	5187	5657	6169
Exposed1	−0.015	0.048	−1.534	−3.828	−3.370	−4.962*	−4.330	−2.639	−4.001	−2.179	−2.047	−1.364	1.158	2.452	1.986	3.117	6.343**	5.494**	3.782	3.928	2.498	2.639
	(2.230)	(2.697)	(2.474)	(2.976)	(2.861)	(2.535)	(3.050)	(3.111)	(2.664)	(2.285)	(2.384)	(2.657)	(2.467)	(2.339)	(2.209)	(2.349)	(2.266)	(2.499)	(2.868)	(3.579)	(3.754)	(2.918)
Session	−0.569*	−0.062	−0.097	0.048	−0.303	−0.287	−0.329	−0.358	−0.574*	−0.146	−0.171	0.184	0.507	0.524	0.380	0.744	0.937**	0.786*	0.169	0.174	0.506	−0.032
	(0.324)	(0.524)	(0.362)	(0.533)	(0.278)	(0.294)	(0.418)	(0.307)	(0.318)	(0.457)	(0.414)	(0.398)	(0.550)	(0.358)	(0.449)	(0.526)	(0.357)	(0.451)	(0.551)	(0.576)	(0.638)	(0.581)
Exposed1:Session	0.228	−0.199	−0.368	−0.047	0.255	0.196	0.187	0.024	0.578	0.363	0.195	−0.148	−0.648	−0.591	−0.197	−0.668	−1.111***	−1.153**	−0.488	−0.859	−0.850	−0.248
	(0.362)	(0.586)	(0.404)	(0.596)	(0.311)	(0.329)	(0.467)	(0.343)	(0.355)	(0.511)	(0.463)	(0.445)	(0.615)	(0.400)	(0.502)	(0.591)	(0.400)	(0.505)	(0.616)	(0.644)	(0.713)	(0.649)
Intercept	2.868	3.384	5.313**	9.601***	9.928***	7.866***	10.138***	7.798***	6.947***	2.724	4.914**	3.462	2.505	−2.533	−3.166	−3.684*	−5.350**	−5.346**	−1.429	−0.268	0.860	4.627*
	(1.995)	(2.412)	(2.213)	(2.662)	(2.559)	(2.268)	(2.728)	(2.783)	(2.383)	(2.043)	(2.133)	(2.377)	(2.207)	(2.092)	(1.976)	(2.090)	(2.026)	(2.236)	(2.565)	(3.201)	(3.358)	(2.610)
Observations	60	60	60	60	60	60	60	60	60	60	60	60	60	60	60	59	60	60	60	60	60	60

Note: (standard error) *p<0.1; **p<0.05; ***p<0.01

APPENDIX VI

COMPLIMENTARY QUANTILE-QUANTILE PLOT FOR CHAPTER 6

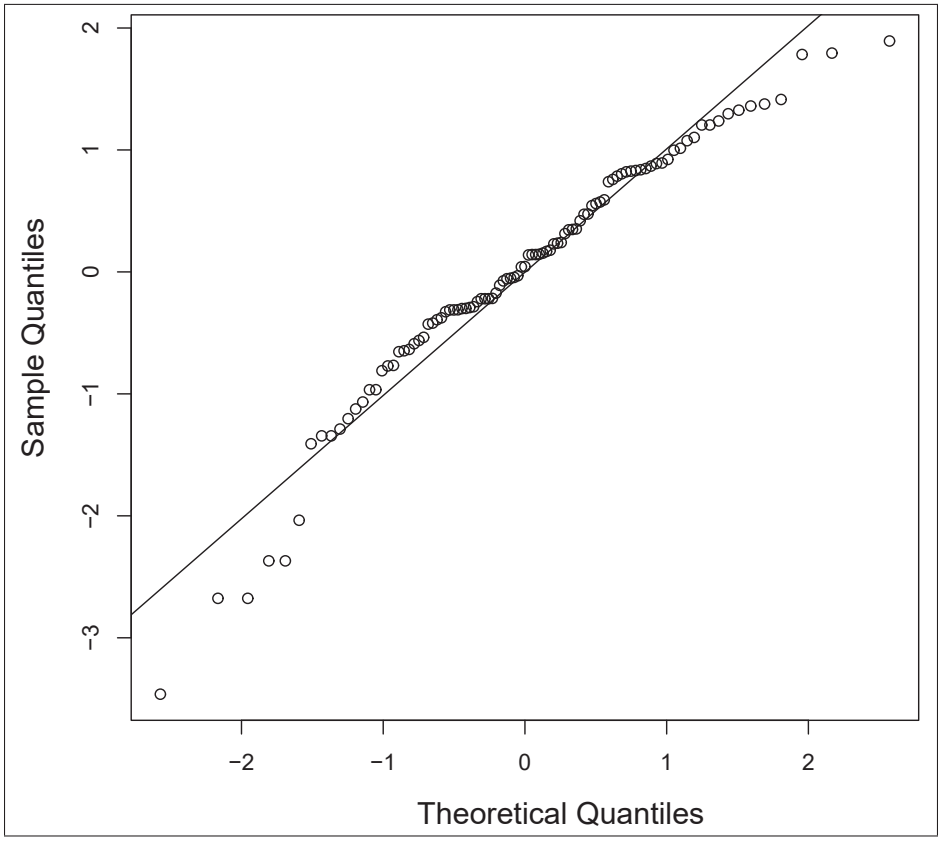

Figure-A VI-1 Quantile-Quantile plot for the residuals of the CAS DPOAE suppression model for DPOAE frequency f_2 = 1682 Hz

REFERENCES

3M. (2020). What is hearing protection fit testing? Consulted at https://safetytownsquare .3mcanada.ca/articles/what-is-hearing-protection-fit-testing.

Alberti, P. W. (1992). Noise induced hearing loss. *BMJ: British Medical Journal*, 304(6826), 522.

Allen, J. B. (1986). Measurement of eardrum acoustic impedance. In *Peripheral auditory mechanisms* (pp. 44–51). Springer.

ANSI. (2007). Methods of Estimating Effective A-Weighted Sound Pressure Levels When Hearing Protectors Are Worn. *American National Standard, ANSI S12. 68*.

ANSI. (2008). *Methods for measuring the real-ear attenuation of hearing protectors*. ANSI/ASA S12.6. Washington, D.C., USA: American National Standards Institute.

Attias, J., Bresloff, I., Reshef, I., Horowitz, G. & Furman, V. (1998). Evaluating noise induced hearing loss with distortion product otoacoustic emissions. *British journal of audiology*, 32(1), 39–46.

AudSim. (2019). The Hughson-Westlake Method of Obtaining Threshold. Consulted at http:// audsim.com/docs/h-w.shtml.

Berger, E. H. (2010). *What is a Personal Attenuation Rating (PAR)?* (Report n°2.31). 3M Occupational Health & Environmental Safety Division E•A•RCAL Laboratory.

Berger, E. (1985). Is real-ear attenuation at threshold a function of hearing level? *The Journal of the Acoustical Society of America*, 78(5), 1588–1595.

Berger, E. & Kerivan, J. (1983). Influence of physiological noise and the occlusion effect on the measurement of real-ear attenuation at threshold. *The Journal of the Acoustical Society of America*, 74(1), 81–94.

Berger, E. H. (2003). *The noise manual*. Aiha.

Berger, E. H., Franks, J. R., Behar, A., Casali, J. G., Dixon-Ernst, C., Kieper, R. W., Merry, C. J., Mozo, B. T., Nixon, C. W., Ohlin, D. et al. (1998). Development of a new standard laboratory protocol for estimating the field attenuation of hearing protection devices. Part III. The validity of using subject-fit data. *The journal of the acoustical society of america*, 103(2), 665–672.

Bharadwaj, H. M., Masud, S., Mehraei, G., Verhulst, S. & Shinn-Cunningham, B. G. (2015). Individual Differences Reveal Correlates of Hidden Hearing Deficits. *Journal of Neuroscience*, 35(5), 2161–2172. doi: 10.1523/JNEUROSCI.3915-14.2015.

Bohne, B. A., Kimlinger, M. & Harding, G. W. (2017). Time course of organ of Corti degeneration after noise exposure. *Hearing Research*, 344, 158–169. doi: 10.1016/j.heares.2016.11.009.

Bolger, N. & Laurenceau, J.-P. (2013). *Intensive longitudinal methods: An introduction to diary and experience sampling research*. Guilford Press.

Bonnet, F. (2019). *Méthode de mesure individuelle de l'exposition sonore effective intra-auriculaire en milieu de travail*. (Ph.D. thesis, École de technologie supérieure, Montréal (Canada)).

Bonnet, F., Voix, J. & Nélisse, H. (2015). The opportunities and challenges of in-ear noise dosimetry. *Canadian Acoustics*, 43(3), 2.

Bonnet, F., Nélisse, H., Nogarolli, M. A. & Voix, J. (2019a). In-ear noise dosimetry under earplug: Method to exclude wearer-induced disturbances. *International Journal of Industrial Ergonomics*, 74, 102862.

Bonnet, F., Nélisse, H. & Nogarolli, M. A. C. (2019b). An in-ear noise dosimetery method that excludes the sounds generated by individuals wearing earplugs: preliminary field study. *International Congress on Sound and Vibration*.

Bonnet, F., Nélisse, H., Nogarolli, M. A. & Voix, J. (2020). Individual in situ calibration of in-ear noise dosimeters. *Applied Acoustics*, 157, 107015.

Borg, E., Nilsson, R. & Lidén, G. (1979). Fatigue and recovery of the human acoustic stapedius reflex in industrial noise. *The Journal of the Acoustical Society of America*, 65(3), 846–848.

Borgh, M., Lindström, F., Waye, K. P. & Claesson, I. (2008). The effect of own voice on noise dosimeter measurements: a field study in a day-care environment, including adults and children. *Internoise*.

Bramhall, N., Beach, E. F., Epp, B., Le Prell, C. G., Lopez-Poveda, E. A., Plack, C. J., Schaette, R., Verhulst, S. & Canlon, B. (2019). The search for noise-induced cochlear synaptopathy in humans: Mission impossible? *Hearing research*, 377, 88–103.

Bramhall, N. F., Konrad-Martin, D., McMillan, G. P. & Griest, S. E. (2017). Auditory Brainstem Response Altered in Humans With Noise Exposure Despite Normal Outer Hair Cell Function. *Ear and Hearing*, 38(1), e1–e12.

Byrne, D. & Reeves, E. (2008). Analysis of Nonstandard Noise Dosimeter Microphone. *Journal of Occupational and Environmental Hygiene*, 5(3), 197–209.

Canetto, P. (2009). Hearing protectors: Topicality and research needs. *International Journal of Occupational Safety and Ergonomics*, 15(2), 141–153.

Carnegie Mellon University. (1992). NOISEX-92 database.

CCOHS. (2019a). Noise - Hearing Conservation Program. Consulted at https://www.cchst.ca/oshanswers/phys_agents/hearing_conservation.html.

CCOHS. (2019b). Noise - Occupational Exposure Limits in Canada. Consulted at https://www.ccohs.ca/oshanswers/phys_agents/exposure_can.html.

Charaziak, K. K. & Shera, C. A. (2017). Compensating for ear-canal acoustics when measuring otoacoustic emissions. *The Journal of the Acoustical Society of America*, 141(1), 515–531. doi: 10.1121/1.4973618.

CNESST. (2011). Statistiques annuelles. Quebec, Canada. Consulted at http://www.csst.qc.ca/publications/200/Documents/DC200_1046_19web.pdf.

CNESST. (2015). Surdité professionnelle : le boom d'un mal silencieux. Consulted at http://preventionautravail.com/reportages/266-surdite-professionnelle-le-boom-d-un-mal-silencieux.html.

CNESST. (2017). *Statistiques annuelles 2017*. Consulted at https://www.cnesst.gouv.qc.ca/Publications/200/Documents/DC200-1046web.pdf.

Cody, A. & Johnstone, B. (1981). Acoustic trauma: Single neuron basis for the"half-octave shift". *The Journal of the Acoustical Society of America*, 70(3), 707–711.

Creutzfeldt, O., Ojemann, G. & Lettich, E. (1989). Neuronal activity in the human lateral temporal lobe. *Experimental Brain Research*, 77(3), 451–475.

CRITIAS. (2019). NSERC-EERS Industrial Research Chair in In-Ear Technologies (CRITIAS) - Auditory Research Platform (ARP). Consulted at http://critias.etsmtl.ca/the-technology/arp/.

Czyżewski, A., Kotus, J. & Kostek, B. (2007). Determining the noise impact on hearing using psychoacoustical noise dosimeter. *Archives of Acoustics*, 32(2), 215–229.

Davis, R. I., Qiu, W., Heyer, N. J., Zhao, Y., Yang, M. Q., Li, N., Tao, L., Zhu, L., Zeng, L., Yao, D. et al. (2012). The use of the kurtosis metric in the evaluation of occupational hearing

loss in workers in China: Implications for hearing risk assessment. *Noise and Health*, 14(61), 330.

Davis, S. K., Calamia, P. T., Murphy, W. J. & Smalt, C. J. (2019). In-ear and on-body measurements of impulse-noise exposure. *International journal of audiology*, 58(sup1), S49–S57.

de Toro, M. A. A., Ordoñez, R., Reuter, K., Hammershøi, D. & others. (2010). Recovery of distortion-product otoacoustic emissions after a 2-kHz monaural sound-exposure in humans: Effects on fine structures. *The Journal of the Acoustical Society of America*, 128(6), 3568–3576.

Dreisbach, L. E. & Siegel, J. H. (2005). Level dependence of distortion-product otoacoustic emissions measured at high frequencies in humans. *The Journal of the Acoustical Society of America*, 117(5), 2980. doi: 10.1121/1.1880792. 00013.

École de technologie supérieure. (2019). Comité d'éthique à la recherche - Numéro de référence : H20170204. Consulted at https://www.etsmtl.ca/Recherche/Soutien-aux-chercheurs%20/Comite-ethique-ets.

Eddins, A. C., Zuskov, M. & Salvi, R. J. (1999). Changes in distortion product otoacoustic emissions during prolonged noise exposure. *Hearing research*, 127(1-2), 119–128.

Eleftheriou, P. C. (2002). Industrial noise and its effects on human hearing. *Applied Acoustics*, 63(1), 35–42.

Engdahl, B. (1996). Effects of noise and exercise on distortion product otoacoustic emissions. *Hearing Research*, 93(1-2), 72–82.

Engdahl, B. & Kemp, D. T. (1996). The effect of noise exposure on the details of distortion product otoacoustic emissions in humans. *The Journal of the Acoustical Society of America*, 99(3), 1573–1587.

Etymotic Research. (2019a). ER-10B+. Consulted at https://www.etymotic.com/auditory-research/microphones/er-10b.html.

Etymotic Research. (2019b). ER-10x. Consulted at https://www.er10x.com/downloads/documents/.

Feder, K., Michaud, D., McNamee, J., Fitzpatrick, E., Davies, H. & Leroux, T. (2017). Prevalence of hazardous occupational noise exposure, hearing loss, and hearing protection usage among a representative sample of working Canadians. *Journal of occupational and environmental medicine*, 59(1), 92.

Feeney, M., Schairer, K., Keefe, D. H., Fitzpatrick, D., Putterman, D., Garinis, A., Kurth, M., Kolberg, E., McGregor, K. & Light, A. (2018). Comparison of wideband and clinical acoustic reflex thresholds in patients with normal hearing and sensorineural hearing loss. *The Journal of the Acoustical Society of America*, 144(3), 1834–1834.

Fernandez, K. A., Jeffers, P. W., Lall, K., Liberman, M. C. & Kujawa, S. G. (2015). Aging after noise exposure: acceleration of cochlear synaptopathy in "recovered" ears. *Journal of Neuroscience*, 35(19), 7509–7520.

Furman, A. C., Kujawa, S. G. & Liberman, M. C. (2013). Noise-Induced Cochlear Neuropathy Is Selective for Fibers With Low Spontaneous Rates. *Journal of Neurophysiology*, 110(3), 577–86. doi: 10.1152/jn.00164.2013.

Gates, G. A. & Mills, J. H. (2005). Presbycusis. *The lancet*, 366(9491), 1111–1120.

Gates, G. A., Mills, D., Nam, B.-h., D'Agostino, R. & Rubel, E. W. (2002). Effects of age on the distortion product otoacoustic emission growth functions. *Hearing Research*, 163(1-2), 53–60.

Gehr, D. D., Janssen, T., Michaelis, C. E., Deingruber, K. & Lamm, K. (2004). Middle ear and cochlear disorders result in different DPOAE growth behaviour: implications for the differentiation of sound conductive and cochlear hearing loss. *Hearing research*, 193(1-2), 9–19.

Goley, G. S., Song, W. J. & Kim, J. H. (2011). Kurtosis corrected sound pressure level as a noise metric for risk assessment of occupational noises. *The Journal of the Acoustical Society of America*, 129(3), 1475–1481.

Groenewold, M. R., Masterson, E. A., Themann, C. L. & Davis, R. R. (2014). Do hearing protectors protect hearing? *American journal of industrial medicine*, 57(9), 1001–1010.

Grundström, B. (2019). Bandsaw. Consulted at https://thenounproject.com/term/bandsaw/883733/.

Guinan Jr, J. J., Backus, B. C., Lilaonitkul, W. & Aharonson, V. (2003). Medial olivocochlear efferent reflex in humans: otoacoustic emission (OAE) measurement issues and the advantages of stimulus frequency OAEs. *Journal of the Association for Research in Otolaryngology*, 4(4), 521–540.

Guinan Jr, J. J. (2006). Olivocochlear efferents: anatomy, physiology, function, and the measurement of efferent effects in humans. *Ear and hearing*, 27(6), 589–607.

Hauser, R. & Probst, R. (1991). The influence of systematic primary-tone level variation L2- L1 on the acoustic distortion product emission 2f1- f2 in normal human ears. *The Journal of the Acoustical Society of America*, 89(1), 280–286.

Hiipakka, M. & Tikander, M. (2009). Modeling of external ear acoustics for insert headphone usage. *126th Convention*, pp. 1–11. Consulted at http://www.aes.org/e-lib/browse.cfm ?elib=15253.

HSE. (2019a). Health and safety executive : Removal of hearing protectors severely reduces protection . Consulted at http://www.hse.gov.uk/noise/hearingprotection/index.htm/.

HSE. (2019b). Health and Safety Executive : Over-protection. Consulted at http://www.hse.gov .uk/noise/goodpractice/hearingoverprotect.htm.

Huang, G. T., Rosowski, J. J., Puria, S. & Peake, W. T. (2000). A noninvasive method for estimating acoustic admittance at the tympanic membrane. *The Journal of the Acoustical Society of America*, 108(3), 1128. doi: 10.1121/1.1287024.

Huang, Q. & Tang, J. (2010). Age-related hearing loss or presbycusis. *European Archives of Oto-rhino-laryngology*, 267(8), 1179–1191.

Interacoustics. (2019). A Guide to Otoacoustic Emissions. Consulted at https://diatec.ch/ wp-content/uploads/2019/04/OAE-Guide_EN.pdf.

ISO. (1991). ISO 389:1991 ACOUSTICS – STANDARD REFERENCE ZERO FOR THE CALIBRATION OF PURE-TONE AIR CONDUCTION AUDIOMETERS. Consulted at https://www.iso.org/standard/4375.html.

ISO. (2002). *Acoustics — Determination of sound immission from sound sources placed close to the ear — Part 1: Technique using a microphone in a real ear (MIRE technique)*. ISO 11904-1:2002. Geneva, Switzerland: International Organization for Standardization.

ISO. (2013). ISO 1999:2013 - Acoustics – Estimation of noise-induced hearing loss. Consulted at http://www.iso.org/iso/catalogue_detail.htm?csnumber=45103.

José Pinheiro, Douglas Bates, Saikat DebRoy, Deepayan Sarkar, EISPACK authors, Siem Heisterkamp, Bert Van Willigen, R-core. (2019). Package nlme. Consulted at https:// cran.r-project.org/web/packages/nlme/nlme.pdf.

Katz, J., Medwetsky, L., Burkard, R. & Hood, L. (2009). In *Handbook of Clinical Audiology* (ed. 6th, pp. 1056). Lippincott Williams & Wilkins.

Keefe, D. H. (2002). Spectral shapes of forward and reverse transfer functions between ear canal and cochlea estimated using DPOAE input/output functions. *The Journal of the Acoustical Society of America*, 111(1), 249–260.

Keefe, D. H., Ling, R. & Bulen, J. C. (1992). Method to measure acoustic impedance and reflection coefficient. *The Journal of the Acoustical Society of America*, 91(1), 470–485. doi: 10.1121/1.402733.

Kemp, D. T., Ryan, S. & Bray, P. (1990). A guide to the effective use of otoacoustic emissions. *Ear and hearing*, 11(2), 93–105.

Kemp, D. (1986). Otoacoustic emissions, travelling waves and cochlear mechanisms. *Hearing research*, 22(1), 95–104.

Keppler, H., Dhooge, I., Maes, L., D'haenens, W., Bockstael, A., Philips, B., Swinnen, F. & Vinck, B. (2010a). Transient-evoked and distortion product otoacoustic emissions: A short-term test-retest reliability study. *Int. J. Audiol.*, 49(2), 99–109.

Keppler, H. (2010). *Optimization of the diagnosis of noise-induced hearing loss with otoacoustic emissions*. (Ph.D. thesis, Ghent University). Consulted at https://biblio.ugent.be/publication/1079594.

Keppler, H., Dhooge, I., Corthals, P., Maes, L., D'haenens, W., Bockstael, A., Philips, B., Swinnen, F. & Vinck, B. (2010b). The effects of aging on evoked otoacoustic emissions and efferent suppression of transient evoked otoacoustic emissions. *Clinical Neurophysiology*, 121(3), 359–365. doi: 10.1016/j.clinph.2009.11.003. 00031.

Kim, S., Frisina, R. D. & Frisina, D. R. (2006). Effects of age on speech understanding in normal hearing listeners: Relationship between the auditory efferent system and speech intelligibility in noise. *Speech communication*, 48(7), 855–862.

Kirk, D. & Patuzzi, R. (1997). Transient changes in cochlear potentials and DPOAEs after low-frequency tones: the two-minute bounce revisited. *Hearing research*, 112(1), 49–68.

Kuba Mazur. (2016). *Auditory Research Platform : Twenty-Four Hour In-Ear Dosimetry*. (Master's thesis, École de technologie supérieure, Montréal (QC), Canada).

Kujawa, S. G. & Liberman, M. C. (2006). Acceleration of age-related hearing loss by early noise exposure: evidence of a misspent youth. *J Neurosci*, 26(7), 2115–23. doi: 10.1523/jneurosci.4985-05.2006.

Kujawa, S. G. & Liberman, M. C. (2009). Adding Insult to Injury: Cochlear Nerve Degeneration After "Temporary" Noise-Induced Hearing Loss. *The Journal of Neuroscience*, 29(45),

14077–14085.

Kujawa, S. G. & Liberman, M. C. (2015). Synaptopathy in the noise-exposed and aging cochlea: Primary neural degeneration in acquired sensorineural hearing loss. *Hearing Research*, 330, 191–199. doi: 10.1016/j.heares.2015.02.009. 00038.

Lapsley Miller, J. A., Marshall, L. & Heller, L. M. (2004). A longitudinal study of changes in evoked otoacoustic emissions and pure-tone thresholds as measured in a hearing conservation program. *International journal of audiology*, 43(6), 307–322. Consulted at http://www.tandfonline.com/doi/abs/10.1080/14992020400050040. 00071.

Laroche, C., Hetu, R. & Poirier, S. (1989). The growth of and recovery from TTS in human subjects exposed to impact noise. *The Journal of the Acoustical Society of America*, 85(4), 1681–1690.

Le Prell, C. G. (2019). Effects of noise exposure on auditory brainstem response and speech-in-noise tasks: A review of the literature. *International journal of audiology*, 58(sup1), S3–S32.

Lebeau, M. (2014). Maladies professionnelles : impact économique au Québec, colloque IRSST. Consulted at https://medias.irsst.qc.ca/videos/1411_au_co_HD_impactEconomique_fr_pdf.pdf.

Lee D. Hager. (2019). Hearing Protection: Prevention is the Answer. Consulted at https://www.audiologyonline.com/articles/hearing-protection-prevention-answer-1143.

Liberman, M. C. & Kujawa, S. G. (2017). Cochlear synaptopathy in acquired sensorineural hearing loss: Manifestations and mechanisms. *Hearing research*, 349, 138–147.

Liberman, M. C., Epstein, M. J., Cleveland, S. S., Wang, H. & Maison, S. F. (2016). Toward a differential diagnosis of hidden hearing loss in humans. *PloS one*, 11(9), 15.

Liberman, M. (2016). Noise-Induced Hearing Loss: Permanent Versus Temporary Threshold Shifts and the Effects of Hair Cell Versus Neuronal Degeneration. In *Advances in Experimental Medicine and Biology* (pp. 1–7). Springer New York LLC.

Lichtenhan, J., Wilson, U., Hancock, K. & Guinan, J. (2016). Medial olivocochlear efferent reflex inhibition of human cochlear nerve responses. *Hearing research*, 333, 216–224.

Lin, H. W., Furman, A. C., Kujawa, S. G. & Liberman, M. C. (2011). Primary neural degeneration in the Guinea pig cochlea after reversible noise-induced threshold shift. *Journal of the Association for Research in Otolaryngology*, 12(5), 605–616.

Lutman, M. E., Davis, A. C. & Ferguson, M. A. (2008). *Epidemiological Evidence for the Effectiveness of the Noise at Work Regulations* (Report n°Res. Rept. RR669). Norwich, UK: Health Safety Executive.

Maison, S. F. & Liberman, M. C. (2000). Predicting vulnerability to acoustic injury with a noninvasive assay of olivocochlear reflex strength. *Journal of Neuroscience*, 20(12), 4701–4707.

Maison, S. F., Usubuchi, H. & Liberman, M. C. (2013). Efferent feedback minimizes cochlear neuropathy from moderate noise exposure. *The Journal of Neuroscience*, 33(13), 5542–5552.

Marshall, L., Miller, J. A. L., Heller, L. M. et al. (2001). Distortion-product otoacoustic emissions as a screening tool for noise-induced hearing loss. *Noise and Health*, 3(12), 43.

Mathworks. (2018). Matlab 2018b.

Melnick, W. (1991). Human temporary threshold shift (TTS) and damage risk. *The Journal of the Acoustical Society of America*, 90(1), 147–154.

Microsoft. (2019). Critical Section Objects. Consulted at https://docs.microsoft.com/en-us/windows/win32/sync/critical-section-objects.

Moulin, A. (2000a). Influence of primary frequencies ratio on distortion product otoacoustic emissions amplitude. I. Intersubject variability and consequences on the DPOAE-gram. *The Journal of the Acoustical Society of America*, 107(3), 1460–1470.

Moulin, A. (2000b). Influence of primary frequencies ratio on distortion product otoacoustic emissions amplitude. II. Interrelations between multicomponent DPOAEs, tone-burst-evoked OAEs, and spontaneous OAEs. *The Journal of the Acoustical Society of America*, 107(3), 1471–1486.

Mukerji, S., Windsor, A. M. & Lee, D. J. (2010). Auditory brainstem circuits that mediate the middle ear muscle reflex. *Trends in amplification*, 14(3), 170–191.

Müller, J. & Janssen, T. (2008). Impact of occupational noise on pure-tone threshold and distortion product otoacoustic emissions after one workday. *Hearing research*, 246(1), 9–22.

Nadon, V. (2014). *Développement d'une oreillette pour la mesure des émissions otoacoustiques*. (Master's thesis, École de technologie supérieure).

Nadon, V. (2016). *Development of a method and algorithms for the combined measurement - inside the ear with a hearing protector - of the noise exposure dose and the induced hearing fatigue as measured with otoacoustic emissions*. DGA1033 - Proposed research plan.

Nadon, V., Voix, J., Bockstael, A. & Botteldooren, D. (2014). Signal processing techniques for continuous monitoring of distortion product otoacoustic emissions in noisy industrial environments. *Forum Acusticum 2014*.

Nadon, V., Bockstael, A., Botteldooren, D., Lina, J.-M. & Voix, J. (2015a). Individual monitoring of hearing status: Development and validation of advanced techniques to measure otoacoustic emissions in suboptimal test conditions. *Applied Acoustics*, 89, 78–87. 00005.

Nadon, V., Bockstael, A., Botteldooren, D. & Voix, J. (2015b). Assessment of otoacoustic emission probe fit at the workfloor. *10th European Congress and Exposition on Noise Control Engineering (Euronoise 2015)*, pp. 1955–1960.

Nadon, V., Bockstael, A., Botteldooren, D. & Voix, J. (2015c). Assessment of otoacoustic emission probe fit at the workfloor. *10th European Congress and Exposition on Noise Control Engineering (Euronoise 2015)*, pp. 1955–1960.

Nadon, V., Voix, J., Bockstael, A., Botteldooren, D. & Jean-Marc, L. (2015d). Method and device for continuous in-ear hearing health monitoring on a human being. Google Patents. US Patent App. 15/319,934.

Nadon, V., Bockstael, A., Botteldooren, D., Lina, J.-M. & Voix, J. (2017a). Design Considerations for Robust Noise Rejection in Otoacoustic Emissions Measured In-Field Using Adaptive Filtering. *Acta Acustica united with Acustica*, 103(2), 299–310.

Nadon, V., Bockstael, A., Botteldooren, D. & Voix, J. (2017b). Field monitoring of otoacoustic emissions during noise exposure: Pilot study in controlled environment. *American journal of audiology*, 26(3S), 352–368.

Nadon, V., Bonnet, F., E. Bouserhal, R., Bernier, A. & Voix, J. (2019). Method for protected noise exposure level assessment under an in-ear hearing protection device: a pilot study. *International Journal of Audiology*. Submitted.

National Association of Broadcasters. (1986). Modulation, Overmodulation, and Occupied Bandwidth.

Neely, S. & Liu, Z. (1994). *EMAV: Otoacoustic emission averager*.

Neitzel, R. & Fligor, B. (2017). Geneva: World Health Organization - Determination of risk of noise-induced hearing loss due to recreational sound: review. Consulted at https://www.who.int/pbd/deafness/Monograph_on_determination_of_risk_of_HL_due_to_exposure_to_recreational_sounds.pdf.

Neitzel, R., Somers, S. & Seixas, N. (2006). Variability of real-world hearing protector attenuation measurements. *The Annals of occupational hygiene*, 50(7), 679–691.

Nélisse, H., Gaudreau, M.-A., Boutin, J., Voix, J. & Laville, F. (2011). Measurement of hearing protection devices performance in the workplace during full-shift working operations. *Annals of occupational hygiene*, 56(2), 221–232.

NIOSH. (1998). Criteria for a recommended standard: Occupational noise exposure, revised criteria 1998. NIOSH Cincinnati, OH.

NIOSH. (2016). National Institute for Occupational Safety and Health : NOISE AND HEARING LOSS PREVENTION. Consulted at https://www.cdc.gov/niosh/topics/noise/.

NIOSH. (2019). NOISE AND HEARING LOSS PREVENTION. Consulted at https://www.cdc.gov/niosh/topics/noise/default.html.

Ockel. (2019). Ockel Sirius A. Consulted at https://www.ockelcomputers.com/sirius-a/.

OSHA. (2019a). OSHA Fact Sheet: Laboratory Safety Noise. Consulted at https://www.osha.gov/Publications/laboratory/OSHAfactsheet-laboratory-safety-noise.pdf.

OSHA. (2019b). Differentiation between the 80 dBA threshold for hearing conservation and the 90 dBA PEL. Consulted at https://www.osha.gov/laws-regs/standardinterpretations/2001-09-26.

Otodynamics Ltd. (2019). Echoport. Consulted at https://www.otodynamics.info/product/echoport/.

PJRC store. (2019). Audio Adaptor Board for Teensy 3.0 - 3.6. Consulted at https://www.pjrc.com/store/teensy3_audio.html.

Plack, C. J., Leger, A., Prendergast, G., Kluk, K., Guest, H. & Munro, K. J. (2016). Toward a Diagnostic Test for Hidden Hearing Loss. *Trends in Hearing*, 20(0), 9. doi: 10.1177/2331216516657466. 00000.

Plack, C. J., Barker, D. & Prendergast, G. (2014). Perceptual Consequences of "Hidden" Hearing Loss. *Trends in Hearing*, 18, 233121651455062. doi: 10.1177/2331216514550621.

Preyer, S., Baisch, A., Bless, D. & Gummer, A. W. (2001). Distortion product otoacoustic missions in human hypercholesterolemia. *Hearing Research*, 152, 139–151.

Prince, M. M., Stayner, L. T., Smith, R. J. & Gilbert, S. J. (1997). A re-examination of risk estimates from the NIOSH Occupational Noise and Hearing Survey (ONHS). *The Journal of the Acoustical society of America*, 101(2), 950–963.

Probst, R., Lonsbury-Martin, B. L. & Martin, G. K. (1991). A review of otoacoustic emissions. *The Journal of the Acoustical Society of America*, 89(5), 2027–2067.

Purves, D. (Ed.). (2004). *Neuroscience* (ed. 3rd ed). Sunderland, Mass: Sinauer Associates, Publishers.

Qiu, W., Hamernik, R. P. & Davis, R. I. (2013). The value of a kurtosis metric in estimating the hazard to hearing of complex industrial noise exposures. *The Journal of the Acoustical Society of America*, 133(5), 2856–2866.

Rabinowitz, P. M., Galusha, D., Dixon-Ernst, C., Clougherty, J. E. & Neitzel, R. L. (2013). The dose-response relationship between in-ear occupational noise exposure and hearing loss. *Occupational and environmental medicine*, 70(10), 716–21. Consulted at http://www.ncbi.nlm.nih.gov/pubmed/23825197.

Randall, R. B. & Tech, B. (1987). *Frequency analysis*. Brüel & Kjær.

Richmond, S. A., Kopun, J. G., Neely, S. T., Tan, H. & Gorga, M. P. (2011). Distribution of standing-wave errors in real-ear sound-level measurements. *The Journal of the Acoustical Society of America*, 129(5), 3134–3140.

Rosati, M. V., Tomei, F., Loreti, B., Casale, T., Cianfrone, G., Altissimi, G., Tomei, G., Bernardini, A., Di Marzio, A., Sacco, C. et al. (2018). Distortion-product otoacoustic emissions in workers exposed to urban stressors. *Archives of environmental & occupational health*, 73(3), 176–185.

Ruberg, K. (2019). Untreated Disabling Hearing Loss Costs Billions – in the US and the Rest of the World. Consulted at https://www.hearingreview.com/practice-building/marketing/surveys-statistics/untreated-disabling-hearing-loss-costs-billions-us-rest-world.

SAS. (2016). SAS/STAT(R) 9.2 User's Guide, Second Edition. Overview: MIXED Procedure. Consulted at https://support.sas.com/documentation/cdl/en/statug/63033/HTML/default/viewer.htm#statug_mixed_sect001.htm.

Schaette, R. & McAlpine, D. (2011). Tinnitus With a Normal Audiogram: Physiological Evidence for Hidden Hearing Loss and Computational Model. *The Journal of Neuroscience*,

31(38), 13452–13457.

Scheperle, R. A., Neely, S. T., Kopun, J. G. & Gorga, M. P. (2008). Influence of *in situ* , sound-level calibration on distortion-product otoacoustic emission variability. *The Journal of the Acoustical Society of America*, 124(1), 288–300. doi: 10.1121/1.2931953. 00000.

Scheperle, R. A., Goodman, S. S. & Neely, S. T. (2011). Further assessment of forward pressure level for *in situ* calibration. *The Journal of the Acoustical Society of America*, 130(6), 3882–3892. doi: 10.1121/1.3655878.

Sergeyenko, Y., Lall, K., Liberman, M. C. & Kujawa, S. G. (2013). Age-related cochlear synaptopathy: an early-onset contributor to auditory functional decline. *The Journal of Neuroscience*, 33(34), 13686–13694.

Siegel, J. H. (1994). Ear-canal standing waves and high-frequency sound calibration using otoacoustic emission probes. *The Journal of the Acoustical Society of America*, 95(5), 2589–2597.

Siegel, J. H. (1995). Cross-talk in otoacoustic emission probes. *Ear and hearing*, 16(2), 150–158.

Singer, J. D., Willett, J. B., Willett, J. B. et al. (2003). *Applied longitudinal data analysis: Modeling change and event occurrence*. Oxford university press.

Sliwinska-Kowalska, M., Kotylo, P. et al. (2001). Otoacoustic emissions in industrial hearing loss assessment. *Noise and Health*, 3(12), 75.

Smalt, C. J., Lacirignola, J., Davis, S. K., Calamia, P. T. & Collins, P. P. (2017). Noise dosimetry for tactical environments. *Hearing research*, 349, 42–54.

Smith, P. S., Monaco, B. A. & Lusk, S. L. (2014). Attitudes toward use of hearing protection devices and effects of an intervention on fit-testing results. *Workplace health & safety*, 62(12), 491–499.

Smith, S., Kei, J., McPherson, B. & Smyth, V. (2001). Effects of speech babble on transient evoked otoacoustic emissions in normal-hearing adults. *JOURNAL-AMERICAN ACADEMY OF AUDIOLOGY*, 12(7), 371–378. Consulted at http://www.audiology.org/sites/default/files/journal/JAAA_12_07_05.pdf. 00000.

Sonomax. (2016). SonoFit. Consulted at http://sonomax.com/assets/files/pdf/Sonomax-SonoFitSystem-Sheet.pdf.

Starck, J., Toppila, E., Pyykko, I. et al. (2003). Impulse noise and risk criteria. *Noise and Health*, 5(20), 63.

Starck, J. & Pekkarinen, J. (1987). Industrial impulse noise: crest factor as an additional parameter in exposure measurements. *Applied Acoustics*, 20(4), 263–274.

Stuart, A. & Cobb, K. M. (2015). Reliability of measures of transient evoked otoacoustic emissions with contralateral suppression. *Journal of Communication Disorders*, 58, 35–42. doi: 10.1016/j.jcomdis.2015.09.003. 00000.

Sun, X.-M. (2008). Contralateral suppression of distortion product otoacoustic emissions and the middle-ear muscle reflex in human ears. *Hearing Research*, 237(1-2), 66–75. doi: 10.1016/j.heares.2007.12.004. 00039.

Sutton, L. A., Lonsbury-Martin, B. L., Martin, G. K. & Whitehead, M. L. (1994). Sensitivity of distortion-product otoacoustic emissions in humans to tonal over-exposure: time course of recovery and effects of lowering L2. *Hearing Research*, 75(1-2), 161–174.

Tantranont, K. & Codchanak, N. (2017). Predictors of hearing protection use among industrial workers. *Workplace health & safety*, 65(8), 365–371.

Theis, M. A., Gallagher, H. L., McKinley, R. L. & Bjorn, V. S. (2012). Hearing Protection With Integrated In-Ear Dosimetry: A Noise Dose Study. *ASME 2012 Noise Control and Acoustics Division Conference*, pp. 237. doi: 10.1115/NCAD2012-0636.

Themann, C. L. & Masterson, E. A. (2019). Occupational noise exposure: A review of its effects, epidemiology, and impact with recommendations for reducing its burden. *The Journal of the Acoustical Society of America*, 146(5), 3879–3905.

Thiery, L. & Meyer-Bisch, C. (1988). Hearing loss due to partly impulsive industrial noise exposure at levels between 87 and 90 dB (A). *The Journal of the Acoustical society of America*, 84(2), 651–659.

Tracy, S. (2001). *Examination of the 2f2-fl distortion-product otoacoustic emission in normal-hearing and hearing-impaired ears and its potential for use in the detection of hearing loss*. (Ph.D. thesis, The graduate school of Syracuse University).

Trawick, J. A., Slagley, J. & Eninger, R. M. (2019). Occupational Noise Dose Reduction via Behavior Modification Using In-Ear Dosimetry among United States Air Force Personnel Exposed to Continuous and Impulse Noise. doi: 10.4236/ojsst.2019.92005.

Venet, T., Campo, P., Rumeau, C., Thomas, A. & Parietti-Winkler, C. (2014). One-day measurement to assess the auditory risks encountered by noise-exposed workers. *International*

journal of audiology, 53(10), 737–744.

Vijay K., M. & Douglas B., W. (1999). In *Digital Signal Processing Handbook* (ed. 1st, pp. 1690). CRC (Chemical Rubber Company) Press, USA.

Vinck, B. M., Van Cauwenberge, P. B., Leroy, L. & Corthals, P. (1999). Sensitivity of transient evoked and distortion product otoacoustic emissions to the direct effects of noise on the human cochlea. *Audiology*, 38(1), 44–52.

Voix, J. (2006). *Mise au point d'un bouchon d'oreille" intelligent"*. (Ph.D. thesis, École de technologie supérieure).

Voix, J. & Laville, F. (2009). The objective measurement of individual earplug field performance. *The Journal of the Acoustical Society of America*, 125(6), 3722–3732. doi: 10.1121/1.3125769. 00039.

Voix, J., Smith, Pegeen & Berger, Elliott. (2019). Field Attenuation Measurement Procedures. In *The Noise Manual* (ed. 6). Am. Ind. Hyg. Assoc. J.

Whitehead, M., Stagner, B., Lonsbury-Martin, B. L. & Martin, G. K. (1994). Measurement of otoacoustic emissions for hearing assessment. *Engineering in Medicine and Biology Magazine, IEEE*, 13(2), 210–226.

William Hollender. (2019). Super Audio Board. Consulted at https://github.com/whollender/SuperAudioBoard.

Withnell, R. H. & Yates, G. K. (1998). Onset of basilar membrane non-linearity reflected in cubic distortion tone input-output functions. *Hearing research*, 123(1-2), 87–96.

Xiong, M., Yang, C., Lai, H. & Wang, J. (2014). Impulse noise exposure in early adulthood accelerates age-related hearing loss. *European Archives of Oto-Rhino-Laryngology*, 271(6), 1351–1354.

Yakunina, N., Kim, J. & Nam, E.-C. (2018). The effect of primary levels and frequencies on the contralateral suppression of distortion product otoacoustic emission. *Journal of audiology & otology*, 22(2), 89.

Yuntab. (2019). Yuntab Wintel Mini PC. Consulted at https://www.walmart.com/ip/Yuntab-GB01-Wintel-Mini-PC-Box-Atom-Processor-Z3735F-Quad-core-CPU-with-Windows-10-Ram-2GB-EMMC-64GB-Bluetooth-4-0-4K-Ultra-HD-Wifi-2-4G-5G/518647868.

Zare, S., Nassiri, P., Monazzam, M. R., Pourbakht, A., Azam, K. & Golmohammadi, T. (2015). Evaluation of Distortion Product Otoacoustic Emissions (DPOAEs) among workers at

an Industrial Company exposed to different industrial noise levels in 2014. *Electronic physician*, 7(3), 1126.

Zechmann, E. (2019). Continuous Sound and Vibration Analysis - File Exchange - MATLAB Central. Consulted at https://www.mathworks.com/matlabcentral/fileexchange/21384-continuous-sound-and-vibration-analysis.

Zoom. (2019). Zoom H5. Consulted at https://www.zoom.co.jp/products/field-video-recording/field-recording/h5-handy-recorder.